Mechanism of Action of Membrane-Active Marine Natural Products Theonellamide A and Amphidinol 3

（膜作動性海洋天然物セオネラミドＡと
アンフィジノール３の作用機構解析）

A Thesis Submitted to the
Graduate School of Science
Osaka University

In Partial Fulfillment of the
Requirements for the Degree of
Doctor of Philosophy (Ph.D.) in Chemistry

By

Rafael Atillo Espiritu

Department of Chemistry
Graduate School of Science
Osaka University
2013

Mechanism of Action of Membrane-Active Marine Natural Products Theonellamide A and Amphidinol 3

（膜作動性海洋天然物セオネラミドＡと
アンフィジノール３の作用機構解析）

Rafael Atillo Espiritu

Department of Chemistry
Graduate School of Science
Osaka University
2013

Abstract

Marine organisms are a rich source of numerous structurally unique and biologically active secondary metabolites that may find potential use as effective therapeutics. Among the several promising compounds include the sponge-derived theonellamides (TNMs) and dinoflagellate-derived amphidinols (AMs).

Theonellamides are antifungal and cytotoxic bicyclic dodecapeptides isolated from the marine sponge *Theonella* sp. Recently, it has been shown that TNMs recognize 3β-hydroxysterol-containing membranes, induce glucan overproduction, and damage cellular membranes. However, to date, the detailed mode of sterol-binding at a molecular level has not been determined. To gain insight into the mechanism of sterol-recognition of TNM in lipid bilayers, surface plasmon resonance (SPR) experiments and solid state deuterium nuclear magnetic resonance (^{2}H NMR) measurements were performed on theonellamide A (TNM-A). SPR results revealed that the incorporation of 10 mol% of cholesterol or ergosterol into 1-palmitoyl-2-oleoyl-*sn*-glycero-3-phosphocholine (POPC) membranes significantly enhances the affinity of the peptide for the membrane, particularly in the initial binding process, to the membrane surface, while binding to epicholesterol (3α-cholesterol)-containing membranes was significantly weaker. This increase in affinity is due to direct intermolecular interaction between the 3β-hydroxysterols in membranes and TNM-A as evidenced by characteristic changes in the solid state ^{2}H NMR spectra. These results demonstrate that TNM-A recognizes the 3β-OH moiety of sterols, greatly facilitating its binding to bilayer membranes.

It has also become apparent that membrane action of TNM-A does not involve the formation of clear and distinct pores but more likely morphological changes or deformations. To observe these morphological changes, solid state ^{31}P NMR and differential interference and confocal fluorescence microscopy were performed. Solid state ^{31}P NMR revealed the presence of isotropic signals both in cholesterol-containing and sterol-free POPC liposomes indicating disruption of the membrane, consistent with previous dye leakage experiments. These were most likely due to regions of high membrane curvature than small fast-tumbling structures based on dynamic light scaterring (DLS) measurements. Differential interference and confocal microscopy images using giant unilamellar vesicels (GUVs) showed clear fluctuations in membrane surface structure indicating regions of high curvature both in cholesterol-containing (5 mol%) and sterol-free POPC liposomes, which occurs more frequently in the former. These deformations also appear to allow the influx of bulk solution into the vesicles as observed with a fluorescent TNM-A derivative. Interestingly, a membrane

fission process was also detected in both types of liposomes that may account for vacuolar fragmentation reported earlier.

Amphidinols (AMs) are polyketide metabolites from the dinoflagellate *Amphidinium klebsii* whose structure is characterized by a polyol and polyene chains separated by two tetrahydropyran rings. These compounds show potent antifungal and hemolytic properties which is believed to arise from its interaction with the lipid bilayer. Indeed, amphidinol 3 (AM3) has been demonstrated to permeabilize sterol-containing liposomes and its membrane-bound structure where the polyol and polyene chains are located in the membrane surface and interior, respectively, supported a toroidal pore mechanism. Despite these findings, a detailed molecular basis on how AMs recognize sterols on membranes and how the pore/lesion forms in still unclear. Here, it was demonstrated that pore formation by AM3 was found to occur exclusively in liposomes with 3β-hydroxysterols, suggesting the importance of sterol in the pore complex. Similarly with TNM-A, SPR analysis showed AM3 to have very weak affinity towards epicholesterol-containing membranes, in contrast with 3β-hydroxysterol-containing liposomes. This is brought about by the lack of direct intermolecular interaction in the former compared with the latter based on solid state ^{2}H NMR data. Interestingly, however, in contrast to the assumed toroidal pore formed by AM3, no such structure was apparent based on solid state ^{31}P NMR spectra indicating that AM3 does not cause significant disruption of surrounding phospholipids.

Table of Contents

List of Abbreviations

µ	micro
Å	angstrom
AM3	amphidinol 3
AM	amphidinol
AMP	antimicrobial peptide
CDC	cholesterol-dependent cytolysin
CP-MAS	cross polarization-magic angle spinning
CSA	chemical shift anisotropy
d	deuterated
DLS	dynamic light scattering
DMSO	dimethyl sulfoxide
EC_{50}	half maximal effective concentration
EDC	1-Ethyl-3-[3-(dimethylamino)propyl]carbodiimide
EDTA	ethylenediamine tetraacetic acid
g	gram
GUV	giant unilamellar vesicle
HPLC	high performance liquid chromatography
Hz	hertz
IC_{50}	half maximal inhibitory concentration
k	kilo
L	liter
LUV	large unilamellar vesicle
m	milli / meter
M	molar
MEC	minimum effective concentration
MeCN	acetonitrile
MeOH	methanol
min	minute
mol	mole
MLV	multilamellar vesicle
NaOH	sodium hydroxide
NHS	*N*-hydroxysuccnimide
NMR	nuclear magnetic resonance

ODS	octyldodecylsilane
PBS	phosphate buffered saline
PC	phosphatidylcholine
ppm	parts per million
POPC	1-palmitoyl-2-oleoyl-*sn*-glycero-3-phosphocholine
PrOH	propanol
RU	resonance (response) unit
s	second
SUV	small unilamellar vesicle
SPR	surface plasmon resonance
TLC	thin layer chromatography
TNM	theonellamide
TNM-A	theonellamide-A
TNM-FL	fluorescein-labeled theonellamide A

List of Figures

List of Tables

List of Schemes

Chapter 1

General Introduction – Mechanism of Action of Membrane-Active Compounds

1.1 Membrane-Active Compounds

Biological membranes (Figure 1-1) are fundamental cellular structures that mainly function as a barrier separating the inside of the cell from the external environment. At the same time, it acts as a semi-permeable membrane that allows the passage of certain ions or

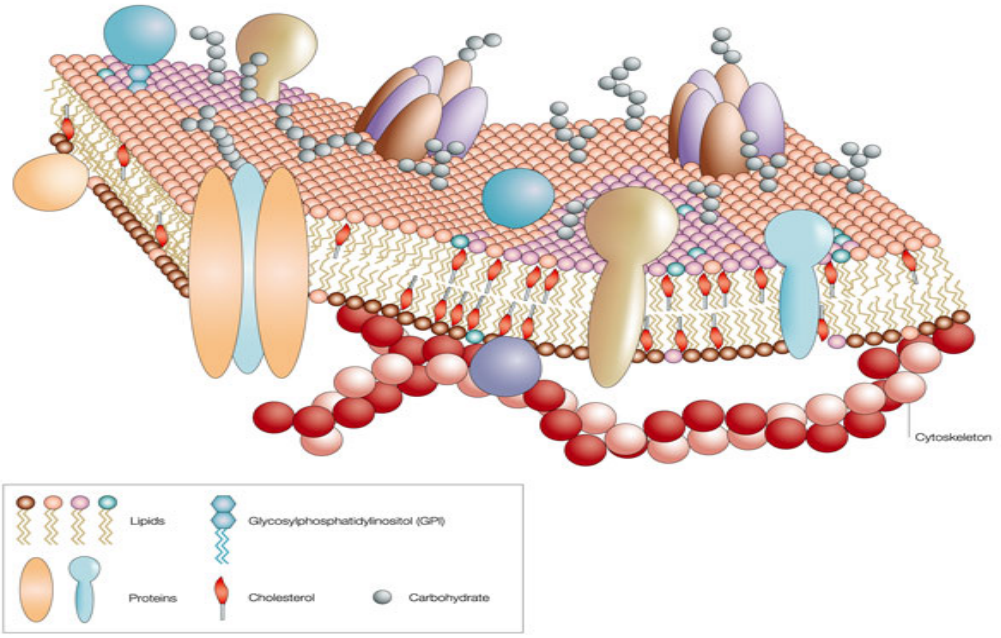

Figure 1-1. Fluid mosaic representation of a biological membrane. Reprinted with permission from *Horizon Symposia: Living Frontier*, **2004**, 1-4.[2] Copyright © (2004) Nature Publishing Group.

molecules while excluding others. The currently accepted representation of a biological membrane is the so-called fluid mosaic model proposed by Singer and Nicholson which states that the membrane is a fluid phospholipid bilayer dispersed with integral and peripheral

membrane proteins, and other constituents such as sterols (in eukaryotic cells), that can freely diffuse laterally.[1,2]

Given the importance of membranes in ensuring cell integrity and survival as well as compartmentalizing the entire cell and the organelles inside them, disruption of membrane function results in significant biological problems. It is therefore not surprising to find a lot of compounds, both natural and synthetic, that are known to target the membrane to be able to exert their biological activity. For instance, integral membrane proteins are the target of more than 60% of current commercially available drugs.[3] Cholesterol-dependent cytolysins (CDCs), toxins secreted by certain Gram-positive bacteria that contribute to their pathogenesis, show

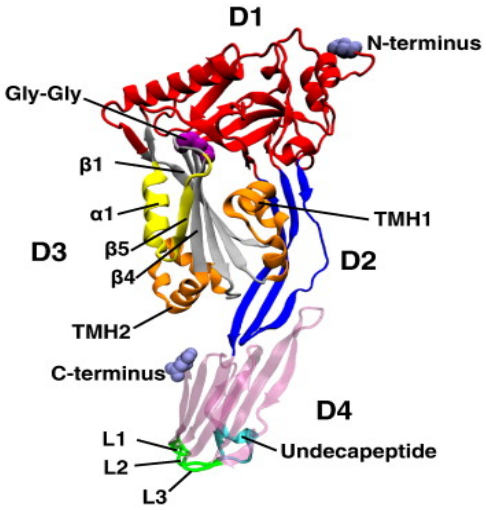

Figure 1-2. Molecular structure of the CDC from *Clostridium perfringens,* perfringolysin O. Reprinted with permission from *Biochim, Biophys. Acta*., **2012**, 1818, 1028-1038., and *Cell*, **1997**, 89, 685-692.[4,45] Copyright © (2012 and 1997) Elsevier.

an absolute dependence on the presence of membrane cholesterol for its activity.[4] These proteins have been previously identified exclusively with Gram-positive organisms, but recently the first CDCs from two species of Gram-negative bacteria, not known to cause harm or disease in humans or animals, were reported.[5] Another group of well known sterol-binders are the polyene macrolide antibiotics that include amphotericin B, natamycin, nystatin A1 and filipin III.[6] Meanwhile, antimicrobial peptides (AMPs) produced by a great variety of organisms including animals, plants, invertebrates, and bacteria, like the well studied magainin and melittin, are widely believed to target the membrane itself and/or certain phospholipid components more prevalent in bacteria than mammals and are thus proposed as

possible candidate drugs to combat antibiotic- resistant bacteria.[7,8] The structures of some of these membrane-active compounds are shown in Figure 1-2 and 1-3.

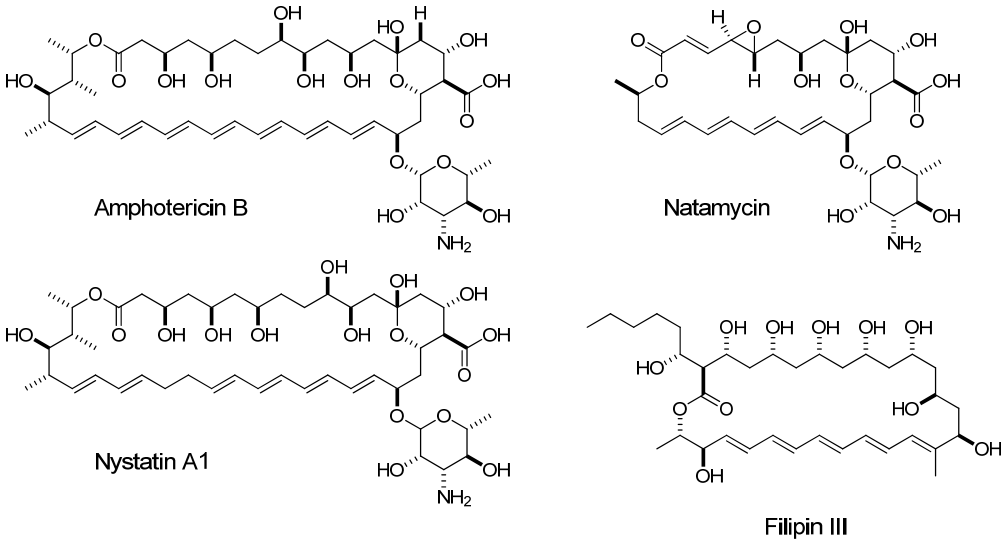

Melittin : G-I-G-A-V-L-K-V-L-T-T-G-L-P-A-L-I-S-W-I-K-R-K-R-Q-Q
Magainin 1: G-I-G-K-F-L-H-S-A-G-K-F-G-K-A-F-V-G-E-I-M-K-S
Magainin 2: G-I-G-K-F-L-H-S-A-K-K-F-G-K-A-F-V-G-E-I-M-N-S

Figure 1-3. Chemical structures of several polyene macrolide antibiotics and the primary amino acid sequence of melittin and magainin 1 and 2.

Components of the membrane are varied, ranging from proteins, phospholipids and sterols, and recognition of these components by their appropriate biomolecular partner is critical for different membrane and cellular processes. This is more pronounced in the case of drugs used to treat human diseases; in fact an extremely high selectivity and affinity are two of the most desired characteristics of drug molecules.[9] In general, increasing the selectivity of drugs for their targets, such as membrane proteins, involves functionalizing the compound with non-polar or polar groups that could induce the most favorable interactions with the protein's binding pocket in thermodynamic terms.[9] Some molecules also take advantage of certain cellular deficiencies to account for their selectivity such as the small molecule lanperisone which works by inducing reactive oxygen species that some cancer cells cannot effectively scavenge leading to oxidative stress and ultimately, cell death.[10]

Selective toxicity of CDCs for mammalian cells, on the other hand, arises from its absolute dependence on membrane cholesterol,[4] which is predominant in mammalian membranes. Cholesterol acts as the membrane receptor for this class of compounds, binding to which leads to a cascade of events resulting in pore formation. Interestingly, a few CDCs use human CD59 as their receptor, rather than cholesterol, but presence of this sterol is still a requirement for pore formation.[4] Efficacy of polyene macrolide antibiotics, e.g. amphotericin B, in the treatment of systemic fungal infections is widely attributed to its higher binding affinity to ergosterol, the main fungal sterol, compared with cholesterol in mammalian membranes.[11,12] Nevertheless, this does not preclude the serious side effects of the drug, most notably its nephrotoxoctiy, which sometimes necessitates the discontinuation of its use even in severe fungal infections.[13]

Antimicrobial peptides have recently gained considerable attention due to their potential use in combating the increasing incidence of bacteria resistant to traditional antibiotics.[14] The marked selectivity and lethality of AMPs towards microbes rather than the host cells is most commonly associated with the preferential ionic interaction between the usually cationic AMPs and the anionic constituents of bacterial membranes coupled with the lack of rigidifying lipids like cholesterol; eukaryotic membranes, on the other hand are zwitterionic and contain sterols.[7,8,14-17] Some of these AMPs also show a selective cytotoxicity towards cancer cells which is also due to the preponderance of anionic membrane components in these cells: the expression of anionic molecules such as phosphatidylserine, O-glycosylated mucins, sialilated gangliosides, and heparin sulfates are elevated in cancer cells.[18] Another subset in these big group of AMPs are those that usually have high activity on a specific target bacterium and act via a receptor-mediated mechanism.[14] These high target specificity peptides both have a receptor-binding region and a pore-forming region, and it includes nisin Z and mesentercicin Y.[19]

1.2 Mechanisms of Membrane Permeabilization

The afore-mentioned compounds, specifically the CDCs, polyene macrolides, and AMPs exert their biological action through membrane interactions and there is sufficient evidence to suggest that their toxicity arises from permeabilization of the membrane subsequently leading to cell lysis.[4,6-8,11,12,14-19] Membrane permeabilization by these compounds can occur via formation of distinct transmembrane pores or non-pore defects, both of which are able to dissipate membrane potential as well as cause leakage of cellular solutes and/or components.

1.2.1 Transmembrane Pore Models

Pore formation of membranes can occur in any of two possible mechanisms: barrel-stave or toroidal pore.

In a ***barrel-stave pore***, membrane-bound compounds aggregate and form oligomeric structures able to span the entire length of the membrane. The extraordinarily large CDC pore is usually composed of about 35-50 monomers with a diameter ranging from 250-300 Å,[4] while the amphotericin B-sterol pore complex is normally composed of 4-8 pairs of amphotericin B and sterol molecules with a pore diameter of about 6-9 Å.[12,20] Pore formation by AMPs, in general, is unique and only a few of them qualify as true pore formers.[7,8,14] In the barrel-stave mechanism (Figure 1-4), penetration of the hydrophobic membrane core is essential, thus interaction between the peptides and membranes is primarily governed by hydrophobic interactions, with the hydrophobic residues facing the lipid core while the hydrophilic ones line the water-filled pore lumen.[14] For this reason, these peptides necessarily have to be non-cell selective, permeabilizing both zwitterionic and anionic membranes, as is the case with alamethicin, which forms a barrel-stave pore with an inner diameter of about 18 Å.[7,8,14]

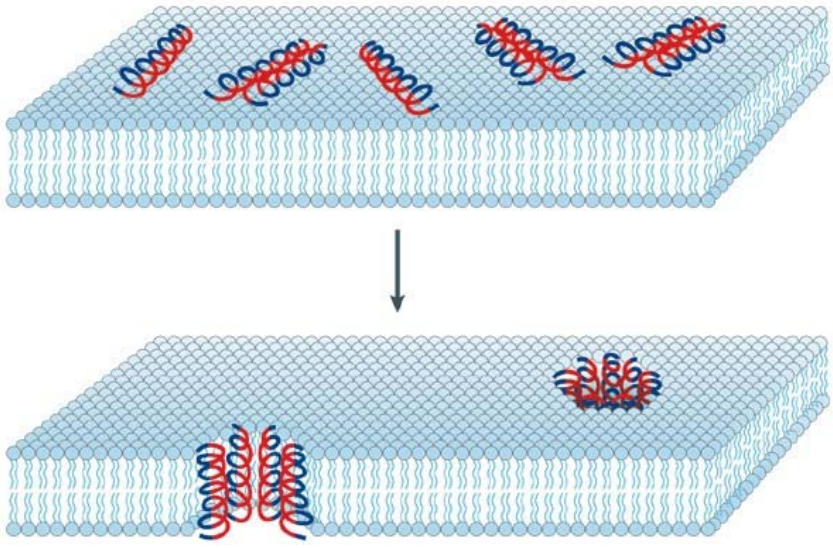

Figure 1-4. Cartoon representation of barrel-stave pore formation by antimicrobial peptides. Blue and red regions represent the hydrophobic and hydrophilic portions of AMPs, respectively. Reprinted with permission from *Nat. Rev. Microbiol.*, **2005**, 3, 238-250., and *Biopolymers*, **1998**, 47, 451-463.[7,46] Copyright © (2005) Macmillan Publishers Ltd. and (1998) John Wiley & Sons, Inc.

In the ***toroidal-pore*** model, membrane-bound peptides, for instance, insert and cooperatively affect the local curvature by inducing the membrane to bend back on itself continuously such that the water-filled pore is lined by both the peptides and the phospholipid head groups, forming a toroid of high curvature (Figure 1-5).[7,8] The defining characteristic of a toroidal pore is that the peptides are always associated with the lipid headgroups. Melittin and magainin are examples of AMPs that are believed to permeabilize membrane via toroidal pore formation, and in the case of magainin, it forms a larger pore compared with alamethicin having an inner of about 30-50 Å, which is thought to contain approximately 4-7 peptides and ~90 lipid molecules.[7] Aside from small, cationic antimicrobial peptides, toroidal pore formation has also been proposed as the mode of action of proteinous toxins (>20 kDa), specifically equinatoxin II and sticholysins obtained from sea anemones.[21,22]

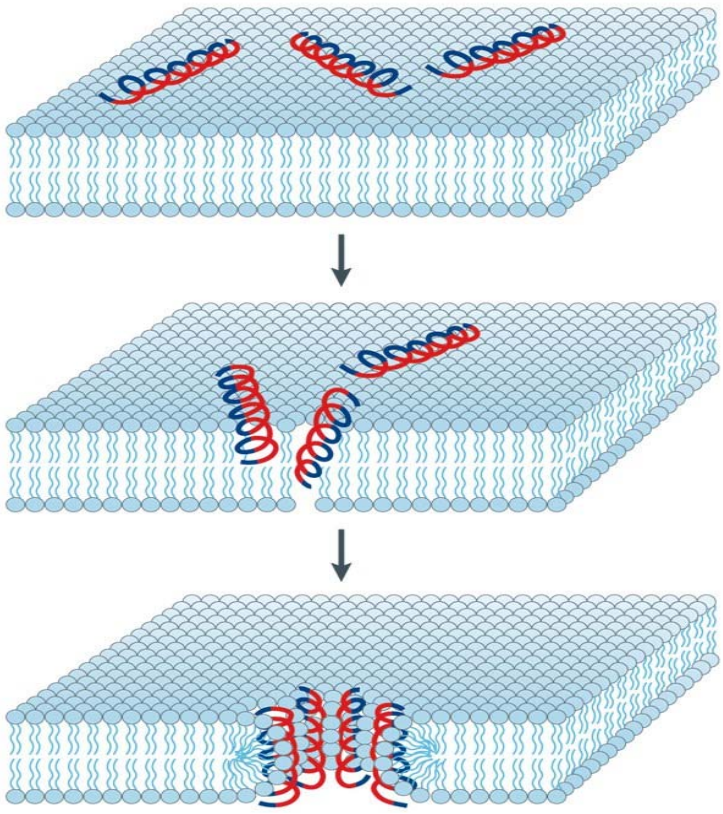

Figure 1-5. Cartoon representation of toroidal pore formation by antimicrobial peptides. Blue and red regions represent the hydrophobic and hydrophilic portions of AMPs, respectively. Reprinted with permission from *Nat. Rev. Microbiol.*, **2005**, 3, 238-250., and *Phys. Rev. Lett.*, **2004**, 92, 198304-1 – 198304-4.[7,47] Copyright © (2005) Macmillan Publishers Ltd., and (2004) American Physical Society.

The fundamental difference between these two pore models is that a barrel-stave works with the hydrophobic membrane core using it as a basis to form the channel, while a toroidal pore works against it, disrupting non-polar-polar segregation of the membrane with alternative regions where these parts can have more favorable interactions.[8]

1.2.2 Non-Pore Models

Pore formation by AMPs is quite a unique phenomenon.[8,15] However, conclusive evidence on the presence of these water-filled pores formed by most of the so called "pore-forming peptides" are still lacking.[8] In addition, pore-forming peptides should theoretically be bactericidal at very low concentrations; lower than the experimentally observed micromolar levels, since they will be lethal once they penetrate the membrane where pores can be formed by as few as three monomers.[14] Simulation studies have also demonstrated that a single, 10 Å water-filled pore will have a release rate of 50,000 ions per second,[8] while that of the gramicidin, a well-studied AMP, ion channel is known to pass up to 10^6-10^7 ions per second.[23] Since a typical large unilamellar vesicle can only contain hundreds to a few thousand probe molecules, complete release should be observed within a fraction of a second. However, experimentally, only a fraction of vesicle contents are released with rates that are at least 3 orders of magnitude below the theoretical rate (Figure 1-6). In addition, a typical vesicle experiment, for instance using giant unilamellar vesicles, has bound peptide to lipid ratio that is quite high (~ 1:50). This would translate to about 2 x 10^7 bound peptides enough to form 2 million pores (assuming decameric structures) but leakage of contents remain inefficient.[8] Thus significant leakage via pore formation is really a rare occurrence, instead, what could actually happen is a more general disruption of membrane integrity.[8]

The most commonly-cited non-pore permeabilization mechanism is the so-called ***carpet or detergent model*** (Figure 1-7).[7,8,14,15] In this model, the peptides bind parallel to the membrane surface with their hydrophobic regions oriented towards the lipidic core while their hydrophilic portions contact the polar phospholipid headgroup, and cover the membrane surface like a carpet. Only when the peptides reach a threshold concentration, they insert and permeate the membrane leading to disruption of membrane integrity. At this concentration, the peptides may also form transient toroidal holes which could facilitate translocation of the peptide into the inner membrane leaflet leading to formation of mixed micelles and a disastrous collapse of the membrane. This mode of action is proposed to account for the activity of the majority of AMPs since it does not require specific interaction between membrane-bound monomers, peptide insertion into hydrophobic core or channel formation. In

contrast, it appears that an appropriate hydrophobicity and net positive charge is enough for activity.[15]

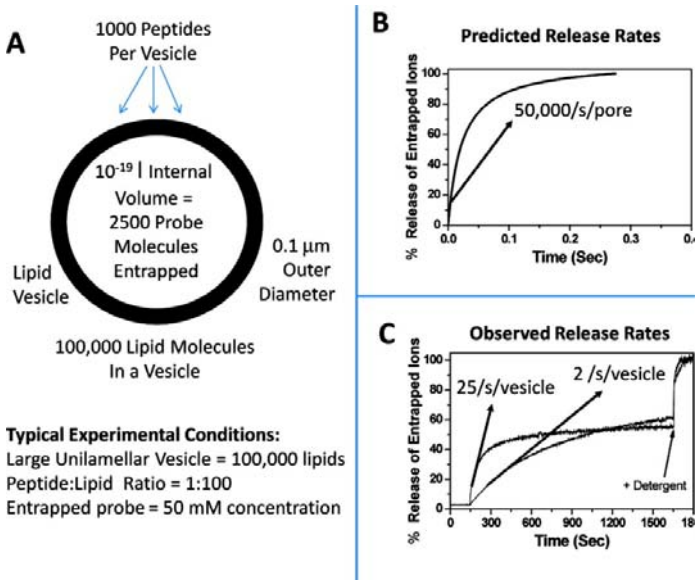

Figure 1-6. Release of vesicle-entrapped molecules. (A) Typical experimental conditions, (B) theoretical release rate, (C) experimental release rate. Reprinted with permission from *ACS Chem. Biol.,* **2010**, 5, 905-917.[8] Copyright © (2010) American Chemical Society.

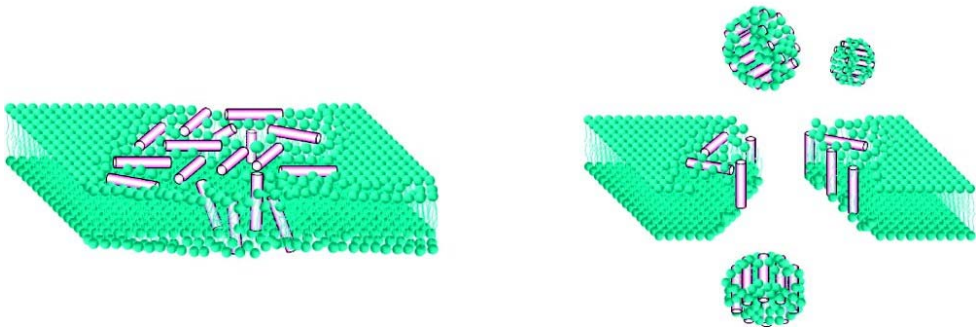

Figure 1-7. Cartoon representation of the carpet/detergent mode of action by antimicrobial peptides. Reprinted with permission from *ACS Chem. Biol.,* **2010**, 5, 905-917.[8] Copyright © (2010) American Chemical Society.

Other non-pore models that have been previously proposed include the sinking raft model,[24,25] charge cluster mechanism,[26,27] leaky slit model,[28] and the interfacial activity model.[8] It is worth pointing out, however, that these models most likely complement each

other, rather than any single one being the exclusive mechanism of antimicrobial peptide-induced membrane permeabilization.

In the ***sinking raft model*** (Figure 1-8), a mass imbalance between the outer and inner membrane leaflets is generated because of peptide binding on the former. This mass imbalance creates curvature strain and to relieve the stress, peptides "sink" into the bilayer with concomitant lipid flip-flop and efflux of intracellular metabolites. When the peptides reach the cytoplasmic side of the membrane and equilibrium is re-established, lipid flip-flop and efflux stops. This model was proposed to account for the graded dye release observed with *Staphylococcus aureus* lytic peptide δ-lysin.[24,25]

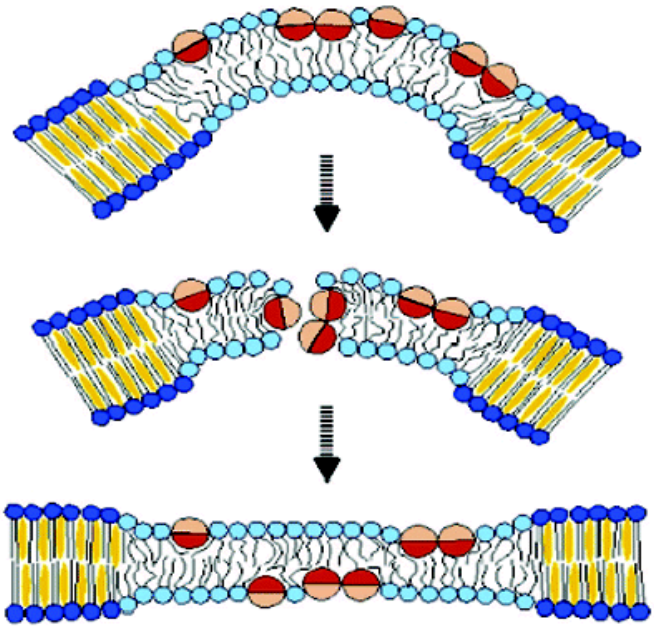

Figure 1-8. Representation of the sinking raft model. Peptides are shown as circles, with dark and light regions corresponding to the molecules' hydrophobic and hydrophilic portions, respectively. Reprinted with permission from *Biochemistry,* **2004**, 43, 8846-8857., and *Biochemistry,* **2005**, 44, 9538-9544.[24,25] Copyright © (2004 and 2005) American Chemical Society.

Bacterial plasma membrane contains a greater proportion of anionic lipids than zwitterionic ones, and clustering of the former by some cationic antimicrobial peptides is proposed to contribute to their bactericidal action.[26,27] The ***charge cluster mechanism*** (Figure 1-9) arises from the preferential interaction between cationic AMPs and anionic lipids and subsequent clustering of the latter leading to formation of lipid-peptide domains that excludes the zwitterionic membrane components. This causes a large reorganization of the bacterial

membrane and an increase in concentration of anionic lipids and peptides within certain domains will result in boundary defects leading to membrane permeabilization and/or functional impairment of membrane proteins normally associated with anionic lipids. Furthermore, this clustering may cause existing bacterial membrane domains to be unstable and/or to have altered properties which ultimately could lead to cell death. Antimicrobial peptides that are highly cationic (+6 to +10 net charge) served as a model for this mechanism.

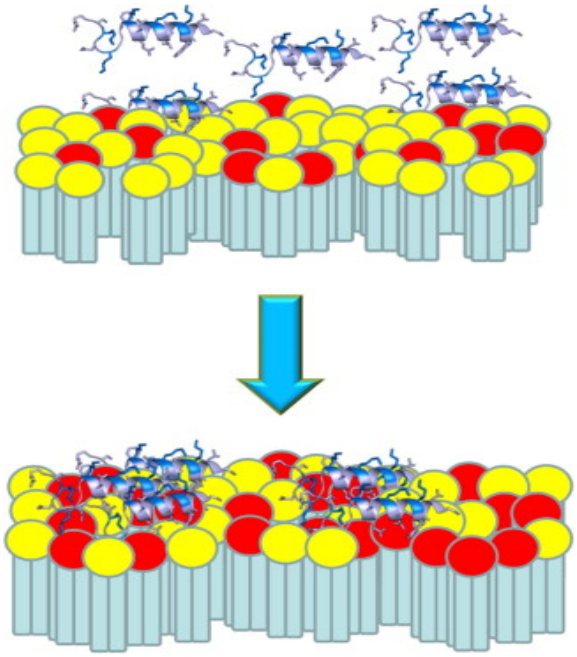

Figure 1-9. Clustering on anionic lipids (red) by cationic antimicrobial peptides leading to formation of peptide-lipid domains and segregation of zwitterionic lipids (yellow). Reprinted with permission from *Prog. Lipid Res.*, **2012**, 51, 149-177.[17] Copyright © (2012) Elsevier.

The ***leaky slit model*** (Figure 1-10) was proposed as a possible mechanism to account for the toxicity of plantaricin A and other fiber forming proteins and peptides.[28] Fibril formation by various proteins and peptides has been reported to be induced by negatively-charged phospholipids, particularly phosphatidylserine, present in membranes.[29] In this model, bound peptides arrange themselves in a linear configuration with their hydrophobic regions facing the membrane core. Toxicity lies in the hydrophilic regions of the peptide (interactions between these regions account for the aggregation and formation of fibrilliar oligomers) which will not be able to make contact with the opposing hydrophobic layer. This will then

force the membrane to adopt a highly positive curvature, forming a "leaky slit" facilitating movement of solutes across the membrane causing the cell to be irreparable. Given these, the

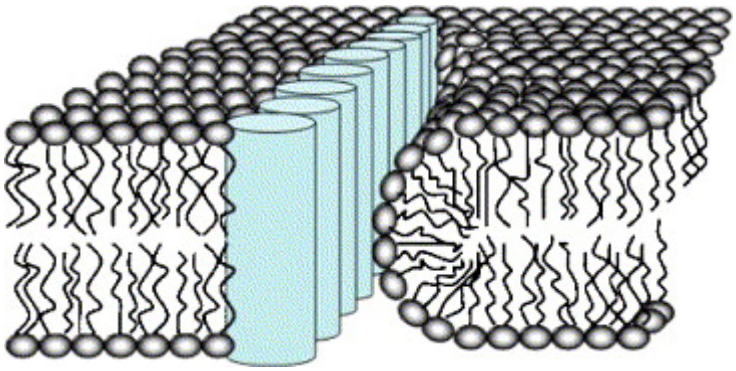

Figure 1-10. Cartoon representation of a membrane leaky slit induced by fiber-forming peptides. Reprinted with permission from *Biochim. Biophys. Acta.*, **2006**, 1758, 1461-1474.[28] Copyright © (2006) Elsevier.

only requirement for the formation of a leaky slit appears to be the capacity of the peptide to aggregate into fibers having an amphiphatic nature able to span the membrane.

Another probable mechanism of AMP action was proposed based on the activity of the peptides in the interfacial region of the membrane. The hydrophobic core of the membrane, which acts as a semi-permeable barrier, is sandwiched between a region about 10-15 Å thick containing lipid polar head groups, water, counterions, and a small fraction of hydrocarbon groups, called the interfacial region.[8] The ***interfacial activity model*** describes the capacity of an imperfectly amphiphatic peptide, those that are amphiphatic but with imperfect segregation of polar and non-polar residues, to partition in this region resulting in the perturbation of the strict permeability barrier imposed by the membrane core. This perturbation arises from local membrane rearrangements affecting the separation of the hydrophobic core and the interfacial groups, formation of which carries polar solutes along with the peptides and lipids across the membrane resulting in leakage associated with AMPs. It is also proposed that an interfacially-active peptide will be active even at low concentrations, and that translocation of these peptides will always be coupled with lipid flip-flop and membrane leakage.[8] This model is represented in a molecular dynamics simulation shown in Figure 1-11.

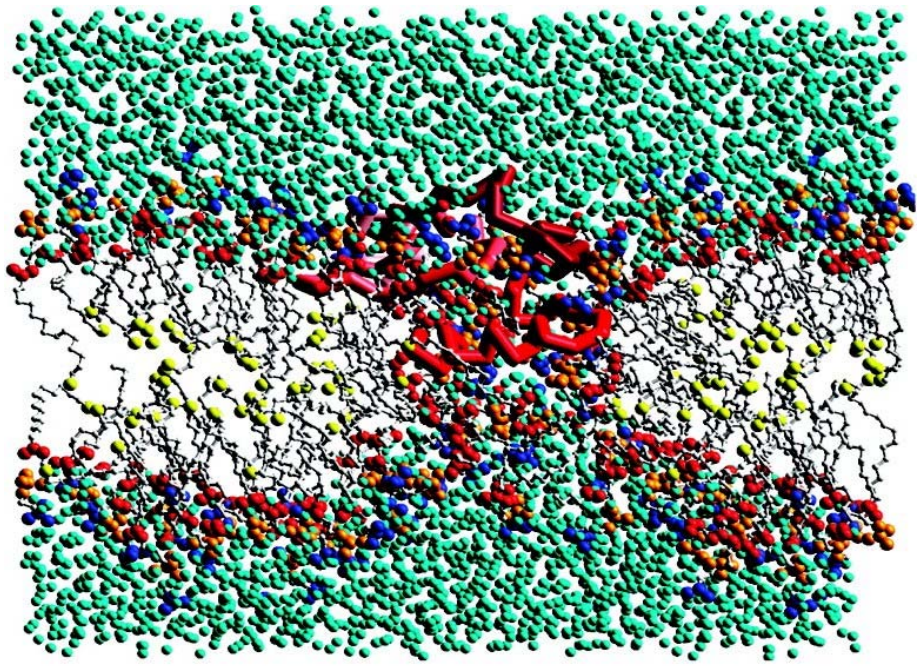

Figure 1-11. Molecular dynamics simulation that could represent the interfacial activity. Water, choline, phosphate, carbonyl, and terminal methyl groups are represented by blue-green, blue, orange, red, and yellow spheres. Reprinted with permission from *ACS Chem. Biol.*, **2010**, 5, 905-917., and *Biochim. Biophys. Acta*, **2008**, 1778, 2308-2317.[8,48] Copyright © (2010) American Chemical Society and (2008) Elsevier.

1.3 Methods to Study Membrane Interactions

Interactions between bioactive molecules and cell membranes play a key role in the regulation of several cellular processes such as signal transduction, ion channel formation, and the action of antimicrobial and cytotoxic peptides. Among a wide range of techniques employed to investigate these interactions,[30,31] SPR has been proven to be an excellent tool to examine the binding behavior of biomolecules to membranes.[30,32] This technique was successfully employed to characterize the interaction of cationic amphiphilic drugs and antimicrobial peptides with artificial membranes.[33-35] Recently, using SPR, the binding of amphotericin B[36] to POPC liposomes was also evaluated, which revealed that the affinity of this molecule to the vesicles is significantly enhanced by incorporating cholesterol or ergosterol into the lipid bilayer. In this earlier study, a dodecylamine-modified CM5 sensor chip was developed to minimize non-specific interaction between amphotericin B and the dextran matrix on the chip thus providing a more accurate evaluation of the binding interaction between the drug and liposomes.[36]

Solid-state ^{2}H NMR spectroscopy is an invaluable tool in the study of lipid and sterol dynamics in model membranes, e.g. the membrane perturbing effects induced by antimicrobial peptides can be directly observed by the change in quadrupole splitting of deuterated acyl chain segments of phospholipids.[37] Recently, ^{2}H NMR was used to reveal the dynamics of sterols affected by the presence of amphotericin B.[38] This study has showed that amphotericin B inhibits the fast rotational motion of ergosterol in membranes, thus unequivocally demonstrating the direct amphotericin B-ergosterol interaction in lipid bilayers.

Membrane morphological changes or deformations have been observed to be induced by certain compounds, most notably antimicrobial peptides, and is postulated to be linked with their reported biological activities.[15,27,39-41] These peptides cause a wide range of effects including positive and negative curvature strain, induction of cubic lipid phases, clustering of certain phospholipids, membrane thinning, formation of lipid protrusions, and membrane disruptions. Solid state ^{31}P NMR is a sensitive and highly useful tool to study changes in membrane morphology and phospholipid dynamics as exemplified by some antimicrobial peptides.[37-42] Meanwhile, giant unilamellar vesicles (GUVs), whose diameter reaches up to about 100 μm, have gained much attention as suitable tools to carry out fluorescence microscopy experiments and to observe structural details in membrane organization above ~300 nm.[43,44] In addition, the average size of GUVs also approximate that of the plasma membrane of a number of cells, which makes it possible to conduct measurements with single vesicles that mimic the curvature of natural membranes.[43] This latter advantage can be exploited in order to gain more meaningful insight into the effects of certain molecules, such as peptide and proteins, on the structure of the membrane.

References

1. Singer, S.J.; Nicolson, G.L. *Science*. **1975**, 175, 720-731.
2. Pietzsch, J. Mind the membrane. *Horizon Symposia: Living Frontier.* **2004**, 1-4.
3. Arinaminpathy, Y.; Khurana, E.; Engelman, D.M.; Gerstein, M.B. *Drug. Discov. Today*. **2009**, 14, 1130-1135.
4. Hotze, E.M.; Tweten, R.K. *Biochim, Biophys. Acta*. **2012**, 1818, 1028-1038.
5. Hotze, E.M.; Le, H.M.; Sieber, J.R.; Bruxvoort, C.; McInerney, M.J.; Tweten, R.K. *Infect. Immun.* **2013**, 81, 216-225.
6. te Welscher, Y.M.; ten Napel, H.H.; Balagué, M.M.; Souza, C.M.; Riezman, H.; de Kruijff, B.; Breukink, E. *J. Biol. Chem.* **2008**, 283, 6393-6401.
7. Brogden, K.A. *Nat. Rev. Microbiol.* **2005**, 3, 238-250.
8. Wimley, W.C. *ACS Chem. Biol.* **2010**, 5, 905-917.
9. Kawasaki, Y.; Freire, E. *Drug Discov. Today.* **2011**, 16, 985-990.
10. Shaw, A.T.; Winslow, M.M.; Magendantz, M.; Ouyang, C.; Dowdle, J.; Subramanian, A.; Lewis, T.A.; Maglathin, R.L.; Tolliday, N.; Jacks, T. *Proc. Natl. Acad. Sci. USA.* **2011**, 108, 8773-8778.
11. Mouritsen, O.G.; Zuckermann, M.J. *Lipids.* **2004**, 39, 1101-1113.
12. Umegawa, Y.; Nakagawa, Y.; Tahara, K.; Tsuchikawa, H.; Matsumori, N.; Oishi, T.; Murata, M. *Biochemistry.* **2012**, 51, 83-89.
13. Laniado-Laborín, R.; Cabrales-Vargas, M.N. *Rev. Iberoam. Micol.* **2009**, 26, 223-227.
14. Papo, N.; Shai, Y. *Peptides.* **2003**, 24, 1693-1703.
15. Shai, Y. *Biopolymers.* **2002**, 66, 236-248.
16. Strömstedt, A.A.; Ringstad, L.; Schmidtchen, A.; Malmsten, M. *Curr. Opin. Colloid Interface Sci.* **2010**, 15, 467-478.
17. Teixeira, V.; Feio, M.J.; Bastos, M. *Prog. Lipid Res.* **2012**, 51, 149-177.
18. Schweizer, F. *Eur. J. Pharmacol.* **2009**, 625, 190-194.
19. Breukink, E.; de Kruijff, B. *Nat. Rev. Drug. Discov.* **2006**, 5, 321-323.
20. Houdai, T.; Matsuoka, S.; Matsumori, N.; Murata, M. *Biochim. Biophys. Acta.* **2004**, 1667, 91-100.
21. Anderluh, G.; Dalla Serra, M.; Viero, G.; Guella, G.; Maček, P.; Menestrina, G. *J. Biol. Chem.* **2003**, 278, 45216-45223.
22. Álvarez, C.; Mancheño, J.M.; Martínez, D.; Tejuca, M.; Pazos, F.; Lanio, M.E. *Toxicon.* **2009**, 54, 1135-1147.
23. Davis, R.W.; Patrick, E.L.; Meyer, L.A.; Ortiz, T.P.; Marshall, J.A.; Keller, D.J.; Brozik, S.M.; Brozik, J.A. *J. Phys. Chem. B.* **2004**, 108, 15364-15369..

24. Pokorny, A.; Almeida, P.F.F. *Biochemistry.* **2004**, 43, 8846-8857.
25. Pokorny, A.; Almeida, P.F.F. *Biochemistry.* **2005**, 44, 9538-9544.
26. Epand, R.F.; Maloy, W.L.; Ramamoorthy, A.; Epand, R.M. *Biochemistry.* **2010**, 49, 4076-4084.
27. Epand, R.M.; Epand, R.F. *Mol. BioSyst.* **2009**, 5, 580-587.
28. Zhao, H.; Sood, R.; Jutila, A.; Bose, S.; Fimland, G.; Nissen-Meyer, J.; Kinnunen, P.K.J. *Biochim. Biophys. Acta.* **2006**, 1758, 1461-1474.
29. Zhao, H.; Tuominen, E.K.J.; Kinnunen, P.K.J. *Biochemistry.* **2004**, 43, 10302-10307.
30. Mozsolits, H.; Aguilar, M. *Biopolymers.* **2002**, 66, 3-18.
31. Seldon, A.M.; Casey, D.; Law, R.V.; Gee, A.; Templer, R.H.; Ces, O. *Chem. Soc. Rev.* **2009**, 38, 2509-2519.
32. Hall, D. *Anal. Biochem.* **2001**, 288, 109-125.
33. Nussio, M.R.; Sykes, M.J.; Miners, J.O.; Shapter, J.G. *Chem. Med. Chem.* **2007**, 2, 366-373.
34. Papo, N.; Shai, Y. *Biochemistry*. **2003**, 42, 458-466.
35. Hall, K.; Mozsolits, H.; Aguilar, M. *Lett. Pept. Sci.* **2003**, 10, 475-485.
36. Mouri, R.; Konoki, K.; Matsumori, N.; Oishi, T.; Murata, M. *Biochemistry.* **2008**, 47, 7807-7815.
37. Strandberg, E.; Ulrich, A.S. *Concepts. Magn. Reson. A.* **2004**, 23, 89-120.
38. Matsumori, N.; Tahara, K.; Yamamoto, H.; Morooka, A.; Doi, M.; Oishi, T.; Murata, M. *J. Am. Chem. Soc.* **2009**, 131, 11855-11860.
39. Haney, E.F.; Nathoo, S.; Vogel, H.J.; Prenner, E.J. *Chem. Phys. Lipids.* **2010**, 163, 82-93.
40. Mecke, A.; Lee, D.K.; Ramamoorthy, A.; Orr, B.G.; Banaszak Holl, M.M. *Biophys. J.* **2005**, 89, 4043-4050.
41. Arouri, A.; Kiessling, V.; Tamm, L.; Dathe, M.; Blume, A. *J. Phys. Chem. B.* **2011**, 115, 158-167.
42. Bechinger, B.; Salnikov, E.S. *Chem. Phys. Lipids.* **2012**, 165, 282-301.
43. Bagatolli, L.A. Membranes and Fluorescence Microscopy. In *Reviews in Fluorescence*; Geddes, C.D., Ed.; Springer: New York, 2009; Vol. 2007; p 33-51.
44. Wesołowska, O.; Michalak, K.; Maniewska, J.; Hendrich, A.B. *Acta Biochim. Pol.* **2009**, 56, 33-39.
45. Rossjohn, J.; Feil, S.C.; McKinstry, W.J.; Tweten, R.K.; Parker, M.W. *Cell.* **1997**, 89, 685-692.
46. Oren, Z.; Shai, Y. *Biopolymers.* **1998**, 47, 451-463.

47. Huang, H.W. *Phys. Rev. Lett.* **2004**, 92, 198304-1 – 198304-4.
48. Sengupta, D.; Leontiadou, H.; Mark, A.E.; Marrink, S.J. *Biochim. Biophys. Acta*. **2008**, 1778, 2308-2317.

Chapter 2

Interaction between Theonellamide A and Sterols in Lipid Bilayer Membranes

2.1 Introduction – Bioactive Compounds from the Marine Sponge of the Genus *Theonella*

2.1.1 Marine Sponge-Derived Natural Products

Marine sponges are multicellular, filter-feeding, and sessile organisms belonging to the phylum *Porifera* (Latin: "pore-bearer) whose porous bodies facilitate the passage of water through them. These benthic animals are among the most ancient multicellular organisms having first appeared in the world's waters about 700 million years ago, and their simple body structure, which have served them well throughout their existence, have largely remained unchanged.[1,2] Most of the roughly 15,000 sponge species live in polar, tropical, and temperate marine environments, however, a small population of about 1% can be found in freshwater regions.

Perhaps the most remarkable attribute of marine sponges is their ability to house an extremely dense and diverse microbial community that includes prokaryotes, including cyanobacteria, archaea, and unicellular eukaryotes, which are most commonly found in the sponge's mesohyl tissue (Figure 2-1).[2] These microbial clusters can account for as much as 35% of the animal's biomass and is present in densities beyond 10^9 microbial cells per cubic centimeter of sponge tissue, which is 3-4 orders of magnitude greater than that found in the surrounding water.[2]

Marine sponges are a rich source of natural products, largely because of their inclination to produce various structurally unique bioactive secondary metabolites.[3] It is believed that, in some case, these bioactive compounds are actually produced, not by the sponge themselves, but by the diverse and dense microbial community they host,[4] examples of which are shown in Table 2-1.

Sponges produce these various compounds and toxins to serve a multitude of functions necessary for their survival that includes deterrent for predators, to compete for space with other sessile organisms, communication, and for protection against infection.[1]

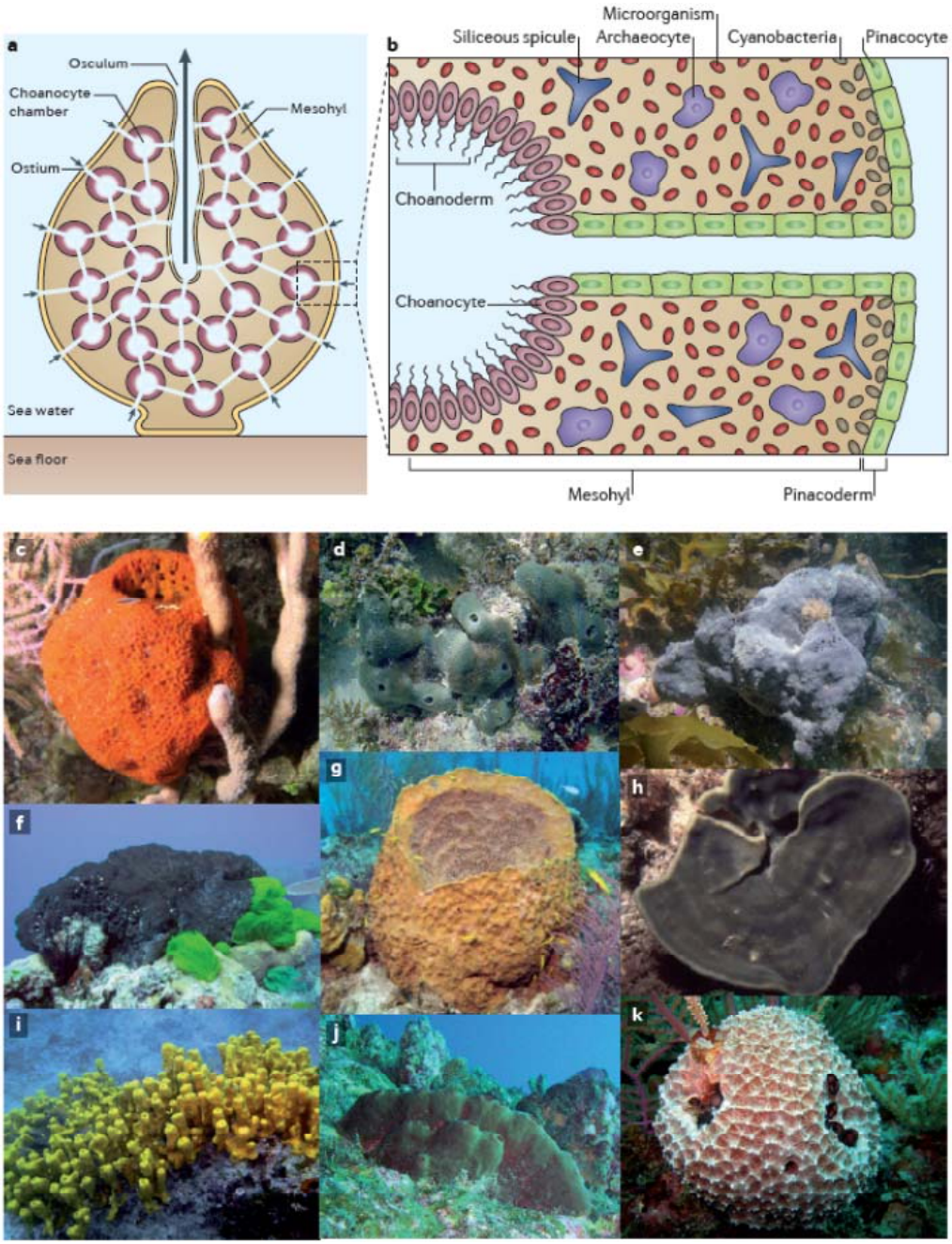

Figure 2-1. Representation and images of sponge. (a) schematic representation of a typical sponge body, (b) enlargement of the sponge internal structure, (c) *Mycale laxissima*, (d) *Amphimedon queenslandica*,[56] (e) *Ancorina alata*,[57] (f) *Rhopaloeides odorabile*,[57] (g) *Xestospongia muta*, (h) *Cymbastela concentric*, (i) *Aplysina aerophoba*,[57] (j) *Theonella swinhoei*, and (k) *Ircinia felix*. Reprinted with permission from *Nat. Rev. Microbiol.*, **2012**, 10, 641-654., and *Environ. Microbiol.*, **2012**, 14, 335-346. [2,57] Copyright © (2012) Macmillan Publishers Ltd., and (2011) Society for Applied Microbiology and Blackwell Publishing Ltd.

Table 2-1. Some natural products suspected or known to be produced by sponge symbionts.[5-9]

Natural Product	Suspected Bacterial Source	Host Sponge
Brominated Biphenyl ethers	*Oscillatoria spongeliae*	*Lamellodysidea spp.*
Chlorinated peptides	*O. spongeliae*	*Lamellodysidea spp.*
Theopalauamide	*Candidatus Entotheonella palauensis*	*Theonella swinhoei*
Swinholide A	Unicellular bacterium	*T. swinhoei*
Onnamide A	Unidentified bacterium	*T. swinhoei*
Psymberin	Unidentified bacterium	*Psammocinia bulbosa*

The prevalence of these varied bioactive compounds offer promising potential for biotechnological and therapeutic purposes. Precandidaspongiolide A and candidaspongiolide A are potent (nM) and selective melanoma inhibitors isolated from a Papua New Guinean *Candidaspongia* sp.[10] Kabiramide J and K are potent antimalarials isolated from *Pachatrissa nux*[11] as well as psammaplysin H obtained from *Pseudoceratina* sp.[12] Sorbicillactone A, an antileukemic compound, was isolated from a symbiont of *Ircinia fasiculata.*[13] The antioxidant meroterpenoid hydroquinone halioxepine was isolated from *Haliclona* sp.[14] Hippolide A from *Hippospongia lachne* is an inhibitor of protein tyrosine phosphatase 1B activity.[15] The cytotoxic peptides callyaerins E[16] and discodermins A-H were isolated from *Callyspongia aerizusa* and *Discodermia kiiensis* respectively,[17,18] while the cytotoxic sphingosine derivatives jaspines A and B from *Jaspis* sp.[19]

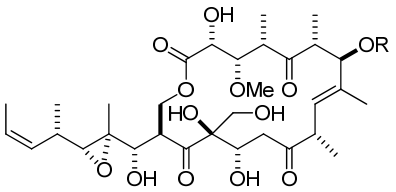

Precandidaspongiolide A: R = H
Candidaspongiolide A: R = Ac

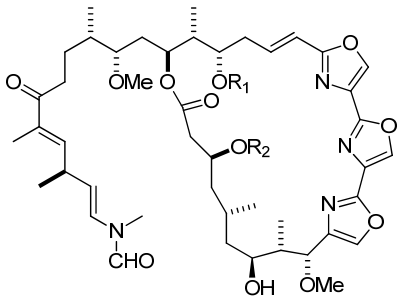

Kabiramide J: R_1 = H R_2 = $CONH_2$
Kabiramide K: R_1 = Me R_2 = H

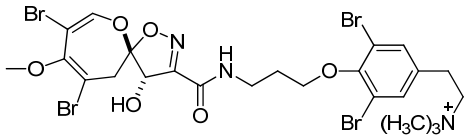

Psammaplysin H

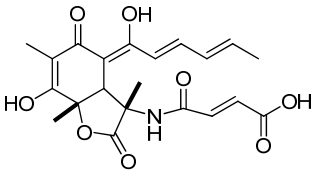

Sorbicillactone A

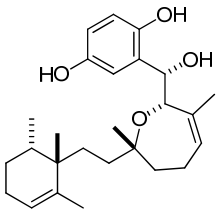

Halioxcepine

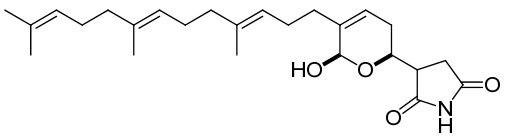

Hippolide A

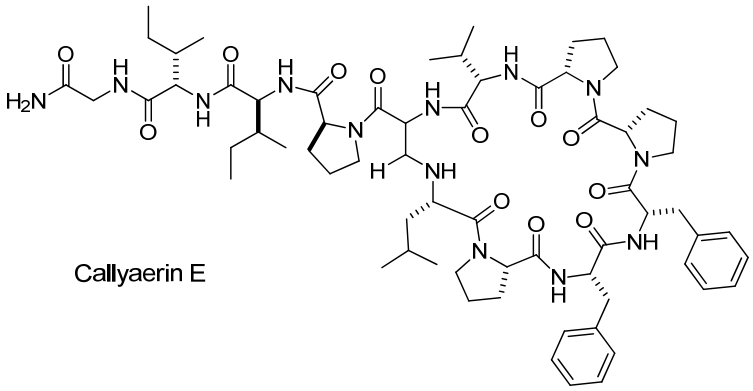

Callyaerin E

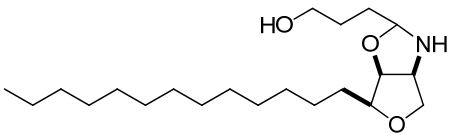

Jaspine A

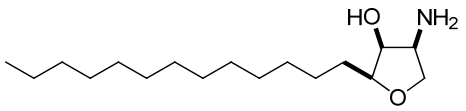

Jaspine B

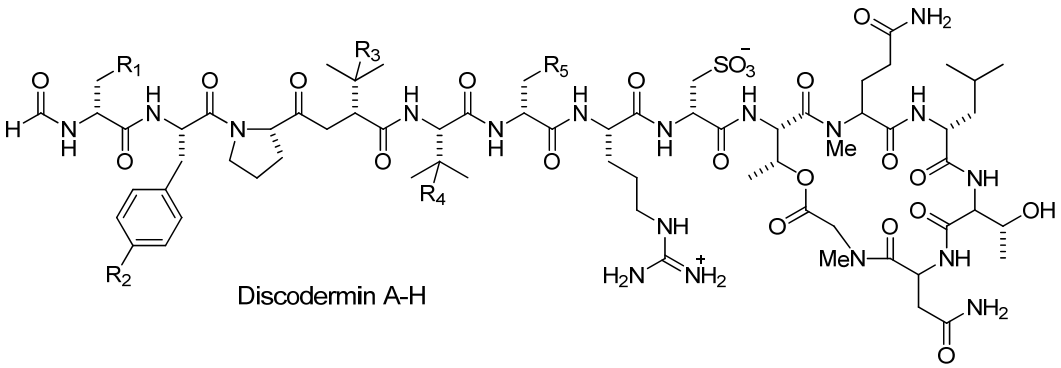

Discodermin A-H

A: R_1=R_2=H, R_3=R_4=Me, R_5=X
B: R_1=R_2=R_3=H, R_4=Me, R_5=X
C: R_1=R_2=R_4=H, R_3=Me, R_5=X
D: R_1=R_2=R_3=R_4=H, R_5=X
E: R_1=R_2=H, R_3=R_4=Me, R_5=Y
F: R_1=R_2=H, R_3=Me, R_4=Et, R_5=X
G: R_1=R_3=R4=Me, R_2=H, R_5=X
H: R_1=H, R_2=OH, R_3=R_4=Me, R_5=X

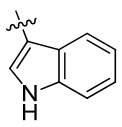

X

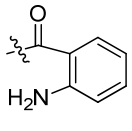

Y

2.1.2 Bioactive Compounds from Sponge of the Genus *Theonella*

The marine sponge *Theonella swinhoei* (Lithistida, Theonellidae) has attracted considerable attention over the past few decades due to its prolific production of diverse natural products with intriguing structures as well as potent biological activities, some of which may have promising therapeutic potential.[20] Among the first compounds reported from this species are the rare 4-methylene-substituted sterols theonellasterol and conicasterol, which up to that time, has never been reported from either marine or terrestrial sources,[21] and the symmetric 44-member macrolide swinholide A.[22] Theonellasterol, together with ten new related polyhydroxy steroids theonellasterol B-H and conicasterol B-D, were recently demonstrated to be selective antagonists of the farnesoid-X-receptor and agonists of the pregnane-X-receptor, widely expressed in mammalian livers, which could make them a promising lead for treating liver diseases such as cholestasis and cirrhosis.[23,24] Meanwhile, swinholide A, which has also been established to be produced by sponge-associated microbes, exhibits potent antifungal and cytotoxic activities against certain cancer cell lines.[25] Moreover, its mechanism of action has been investigated in detail and revealed to involve the

dimerization of actin as well as disruption of the actin cytoskeleton.[26,27] This remarkable characteristic allows it to be used extensively in cell biology studies.[28]

Natural products isolated from worldwide collections of *Theonella swinhoei* can be classified into approximately 9 biosynthetic categories that include sesquiterpenes, polyketides, alkaloids, linear and cyclic peptides, theopedrin derivaties, and glycopeptides and glycosides.[20] Among these, however, peptides represent the most notable group.[29] Solomonamide A is an unprecendented cyclic tetrapeptide isolated recently which showed anti-inflammatory activity (60% edema reduction in mice at a dose of 100μg/kg body weight) in *in vivo* assay;[29] the same species has also previously yielded two new anti-inflammatory cyclic octapeptides, perthamides C and D.[30] *Theonella* species collected from deeper waters revealed the co-occurrence of three different families of peptides, the combination of which appears to define a new *Theonella* chemotype.[31] Interestingly, in this suite of compounds, the cyclic *N*-methylated peptides koshikamides F and H inhibited an HIV entry in a HIV-1 infectivity assay with the IC_{50} values of 2.3 and 5.5 μM, respectively.[31] Their linear counterparts, on the other hand, were inactive suggesting the importance of the exocyclic olefin and its associated conformation as well as the ten-membered lactone ring in the anti-HIV activity of these peptides.[31] Perhaps one of the most extraordinary compound obtained from this species is the linear polypeptide polytheonamide B (pTB) isolated from a sponge collected in Japan.[32] This compound is composed of 48 amino acid residues that includes 13 non-proteinogenic residues which is capped with 5,5-dimethyl-2-oxohexanoate at the *N*-terminus and is by far the largest non-ribosomal peptide known to date. A very intriguing structural feature of pTB is that the entire sequence is made up of alternating D- and L- amino acids that adopts a β-helix structure with 6.3 residues per turn (determined with NMR in methanol/chloroform) with a length of approximately 45 Å and a hydrophilic pore with a 4 Å inner diameter.[33,34] Experiments with planar lipid bilayers demonstrated that the peptide inserts into the bilayer forming channels that showed selectivity towards monovalent cations.[35] pTB is an extremely cytotoxic peptide with the IC_{50} value of 70-80 pg/mL in the MTT assay (in contrast, doxorubicin exhibited an IC_{50} value of 40-90 ng/mL), $IC_{50} < 4$ ng/mL, and $IC_{50} < 1$ ng/mL against P388 murine leukemia cells, L1210 murine lymphocytic leukemia cells, and Neuro-2a mouse neuroblastoma cells, respectively.[34] The total synthesis of pTB has been reported recently.[36]

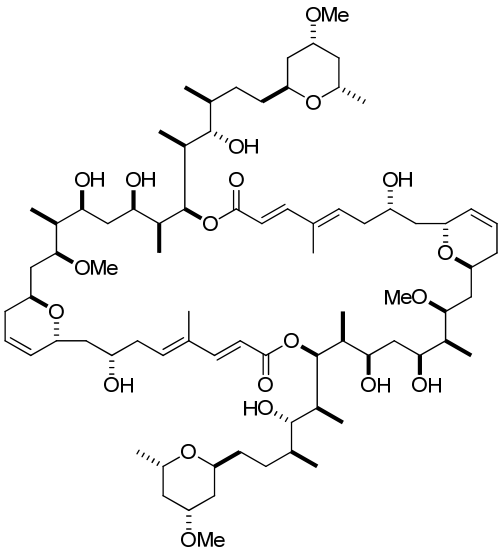

Swinholide A

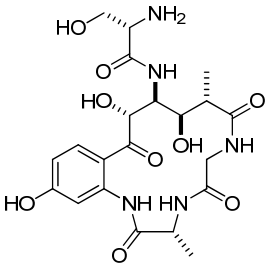

Solomonamide A

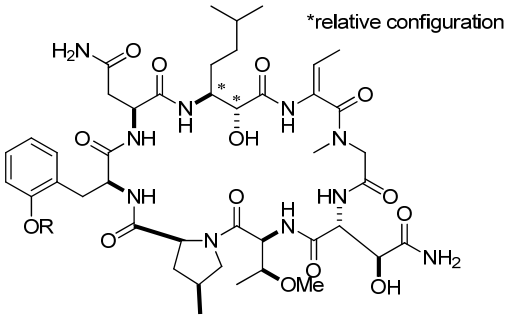

*relative configuration

	R
Perthamide C	OH
Perthamide D	H

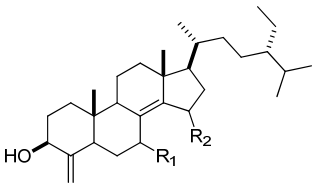

	$R_1 = R_2$
Theonellasterol	H
Theonellasterol F	OH

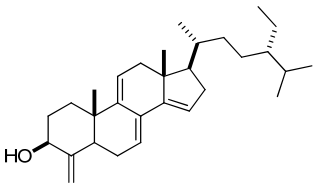

Theonellasterol B

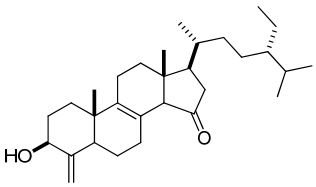

Theonellasterol C

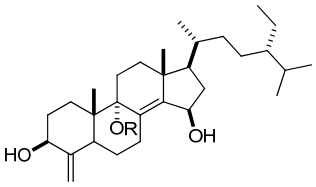

	R
Theonellasterol D	OMe
Theonellasterol E	OH

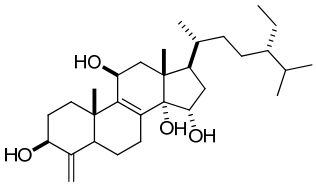

Theonellasterol G

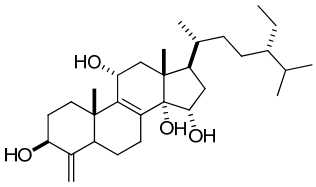

Theonellasterol H

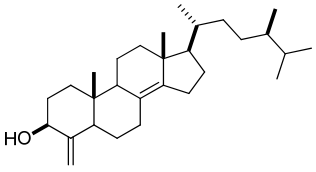

Conicasterol

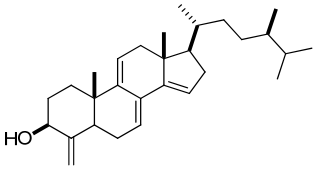

Conicasterol B

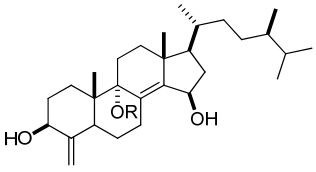

	R
Conicasterol C	OMe
Conicasterol D	OH

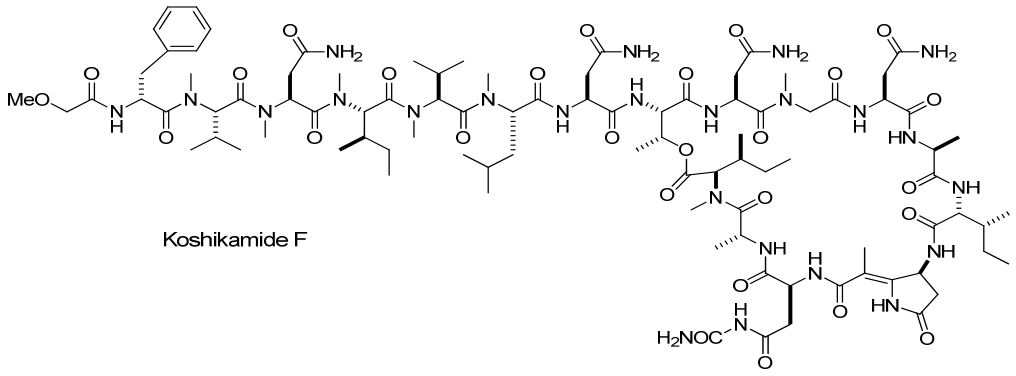

Koshikamide F

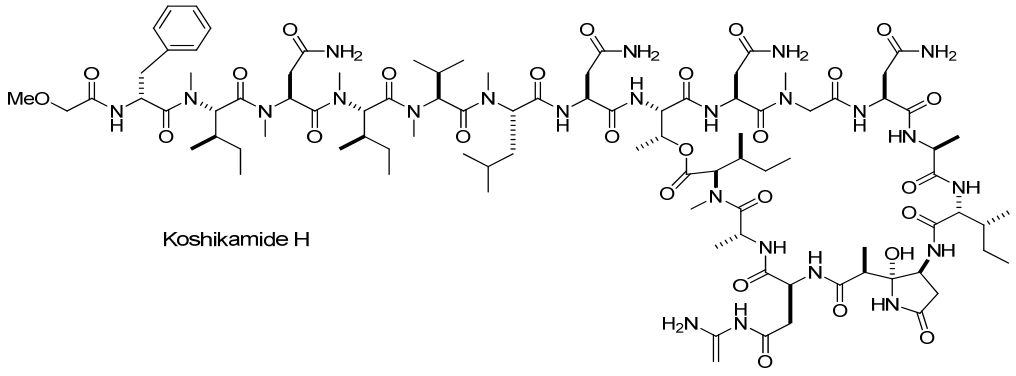

Koshikamide H

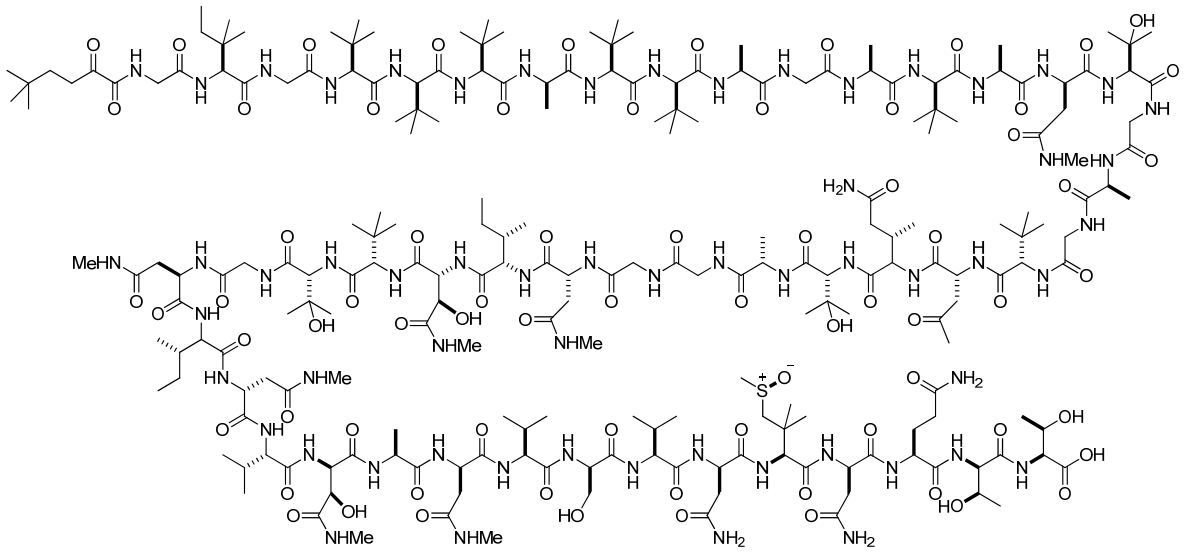

Polytheonamide B

2.1.3 Theonellamides and its Congeners

Investigation on bioactive compounds from *Theonella swinhoei* collected off Hachijo-jima Island in Japan, led to isolation of the first member of this family in 1989 by Matsunaga et. al., which they named theonellamide F.[37] Theonellamide F is a bicyclic dodecapeptide which contains some unusual amino acids and is bridged by an unprecedented histidinoalanine moeity : L-Asn, L-aThr, two residues of L-Ser, L-Phe, βAla, (2S,3R)-3-hydroxyasparagine, (2S,4R)-2-amino-4-hydroxyadipic acid, τ-L-histidino-D-alanine, L-*p*-bromophenylalanine, and (3S,4S,5E,7E)-3-amino-4-hydroxy-6-methyl-8-(*p*-bromophenyl)-5,7-octadienoic acid. Further characterization of the antifungal fraction from the same sponge extracts afforded five related peptides, theonellamides (TNMs) A-E.[38] TNM-A and TNM-B differ in three amino acid residues from TNM-F. Furthermore, TNM-A has a sugar residue, β-D-galactose, attached to the free imidazole nitrogen. Meanwhile, TNM-C is the debromo of TNM-F. Finally TNM-D and TNM-E have the same structure and composition as TNM-F except that they have a β-L-arabinose and β-D-galactose, respectively, attached to the free imidazole nitrogen. TNM-A and TNM-F appears to be the most abundant compounds.

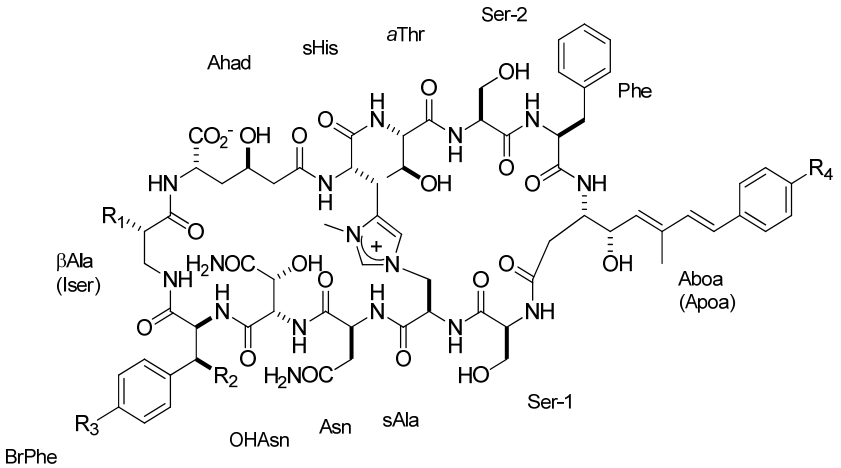

	R_1	R_2	R_3	R_4
Theonellamide F	H	H	Br	Br
Theonellamide B	OH	Me	Br	H
Theonellamide C	H	H	H	Br

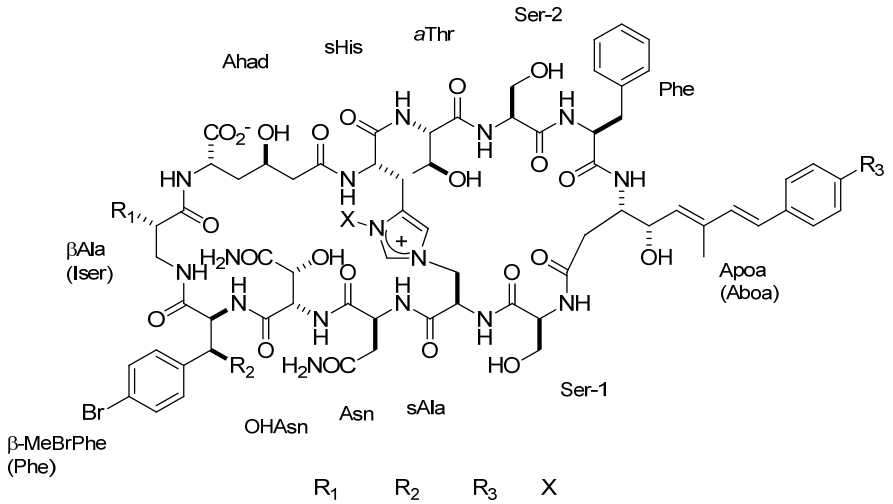

	R_1	R_2	R_3	X
Theonellamide A	OH	Me	H	β-D-Gal
Theonellamide D	H	H	Br	β-L-Ara
Theonellamide E	H	H	Br	β-D-Gal

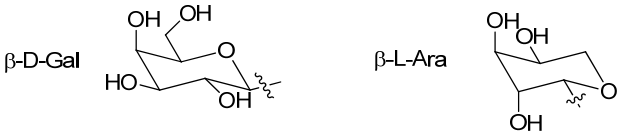

Apoa = (5E,7E)-3-amino-4-hydroxy-6-methyl-8-phenyl-5,7-octadienoic acid
Aboa = (5E,7E)-3-amino-4-hydroxy-6-methyl-8-(p-bromophenyl)-5,7-octadienoic acid
aAla = alanine portion of histidinoalanine
OHAsn = β-hydroxyasparagine
β-MeBrPhe = β-methyl-*p*-bromophenylalanine
BrPhe = *p*-bromophenylalanine
Iser = isoserine
Ahad = α-amino-γ-hydroxyadipic acid
sHis = histidine portion of histidinoalanine
*a*Thr = *allo*-threonine

Very few closely related analogs of theonellamides have been reported. Theonegramide was isolated from a similar sponge species collected off Negros Island, the Philippines and elucidation of its structure and sequence revealed very close similarity to TNM-A except that the hydroxyl group in the Ahad residue as well the sugar in TNM-A were replaced by a hydrogen and an arabinose, respectively, in theonegramide.[39] Meanwhile, theopalauamide and isotheopalauamide were also isolated from same sponge species, but collected off Palau.[40] The latter two peptides were identical to theonegramide but they contained a galactose sugar instead of arabinose. The minor peptide, isotheopalauamide, was established to be a stable conformer formed from TFA-catalyzed equilibration in the isolation process. All of these three congeners showed growth inhibition activity against *Candida albicans* in the standard paper disk assay.

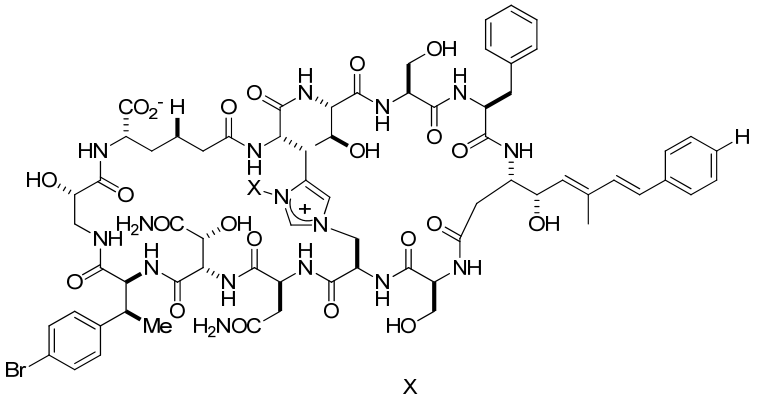

	X
Theonegramide	β-D-Ara
Theopalauamide (1)	β-D-Gal
Isotheopalauamide (2)	β-D-Gal

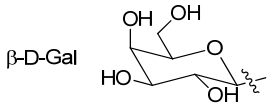

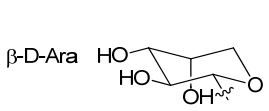

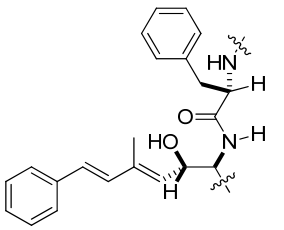

1

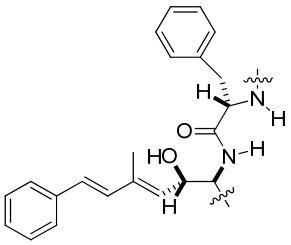

2

2.1.4 Biological Evaluation of Theonellamides

Theonellamide-F (TNM-F) was isolated as a major antifungal metabolite from a bioactive fraction of extracts from the sponge *Theonella swinhoei*.[37] This peptide inhibited the growth of various pathogenic fungi, e.g. *Candida* spp., *Trichophyton* spp., and *Aspergillus* spp., at low concentrations of 3-12 μg/mL. Further characterization of the antifungal extracts afforded other bioactive compounds, TNM-A to E. Some of these later peptides contain a sugar moiety attached to the histidinoalanine bridge making them ideal analogs to determine the effect of such substitution on the peptide's activity. Interestingly, however, it appears that the sugar residue does not play a significant role in their bioactivity as evidenced by their cytotoxic potencies against P388 murine leukemia cells summarized in Table 2-2.[37,38]

It has previously been reported that TNM-F induces the formation of extraordinarily large vacuoles in 3Y1 rat fibroblasts, and that such vacuoles accumulated granules exhibiting

Brownian motion that also appeared to be organelle-like in size.[41] From this observation, it is postulated that TNM-F may affect cellular autophagy and inhibits organelle degradation as well as the breakdown of the cells' own proteins. Furthermore, treatment of the cells with TNM-F did not have any pronounced effect on either cellular morphology or cell viability. Monensin, on the other hand, altered morphology and was lethal to cells, thus TNM-F can be a useful probe to study intracellular membrane structures.[41] A more detailed investigation of this extraordinarily large vacuoles showed that they were acidic,[42] based on colocalization with an acidotropic dye, and inhibition of this process and disappearance of vacuoles upon treatment with bafilomycin A suggested that these vacuoles contained V-ATPase that maintained cellular acidity similar to those induced by the *H. pylori* toxin VacA. Unlike VacA that required the integrity of microtubules and the function of the GTPase rab7 for vacuolar formation, TNM-F action was hardly affected by tubulin-depolymerzing agents and rab7 appears to be important only in certain types of vacuoles and processes. Evidence of this mechanism indicated vacuolar formation of these two compounds were different.[42] In addition, by using TNM-A-conjugated gel beads, glutamate dehydrogenase and 17β-hydroxysteroid dehydrogenase IV were identified as its binding proteins from rabbit liver tissues, and *in vitro* assays revealed that TNM-F activates glutamate dehydrogenase leading to the amination of α-ketoglutarate, although its potency is lower than the known activator adenosine diphosphate.[43]

Table 2-2. Reported cytotoxicties of TNMs.[37,38]

	IC_{50}(μg/mL)
TNM-A	5
TNM-B	1.7
TNM-C	2.5
TNM-D	1.7
TNM-E	0.9
TNM-F	2.7

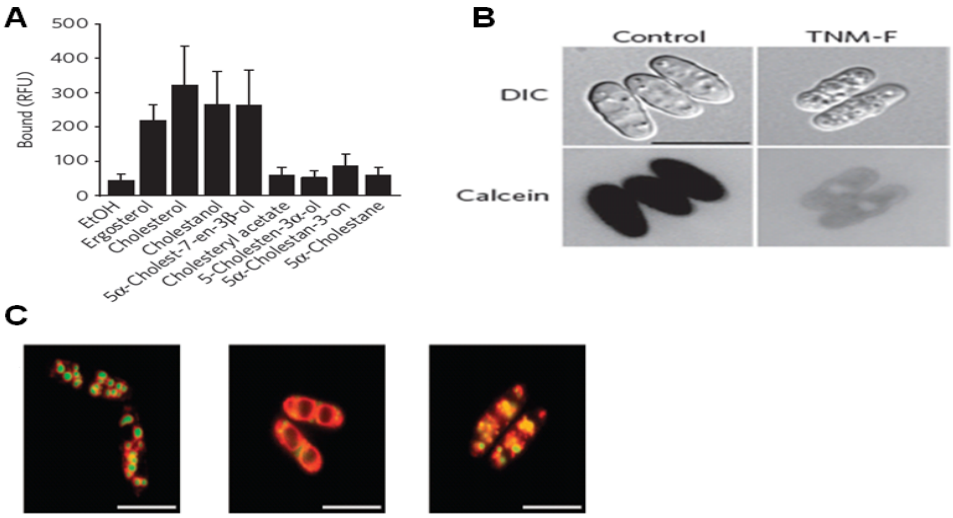

Figure 2-2. Sterol binding and disruption of plasma membrane integrity by TNM-F. (A) Binding of TNM-F to 3β-hydroxysterols, *in vitro*. (B) Passive entry of calcein into TNM-F treated yeast cells. (C) Changes in yeast vacuolar morphology upon treatment with DMSO (left), amphotericin B (middle), and TNM-F (right). Reprinted with permission from *Nat. Chem. Biol.*, **2010**, 6, 519-526.[44] Copyright © (2010) Macmillan Publishers Ltd.

Recently, a series of systematic experiments have provided substantial insights into the mode of action of TNMs and the structurally related theopalauamide.[44,45] Budding yeast genomics, using a collection of molecular barcoded ORF libraries, revealed that theopalauamide is less effective toward mutated cells in the ergosterol biosynthesis pathway.[45] Indeed, theopalauamide permeabilizes liposomes containing ergosterol.[45] Chemical genomic analysis using a fission yeast ORF collection suggested a mechanistic link between TNMs and 1,3-β-D-glucan synthesis, and an overproduction of 1-3-β-D-glucan was observed following the treatment of yeast cells with TNM-F in a Rho1-dependent manner.[44] Furthermore, *in vitro* binding assays, using a fluorescent-labeled TNM derivative, demonstrated that it specifically binds to 3β-hydroxysterols such as cholesterol and ergosterol (Figure 2-2A).[44] The sterol binding is required for the TNM-induced 1-3-β-D-glucan synthesis and subsequent loss of membrane integrity (Figure 2-2B). Judging from the phenotypic changes in yeasts, the membrane action of TNM-F is apparently distinct from that of polyene antifungals such as amphotericin B, which is also known to bind sterols in membranes; e.g., TNM-F caused fragmentation (Figure 2-2C), instead of enlargement, of vacuoles, and exhibited a time-dependent toxicity, as opposed to amphotericin B, which had acute fungicidal activity. Thus, TNMs represent a novel class of sterol-binding compounds whose mode of action is different from that of polyene antibiotics, and therefore are expected to be a new tool for exploring the function and localization of sterols in cells.

2.1.5 Objectives of this Study on the Mode of Action of Theonellamide A

Despite the findings described above, the precise mode by which TNMs recognize sterols in membranes is still unclear. Therefore, a detailed analysis of the bimolecular interaction between TNMs and sterols is indispensable in understanding the mode of action of this class of compounds. To this end, the nature of the binding interaction between TNM-A and POPC liposomes containing cholesterol, ergosterol, or epicholesterol (Figure 2-3), as well as its binding kinetics, was investigated by carrying out SPR measurements. Then, the presence or absence of direct intermolecular interaction between TNM-A and membrane-embedded sterols, which could affect the peptide's binding to the bilayer, was scrutinized with solid state ^{2}H NMR using deuterium-labeled sterols (Figure 2-3). Moreover, to possibly account for the observed biological action of TNM-A, the effects of TNM-A addition to POPC membranes, with or without sterols, were explored with a variety of methods including calcein leakage assay, solid state ^{31}P NMR, and microscopy observations. From the results obtained in these work, a probable mechanism of TNM-A membrane action was proposed.

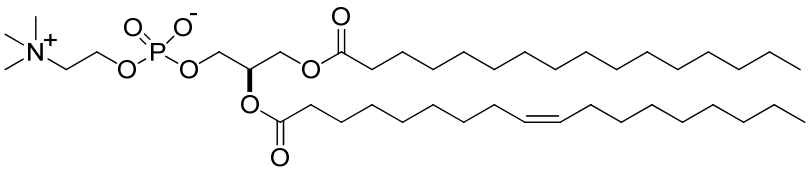

1-palmitoyl-2-oleoyl-*sn*-glycero-3-phosphocholine (POPC)

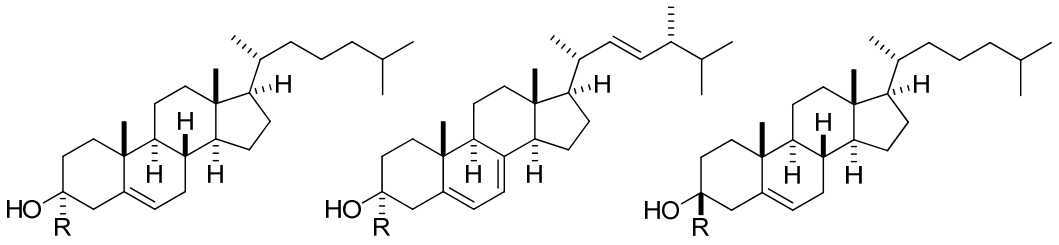

Cholesterol : R = H
3-*d*-Cholesterol : R = D

Ergosterol : R = H
3-*d*-Ergosterol : R = D

Epicholesterol : R = H
3-*d*-Epicholesterol : R = D

Figure 2-3. Structures of lipids used in this study.

2.2 Results and Discussion

2.2.1 Binding of TNM-A to POPC Liposomes Measured by SPR

Several important biological processes begin at the membrane surface by the interaction of certain membrane components with bioactive molecules. Surface plasmon resonance (SPR) has been extensively used in assessing the interaction between bioactive compounds and artificial membranes,[46-50] mainly because it allows for a real-time observation of the binding interaction as well as an evaluation of the binding kinetics, among its other features. Recently, by devising a new SPR method that minimizes non-specific interaction between the analyte and dextran matrix on the sensor surface, a more accurate evaluation of the binding interaction between amphotericin B and POPC membranes was achieved.[51] This same dodecylamine-modified sensor chip was used to examine in more detail the interaction between TNM-A and membranes.

2.2.2 Sensor Chip Modification and Binding Interaction

A dodecylamine-modified CM5 sensor chip (Figure 2-4) was utilized to evaluate the interaction of TNM-A with POPC/sterol (10 mol %) and pure POPC liposomes as was previously reported for amphotericin B.[51] One of two flow cells was modified while the other

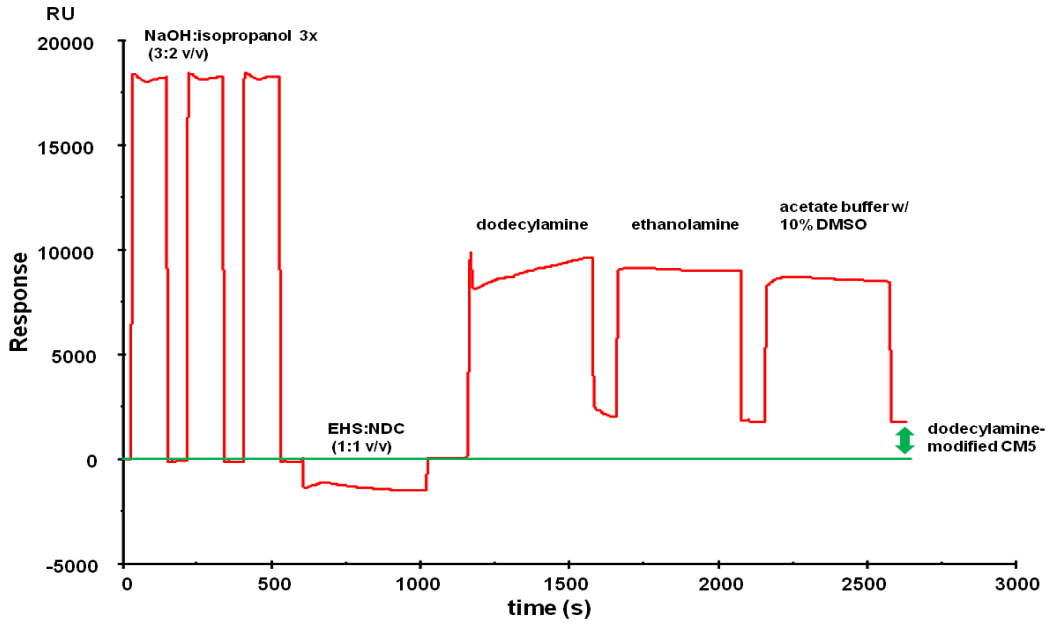

Figure 2-4. Sensorgram of dodecylamine modification of one of CM5 sensor chip's flow cells.

was left intact, serving as the reference cell. A schematic representation of a typical SPR experiment is shown in Figure 2-5. The liposomes, at a concentration of 0.5 mM, were captured by the modified lane with an immobilization level of around 12700 ± 800 RU, which

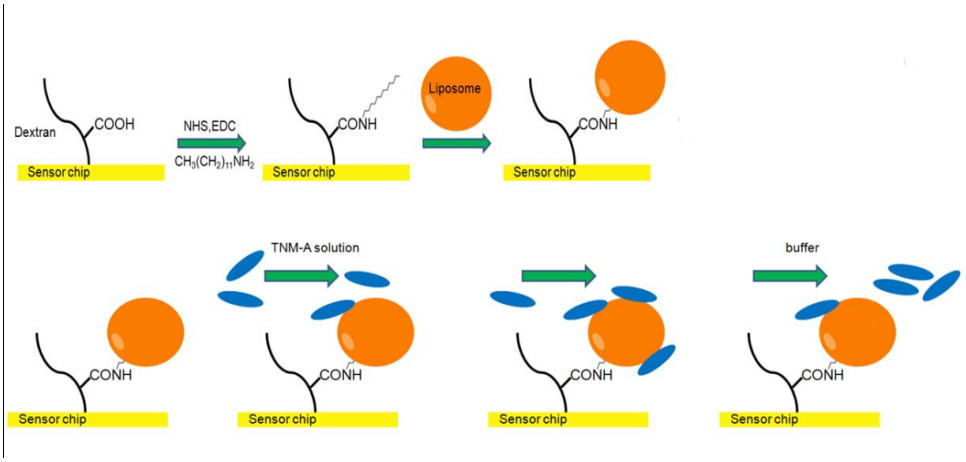

Figure 2-5. Schematic representation of a typical SPR experiment.

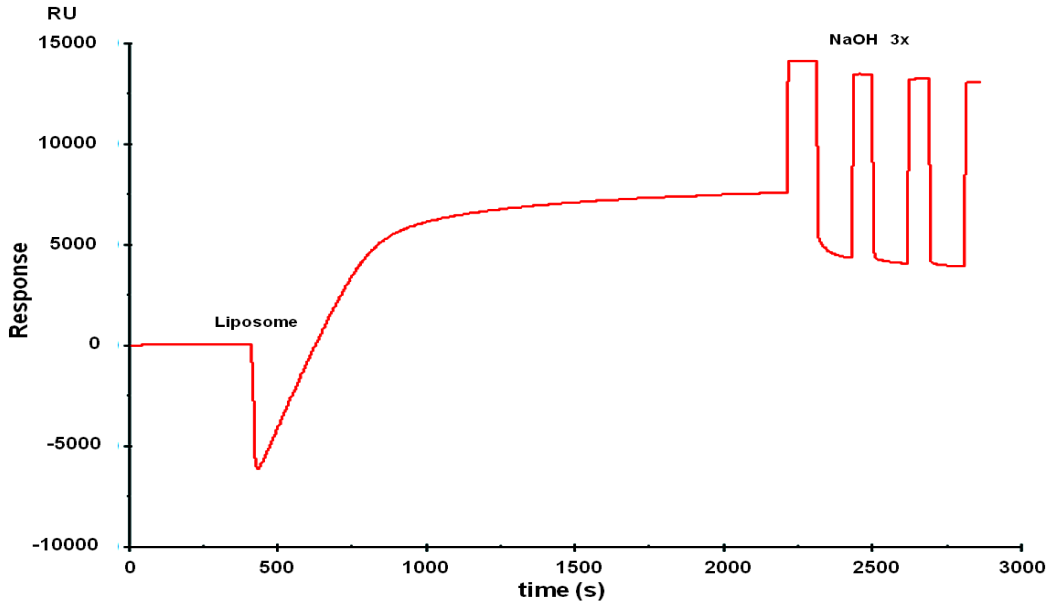

Figure 2-6. Representative sensorgram of POPC:cholesterol liposome immobilization on a dodecylamine-modified sensor surface. A drop in response upon liposome injection is due to the difference in the running buffer (PBS with 5% DMSO) and liposome buffer (PBS).

was stable even after repetitive washing with NaOH (50 mM); a representative sensorgram of liposome capture is shown in Figure 2-6. For kinetic analysis, TNM-A, at various concentrations, was injected and response from the control lane was subtracted from that in the liposome-immobilized lane.

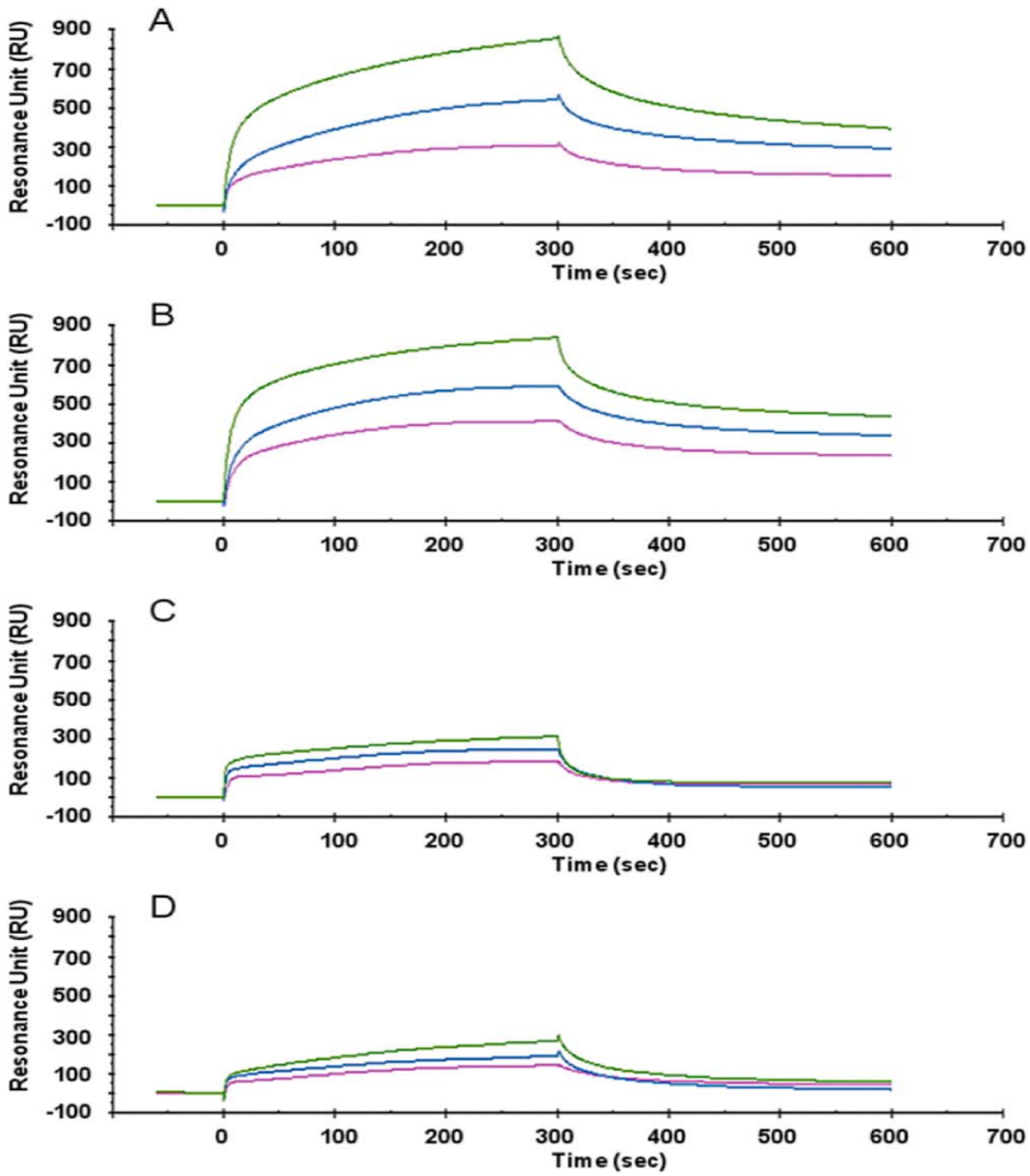

Figure 2-7. SPR sensorgrams for binding of TNM-A to liposomes captured on a dodecylamine-modified CM5 sensor chip: (A) 10 mol % cholesterol-containing POPC liposomes, (B) 10 mol % ergosterol-containing POPC liposomes, (C) 10 mol % epicholesterol-containing POPC liposome, and (D) pure POPC liposomes. Sensorgrams correspond to 20 (green), 15 (blue), and 10 (violet) μM TNM-A.

Figure 2-7 shows typical sensorgrams representing the binding of TNM-A to various POPC liposomes. Interaction of the peptide with the membranes showed clear concentration dependence, regardless of the presence or absence of sterol, indicating that the amount of membrane-bound peptide is directly proportional to the peptide concentration in the bulk solution. Moreover, as evidenced by the RU increase, the presence of cholesterol and ergosterol significantly enhanced the binding of the peptide to POPC liposomes by approximately 3-fold compared with that of pure POPC liposomes, while the binding of the peptide to epicholesterol (3α-cholesterol)-containing liposomes was comparable to that of pure POPC liposomes. These observations clearly demonstrate the preference of the peptide for 3β-hydroxysterols, which is consistent with the previous findings obtained with fluorescently labeled TNM.[44]

2.2.3 Kinetic Evaluation of TNM-A Binding

The kinetics of binding of TNM-A to lipid membranes was analyzed by fitting the experimental curves to those calculated from a theoretical model. On the basis of the possible mechanism of action of antimicrobial and membrane-active peptides,[46,49] the sensorgrams could be fitted to the two-state reaction model (Figure 2-8). This model assumes that the interaction between the peptide and membrane lipids occurs via a two-step process: the first

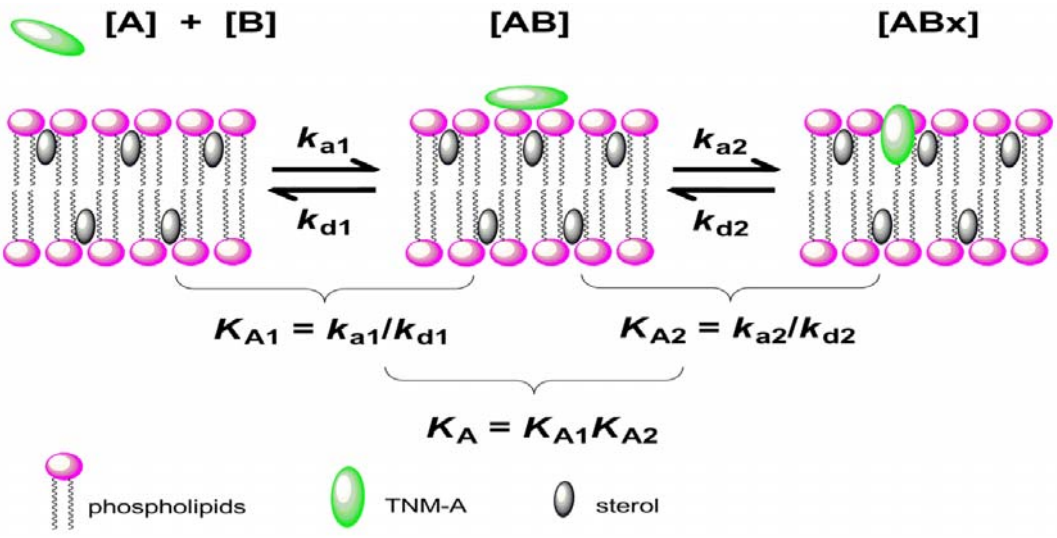

Figure 2-8. Illustration of the two-state reaction model for the interaction between TNM-A and sterol-containing phospholipid membranes.

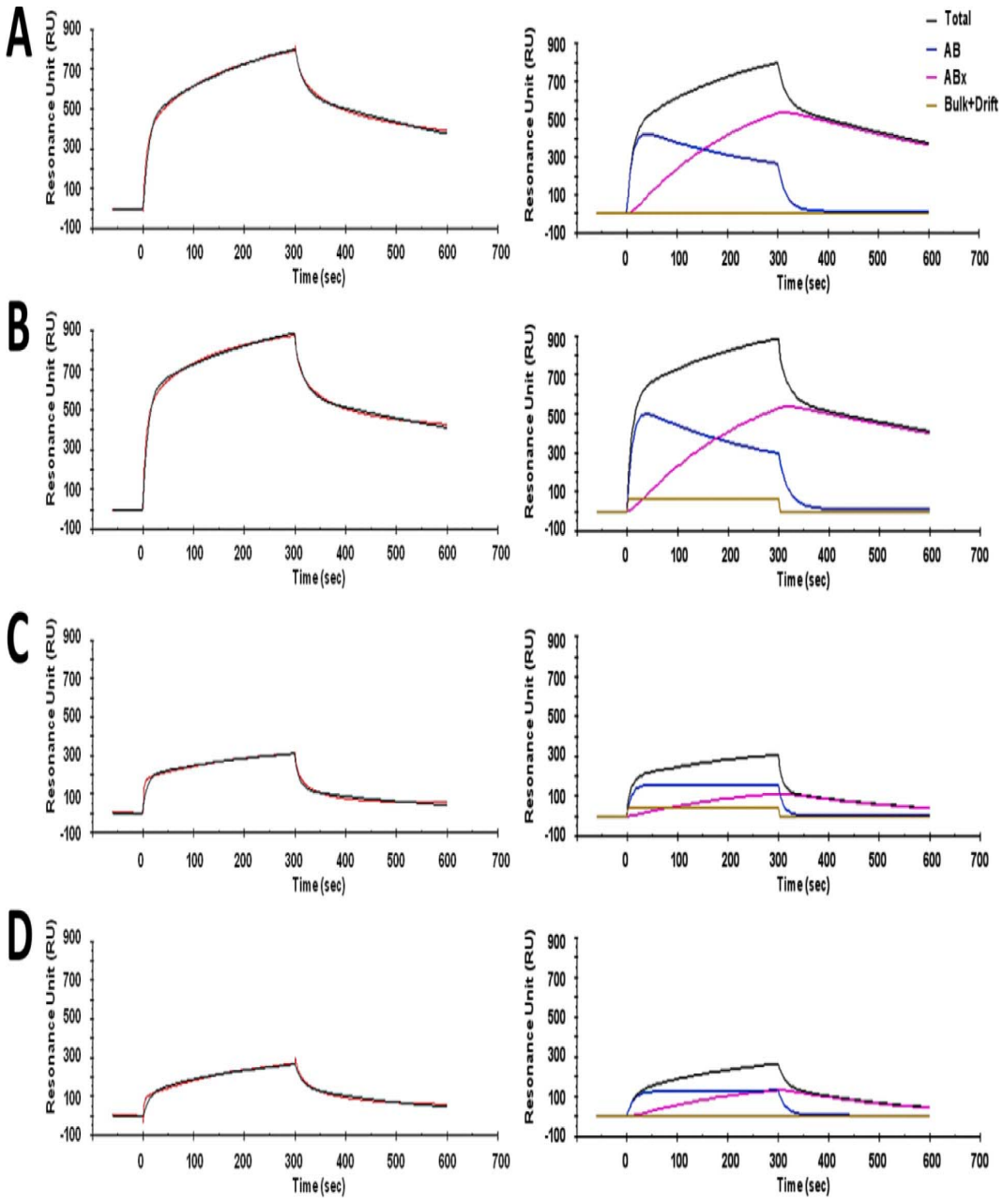

Figure 2-9. Curve fitting of the SPR sensorgrams to the two-state reaction model (left) and components of the fitting curves (right): (A) 10 mol % cholesterol-containing POPC liposomes, (B) 10 mol % ergosterol-containing POPC liposomes, (C) 10 mol % epicholesterol-containing POPC liposomes, and (D) pure POPC liposomes. Experimental RU values were recorded for 20 μM TNM-A. Red and black traces in the left panels depict experimental and theoretical curves, respectively. Blue, pink, and yellow traces in the right panels represent contributions from the AB complex, the ABx complex, and the bulk effect of the solvent, respectively, to the total component (black line).

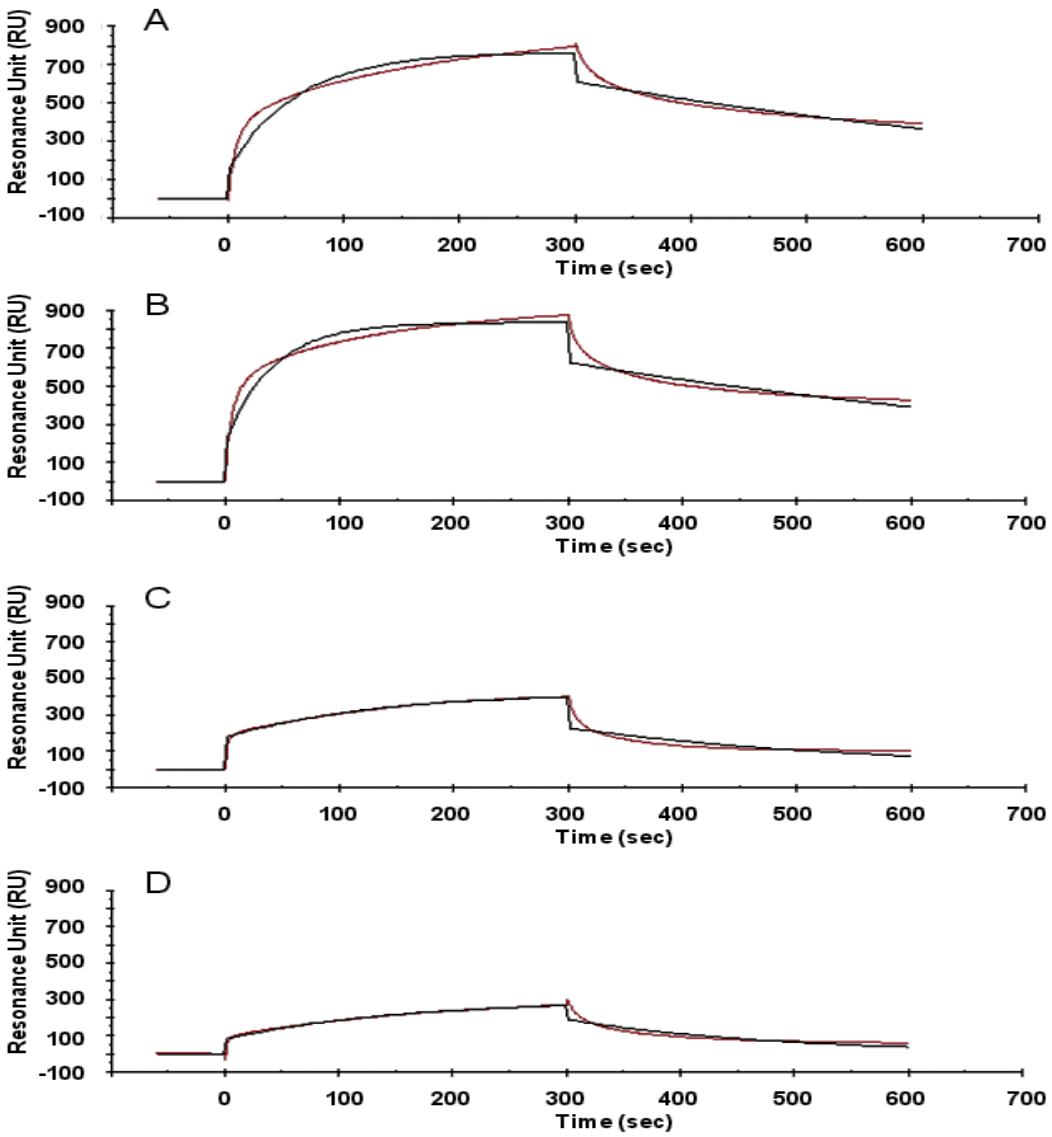

Figure 2-10. Curve fitting of the SPR sensorgrams using the Langmuir or 1:1 bimolecular interaction model for TNM-A (20 μM) binding to POPC liposomes captured on a modified CM5 sensor chip. (A) 10 mol% cholesterol-containing POPC liposomes, (B) 10 mol% ergosterol-containing POPC liposomes, (C) 10 mol% epicholesterol-containing POPC liposomes, and (D) pure POPC liposomes. Red and black traces correspond to experimental and theoretical curves respectively.

step involving the actual binding of TNM-A to the membrane surface and the second step probably corresponding to a conformational or morphological change to form a more stable membrane complex. The two-state analysis was first applied to well-known membrane peptides melittin and magainin[49,50] and then successfully used for the antifungal natural product amphotericin B.[51] For these compounds, the two-state model reproduced the

experimental SPR sensorgrams better than the conventional Langmuir model, which is consistent with the mechanisms of their membrane activities. Figure 2-9 shows the curve fitting of the experimental sensorgrams to the two-state reaction model (Figure 2-8 and Eq. 6-1 to 6-4) together with the components of the theoretical curve, demonstrating that theoretical curves using the two-state model excellently reproduced the experimental sensorgrams. As is evident from the right panels of Figure 2-9, progression of the second step is much slower than that of the first step in all four cases, thus showing that the second step is rate-limiting. The sensorgrams were also fitted to the Langmuir or 1:1 bimolecular interaction model but it could not reproduce the theoretical curve (Figure 2-10), thus supporting the notion that the binding of TNM-A to the lipid bilayers occurs via two different processes. Table 2-3 lists the kinetic and affinity constants obtained from the fitting, showing that the presence of 3β-hydroxysterol, cholesterol, or ergosterol significantly enhanced the affinity (K_A) of TNM-A for the membranes compared with those of epicholesterol (3α-hydroxysterol)-containing and

Table 2-3. Kinetics and affinity constants of the binding of TNM-A to liposomes obtained from the two-state reaction model.[a]

	POPC-cholesterol (10 mol%)	**POPC-ergosterol (10 mol%)**	**POPC-epicholesterol (10 mol%)**	**POPC**
k_{a1} ($\times 10^3$/Ms)	1.6 ± 0.3	2.5 ± 0.2	0.22 ± 0.09	0.15 ± 0.05
k_{d1} ($\times 10^{-2}$/s)	5.3 ± 0.5	4.73 ± 0.06	7.5 ± 3.7	7.7 ± 1.1
k_{a2} ($\times 10^{-3}$/s)	6.6 ± 0.4	5.7 ± 0.2	3.4 ± 0.7	6.1 ± 0.4
k_{d2} ($\times 10^{-3}$/s)	1.8 ± 0.2	1.2 ± 0.1	2.4 ± 1.3	4.7 ± 0.3
K_{A1} ($\times 10^3$/M)	30 ± 4	52 ± 4	3.0 ± 0.5	1.8 ± 0.4
K_{A2}	3.6 ± 0.6	4.8 ± 0.4	1.6 ± 0.5	1.3 ± 0.1
K_A ($\times 10^3$/M)	109 ± 32	250 ± 26	4.9 ± 1.9	2.4 ± 0.5

[a] Concentration of TNM-A was 20 μM.

pure POPC liposomes. This enhanced affinity of the peptide for the 3β-hydroxysterol-containing membranes is mainly due to the first binding step, because the rate constants (k_{a1}) are ~10 times larger in cholesterol- and ergosterol-containing liposomes than in epicholesterol-containing and pure POPC liposomes. In contrast, the second rate constants (k_{a2} and K_{A2}) were approximately the same for all systems tested, thus indicating that the second process is less affected by the presence of 3β-hydroxysterol.

In these measurements, the binding of TNM-A to POPC liposomes was very strong, especially with cholesterol- or ergosterol-containing membranes, such that regeneration of the liposome surface via repeated washing with NaOH was not successful (Figure 2-11). Thus, the liposomes once used for analysis had to be removed, and then fresh liposomes were immobilized on the sensor chip for the next analysis, which resulted in the relatively large standard deviations shown in Table 2-3. Nevertheless, kinetic data can be safely compared because the differences in the kinetic constants between membrane systems significantly exceed the deviations.

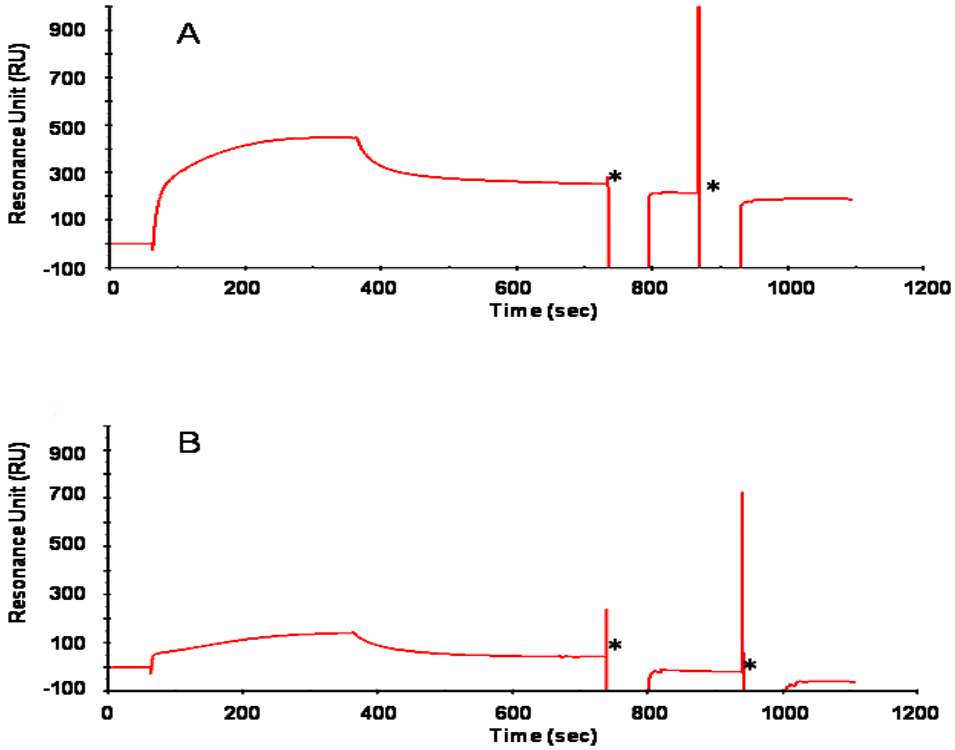

Figure 2-11. Regeneration of (A) 10 mol% ergosterol-containing POPC liposome and (B) pure POPC liposome surface with 50 mM NaOH. TNM-A bound to ergosterol-containing POPC liposomes were hardly removed after NaOH washing such that new liposome surface was immobilized for each TNM-A injection. Asterisk denote the point when NaOH was injected.

2.2.4 Sterol Stereoselectivity of TNM-A Viewed by Solid State ^{2}H NMR

Although the SPR experiments described above clearly show the preferential binding of TNM-A to 3β-hydroxysterol-containing membranes, it does not necessarily indicate that TNM-A directly interacts with 3β-hydroxysterol in lipid bilayers; it is also possible to assume that the presence of 3β-hydroxysterols changes the physicochemical properties of the membrane and consequently enhances the membrane affinity of TNM-A. Hence, to gain decisive evidence of the direct binding of TNM-A to membrane sterols, solid-state ^{2}H NMR measurements using 3-*d*-sterols (Figure 2-3) incorporated into POPC liposomes were conducted. Sterol molecules in lipid bilayers undergo fast lateral diffusion, which can be regarded as an axial rotation in NMR, and quadrupolar splitting observed in the ^{2}H NMR spectra depends both on the tilt angle of the C–^{2}H bond with respect to the rotation axis and the wobbling of the molecule.[52] Figure 2-12 shows the spectra of the 3-*d*-sterols incorporated into POPC bilayers in the absence and presence of TNM-A. In the absence of TNM-A (Figure 2-12A), 3-*d*-cholesterol exhibits a characteristic Pake doublet indicative of fast rotational motion of the sterol in the POPC bilayers. However, upon addition of the peptide, a stark attenuation of the splitting signal is observed (Figure 2-12B), indicating that the molecular rotation falls into an intermediate motional speed with correlation times of 10^{-4} to 10^{-5} s. A similar change in the splitting pattern was observed with 3-*d*-ergosterol (Figure 2-12C, D). On the other hand, in 3-*d*-epicholesterol-containing POPC liposomes (Figure 2-12E, F), the characteristic splitting pattern hardly changed, although the splitting value was slightly reduced by the presence of TNM-A, which may be attributable to a morphological change in the liposome induced by TNM-A that will be discussed shortly. Therefore, this demonstrates that the fast rotational motion of both 3-*d*-cholesterol and 3-*d*-ergosterol slows via direct interaction with TNM-A in lipid bilayers, which is indicative of considerable intermolecular interaction. Conversely, no such inhibition with 3-*d*-epicholesterol means that the fast rotational motion occurs even in the presence of TNM-A, indicative of a weaker intermolecular interaction between these two molecules. In addition, these observations strongly support the fact that the presence of either cholesterol or ergosterol, but not epicholesterol, significantly enhances the affinity of TNM-A for POPC liposomes as was shown explicitly in the SPR experiments (Figure 2-7 and Table 2-3). These results unequivocally prove the direct interaction between TNM-A and 3β-hydroxysterols in lipid bilayers.

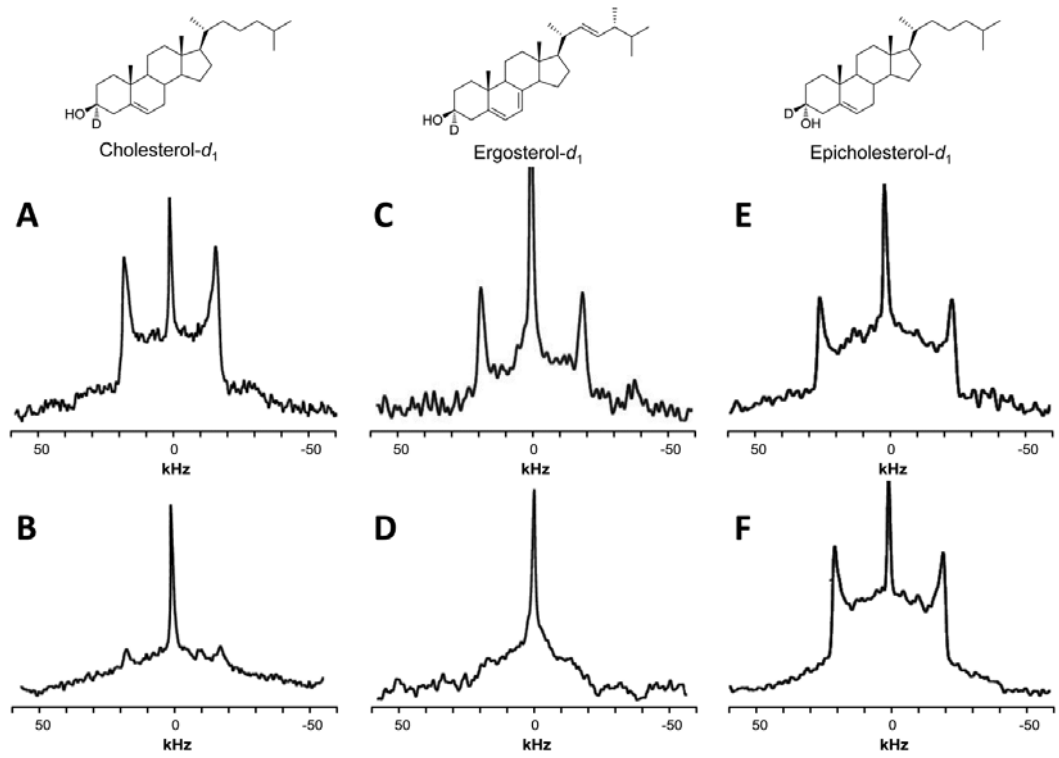

Figure 2-12. ^{2}H NMR spectra of 3-*d*-sterol incorporated into POPC bilayers in the absence (A, C, and E) and presence (B, D, and F) of TNM-A. 3-*d*-cholesterol (A and B), 3-*d*-ergosterol (C and D), and 3-*d*-epicholesterol (E and F) were used. 3-*d*-sterol:TNM-A:POPC molar ratios of 1:0:18 (A, C, and E) and 1:1:18 (B, D, and F) were used. Isotropic signals are mostly from residual deuterium water.

2.2.5 TNM-A and Sterol Bimolecular Interaction in Lipid Bilayer Membranes

Although it had been reported that fluorescently labeled TNMs bind to 3β-sterols,[44] the detailed mode of interaction is yet to be clarified. In this study, to gain a better understanding of the sterol recognition mechanism exhibited by the peptide, the interaction between TNM-A and sterol-containing liposomes was scrutinized using SPR and solid-state ^{2}H NMR and demonstrated for the first time the direct interaction using TNM-A as an intact TNM. Here it should be stressed that, although the concentrations of TNM-A are different by 2 orders of magnitude between the two experiments (20 μM and 2.6 mM), the molar ratios between TNM-A and lipid molecules are almost identical (1:25 and 1:19 for SPR and ^{2}H NMR, respectively), thus rationalizing the concomitant use of both methods.

As described in Chapter 2.1.4, the presence or absence of a sugar moiety in TNM molecules hardly affects the activity based on comparable results obtained from biological tests.[37,38] Theopalauamide, which is structurally closely related to TNM-A and has a sugar

moiety, recognizes sterol molecules as is the case in TNM-F lacking the sugar moiety;[45] therefore, it is reasonable to consider that these results obtained for TNM-A essentially hold true for TNM-F and other TNM congeners.

Using SPR with a dodecylamine-modified CM5 sensor chip that was devised to minimize nonspecific hydrophobic interactions, it was successfully demonstrated in this study that the presence of 3β-hydroxysterols, as seen in cholesterol and ergosterol, significantly increases the affinity of the peptide for POPC membranes (Figure 2-7 and 2-9 and Table 2-3). In contrast, TNM-A showed a lower affinity for epicholesterol-containing or pure POPC liposomes. The kinetic parameters listed in Table 2-3 further revealed that the 3β-sterols markedly promote the initial binding of TNM-A to the membrane surfaces (k_{a1}). The membrane affinity is enhanced by direct interaction between the peptide and the sterols that was explicitly shown by characteristic spectral changes in solid-state ^{2}H NMR. These findings, together with the fact that the alcohol groups of sterols are located close to the membrane interface,[53-55] imply that TNM-A has a direct interaction with the hydroxy moiety of 3β-sterols at the initial binding of TNM-A to the membrane surface, resulting in the greater level of accumulation of the peptide in the shallow area of the membrane. The direct recognition of the sterol hydroxy groups at the membrane surface is consistent with the relatively small difference (a factor of approximately 2) in the affinity between cholesterol and ergosterol (Table 2-3), indicating that TNM-A does not strictly recognize the difference in the steroid skeleton or side chain structure. It is not so far-fetched to assume that intermolecular hydrogen bonds play a crucial functional role in the interaction between TNM-A and the sterol hydroxy group.

In a previous report,[44] it was demonstrated that calcein, a membrane-impermeable fluorescent dye, was able to enter yeast cells in the presence of TNM-F (11 μM), indicating that membrane integrity is compromised by the peptide. Although the presence of 3β-hydroxysterols had a weaker effect on the second step of the binding process (K_{A2} in Table 2-3), the greater level of accumulation of TNM-A on the membrane surface, in the presence of cholesterol or ergosterol, results in an increased level of formation of the second complex (ABx) (Figure 2-9A, B). This presumably corresponds to the relocation of the peptide from the surface-binding form to a more stable membrane-complex form. Observations through microscope and ^{31}P NMR experiments have showed that TNM-A induced microscopic morphological changes in liposome features such as the occurrence of high-curvature regions (to be presented in the next Chapter), which is consistent with the reduced quadrupole splitting value of epicholesterol by the presence of TNM-A (Figure 2-12E, F). Therefore, the second step may correspond to deformation of membrane morphology through the binding of

the peptide. Namely, the accumulated TNM-A in the 3β-sterol-containing membranes could change the membrane morphology and integrity, ultimately resulting in membrane damage as previously reported for yeast cells.[44] In fact, TNM-induced membrane damage as well as cytotoxicity is reported to be time-dependent,[44] consistent with the slow progression of the second process as shown in Figure 2-9.

As described similarly in the Chapter 2.1.4, the membrane action of TNM-F is apparently different from that of amphotericin B, a representative polyene antibiotic forming sterol-dependent pores in fungal membranes; e.g., TNM-F exhibited a time-dependent toxicity, while amphotericin B has acute fungicidal activity.[44] In these experiments using artificial membranes, distinct pore formation by TNM-A could not be observed (Figure 2-13), although it induced hemolysis (Table 2-4). Here it may be meaningful to compare the SPR kinetic parameters of TNM-A with those of amphotericin B. It was previously reported that sterols, particularly ergosterol, prominently promote not only the initial surface binding step of amphotericin B but also the subsequent reorientation process presumably corresponding to pore formation.[51] In particular, the second step of amphotericin B hardly proceeds without sterols in membrane, thus suggesting that the sterol is involved in the pore complex. In contrast, as clearly shown in Table 2-3, the second step of TNM-A binding proceeds without sterols and is not significantly accelerated by the presence of sterols. In addition, amphotericin B shows a more than 10-fold difference in the K_A values between cholesterol and ergosterol, which is largely attributed to the second reorientation step, while TNM-A exhibits a smaller difference (a factor of ~2) as shown in Table 2-3. Taken together, amphotericin B recognizes not only the 3-hydroxy group but also steroid rings and side chains, the latter of which would account for its ergosterol selectivity and promote the second reorientation process corresponding to pore formation, while TNM-A mostly recognizes the sterol hydroxy group in the initial binding process. This difference is consistent with the observation that TNM-A is unlikely to form distinctive pores as does amphotericin B. Rather, as mentioned previously, it is more plausible that the accumulation of TNM-A in the sterol-containing membrane disturbs and damages the bilayer morphology and integrity, which would correspond to the second process in TNM-A binding. Here it should be stressed that the weaker sterol dependency in the second process of the binding of TNM to the membrane does not indicate the lack of the interaction between TNM-A and sterol in the second step, because ^{2}H NMR spectra demonstrate the persistent interaction in the membrane, but rather suggests that TNM-A induces the second step regardless of the presence or absence of its interaction with the sterol molecules.

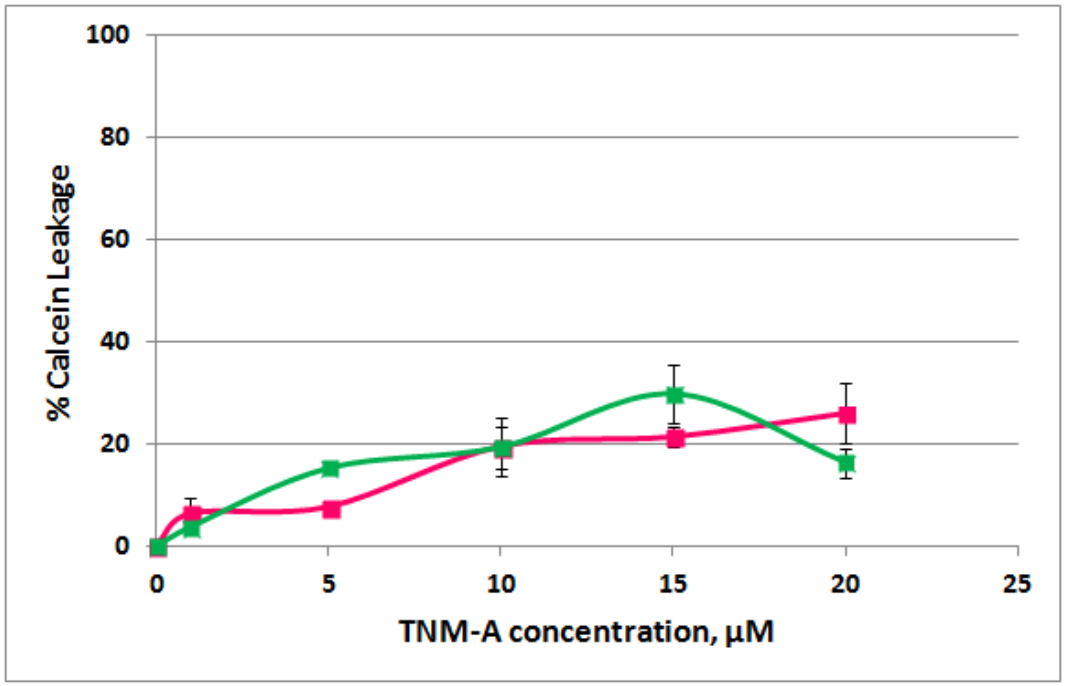

Figure 2-13. TNM-A-induced calcein leakage from POPC (pink) and POPC:cholesterol (10 mol%; green) liposomes. In both cases, final lipid concentration was 27 µM.

Table 2-4. EC_{50} values of TNM-A, amphidinol 3, and amphotericin B-induced hemolysis in human erythrocytes.

	EC_{50} (µM)
Theonellamide-A	0.70
Amphidinol 3	0.58
Amphotericin B	1.62

In conclusion, it was demonstrated using SPR that the presence of cholesterol or ergosterol significantly enhances the affinity of TNM-A for POPC liposomes and the peptide exhibits a preference for sterols with a 3β configuration. This enhanced affinity is caused by direct interaction between the peptide and 3β-hydroxysterols that is explicitly shown by characteristic spectral patterns in solid-state ^{2}H NMR. These results are consistent with the selective binding of fluorescently labeled TNM to 3β-hydroxysterols.[44] Kinetic data obtained in this work show that 3β-hydroxysterols accelerate the initial binding of TNM-A to the

membrane surface, thus suggesting that TNM-A directly recognizes the 3β-OH moiety upon binding to the membrane surface. Although the presence of 3β-hydroxysterols had a weaker effect on the kinetic constants of the second process corresponding to some deformation of bilayer morphology, the accumulation of TNM-A in the sterol-containing membranes eventually promotes the second process, thus causing the damage to the integrity of the membrane as reported previously.[44] However, the nature of these membrane effects as well as that of the molecular recognition is still a subject of further investigation. For this purpose, microscopic and solid state ^{31}P NMR experiments were carried out to observe changes in membrane morphology caused by the peptide, to be presented in the next Chapter.

References

1. Belarbi, E.H.; Contreras Gomez, A.; Christi, Y.; Garcia Camacho, F.; Molina Grima, E. *Biotechnol. Adv.* **2003**, 21, 585-598.
2. Hentschel, U.; Piel, J.; Degnan, S.M.; Taylor, M.W. *Nat. Rev. Microbiol*. **2012**, 10, 641-654.
3. Blunt, W.; Copp, B.R.; Keyzers, R.A.; Munro, M.H.G.; Prinsep, M.R. *Nat. Prod. Rep*. **2013**, 30, 237-323.
4. Taylor, M.W.; Radax, R.; Steger, D.; Wagner, M. *Microbiol. Mol. Biol.* **2007**, 71, 295-347.
5. Unson, M.D.; Holland, N.D.; Faulkner, D.J. *Mar. Biol.* **1994**, 119, 1-11.
6. Flatt, P.M.; Gautschi, J.T.; Thacker, R.W.; Musafija-Girt, M.; Crews, P.; Gerwick, W.H. *Mar. Biol.* **2005**, 147, 761-774.
7. Bewley, C.A.; Holland, N.D.; Faulkner, D.J. *Experientia*, **1996**, 52, 716-722.
8. Piel, J.; Hui, D.; Wen, G.; Butzke, D.; Platzer, M.; Fusetani, N.; Matsunaga, S. *Proc. Natl. Acad. Sci. USA*, **2004**, 101, 16222-16227.
9. Fisch, K.M.; Gurgui, C.; Heyke, N.; van der Sar, S.A.; Anderson, S.A.; Webb, V.L.; Taudien, S.; Platzer, M.; Rubio, B.K.; Robinson, S.J.; Crews, P.; Piel, J. *Nat. Chem. Biol.* **2009**, 5, 494-501.
10. Whitson, E.L.; Pluchino, K.M.; Hall, M.D.; McMahon, J.B.; McKee, T.C. *Org. Lett.* **2011**, 13, 3518-3521.
11. Sirirak, T.; Kittiwisut, S.; Janma, C.; Yuenyongsawad, S.; Suwanborirux, K.; Plubrukarn, A. *J. Nat. Prod.* **2011**, 74, 1288-1292.
12. Xu, M.; Andrews, K.T.; Birrell, G.W.; Tran, T.L.; Camp, D.; Davis, R.A.; Quinn, R.J. *Bioorg. Med. Chem. Lett.* **2011**, 21, 846-848.
13. Bringmann, G.; Gulder, T.A.M.; Lang, G.; Schmitt, S.; Stöhr, R.; Wiese, J.; Nagel, K.; Imhoff, J.F. *Mar. Drugs.* **2007**, 5, 23-30.
14. Trianto, A.; Hermawan, I.; de Voogd, N.J.; Tanaka, J. *Chem. Pharm. Bull.* **2011**, 59, 1311-1313.
15. Piao, S-J.; Zhang, H.J.; Lu, H.Y.; Yang, F.; Jiao, W.H.; Yi, Y.H.; Chen, W.S.; Lin, H.W. *J. Nat. Prod.* **2011**, 74, 1248-1254.
16. Ibrahim, S.R.M.; Min, C.C.; Teuscher, F.; Ebel, R.; Kakoschke, C.; Lin, W.; Wray, V.; Edrada-Ebel, R.; Proksch, P. *Bioorg. Med. Chem.* **2010**, 18, 4947-4956.
17. Ryu, G.; Matsunaga, S.; Fusetani, N. *Tetrahedron Lett.* **1994**, 35, 8251-8254.
18. Ryu, G.; Matsunaga, S.; Fusetani, N. *Tetrahedron.* **1994**, 50, 13409-13416.

19. Ledroit, V.; Debitus, C.; Lavaud, C.; Massiot, G. *Tetrahedron Lett.* **2003**, 44, 225-228.
20. Wegerski, C.J.; Hammond, J.; Tenney, K.; Matainaho, T.; Crews, P. *J. Nat Prod.* **2007**, 70, 89-94.
21. Kho, E.; Imagawa, D.K.; Rohmer, M.; Kashman, Y.; Djerassi, C. *J. Org. Chem.* **1981**, 46, 1836-1839.
22. Carmely, S.; Kashman, Y. *Tetrahedron Lett.* **1985**, 26, 511-514.
23. De Marino, S.; Ummarino, R.; D'Auria, M.V.; Chini, M.G.; Bifulco, G.; Renga, B.; D'Amore, C.; Fiorucci, S.; Debitus, C.; Zampella, A. *J. Med. Chem.* **2011**, 54, 3065-3075.
24. Renga, B.; Mencarelli, A.; D'Amore, C.; Cipriani, S.; D'Auria, M.V.; Sepe, V.; Chini, M.G.; Monti, M.C.; Bifulco, G.; Zampella, A.; Fiorucci, S. *PLoS ONE.* **2012**, 7, e30443.
25. De Marino, S.; Festa, C.; D'Auria, M.V.; Cresteil, T.; Debitus, C.; Zampella, A. *Mar. Drugs.* **2011**, 9, 1133-1141.
26. Klenchin, V.A.; King, R.; Tanaka, J.; Marriott, G.; Rayment, I. *Chem. Biol.* **2005**, 12, 287-291.
27. Allingham, J.S.; Zampella, A.; D'Auria, M.V.; Rayment, I. *Proc. Natl. Acad. Sci. USA.* **2005**, 102, 14527-14532.
28. Braet, F.; Soon, L.; Vekemans, K.; Thordarson, P.; Spector, I. *Protein Rev.* **2008**, 8, 37-49.
29. Festa, C.; De Marino, S.; Sepe, V.; D'Auria, M.V.; Bifulco, G.; Debitus, C.; Bucci, M.; Vellecco, V.; Zampella, A. *Org. Lett.* **2011**, 13, 1532-1535.
30. Festa, C.; De Marino, S.; Sepe, V.; Monti, M.C.; Luciano, P.; D'Auria, M.V.; Debitus, C.; Bucci, M.; Vellecco, V.; Zampella, A. *Tetrahedron*, **2009**, 65, 10424-10429.
31. Plaza, A.; Bifulco, G.; Masullo, M.; Lloyd, J.R.; Keffer, J.L.; Colin, P.L.; Hooper, J.N.A.; Bell, L.J.; Bewley, C.A. *Org. Chem.* **2010**, 75, 4344-4355.
32. Hamada, T.; Sugawara, T.; Matsunaga, S.; Fusetani, N. *Tetrahedron Lett.* **1994**, 35, 719-720.
33. Hamada, T.; Matsunaga, S.; Yano, G.; Fusetani, N. *J. Am. Chem. Soc.* **2005**, 127, 110-118.
34. Hamada, T.; Matsunaga, S.; Fujiwara, M.; Fujita, K.; Hirota, H.; Schmucki, R.; Güntert, P.; Fusetani, N. *J. Am. Chem. Soc.* **2010**, 132, 12941-12945.
35. Iwamoto, M.; Shimizu, H.; Muramatsu, I.; Oiki, S. *FEBS Lett.* **2010**, 584, 3995-3999.
36. Inoue, M.; Shinohara, N.; Tanabe, S.; Takahashi, T.; Okura, K.; Itoh, H.; Mizoguchi, Y.; Iida, M.; Lee, N.; Matsuoka, S. *Nat. Chem.* **2010**, 2, 280-285.

37. Matsunaga, S.; Fusetani, N.; Hashimoto, K.; Wälchli, M. *J. Am. Chem. Soc.* **1989**, 111, 2852-2588.
38. Matsunaga, S.; Fusetani, N. *J. Org. Chem.* **1995**, 60, 1177-1181.
39. Bewley, C.A.; Faulkner, D.J. *J. Org. Chem.* **1994**, 59, 4849-4852.
40. Schmidt, E.W.; Bewley, C.A.; Faulkner, D.J. *J. Org. Chem.* **1998**, 63, 1254-1258.
41. Wada, S.; Matsunaga, S.; Fusetani, N.; Watabe, S. *Mar. Biotechnol.* **1999**, 1, 337-341.
42. Wada, S.; Kantha, S.S.; Yamashita, T.; Matsunaga, S.; Fusetani, N.; Watabe, S. *Mar. Biotechnol.* **2002**, 4, 571-582.
43. Wada, S.; Matsunaga, S.; Fusetani, N.; Watabe, S. *Mar. Biotechnol.* **2000**, 2, 285-292.
44. Nishimura, S.; Arita, Y.; Honda, M.; Iwamoto, K.; Matsuyama, A.; Shirai, A.; Kawasaki, H.; Kakeya, H.; Kobayashi, T.; Matsunaga, S.; Yoshida, M. *Nat. Chem. Biol.* **2010**, 6, 519-526.
45. Ho, C.H.; Magtanong, L.; Barker, S.L.; Gresham, D.; Nishimura, S.; Natarajan, P.; Koh, J.L.Y.; Porter, J.; Gray, C.A.; Andersen, R.J.; Giaever, G.; Nislow, C.; Andrews, B.; Botstein, D.; Graham, T.R.; Yoshida, M.; Boone, B. *Nat. Biotechnol.* **2009**, 27, 369-377.
46. Mozsolits, H.; Aguilar, M. *Biopolymers.* **2002**, 66, 3-18.
47. Hall, D. *Anal. Biochem.* **2001**, 288, 109-125.
48. Nussio, M.R.; Sykes, M.J.; Miners, J.O.; Shapter, J.G. *Chem. Med. Chem.* **2007**, 2, 366-373.
49. Papo, N.; Shai, Y. *Biochemistry*. **2003**, 42, 458-466.
50. Hall, K.; Mozsolits, H.; Aguilar, M. *Lett. Pept. Sci.* **2003**, 10, 475-485.
51. Mouri, R.; Konoki, K.; Matsumori, N.; Oishi, T.; Murata, M. *Biochemistry.* **2008**, 47, 7807-7815.
52. Matsumori, N.; Tahara, K.; Yamamoto, H.; Morooka, A.; Doi, M.; Oishi, T.; Murata, M. *J. Am. Chem. Soc.* **2009**, 131, 11855-11860.
53. Kessel, A.; Ben-Tal, N.; May, S. *Biophys. J.* **2001**, 81, 643-658.
54. Róg, T.; Pasenkiewicz-Gierula, M. *Biophys. J.* **2003**, 84, 1818-1826.
55. Róg, T.; Pasenkiewicz-Gierula, M.; Vattulainen, I. Karttunen, M. *Biochim. Biophys. Acta.* **2009**, 1788, 97-121.
56. Maritz, K.; Calcino, A.; Fahey, B.; Degnan, B.; Degnan, S.M. *Open Mar. Biol. J.* **2010**, 4, 57-64.
57. Webster, N.S.; Taylor, M.W. *Environ. Microbiol*. **2012**, 14, 335-346.

Chapter 3

Morphological Changes of Lipid Bilayers Induced by Marine Sponge Cyclic Peptide Theonellamide A

3.1 Introduction

Theonellamide A (TNM-A) is a potent antifungal peptide produced by the marine sponge *Theonella* sp. The peptide has stereospecific interaction with 3β-hydroxysterols, which is believed be involved in its mechanism of action, for membrane damage.[1] To better understand the nature of TNM-A-sterol interaction in lipid bilayers, SPR and solid state ^{2}H NMR measurements have been carried out, which are described in detail in the preceding Chapter. It was clearly demonstrated that the presence of 3β-hydroxysterols significantly enhance the membrane affinity of TNM-A towards POPC liposomes as opposed to *epi*cholesterol-containing and sterol-free POPC membranes. This enhancement was brought about by direct intermolecular interaction between the peptide and 3β-hydroxysterols, which was explicitly shown in solid state ^{2}H NMR. Nevertheless, interaction between TNM-A and 3β-hydroxysterol-containing membranes were found to result only in moderate membrane permeabilization, which may be due to membrane deformations or morphological changes caused by the peptide, rather than distint pores. Hence, in this Chapter, the effects of TNM-A binding on the morphology of POPC liposomes was investigated, both in the presence and absence of cholesterol, by utilizing solid state ^{31}P NMR, and differential interference/confocal fluorescence microscopy with GUVs.

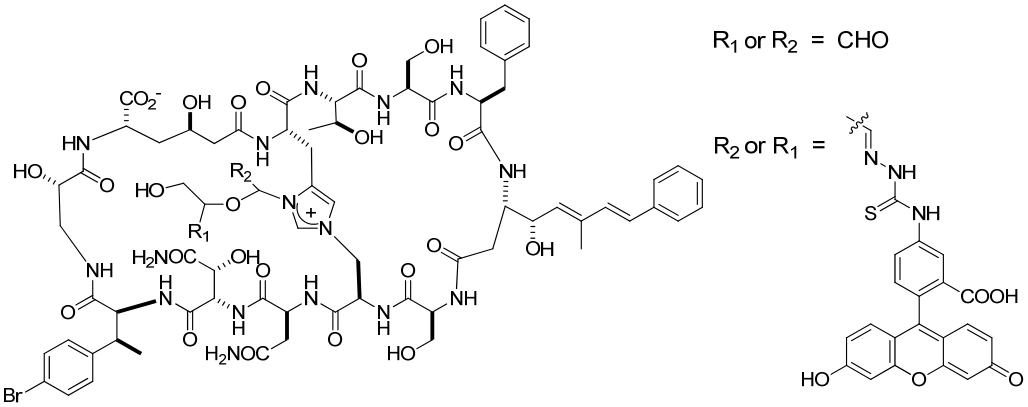

Figure 3-1. Chemical structure of fluorescein-labeled TNM-A (TNM-FL) used in this study.

3.2 Results and Discussion

3.2.1 Effect of TNM-A on Phospholipid Bilayers as Viewed by Solid State ^{31}P NMR

Changes in the phospholipid headgroup region caused by the incorporation of TNM-A in cholesterol-containing and sterol-free POPC liposomes were monitored using solid state ^{31}P NMR spectroscopy. In the absence of TNM-A, line shapes typical for lamellar bilayer structures were observed for both cholesterol-containing and sterol-free POPC liposomes (Figure 3-2A, B). Upon incorporation of 5 mol% TNM-A, however, isotropic signals appeared in both lipid systems as well (Figure 3-2C, D). Isotropic signals are usually assigned to small, fast-tumbling molecules such as lipids in micelles or small unilamellar vesicles, although these could also arise from ^{31}P species undergoing different molecular motions that give rise to isotropic chemical shifts such as regions of high membrane curvature.[2] In any case,

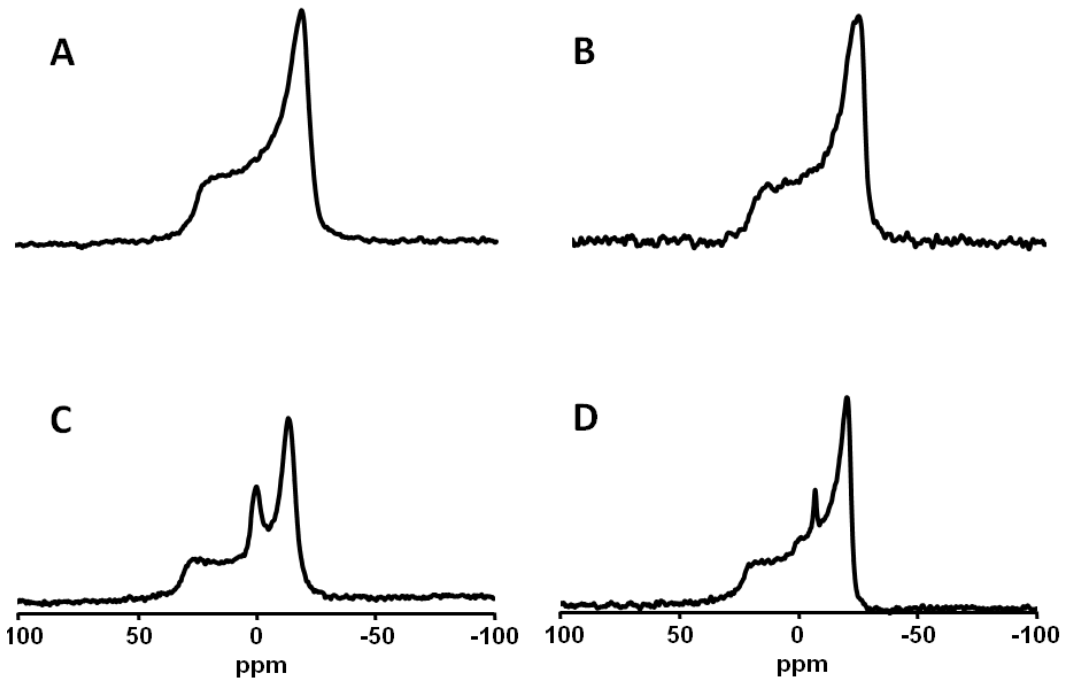

Figure 3-2. Solid State ^{31}P NMR spectra of pure POPC (A and C) and POPC:cholesterol (B and D) liposomes in the absence (A and B) and presence (C and D) of TNM-A. Molar ratios of Cholesterol:TNM-A:POPC were 0:0:18 (A), 1:0:18 (B), 0:1:18 (C) and 1:1:18 (D).

the appearance of these isotropic signals indicates that incorporation of TNM-A into the bilayer results in disruption of the tight phospholipid packing ultimately causing membrane

perturbation or deformation. Moreover, chemical shift anisotropy (CSA) is known to reflect the structural and dynamic response of the lipid head groups as well as the molecular motion, i.e. fluidity, of the phospholipid bilayer and so it may be altered when peptides interact strongly with the phospholipids.[3,4] Disruption of the bilayer integrity by TNM-A, however, appears not to include any significant changes in membrane fluidity as evidenced by the comparable width of the ^{31}P peaks in all four cases (Figure 3-2A-D).

3.2.2 Liposome Size Distribution by Dynamic Light Scattering Measurements

As shown in the solid state ^{31}P NMR in Figure 3-2, isotropic signals were observed when 5 mol% of TNM-A was incorporated into the phospholipid bilayer. These signals may be attributed to one of two possibilities; firstly, TNM-A incorporation induced the emergence

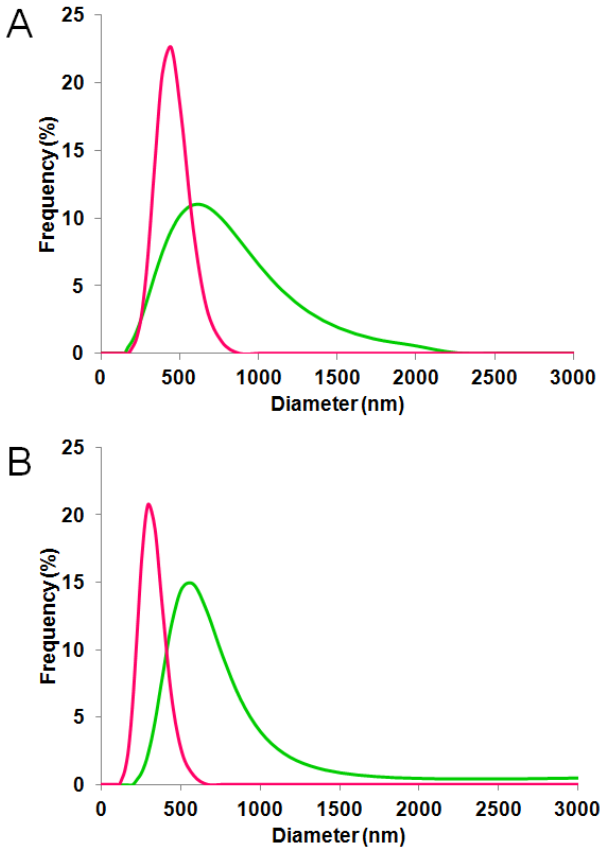

Figure 3-3. Size distribution of cholesterol-free (A) and cholesterol-containing (B) POPC liposomes in the presence (pink) or absence (green) of TNM-A. Components were pre-mixed and molar ratio of Cholesterol:TNM-A:POPC used were 0:1:18 (A, pink), 0:0:18 (A, green), 1:1:18 (B, pink), and 1:0:18 (B, green).

of regions of high membrane curvature, and secondly, addition of the peptide resulted in the formation of small fast-tumbling structures such as micelles, bicelles, or small unilamellar vesicles (SUVs). To distinguish these possibilities, dynamic light scattering measurements were carried out to determine the size distribution profiles of vesicles in the presence of TNM-A. Micelles and bicelles have diameters of about 4.5 nm and 30-100 nm, respectively,[5] while a typical small unilamellar vesicle is approximately 20-50 nm in size.[6] In the presence of TNM-A, however, no such small structures were detected judging from the vesicles' sizes, of which diameters centered at approximately 200 - 500 nm in all four cases (Figure 3-3), well within the reported size of multilamellar vesicles.[6] These results indicate that the presence of isotropic signals in the ^{31}P NMR spectra is likely due to the presence of regions of high membrane curvature induced by TNM-A addition. Another mode of analysis was also performed where TNM-A, at different concentrations, was incubated with pre-formed large unilamellar vesicles (LUVs) for various time, but liposome size distribution also hardly changed (Figure 3-4).

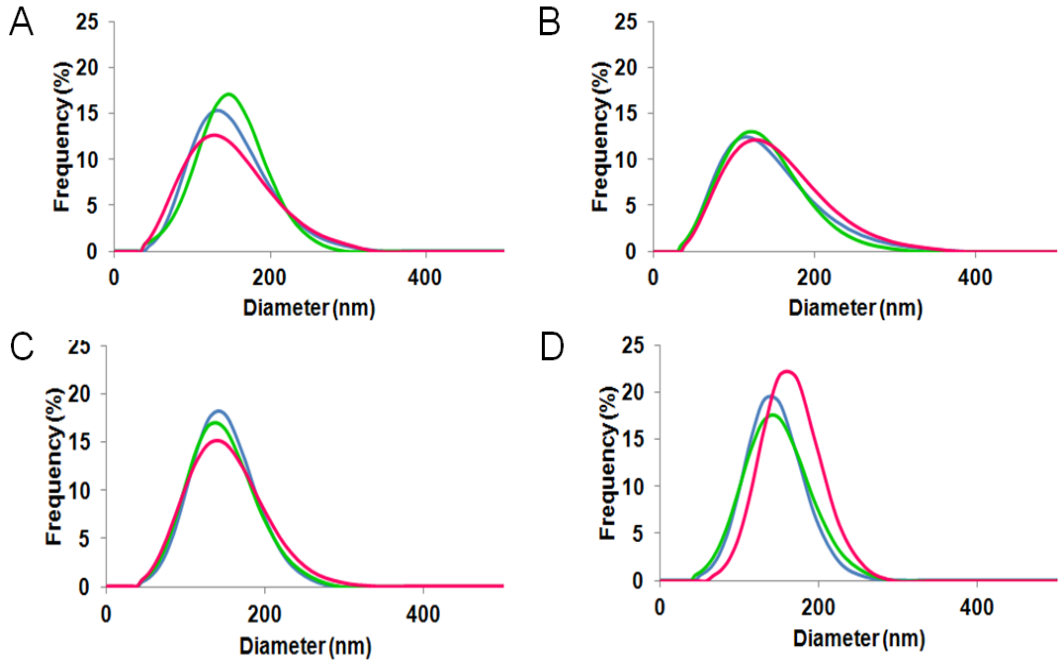

Figure 3-4. Size distribution of POPC:cholesterol (5 mol%) LUVs after incubation with various concentrations of TNM-A for (A) 1, (B) 3, (C) 6, and (D) 21 hours. Blue, green, and pink traces correspond to 0, 5, and 10 μM TNM-A respectively.

3.2.3 Microscopic Observations of Membrane Morphological Changes

In Chapter 2, it was mentioned that TNM-A-induced leakage of vesicle-entrapped calcein was found to be inefficient but comparable, both in sterol-containing and sterol-free POPC liposomes. It is therefore hypothesized that an addition of TNM-A does not result in the formation of distinct pores but causes membrane deformations or morphological changes, which may account for the poor dye leakage activity of TNM-A. This notion was corroborated by results from solid state ^{31}P NMR and dynamic light scattering measurements as shown in Figures 3-2 and 3-3/3-4, respectively, where the isotropic signals observed most likely result from regions of high membrane curvature. To further explore the nature of these deformations or morphological changes, differential interference and confocal fluoresecence microscopy observations were carried out using GUVs.

Addition of TNM-A at various concentrations to POPC GUVs resulted in distinctive morphological changes such as elongation of vesicles and wave-like structures/wrinkling of the membrane surface as indicated by arrows in Figure 3-5. These deformations were found to

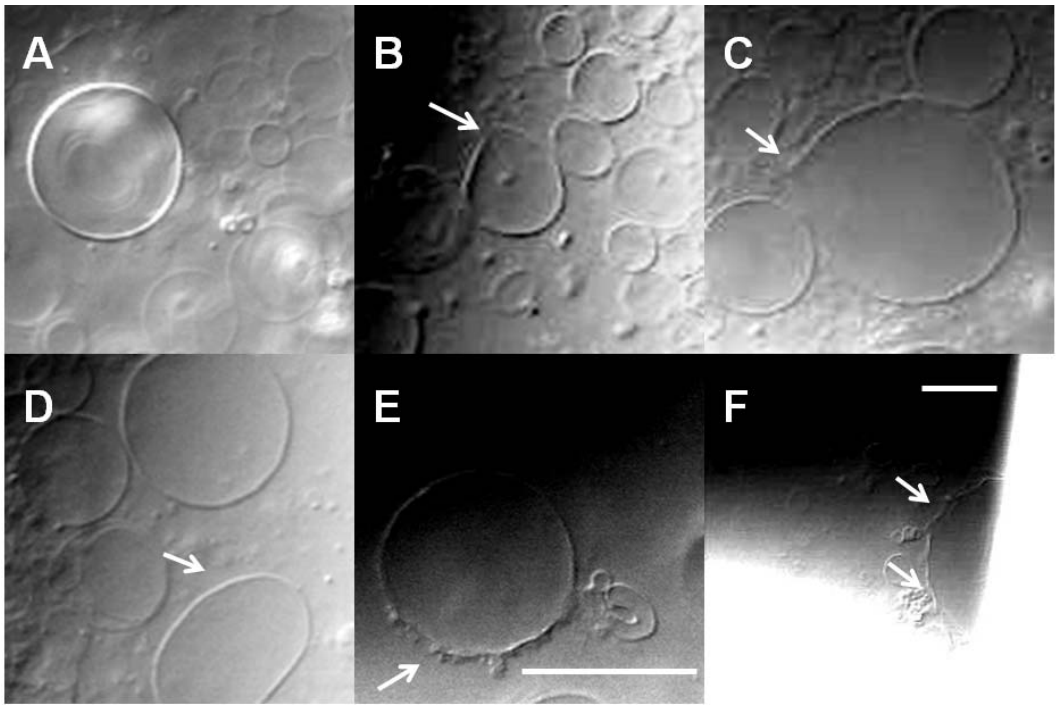

Figure 3-5. Membrane deformations induced by TNM-A. Top (A-C) and bottom panels (D-F) correspond to cholesterol-free and 5 mol% cholesterol-containing POPC GUVs, respectively. Final concentration of TNM-A were 1 μM (A, D), 10 μM (B, E), and 20 μM (C, F). Scale bar (A-E and F) = 25 μm.

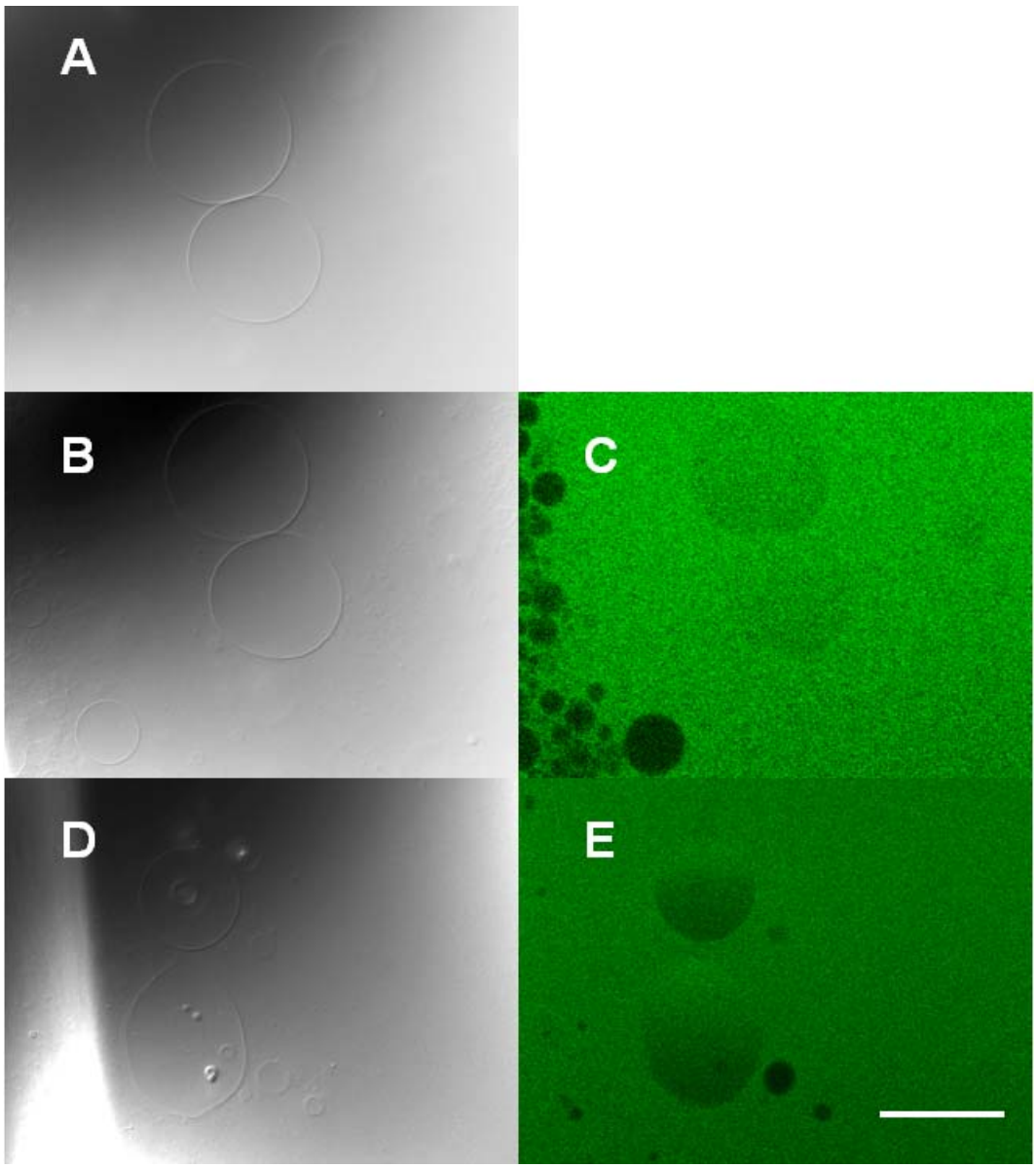

Figure 3-6. TNM-A-induced membrane deformation and permeabilization of 5 mol% cholesterol-containing POPC GUVs. Panels A and B are brightfield images of the same liposomes before and after TNM-A addition, respectively. The corresponding fluorescent image of panel B's is shown in panel C. Panels D and E are the brightfield and fluorescent images, respectively, of a different set of liposomes. To facilitate fluorescent observations, TNM-FL (10 mol% of peptide) was mixed with unmodified TNM-A and added to a final concentration of 20 μM. Scale bar = 50 μm.

be concentration-dependent and occur much more frequently in cholesterol-containing membranes. Furthermore, these defects were detected with TNM-A concentrations as low as 1 μM in cholesterol-containing GUVs (Figure 3-5D), but not in sterol-free liposomes (Figure

3-5A). Moreover, in cholesterol-containing POPC vesicles (Figure 3-5D-F), membrane deformations included vesicle elongation, and some budding and wrinkling of the membranes. On the other hand, elongation was much more prevalent in sterol-free vesicles (Figure 3-5A-C).

To further study the nature of these membrane defects, we also utilized confocal fluorescence microscopy by using a fluorescent derivative of TNM-A, TNM-FL, at 10 mol% of total peptide concentration. In the absence of TNM-A, GUVs clearly appeared spherical (Figure 3-6A). After addition of the peptide, however, a distinguishable deformation of the membrane was observed, both in cholesterol-containing POPC (Figure 3-6B, D) and sterol-free POPC (Figure 3-7A, indicated by an arrow) GUVs. The corresponding fluorescent images (Figure 3-6C, E and Figure 3-7B) shows a predominantly green background due to probe molecules in solution with some vesicles appearing dark because of probe exclusion from the vesicle interior, i.e. unpermeabilized GUVs. Interestingly, the deformed vesicles in Figure 3-6B are almost indistinguishable from that of the background in Figure 3-6C indicating that the extravesicular solution containing the fluorescent probe has diffused to the membrane interior. This phenomenon is more clearly shown in Figure 3-6, D and E, showing the brightfield and fluorescent images of another set of liposomes, respectively, where probe molecules appear to diffuse in the vesicles from their upper region (Figure 3-7E). These observations indicate that TNM-A is capable of inducing both membrane deformation and permeabilization, in which the latter is a result of the former.

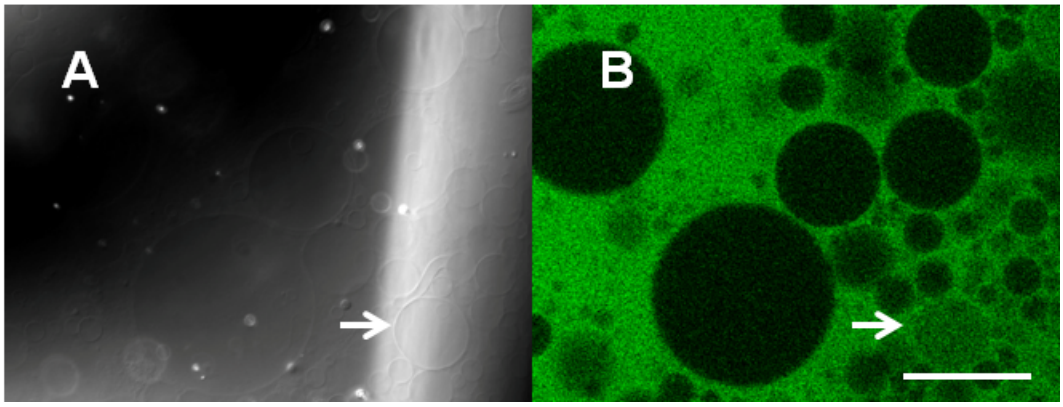

Figure 3-7. Brightfield (A) and fluorescence (B) images of sterol-free POPC GUVs after TNM-A addition, respectively. To facilitate fluorescent observations, TNM-FL (10 mol% of peptide) was mixed with unmodified TNM-A and added to a final concentration of 20 μM. Scale bar = 50 μm.

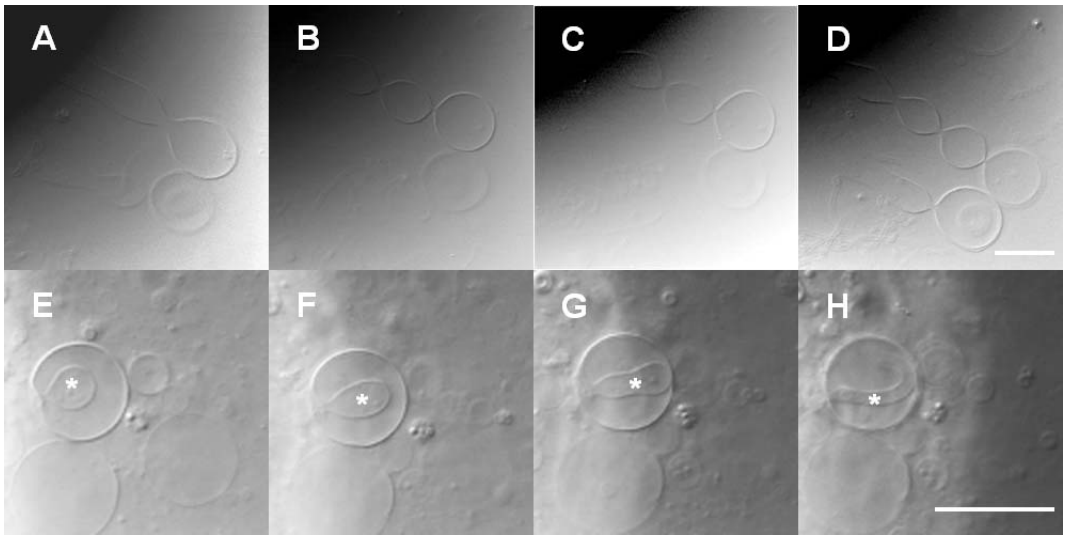

Figure 3-8. Membrane fission induced by TNM-A. Time-lapse images of sterol-free POPC GUVs from A to D and cholesterol-containing (5 mol%) POPC GUVs from E to H showing a fission process in the presence of the peptide. TNM-A was added to a final concentration of 10 μM (A-D) and 5 μM (E-H). Scale bar = 25 μm. Asterisk in panels E-H denote vesicle undergoing fission.

Another finding was that TNM-A appears to promote the fission processes on the membrane. This phenomenon was observed also on both sterol-free (Figure 3-8A-D) and cholesterol-containing (Figure 3-8E-H) POPC GUVs. In the sterol-free GUVs, an originally tubular structure (Figure 3-8A) gave rise to multiple vesicles that are almost completely separated from each other (Figure 3-8B-D) resembling a pearls-on-a-string structure. In cholesterol-containing POPC GUVs, a smaller vesicle (marked with an asterisk) seemed to have completely separated from the bigger one as seen by the appearance of a clear boundary representing a resealed and continuous bilayer (Figure 3-8H). These phenomena progressed with time, but were generally completed within approximately 3-5 minutes in both cases.

The difference in the effects of TNM-A on cholesterol-containing and sterol-free POPC GUVs, as well as the concentration-dependent changes observed in these two systems, are consistent with previous results obtained from SPR. In addition, the observation that some liposomes were deformed while others were not may provide significant insights into the possible mechanism of TNM-A action on the membrane. These will be discussed later.

3.2.4 TNM-A-Induced Morphological Changes in Membrane

Previously, it was reported that a fluorescent derivative of TNM-F specifically binds to 3β-hydrosterols such as cholsesterol and ergosterol *in vitro*, and that sterol binding is required for peptide-induced aberration and toxicity in yeast cells.[1] This work was extended in a recent

report detailed in Chapter 2, and provided insights into the mechanism of TNM-sterol recognition demonstrating by SPR and solid state ^{2}H NMR that TNM-A exhibits direct intermolecular interaction with 3β-hydroxysterols in lipid bilayers leading to peptide accumulation on the shallow region of the membrane. Furthermore, based on moderate dye leakage potency of TNM-A on both sterol-containing and sterol-free POPC liposomes, it was hypothesized that peptide accumulation results in disruption and damage of membrane integrity rather than formation of distinct pores. The results obtained from solid state ^{31}P NMR measurements and microscopy observations further confirmed that TNM-A induces characteristic morphological changes in POPC liposomes either in the presence or absence of sterols, supporting the notion of membrane disruption. It is also worth mentioning that comparison of the results between these two techniques is reasonable when considering that peptide-to-lipid ratio used in ^{31}P NMR was 1:19, while in the lowest TNM-A concentration (1 μM) that induced morphological changes in GUVs, the peptide-to-lipid ratio was 1:57.

The results obtained with TNM-A can also be extended to the other TNM congeners, since, as mentioned in previous studies, the presence or absence of a sugar moiety does not greatly affect the peptides' activities.[7,8] Moreover, theopalauamide, a sugar-containing analogue related to TNM-A, recognizes sterol[9] in the same way as TNM-F bearing no sugar moiety. In addition, the fluorescent analog of TNM-F, with a BODIPY-FL fluorophore attached on the sugar moiety, retained the *in vivo* activity of the unmodified peptide.[1] This rationalizes the use of TNM-FL (Figure 3-1), with the fluorescent probe attached on the same position as in the other analog, in this study where its activity may be safely assumed to be unaffected by this modification.

Using solid state ^{31}P NMR, it was demonstrated that TNM-A disrupts the tight phospholipid packing of the membrane environment, both in the presence and absence of cholesterol as seen in Figure 3-2. Disruption of the membrane is evidenced by appearance of isotropic and narrower anisotropic signals (Figure 3-2C, D), which is likely due to the presence of regions of high membrane curvature rather than small vesicles on the basis of DLS measurements that ruled out the presence of the latter (Figure 3-3 and 3-4). TNM-A-induced disruption of the bilayer integrity in both types of membrane systems would result in an increase in the permeability of the membrane. In fact, comparable dye leakage activity was observed earlier in both cholesterol-containing and sterol-free POPC liposomes upon TNM-A addition.

Kinetic evaluation of the interaction between TNM-A and liposomes using SPR revealed that the second step of TNM-A binding, i.e. membrane deformation, following a two-state reaction model proceeds regardless of the presence or absence of sterols and TNM-

A-sterol interaction. On the other hand, the rate of the first step, i.e. binding on the membrane surface, is greatly enhanced by the presence of 3β-hydroxysterols leading to accumulation of the peptide on the shallow region of the membrane by around three times as much compared with sterol-free POPC liposomes. However, this does not mean an absence of significant sterol-TNM-A interaction since solid state ^{2}H NMR clearly showed the presence of their direct intermolecular interaction. What most likely occurs is that the presence of more TNM-A molecules on the surface of sterol-containing membranes would lead to greater incidence of the second step of the binding, that is, a concentration-dependent disruption of phospholipid headgroups and acyl chain packing in cholesterol-containing membranes. These include vesicle elongation, appearance of surface dents, some wave-like deformations, or wrinkling of the membrane surface, which becomes more pronounced at higher peptide concentrations. These are visibly seen in the microscopy images shown in Figures 3-5. The greater frequency of membrane morphological changes in cholesterol-containing membranes will necessarily translate to more frequent occurrence of regions of high curvature exhibiting isotropic behavior. This could account for the difference in the isotropic signals observed in ^{31}P spectra, e.g. sharper in the case of POPC:cholesterol liposomes (Figure 3-2D). Another possible explanation for this difference in isotropic signals can arise from the smaller vesicles formed in cholesterol-containing liposomes in the presence of the peptide than in sterol-free membranes as depicted in the DLS traces in Figure 3-3. From these results, it can be argued that membrane destabilization and permeabilization by TNM-A is generally independent of the presence or absence of sterols since it probably occurs when the local threshold concentration, i.e. on a specific area of the membrane, is reached and thus is likely governed by non-specific hydrophobic interactions. Indeed, antimicrobial peptides whose mechanism of action is mainly brought about by hydrophobic interactions are necessarily non-cell selective, permeabilizing both zwitterionic and anionic membranes.[10] Still, the presence of both permeabilized and unpermeabilized membranes as seen in Figure 3-6 may suggest an all-or-none mechanism[11] of membrane disruption by TNM-A.

Resistance to bending, fusion and fission is one of the important characteristic of a lipid bilayer since it forms the structural foundation of cell membranes, thus forces and energy have to be applied in order to initiate changes in membrane curvature that will lead to vesicle fission.[12] Remodeling of the membrane, such as a fission process, is an important biological event necessary for proper cellular functions and this is usually driven by specialized proteins such as the N-BAR and dynamin protein families.[13,14] In addition, certain amphiphatic helices have also been demonstrated to sense membrane curvature and subsequently be involved in membrane remodeling.[15] In the latter case, as well as the N-BAR protein family, it has been

shown that insertion of hydrophobic residues in the shallow region of the membrane generating changes in membrane curvature is sufficient enough to drive fission processes.[13,14] This was explained on the basis of the stability of a funnel-like membrane neck, which is an unavoidable intermediate in the fission process.[13] Specifically, shallow insertion of the hydrophic regions into the outer leaflet will necessarily result in the expansion of the bilayer surface with respect to its midplane, thus resulting in stress and destabilization of the neck and favoring its fission. Furthermore, it was predicted that these insertions also accelerate fission by lowering its energy barrier.[13] A similar mechanism was also proposed for fission induced by lyso-PC for GUVs where, beyond a threshold concentration, the funnel-like neck breaks down ultimately resulting in the separation of distinct smaller vesicles.[16] Recently, membrane permeabilization and budding caused by the triterpenoid saponins α- and δ-hederin were proposed to arise from their ability to induce local spontaneous positive curvature.[17] These same events could account for the observed membrane fission induced by TNM-A as shown in Figure 3-8. The hydrophobic phenylalkenyl and neighboring benzyl residues of TNM-A (Figure 3-1) are most likely involved in the shallow penetration of the membrane outer leaflet. It has already been reported that aromatic amino acid residues such as phenylalanine preferentially partition around the membrane-water interface serving as efficient anchors for the proteins, positioned about ~10 Å below the lipid phosphates.[18,19] Thus, it is not far-fetched to hypothesize that insertion of TNM-A phenyl groups could lead to disruption of tight phospholipid packing, expansion of the bilayer surface, and membrane fission. In particular, the phenylalkenyl moiety with the methyl-substituted conjugated diene system may be most critical of the three phenyl-containing side chains in binding and insertion since the rigid diene moiety could provide additional hydrophobic contacts with the membrane shallow interior. The fission process in cholesterol-containing GUVs (Figure 3-8E-F) resulted in vesicle separation, unlike in sterol-free membranes (Figure 3-8A-D). This may be due to a difference in the concentration of membrane-bound peptide where sterol-free membranes have accumulated peptide to a much smaller extent than cholesterol-containing ones. In the context of the funnel-like membrane neck, the threshold concentration needed to break it down may not have been reached in the former.[16] Membrane fission in cholesterol-containing GUVs were observed at lower concentrations of TNM-A (5 μM) compared with pure POPC GUVs (10 μM), and the SPR experiments have demonstrated that more TNM-A are bound in cholesterol-containing membranes. Thus, the rate of fission should be expected to be faster in the former case. This fission brought about by TNM-A may also account for the vesicular fragmentation observed earlier in yeast cells upon addition of the peptide.[1]

Based on the above results and our previous findings, a possible mechanism of membrane destabilization by TNM-A is proposed, summarized in Figure 3-9. In the absence of cholesterol, or ergosterol, only a small number of TNM-A were bound on the membrane surface (Figure 3-9A). It therefore takes time for the peptide to reach its threshold concentration but when it does, membrane deformation can occur. In contrast, the presence of either of these sterols (Figure 3-9B) together with the aid of direct intermolecular interaction, a significantly higher level of peptide accumulation on the membrane surface is reached on a shorter time resulting in more pronounced and faster appearance of membrane morphological changes. In both of these cases, TNM-A probably disrupts only the shallow portion of the membrane interior resulting in morphological changes such as regions of high membrane curvature, wrinkling and dents on the membrane surface, and fission, which also increases the membrane's permeability. This is similar to the proposed interfacial activity model for the action of imperfectly amphiphatic AMPs.[20]

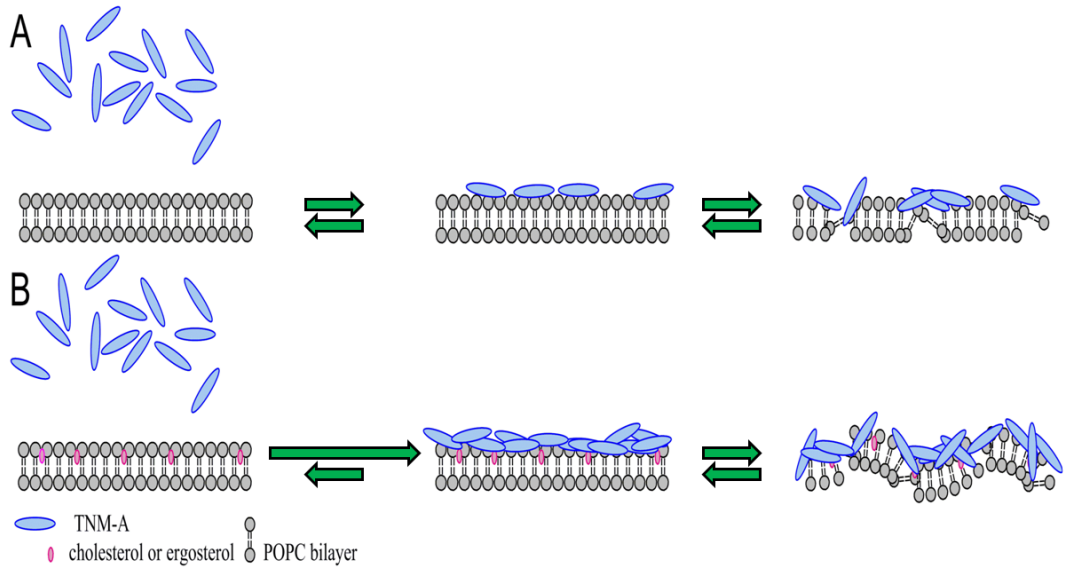

Figure 3-9. Proposed mechanism of membrane disruption by TNM-A on (A) sterol-free and (B) sterol-containing POPC liposomes. Arrows indicate the rate constants, which were determined using SPR and sensorgram fitting to a two-state reaction model detailed in Chapter 2.

In conclusion, we have shown by solid state ^{31}P NMR that TNM-A disrupts both sterol-free and sterol-containing POPC liposomes on the basis of the appearance of characteristic isotropic signals. These isotropic or narrower anisotropic signals probably arose

from regions of high membrane curvature rather than the formation of small vesicles or micelles based of dynamic light scattering measurements. By carrying out microscopy observations, we have verified that TNM-A induces distinct morphological changes in POPC GUVs, which is consistent with the appearance of isotropic signals in solid state ^{31}P NMR. Furthermore, the concentration- and time-dependencies of these morphological changes are consistent with previous findings. Binding of TNM-A on the membrane most likely results in its shallow insertion leading to disruption of the tight phospholipid packing rendering the membrane more permeable as also reported previously.[1] At a higher local concentration that exceeds the threshold concentration, membrane fission could occur which may explain vesicular fragmentation observed earlier.[1] However, additional experiments will have to be carried out to further investigate the fission process, the peptide's binding to only a subset population of liposomes as well as the specific mode of recognition of sterols by the peptide in order to have a more complete understanding of the mode of action of this unique natural product.

References

1. Nishimura, S.; Arita, Y.; Honda, M.; Iwamoto, K.; Matsuyama, A.; Shirai, A.; Kawasaki, H.; Kakeya, H.; Kobayashi, T.; Matsunaga, S.; Yoshida, M. *Nat. Chem. Biol.* **2010**, 6, 519-526.
2. Bechinger, B.; Salnikov, E.S. *Chem. Phys. Lipids*. **2012**, 165, 282-301.
3. Strandberg, E.; Ulrich, A.S. *Concepts. Magn. Reson. A.* **2004**, 23, 89-120.
4. Dave, P. C.; Tiburu, E.K.; Damodaran, K.; Lorigan, G.A. *Biophys. J.* **2004**, 86, 1564-1573.
5. Matsumori, N.; Murata, M. *Nat. Prod. Rep.* **2010**, 27, 1480-1492.
6. Chrai, S.S.; Murari, R.; Ahmad, I. *BioPharm.* **2001**, 14, 10-12,14.
7. Matsunaga, S.; Fusetani, N.; Hashimoto, K.; Wälchli, M. *J. Am. Chem. Soc.* **1989**, 111, 2582–2588.
8. Matsunaga, S.; Fusetani, N. *J. Org. Chem.* **1995**, 60, 1177–1181.
9. Ho, C.H.; Magtanong, L.; Barker, S.L.; Gresham, D.; Nishimura, S.; Natarajan, P.; Koh, J.L.Y.; Porter, J.; Gray, C.A.; Andersen, R.J.; Giaever, G.; Nislow, C.; Andrews, B.; Botstein, D.; Graham, T.R.; Yoshida, M.; Boone, B. *Nat. Biotechnol.* **2009**, 27, 369-377.
10. Papo, N.; Shai, Y. *Peptides.* **2003**, 24, 1693-1703.
11. Apellániz, B.; Nieva, J.L.; Schwille, P.; Garciá-Sáez, A.J. *Biophys. J.* **2010**, 99, 3619-3628.
12. Chernomordik, L.V.; Kozlov, M.M. *Annu. Rev. Biochem.* **2003**, 72, 175-207.
13. Boucrot, E.; Pick, A.; Çamdere, G.; Liska, N.; Evergren, E.; McMahon, H.T.; Kozlov, M.M. *Cell.* **2012**, 149, 124-136.
14. Shnyrova, A.V.; Bashkirov, P.V.; Akimov, S.A.; Pucadyil, T.J.; Zimmerberg, J.; Schmid, S.L.; Frolov, V.A. *Science.* **2013**, 339, 1433-1436.
15. Drin, G.; Antonny, B. *FEBS Lett.* **2010**, 584, 1840-1847.
16. Tanaka, T.; Sano, R.; Yamashita, Y.; Yamazaki, M. *Langmuir.* **2004**, 20, 9526-9534.
17. Lorent, J.; Le Duff, C.S.; Quetin-Leclercq, J.; Mingeot-Leclercq, M.P. *J. Biol. Chem.* **2013**, 288, 14000-14017.
18. de Planque, M.R.R.; Boots, J.P.; Rijkers, D.T.S.; Liskamp, R.M.J. Greathouse, D.V.; Killian, J.A. *Biochemistry.* **2002**, 41, 8396-8404.
19. Victor, K.G.; Cafisco, D.S. *Biophys. J.* **2001**, 81, 2241-2250.
20. Wimley, W.C. *ACS Chem. Biol.* **2010**, 5, 905-917.

Chapter 4

Amphidinol 3 – Sterol Interaction and Pore Formation in Lipid Bilayer

4.1 Introduction – Bioactive Compounds from the Marine Dinoflagellates of the Genus *Amphidinium*

4.1.1 Dinoflagellate-Derived Toxins

Microalgae, most notably phytoplanktons, perform a critical role in maintaining a viable marine environment. By occupying the bottom of the marine food chain, they provide a significant proportion of biomass to support higher lifeforms such as filter-feeding organisms (clams, shellfish, mussels, etc); they also produce a considerable amount of oxygen, through photosynthesis, that is essential to human life.[1,2] The over 5,000 known species of phytoplanktons are classified into one of eight main phylogenetic groups comprised of the Chlorophyta (green algae), Chrysophyta (golden algae), Phaenophyta (brown algae), Dinophyta (dinoflagellata), Euglenophyta, Rhodophyta (red algae), Diatoms (yellow or brown unicellular organisms) and Cyanobacteria (blue-green algae). Extensive proliferation of algae population results in so-called algal blooms that show distinctive and visible colored patches on the ocean surface commonly referred to as "red or brown tides." In some instances, these blooms are harmless; however, in the case of toxic microalgae, referred to as harmful algal bloom or HAB, it often leads to mortality in fish, birds, and mammals (including humans). Although a natural phenomena, HABs have become economically detrimental and a serious health problem, among other things, due to its frequency and with nearly every country with marine waters being affected.[1,3] Of the documented species of phytoplanktons, only around 85 are known to produce potent toxins capable of inflicting harm to other organisms; flagellated microalgae account for about 90% of harmful algal blooms, of which more or less 75% are dinoflagellates.[2]

Dinoflagellate toxins normally accumulate in tissues of, e.g., bivalves filter-feeders, causing no observable damage. In cases where HABs are present, however, the accumulated toxins can increase to critically high levels which then become toxic, even fatal, for organisms higher on the food chain. These toxins associated with harmful algal blooms that cause seafood poisoning are classified into 6 categories traditionally named after the human symptoms observed upon consumption of the toxic seafood: paralytic shellfish poisoning (PSP), ciguatera fish poisoning (CFP), neurotoxic shellfish poisoning (NSP), diarrhetic

shellfish poisoning (DSP), azaspiracid shellfish poisoning (AZP), spiroimine shellfish poisoning (SSP), and possible estuary-associated syndrome (PEAS). [1-5] The last class of shellfish poisoning, amnesic shellfish poisoning (ASP), due to the toxin domoic acid is the only known intoxication caused by a diatom and the only one not caused by dinoflagellates.[2]

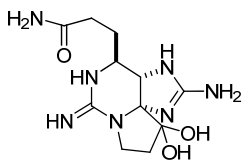

Saxitoxin 1

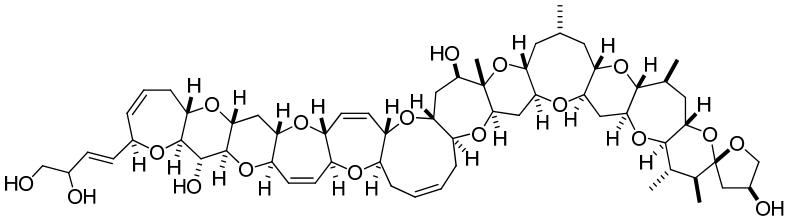

Ciguatoxin

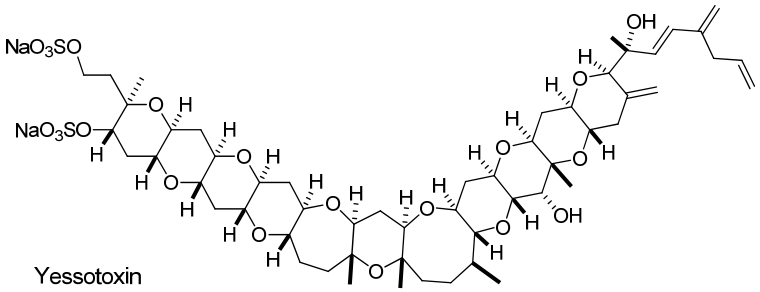

Yessotoxin

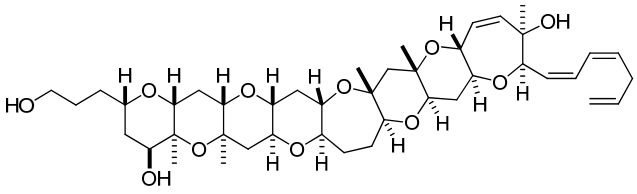

Gambierol

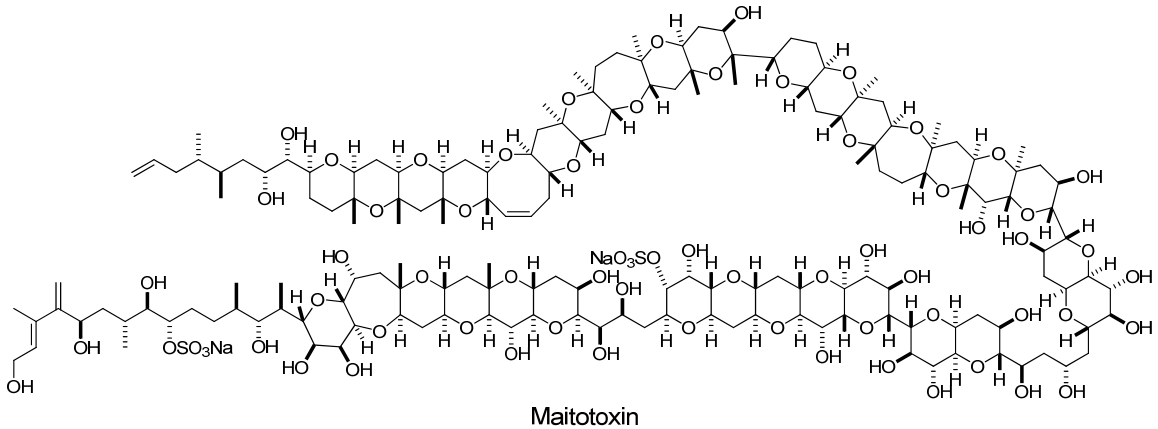

Maitotoxin

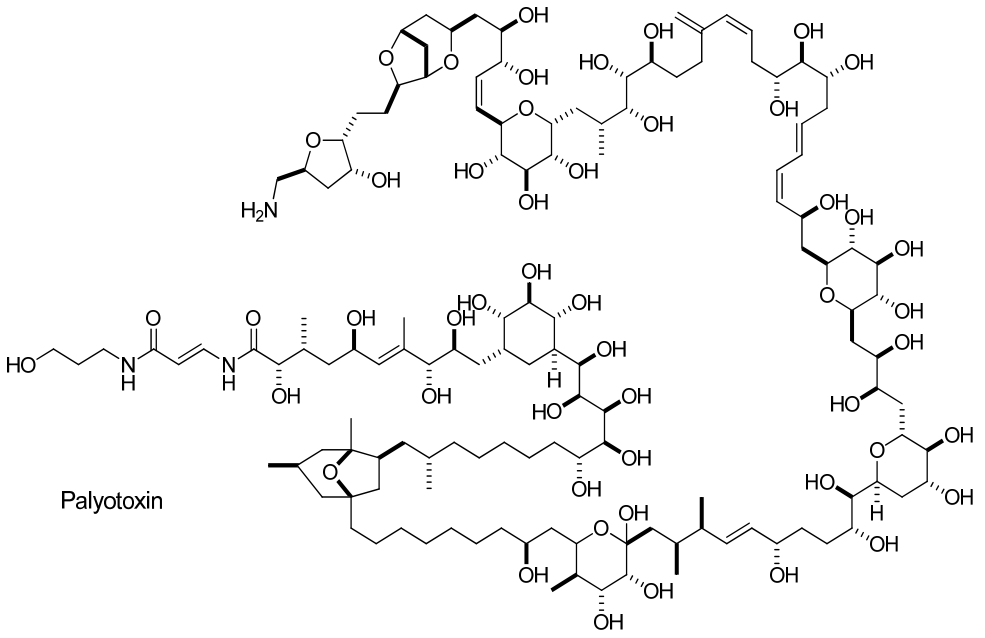

Palyotoxin

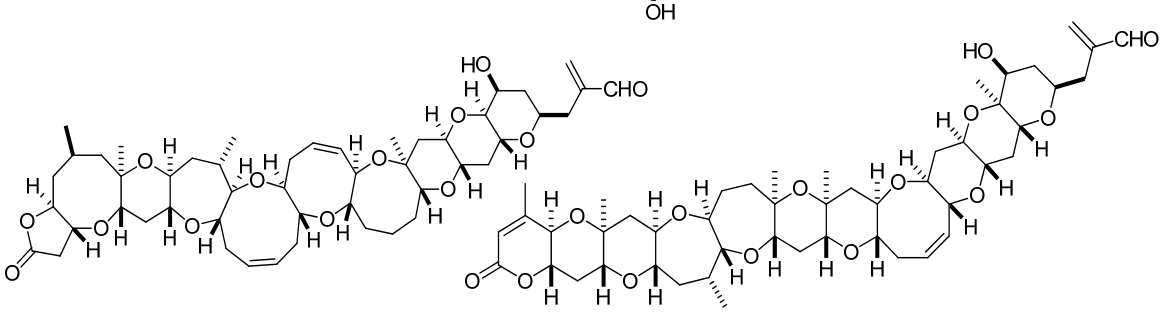

Brevetoxin A

Brevetoxin B

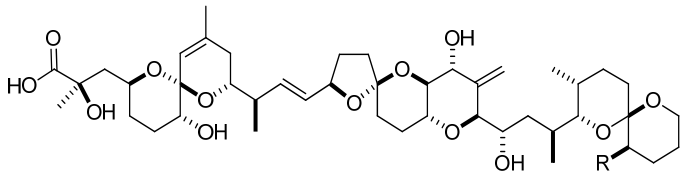

Okadaic acid: R = H

Dinophysistoxin 1: R = Me

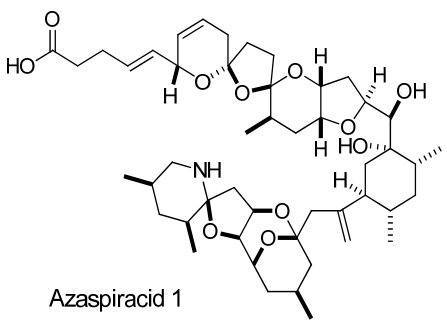

Azaspiracid 1

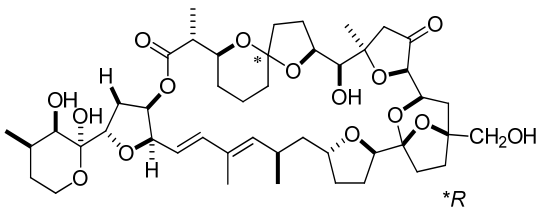

Pectenotoxin 1

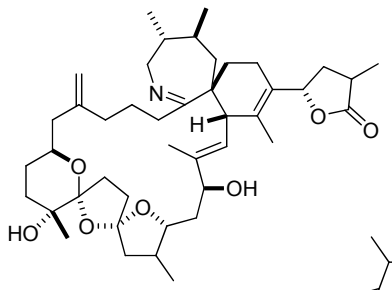

Spirolide C

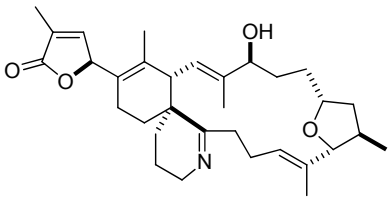

Gymnodimine A

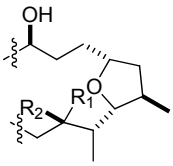

	R_1	R_2
Gymnodimine B	OH	H
Gymnodimine C	H	OH

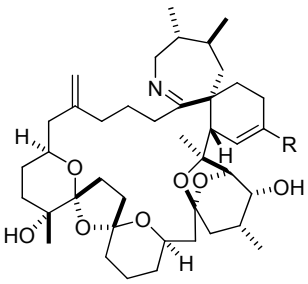

	R
Pinnatoxin A	COOH
Pinnatoxin B	CO_2H, NH_2
Pinnatoxin C	CO_2H, NH_2

PSP is attributed to the heterocyclic guanidine toxins produced by the species in the genera *Alexandrium*, *Gymnodinium*, and *Pyrodinium* represented by the neurotoxic alkaloid saxitoxin, the most researched PSP toxin.[3,6] CFP is the most prevalent case among the seven and is caused by ingestion of reef fish contaminated with ciguatoxins and its analogs maitotoxin, palytoxin and gambierol, which is primarily produced by *Gambierdiscus toxicus*.[2,4,7-9] Incidentally, maitotoxin and palytoxin are the two biggest and most potent non-peptide, non-polymeric toxin known to date. NSP are caused by the cyclic polyether brevetoxins produced primarily by the unarmoured dinoflagellate *Karenia brevis*.[4] These three kinds of seafood intoxication result from the toxins' action on potassium and/or sodium ion channels. DSP is a non-fatal condition associated with polyether toxins mainly produced by species in the genera *Dinophysis* and *Prorocentrum* that includes okadaic acid, dinophysistoxins, and pectenotoxins.[1,10] Yessotoxins were earlier misclassified as DSP toxin, but further studies showed they did not inhibit known targets of the other DSP toxins and was

Table 4-1. Seafood poisoning and their associated dinoflagellates and toxins. [1,2,4,5,11,12]

Seafood poisoning	Causative dinoflagellates	Main toxins
Paralytic shellfish poisoning (PSP)	*Alexandrium catenalla, A. cohorticula, A. fundyense, A. fraterculus, A. leei, A. minutum, A. tamarense, A. andersonii, A. ostenfeldii, A.tamiyavanichii, Gymnodinium catenatum, Pyrodinium bahamanse* var. *compressum*	Saxitoxins (STXs)
Ciguatera fish poisoning (CFP)	*Gambierdiscus toxicus, Prorocentrum* spp.*, P. lima, P. concavum, P. hoffmannianum, P. mexicanum, P. rhathytum, Gymnodinium sangieneum, Gonyaulax polyedra, Ostreopsis* spp., *O. lenticularis, O. siamensis.*	Ciguatoxins (CTXs), Maitotoxins (MTXs), palytoxin, gambierol
Neurotoxic shellfish poisoning (NSP)	*Karenia brevis, K. papilonacea, K. sellformis, K. bicuneiformis, K. concordia, Procentrum borbonicum*	Brevetoxins (PbTxs)
Diarrhetic shellfish poisoning (DSP)	*Dinophysis acuta, D. caudate, D. fortii, D. norvegica, D. mitra, D. rotundata, D. sacculus, D. mile, D. tripos, Prorocentrum lima, P. arenarium, P.belizeanum, P. cassubicum, P. concavum, P.faustiae, P. hoffmannianum,P. maculosum, Coolia* sp., *Protoperidium oceanicum, P. pellucidum,Phalacroma rotundatum.*	Okadaic acid, dinophysis toxins (DTXs), pectenotoxins (PTXs)
Azaspiracid shellfish poisoning (AZP)	*Protoperidinium crassipes*	Azaspiracids (AZAs)
Spiroimine shellfish poisoning (SSP)	*A. ostenfeldii, A. peruvianum, K. selliformis, Vulcanodinium rugosum*	Spirolides, gymnodimines, pinnatoxins
Possible estuary-associated syndrome (PEAS)	*Pfiesteria piscicida*	Cu-ligated toxin (uncharacterized)

more lethal in mice; however, its mechanism is still unclear.[4] AZP is caused by the neurotoxin azaspiracids, whose pharmacology is still unclear, and is produced by the heterotrophic dinoflagellate *Protoperidinium crassipes*.[2,3] SSP has been recently proposed as another class of shellfish poisoning caused by toxins containing a spiroimine unit, specifically spirolides and the other fast- acting toxins gymnodimines and pinnatoxins.[2] The spirolide, gymnodimine, and pinnatoxin family of toxins are produced by the dinoflagellates *Alexandrium ostenfeldii* and *A. peruvianum*, *Karenia selliformis*, and *Vulcanodinium rugosum*, respectively.[2,11,12] A summary of these intoxications, causative dinoflagellates and main toxins involved are shown in Table 4-1.[1,2,4,5,11,12]

Some metabolites associated with dinoflagellates reported so far are of polyketide origin.[4] Secondary metabolites produced by dinoflagellates, and phytoplanktons in general, serve a multitude of functions. These compounds can act as predator defense, for instance, by poisoning grazers; it can also work against competitors, which are mainly other photoautotrophic organisms, by inhibiting photosynthesis, killing of the competitor, or excluding them within the vicinity of the metabolite-producing organism.[13] These metabolites may also compensate competitive disadvantage such as low growth rate and nutrient uptake, [13] enhance interspecific competition under nutrient limitation by redirecting grazers towards non-toxic phytoplanktons,[14] act as pheromones to promote mating,[15] and as means to stun their prey before ingestion.[16]

4.1.2 Bioactive Compounds from Dinoflagellates of the Genus *Amphidinium*

Dinoflagellates belonging to the genus *Amphidinium* are widely considered a prolific source of polykeyide metabolites with unique and intriguing structures that also exhibit fascinating bioactivities, and over the years have attracted considerable attention due to production of ichthyotoxic compounds by some species.[17,18] This genus contains approximately 120 species.[17] One of the most remarkable compounds isolated from the dinoflagellates that is a symbiont of the Okinawan marine flatworm *Amphiscolops* sp., are the potent cytotoxic macrolide family designated as amphidinolides of which around 40 members have been reported.[18,19] Ammphidinolide C, for instance, exhibits cytotocity against murine lymphoma L1210 and human epidermoid carcinoma KB cells in the nanomolar region.[19] Other macrolides reported from *Amphidinium* sp. includes the amphidinolactones,[20] iriomoteolides,[21,22] and caribenolide.[19] Moreover, linear polyketides, the amphidinins, have also been reported from the same dinoflagellates.[23,24] All of these compounds exhibit modest to very potent cytotoxicites. In addition, unique polyhydroxy compounds called the colopsinols, have been isolated from the same dinoflagellates that produced the

amphidinolides and so far, five analogs are known.[25-27] These compounds contain a gentiobioside (β-D-glucopyranosyl-(1→6)-β-D-glucopyranoside) moiety and a sulfate ester. While colopsinols C and E showed cytotoxic activity against L1210 murine leukemia cells, the other three analogs were inactive. However, colopsinol A exhibited, instead, inhibitory activity against DNA polymerase α and β.

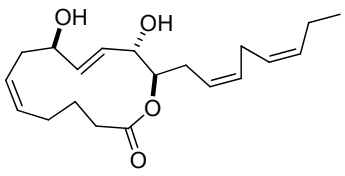

Amphidinolactone A

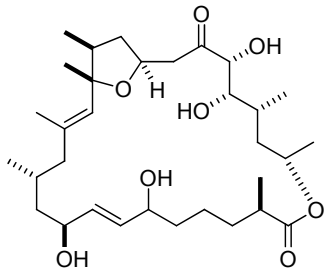

Amphidinolactone B

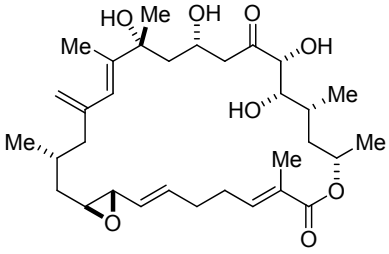

Amphidinolide B

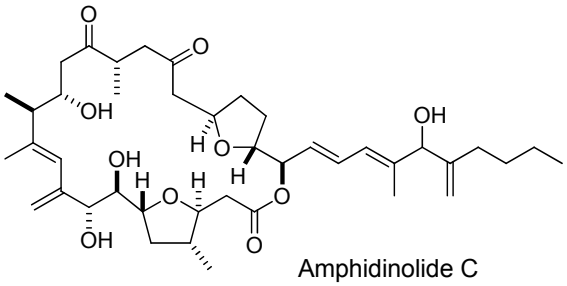

Amphidinolide C

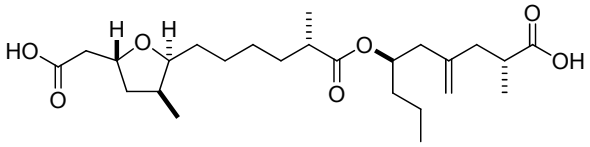

Amphidinin B

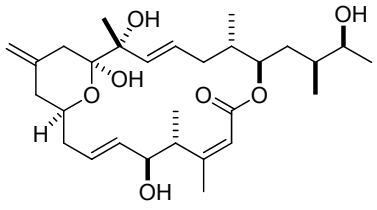

Iriomoteolide-1a

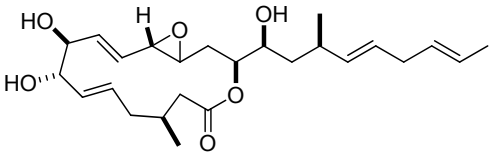

Iriomoteolide-3a

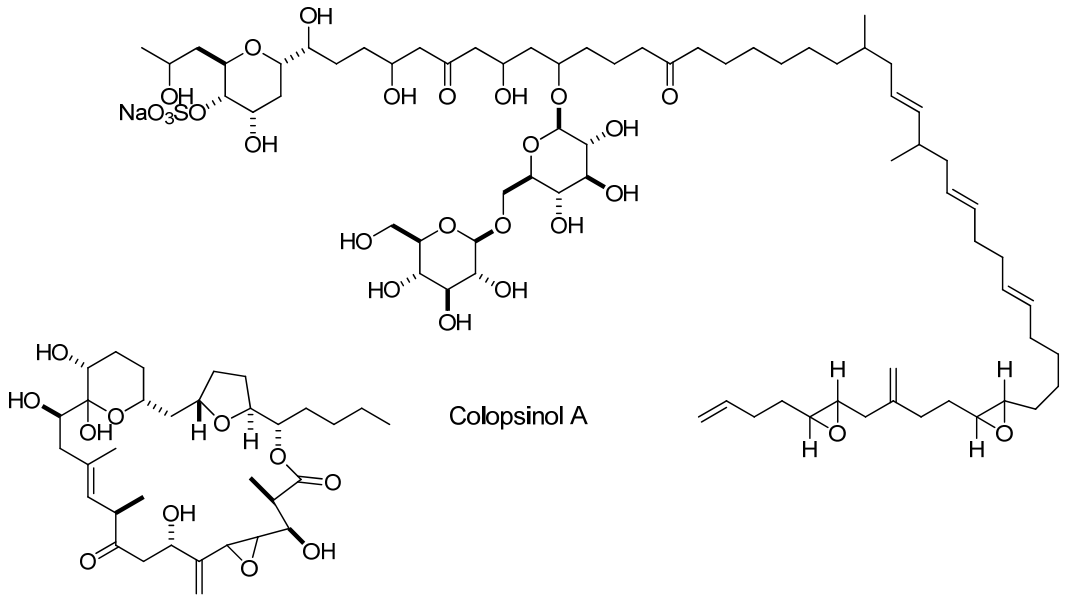

4.1.3 Amphidinols

Initial screening of the dinoflagellate *Amphidinium klebsii* collected at Ishikagi Island, Japan for novel bioactive compounds afforded the very first member of this polyhydroxy polyene class of metabolites, in 1991, which was subsequently called amphidinol (synonymous with amphidinol 1).[28] Since then, nearly 20 closely related compounds collectively termed as amphidinols (AMs) have been isolated.[29-35] The defining structural features of these family of natural products include a polyol and polyene chain, conferring on them amphiphatic properties, which is separated by an intermediate C_{16} section that contains two tetrahydropyran rings connected by a short aliphatic chain (C_6). This middle region of the molecule containing the tetrahydropyran rings is basically conserved among the amphidinol homologues and the variation in AM structures mainly arise from differences in the length and substitution pattern both on the polyol and polyene chains.[35]

The majority of the reported AMs have been isolated from dinoflagellates collected in Japan. The first member, amphidinol 1 (AM1) was obtained from cultured *A. klebsii* found in Ishigaki Island.[28] AM2 – AM6 were extracted from a strain of *A. klebsii* found in the surface wash of seaweeds collected at Aburatsubo Bay in Miura Peninsula, Japan (deposited in the Microbial Culture Collection of the National Institute for Environmental Studies and identified as NIES 613). Further screenings performed much more recently on this same strain

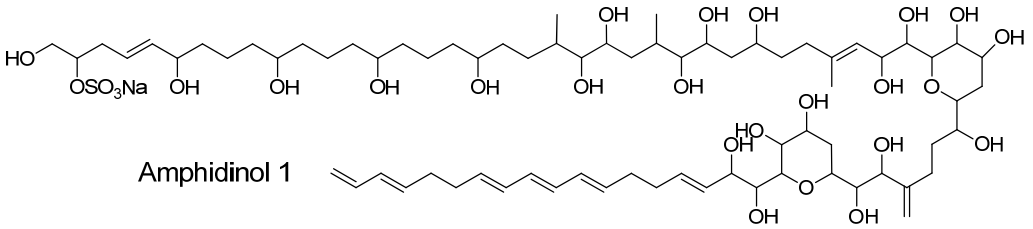

Amphidinol 1

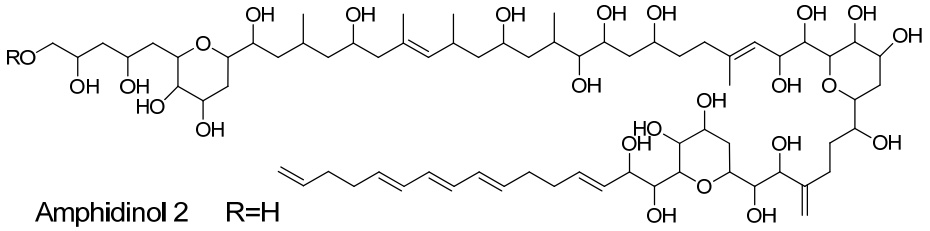

Amphidinol 2 R=H
Amphidinol 11 R=SO_3Na

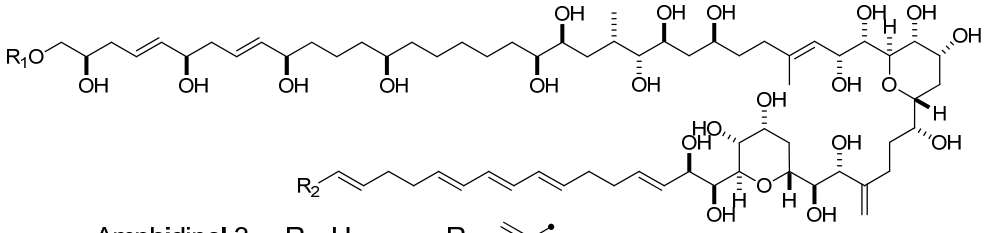

Amphidinol 3 R_1=H R_2=
Amphidinol 4 R_1=H R_2=H
Amphidinol 12 R_1=SO_3Na R_2=H

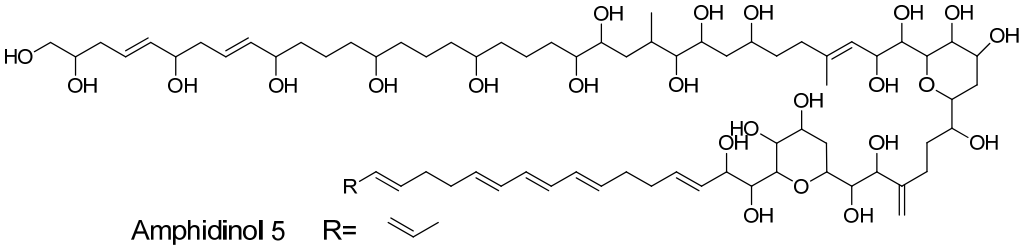

Amphidinol 5 R=
Amphidinol 6 R=H

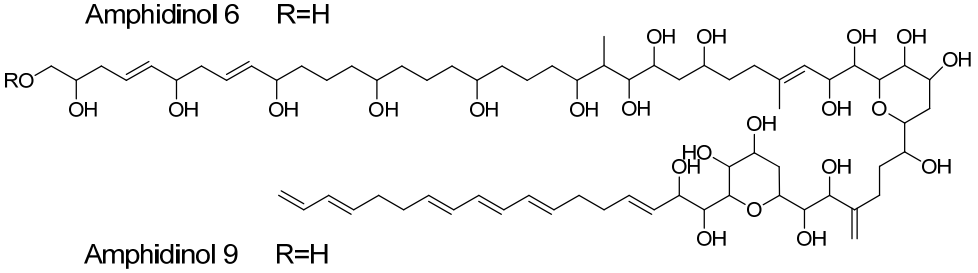

Amphidinol 9 R=H
Amphidinol 13 R=SO_3Na

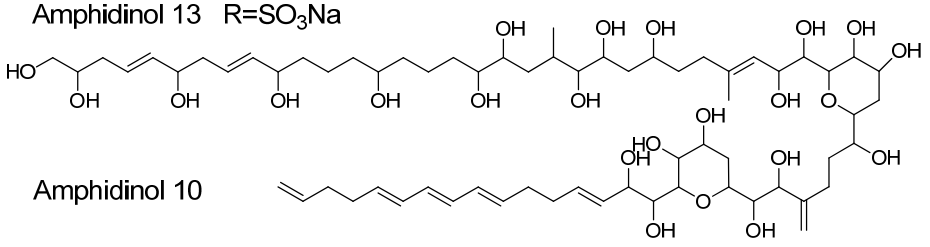

Amphidinol 10

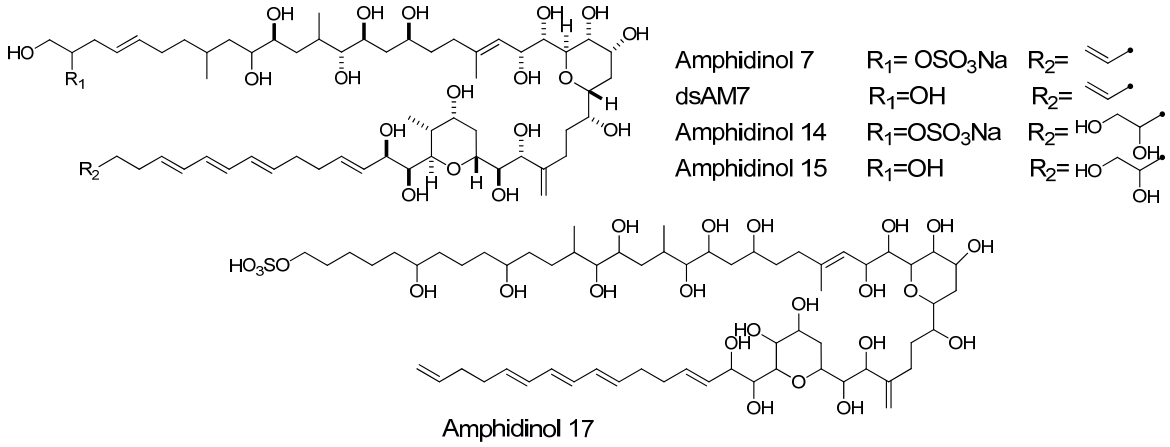

of *A. klebsii* (NIES 613) have afforded AM7, AM14, and AM15.[32,34] Incidentally, AM7 has the shortest carbon backbone among the known AMs as well as possessing the smallest molecular weight. The isolation of AM8 has been reported but its structure has not been elucidated.[30]

The other AM analogues were obtained from dinoflagellates found in other countries. From *A. carterae* collected at Kauauroa, South Island, New Zealand, AM9-AM13 were isolated and up to that time, was the first report of AMs obtained from outside of Japan as well as not from *A. klebsii*.[33] Much more recently, AM17 was also reported from *A. carterae* collected from Little San Salvadore Island, Bahamas.[35] These findings indicate the wide distribution of AMs within the *Amphidinium* spp. as well as AM production that varied from strain to strain, similarly observed with other toxigenic dinoflagellates.[33]

4.1.4 Amphidinol Congeners

Numerous amphidinol congeners have been reported so far both from *Amphidinium* sp. and other species of dinoflagellates. Luteophanols A-D were isolated from *Amphidinium* sp. (strain number Y-52) obtained from the inside of the cells of the Okinawan marine acoel flatworm *Pseudaphanostoma luteocoloris*.[36-38] These compounds exhibited no antifungal activity; however, they showed weak antibacterial action against certain microorganisms. Meanwhile, *Amphidinium* sp. from the surface wash of seaweeds obtained from Lingshui Bay, Hainan Province, China, afforded lingshuiols A and B, later on demonstrated to possess cytotoxic activity against primary rat hepatocytes (IC_{50} value of 0.21 μM) that was attributed to possible membrane permeabilizing properties.[39,40] An enantiomer of lingshuiol B, named symbiopolyol, was recently reported from a symbiont dinoflagellate of the Papuan jellyfish *Mastigias papua* that exhibited significant inhibitory activity against the expression of

vascular cell adhesion molecule-1 (VCAM-1) involved in inflammation.[41] Karatungiols A and B, on the other hand were isolated from *Amphidinium* sp. found in an unidentified marine acoel flatworm from Karatung Island, Indonesia.[42] Karatungiol A exhibited both antifungal (*Aspergillus niger*, 12 μg/disk) and antiprotozoan activities (*Trichomonas foetus*, 1 μg/mL).

A different lab-cultured dinoflagellate, *A. carterae*, yielded the polyhydroxy ichthyotoxin carteraol E which, aside from its potent ichthyotoxicity (LD50 value of 0.28 μM), also exhibits antifungal properties against *A. niger* (15 μg/disk).[43] In addition, a suite of water-slouble toxins, designated as karlotoxins, were isolated from a co-occurring dinoflagellate, *Karlodinium veneficum*, in massive fish kills in Maryland and in many other places since.[44-46] The function of these compounds appear to be non-specifically increasing the ion permeability of membranes leading to osmotic lysis, and they are thought to kill fish by damaging sensitive gill epithelial tissues.[44]

Very recently, a further two related compounds to AMs were isolated. Prorocentrol was reported from *Prorocentrum hoffmannianum*, the very first long carbon chain compound that is linear in nature isolated from the genus *Prorocentrum*.[47] Although prorocentrol was not a potent hemolytic and antifungal compound, it nevertheless showed cytotoxic (against P388 cells) and antidiatom (against *Nitzschia* sp.) activities at 16 μg/mL and 50 μg/mL, respectively. Amdigenol A, on the other hand, was isolated from the dinoflagellate *Amphidinium* sp. that was present on the surface of the marine alga *Digenea simplex*.[48] This compound is large, with a C_{98}- linear carbon backbone that includes the two core structures of AM analogs: the sulfate ester side is similar to that of lingshuiol B, luteophanol A, and symbiopolyol, while the olefinic side chain is analogous to luteophanol D and so it was hypothesized to arise from a linear combination of two AM analogs.

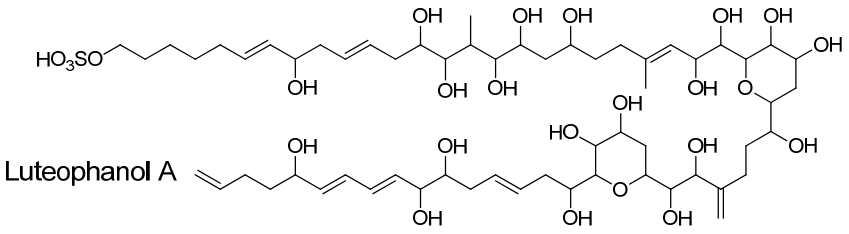

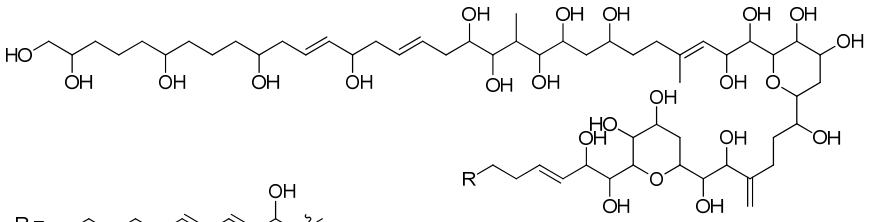

R =

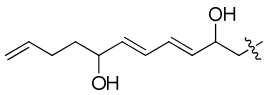

Luteophanol B

R =

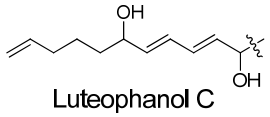

Luteophanol C

R =

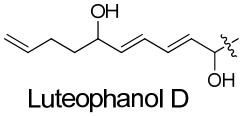

Luteophanol D

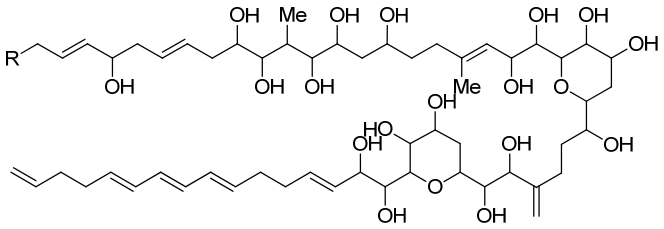

Lingshuiol A: R =

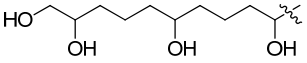

Lingshuiol B: R =

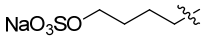

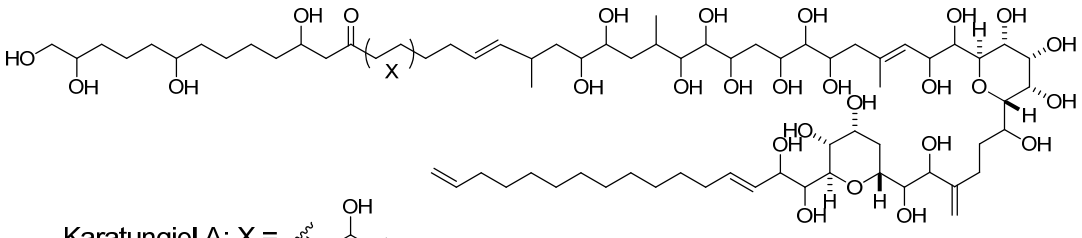

Karatungiol A: X =

Karatungiol B: X =

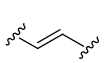

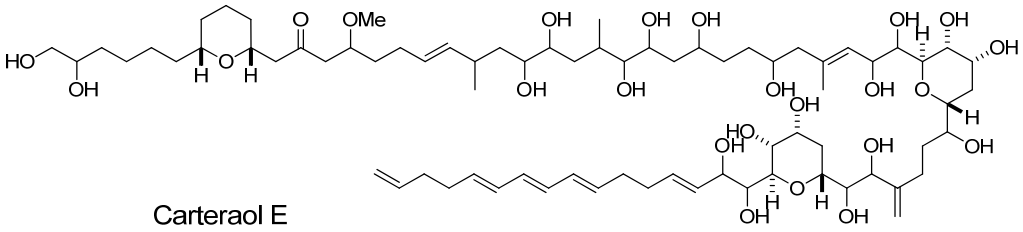

Carteraol E

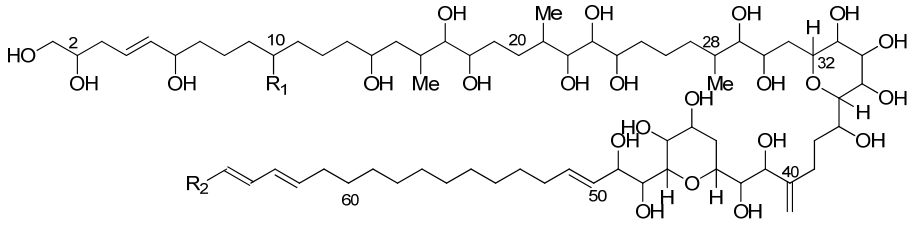

Karlotoxin 1 (KmTx1) $R_1 = OH$; $R_2 = H$
65-E-chloro-KmTx1 $R_1 = OH$; $R_2 = Cl$
10-O-sulfo-KmTx1 $R_1 = OSO_3H$; $R_2 = H$

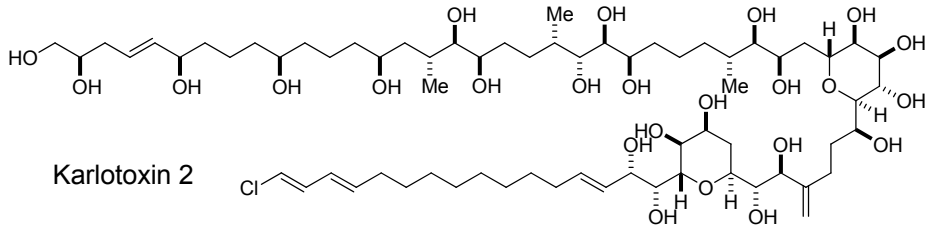

Karlotoxin 2

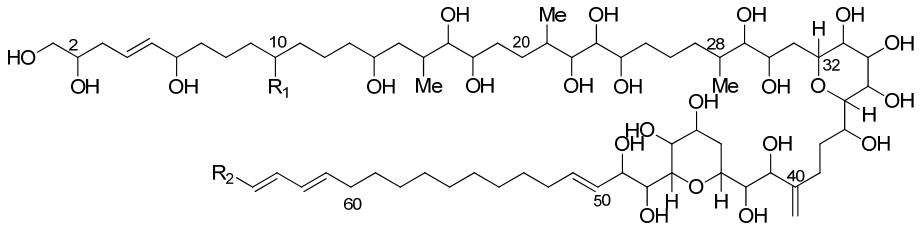

Karlotoxin 3 (KmTx3) $R_1 = OH$; $R_2 = H$
64-E-chloro-KmTx3 $R_1 = OH$; $R_2 = Cl$
10-O-sulfo-KmTx3 $R_1 = OSO_3H$; $R_2 = H$

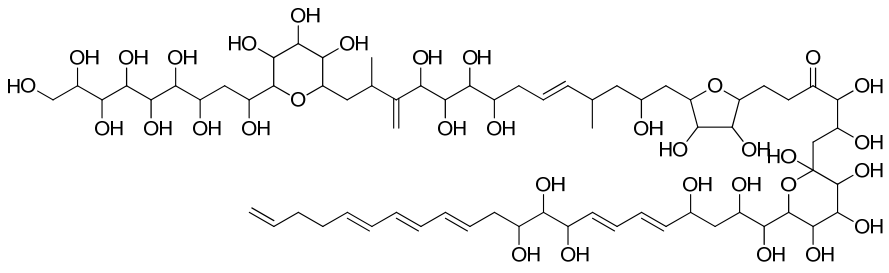

Prorocentrol

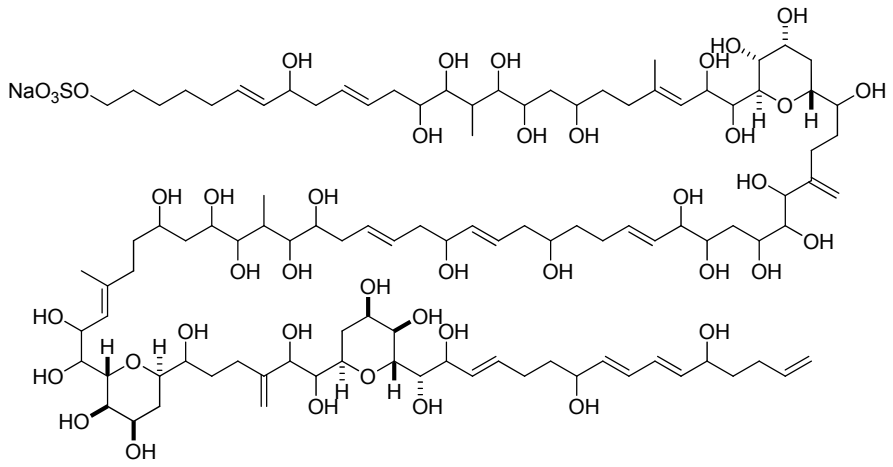

Amdigenol A

4.1.5 Structure-Activity Relationship of Amphidinols

During the course of screening for bioactive metabolites from the cultures of dinoflagelletes, a potent antifungal and hemolytic constituent was isolated and named amphidinol (amphidinol 1 or AM1), a polyhydroxypolyene compound.[28] This compound contained a terminal sulfate ester moiety on its polyhydroxyl part, which was later on demonstrated to have no significant effect or even inhibitory on the activity of these class of compounds based on the isolation and biological evaluation of other AMs lacking the sulfate ester.[34]

With the succeeding isolation of AM7,[32] additional insights into the structure-function relationship in AMs were further obtained mainly because this analog had the shortest polyhydroxyl chain as well as smallest molecular weight among the known AMs, which incidentally also contains a sulfate ester moiety. Specifically, the effect of the length of the polyhydroxyl portion on bioactivity was investigated by preparing a desulfo-AM7 (DsAM7) by hydrolysis of the sulfate ester.[34] Both AM7 and dsAM7 showed antifungal and hemolytic activities albeit weaker compared with AM3, the most potent among the homologs. DsAM7 was slightly more hemolytic than AM6, which possess a long polyhydroxyl chain, but weaker compared with AM3 suggesting that the ideal length of the polyol chain for maximum erythrocyte lysis was that of AM3. Furthermore, the importance of the polyene region on the other side of the molecule was also demonstrated. Both AM14 and AM15, with a hydrophilic dihydroxyl group on the terminal polyene portion, were inactive as hemolytic and antifungal

Table 4-2. Hemolytic and antifungal activities of some amphidinols.[34]

	Hemolytic activity[a] (EC_{50} in µM)	Antifungal activity[b] (MEC in µg/disk)
AM3	0.4	6
AM6	2.9	6
AM7	3.0	10
dsAM7	1.2	8
AM14	>50	>60
AM15	>50	60

[a] against human erythrocytes
[b] against *Aspergillus niger*

Table 4-3. Comparison of the antifungal activites of AM2 and AM3.*

IC_{50} µg/mL	AM2	AM3
Candida albicans	9.73	2.63
Candida glabrata	5.59	1.47
Candida parapsilosis	4.94	3.27
Candida tropicalis	9.77	4.49
Saccharomyces cerevisiae	3.14	0.66
Aspergillus fumigatus	0.24	0.08
Aspergillus flavus	>10	2.88
Aspergillus niger	4.54	1.86

*Results kindly provided by Shionogi Pharmaceutical Company, Osaka, Japan.

agents. This is in contrast to AM7 and dsAM7, their vinyl homologues, which showed activity on both assays. These results highlight the significance of the hydrophobic polyene chain for activity, particularly in the antifungal activities of AM2 and AM3, where the latter has a longer polyene chain. These are summarized in Table 4-2 and 4-3.

In addition, by comparing the activities of AM4 and AM9, it became apparent that location of hydroxyl groups and the terminal double bond did not have any significant adverse nor beneficial effect on their respective activities. Furthermore, the presence of the sulfate ester moiety on the terminal polyhydroxy chain resulted in significantly attenuated activities as shown by AM11, AM12, and AM13. This is in contrast to those of AM2, AM4, and AM9 which differ from the previous three only in the absence of the sulfate ester group.[33] These results are summarized in Table 4-4.

Table 4-4. Biological activites of AM2, AM4, AM9-AM13, and AM17.[33,35]

	Hemolytic activity[a] (μM)	**Antifungal activity[b] (μg/disk)**	**Cytotoxicity[c] (μg/mL)**
AM2	1.16	44.3	14.8
AM4	0.21	58.2	25.3
AM9	0.18	32.9	36.5
AM10	6.53	154	35.2
AM11	28.9	257	23.0
AM12	3.00	>100	26.8
AM13	2.02	132	32.5
AM17	4.90	inactive	not tested

[a] against mouse erythrocytes, except AM17 which was against human erythrocytes
[b] against *Aspergillus niger*
[c] against mouse lymphoid P388 D_1 cells

Lastly, osmotic protection experiments, used to estimate the size of the pore formed by various AMs on erythrocytes, revealed a comparable sized pore formed by AM6, AM7, and

DsAM7.[34] From this data, it can be said therefore that the pore size is not a critical deciding factor for their bioactivities since they had differing hemolytic effects but still forms rather large pores of roughly the same size. In addition, the length of the polyhydroxyl chain also does not greatly influence pore size as AM7, with the shortest polyol chain, had comparable results with AM6, which possesses a longer chain.

4.1.6 Amphidinol – Phospholipid Bilayer Membrane Interactions

The potent antifungal property and hemolytic action of amphidinols are believed to arise from its interaction with the phospholipid membrane ultimately leading to its permeabilization. In addition, studies with artificial membranes demonstrated that AMs bind to them and cause leakage of vesicle contents.[30,49] Investigations in the biological activities of the various amphidinol homologues have revealed significant insights into the role of the polyhydroxy and polyene portions of the molecule in binding and the subsequent permeabilization of the membranes. It was demonstrated that the ideal length of the polyhydroxyl chain for the most efficient lysis of erythrocytes belongs to that of AM3 and that different substitution patterns on this region are not particularly deleterious on the biological activity.[33,34] Furthermore, the presence of a sulfate ester moiety on the terminal polyhydroxy part generally resulted in slight attenuation of their biological action.[35] In contrast, the polyene portion of AMs appears to have a very significant role in their activity, specifically, preserving its hydrophobicity since analogues with dihydroxyl substitution on the terminal polyene region did not exhibit any detectable hemolytic and antifungal properties.[33] In addition, partition coefficients of AMs to vesicles, among which AM3 has the most pronounced partitioning to membrane, clearly highlight the significance of polyolefin region in membrane binding.[49]

The activity of AMs in sterol-containing membrane was also assessed and the initial report on the leakage of calcein entrapped in SUVs induced by AM5 showed a clear sterol dependency: a 27-fold increase in leakage potency was observed upon addition of 33 mol% cholesterol in the membranes.[30] In addition to the hemolytic properties of AMs described in the preceding paragraphs, the diameter of the pore formed by these compounds in erythrocytes was also estimated to be approximately 2 – 2.9 nm, much bigger than that formed by amphotericin B.[50] The membrane permeabilizing properties of AM2 and AM3 in LUVs with varying lipid composition were also investigated by leakage of vesicle-entrapped calcein and showed potent activity on sterol-containing membranes.[51] Both amphidinols did not show activity in vesicles composed of saturated phosphatidylcholines (PC) without sterol. Interestingly, in unsaturated PC without sterol, AM2 still exhibited membrane permeabilizing

action, but not AM3, even at high concentration, which might point out to a possible difference in the mechanism of action of these two molecules (Figure 4-1). Furthermore, sterol content as low as 0.5 mol% is enough to elicit leakage of entrapped dye and the importance of the 3-OH group in sterol was demonstrated since its esterification was inhibitory to the action of AMs. In addition, the activity of AMs was also found to be hardly affected by membrane thickness (Figure 4-2) suggesting marked differences in its mode of action compared with another potent antifungal, amphotericin B; that is AM3 may form toroidal pores. In a recent report using SPR, this higher activity in sterol-containing membranes of AM3 was determined to arise from its higher affinity to ergosterol- and cholesterol-containing membranes compared with sterol-free ones, which was approximated to be about 5300 and 1000 times higher, respectively.[52]

Studies on the conformation of AM3 in micelles and isotropic small bicelles have provided additional basis for its molecular mode of action.[49,53] Findings from these NMR experiments revealed that AM3 takes a hairpin turn around the two tetrahydropyran rings stabilized by hydrogen bonds in amphiphatic environments, with the hydrophilic polyhydroxy region, assumed to be responsible for formation of pores/lesions, predominantly present on the membrane surface while the hydrophobic polyene region, responsible for membrane binding, penetrates the membrane interior. These findings also support the notion of a toroidal pore since in this conformation, AM3 may be too short to span the entire membrane making toroidal pore formation much more feasible.

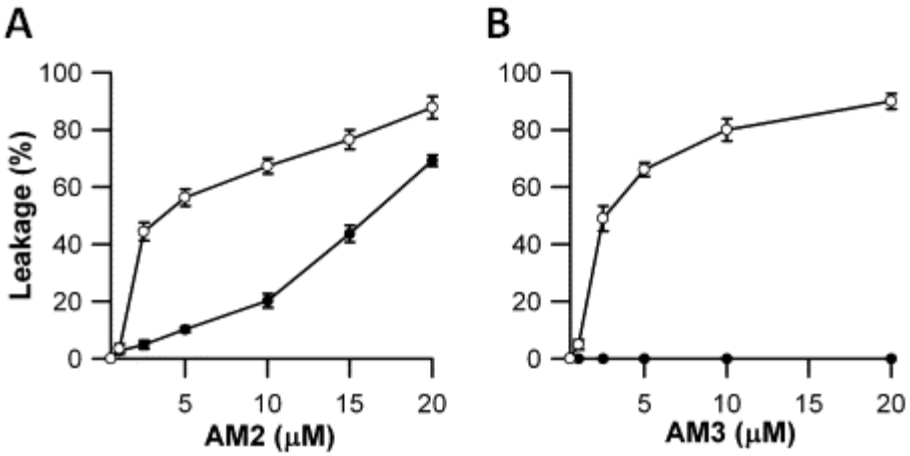

Figure 4-1. Calcein leakage potency of AM2 (A) and AM3 (B) in cholesterol-containing (open circles) and sterol-free (closed circles) POPC liposomes. Phospholipid concentration was 27 μM. Reprinted with permission from *Bioorg. Med.Chem.,* **2008**, 16, 3084-3090.[7] Copyright © (2008) Elsevier.

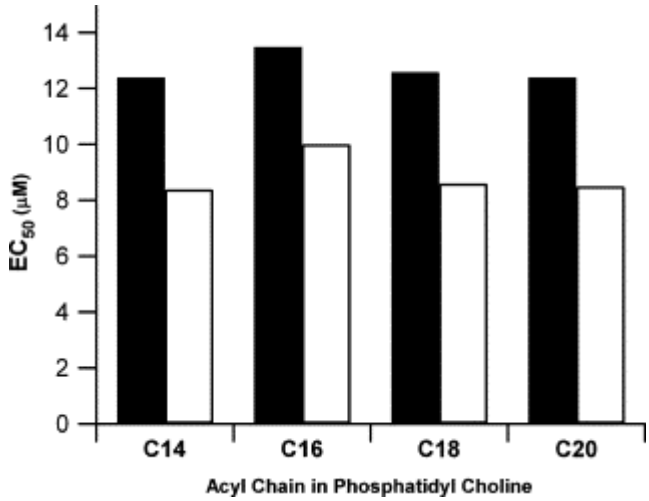

Figure 4-2. Calcein leakage activity of AM2 (filled bars) and AM3 (open bars) in liposomes composed of phosphatidylcholine with varying acyl chain lengths. Reprinted with permission from *Bioorg. Med.Chem.,* **2008**, 16, 3084-3090.[7] Copyright © (2008) Elsevier.

4.1.7 Objectives of this Study on the Mode of Action of Amphidinol 3

Despite these findings, a detailed molecular basis on how AMs recognize sterols on membranes and how the pore/lesion forms in still unclear. For this purpose, the effect of sterol stereochemistry on the membrane permeabilizing activity of AM3 was investigated by observing leakage of trapped dye from liposomes. Activity or inactivity of AM3 towards liposomes with various sterols were then correleated on the basis of its affinity to such membranes using SPR. Furthermore, the presence or absence of direct intermolecular interaction between sterols in membranes and AM3 was also probed with solid state ^{2}H NMR using labeled sterols (Figure 2-3). Finally, to obtain a much more conclusive proof on the initial hypothesis that AM3 may form toroidal pores in membranes, solid state ^{31}P NMR measurements of POPC liposomes, with or without sterol, in the presence or absence of AM3 were carried out. From these data, considerable insights into the mode of membrane action of AM3 were obtained.

4.2 Results and Discussion

4.2.1 Effect of 3α-OH Group on AM3 Activity

As shown in Figure 4-1, the pore-forming activity of AM3 is absolutely dependent on membrane cholesterol, i.e. the absence of which renders the compound inactive.[51] Although SPR results have suggested a functional role of the sterols in increasing AM3 affinity for the membrane,[52] it is still not clear whether this involves direct intermolecular interaction between AM3 and sterol (to be addressed in the next section), or if the stereochemistry of the 3-OH group is critical in the activity. To answer the latter question, calcein leakage measurements were performed with epicholesterol (3α-cholesterol)-containing POPC liposomes and compared with the activity in 3β-hydroxysterol (cholesterol or ergosterol)-containing and pure POPC membranes (for lipid structures, see Figure 2-3). As shown in Figure 4-3, AM3 did not show any significant pore-forming activity in epicholesterol (3α-cholesterol)-containing POPC liposomes; in fact it was almost identical to that in pure POPC membranes. This was in contrast to its high activity in cholesterol- or ergosterol-containing liposomes. These data suggest that membrane permeabilization by AM3, assumed to proceed via formation of pores, also requires that the 3-OH group of sterols be in the β conformation.

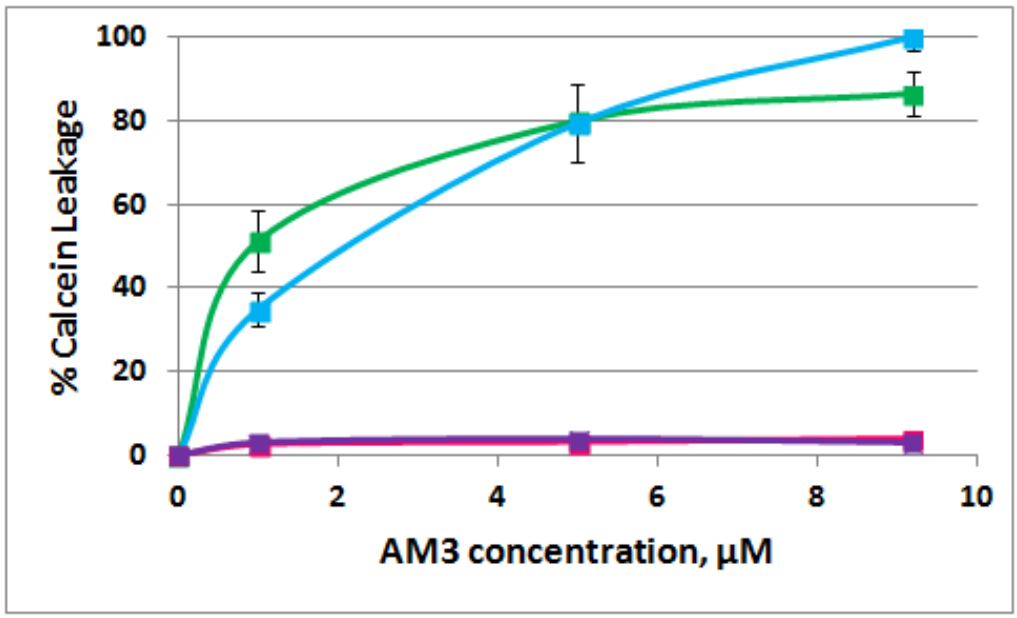

Figure 4-3. AM3-induced calcein leakage from POPC (pink), POPC:cholesterol (green), POPC:ergosterol (blue) and POPC:epicholsterol (purple) liposomes. Mole ratio of POPC:sterol used was 9:1. In all cases, final lipid concentration was 27 µM.

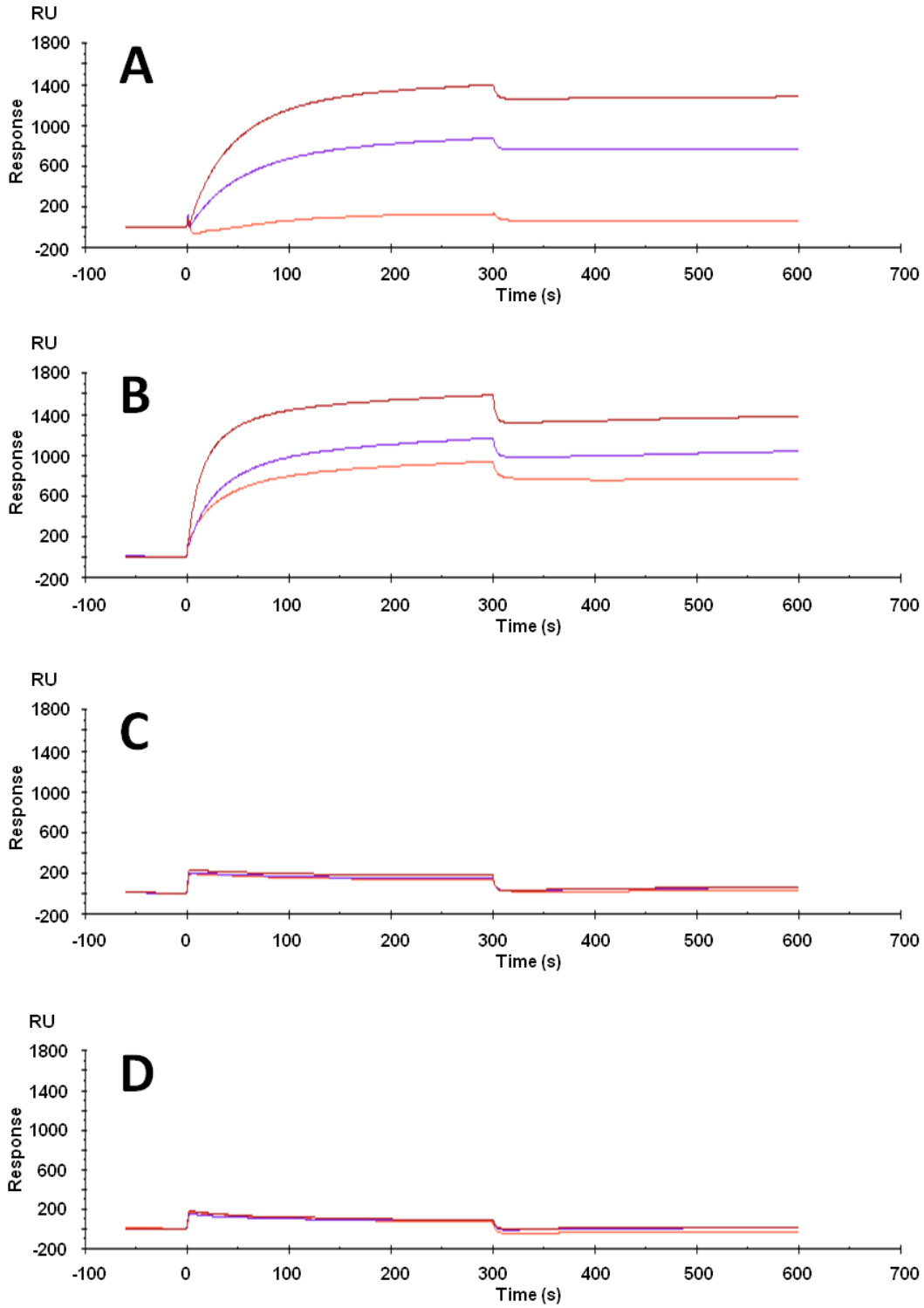

Figure 4-4. SPR sensorgrams for binding of AM3 to liposomes captured on a dodecylamine-modified CM5 sensor chip: (A) 10 mol % cholesterol-containing POPC liposomes, (B) 10 mol % ergosterol-containing POPC liposomes, (C) 10 mol % epicholesterol-containing POPC liposome, and (D) pure POPC liposomes. Sensorgrams correspond to 50 (red), 40 (purple), and 30 (orange) μM AM3.

The absence of pore formation in epicholesterol-containing membranes was also found to be correlated with poor affinity of AM3 towards such liposomes, from a qualitative point of view. This was determined based on SPR experiments using the same protocols as in TNM-A described in Chapter 2.2.1 and 2.2.2, with liposome immobilization levels comparable to that shown in Figure 2-6. Concentration-dependent binding of AM3 was observed in cholesterol- or ergosterol-containing membranes (Figure 4-4A,B) indicating that membrane binding is directly proportional to the concentration of AM3 in the bulk solution, just like TNM-A. Furthermore, as evidenced from RU changes in these two lipid systems, which was approximately 7 seven times as much compared with epicholesterol-containing and pure POPC liposomes (Figure 4-4C,D), it clearly shows the preference of AM3 towards the 3β-hydroxysterols, consistent with the compound's membrane permeabilizing potency shown in Figure 4-3.

4.2.2 Sterol Stereoselectivity of AM3 Viewed by Solid State ^{2}H NMR

Despite preferential binding of AM3 to 3β-hydroxysterol-containing membranes demonstrated by SPR measurement, direct interaction between AM3 and sterols in lipid bilayers cannot be readily assumed to result in the observed increase in membrane affinity. As in the case of TNM-A described in Chapter 2.2.4, solid state ^{2}H NMR experiments were also carried out to obtain evidence of direct interaction between AM3 and different 3-*d*-sterols (Figure 2-3) incorporated into POPC liposomes.

Figure 4-5 shows the spectra of 3-*d*-sterols incorporated into POPC membranes in the absence and presence of AM3. In the absence of AM3 (Figure 4-5A), cholesterol in membranes undergoes fast rotational motion exemplified by the characteristic Pake doublet. This splitting pattern was significantly reduced in the presence of AM3 (Figure 4-5B) implying that molecular motion was considerably inhibited, falling in the range with correlation times of between 10^{-4} and 10^{-5} s.[54] A similar change in the splitting pattern was recorded with 3-*d*-ergosterol (Figure 4-5C,D). These observations were in stark contrast with 3-*d*-epicholesterol where the Pake doublet intensity was comparable, both in the absence and presence of AM3 (Figure 4-5E,F).

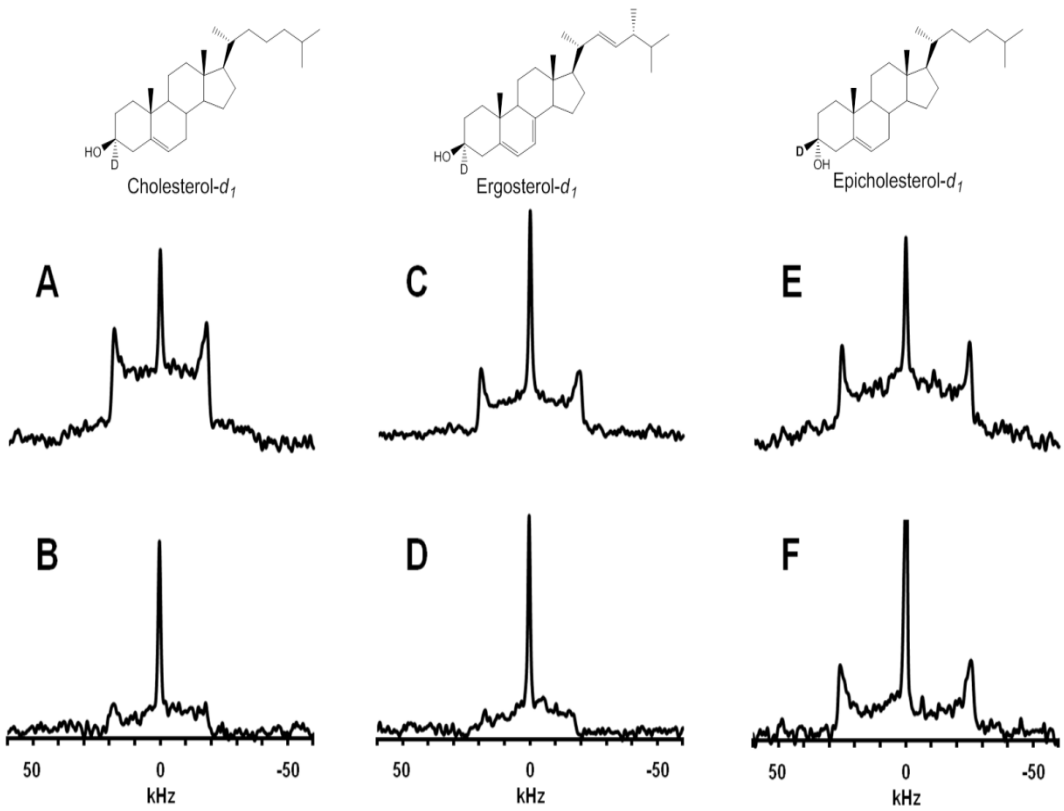

Figure 4-5. ^{2}H NMR spectra of 3-*d*-sterol incorporated into POPC bilayers in the absence (A, C, and E) and presence (B, D, and F) of AM3. 3-*d*-cholesterol (A and B), 3-*d*-ergosterol (C and D), and 3-*d*-epicholesterol (E and F) were used. 3-*d*-sterol:AM3:POPC molar ratios of 1:0:18 (A, C, and E) and 1:1:18 (B, D, and F) were used. Isotropic signals are mostly from residual deuterium water.

These changes in the spectral pattern obtained in the absence and presence of AM3 clearly indicate that the fast rotational motion of both 3-*d*-cholesterol and 3-*d*-ergosterol were considerably inhibited as a result of direct, and significantly stronger, intermolecular interaction between AM3 and these sterols in membranes. In contrast, no noticeable inhibition of fast rotational motion was observed with 3-*d*-epicholesterol indicating a weaker intermolecular interaction between the two molecules. Moreover, these results support the lack of membrane-permeabilizing activity of AM3 (Figure 4-3) and the lower RU response in epicholesterol-containing liposomes as shown by SPR (Figure 4-4) and explicitly demonstrates the direct intermolecular interaction between AM3 and 3β-hydroxysterols in membranes.

4.2.3 Pore Formation by AM3 Viewed by Solid State ^{31}P NMR

The membrane-disrupting activity of AM3 is thought to arise from its interaction with phospholipid bilayers and evidence obtained previously has suggested that AM3 permeabilize the membrane via formation of toroidal pores.[49,51,53] Specifically, the hairpin conformation of AM3, with the polyhydroxy chain located on the membrane surface and the polyene portion penetrating the membrane interior, likely results in the hydrophobic chain of the compound being too short to span the bilayer as in the case of a barrel-stave pore.[49,53] Furthermore, the fact that membrane thickness does not greatly affect AM3 activity supports the notion of toroidal pore formation.[51] To get more conclusive data on whether AM3 forms toroidal pores, the solid state ^{31}P NMR spectra of POPC liposomes with or without sterols were recorded in the absence and presence of AM3. Solid state ^{31}P NMR is a valuable tool to study changes in membrane morphology and phospholipid dynamics. This technique has been extensively utilized to study antimicrobial peptides that form toriodal pores or disrupt the membranes via the carpet mechanism, whose spectra show characteristic isotropic signals.[55-58]

Figure 4-6 and 4-7 shows the solid state ^{31}P NMR spectra of cholesterol- or ergosterol-containing POPC liposomes, respectively, in the absence and presence of AM3. In the absence of AM3 (Figure 4-6A), cholesterol-containing POPC liposomes exhibit typical bilayer lamellar structure as evidenced by the characteristic powder pattern. However, in the presence of 5 mol% AM3 (Figure 4-6B), the spectra hardly changed and no isotropic signals were observed that could suggest phospholipids in a toroidal pore. This was also the case even at a higher AM3 concentration of 15 mol% (Figure 4-6C). A similar observation was recorded in ergosterol-containing POPC liposomes (Figure 4-7A,B) as well as in sterol-free POPC membranes, where it is inactive (Figure 4-8A,B).

AM3, at this sterol concentration (5 mol%), is expected to be active since as low as 0.5 mol% sterol was enough to induce membrane permeabilization,[51] and the lack of distinctive isotropic signals suggests that the compound permeabilizes the membrane without any significant disturbance of the surrounding lipids, in contrast to the assumed toroidal pore model of AM3 action.

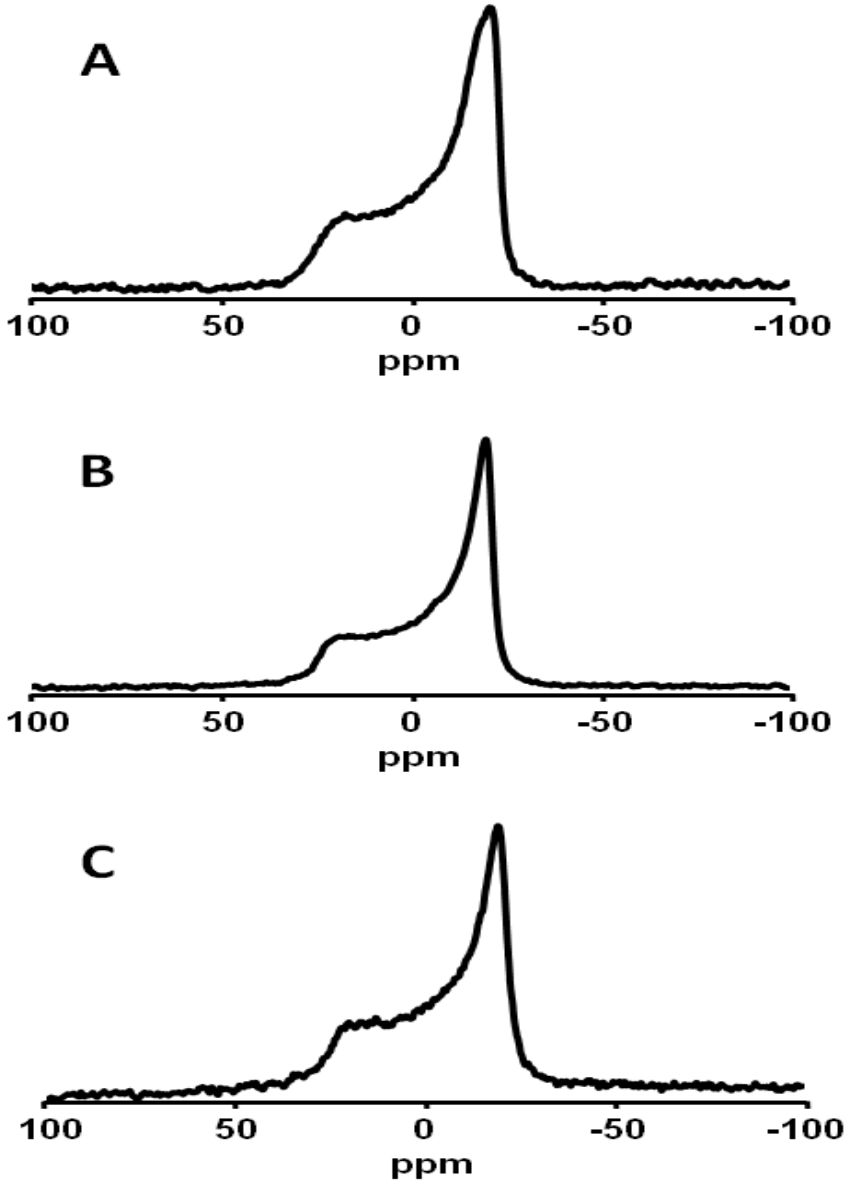

Figure 4-6. ^{31}P NMR spectra of POPC:cholesterol bilayers in the absence (A) and presence (B and C) of AM3. Cholesterol:AM3:POPC molar ratios of 1:0:18 (A), 1:1:18 (B) and 1:3:16 (C) were used.

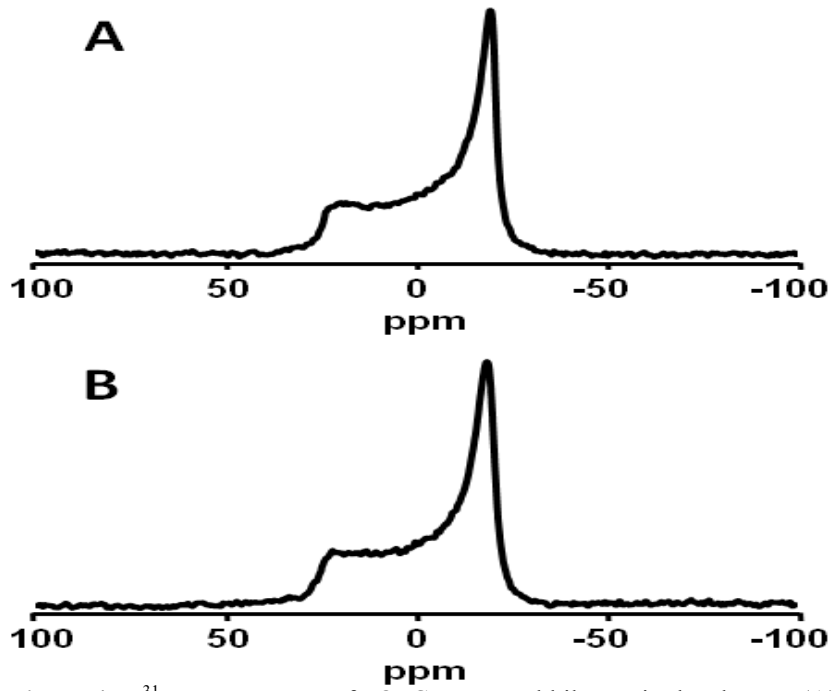

Figure 4-7. ^{31}P NMR spectra of POPC:ergosterol bilayers in the absence (A) and presence (B) of AM3. Ergosterol:AM3:POPC molar ratios of 1:0:18 (A) and 1:1:18 (B) were used.

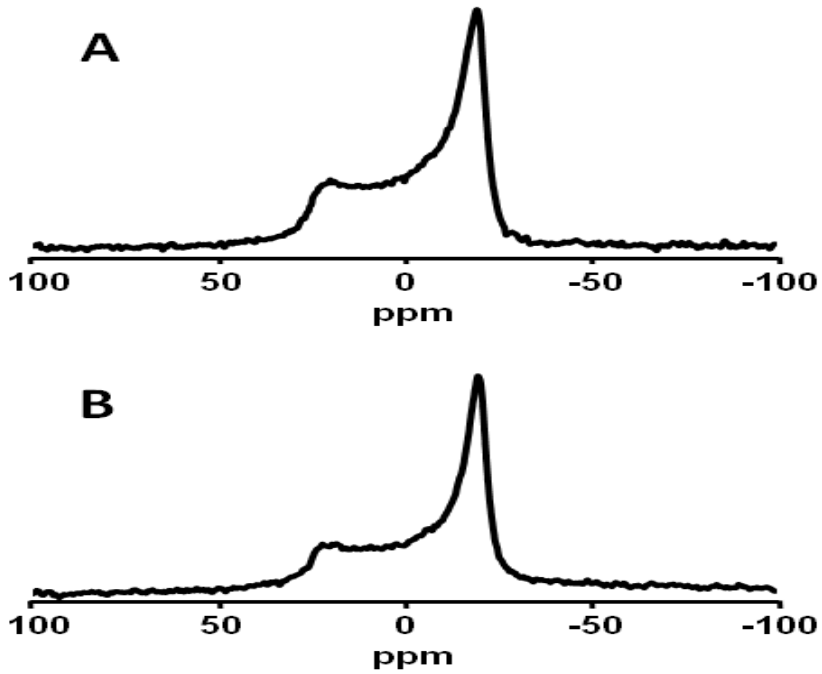

Figure 4-8. ^{31}P NMR spectra of sterol-free POPC bilayers in the absence (A) and presence (B) of AM3. Sterol:AM3:POPC molar ratios of 0:0:18 (A) and 0:1:18 (B) were used.

4.2.4 AM3 - Sterol Bimolecular Interaction and Pore Formation in Lipid Bilayers

Interaction of AMs with phospholipid membranes and subsequent binding is thought to contribute to its observed membrane permeabilizing activity, demonstrated by the compound's ability to release vesicle contents.[30,49] AM3 activity was additionally shown to require the presence of cholesterol or ergosterol in membranes; unlike AM2, which had the activity in the absence of sterols.[51] This was supported by previous SPR experiments detailing a more than 3 orders of magnitude increase in affinity of AM3 towards sterol-containing POPC membranes compared with sterol-free liposomes.[52] Despite these, an in depth understanding of AM3-sterol interaction as well as how the AM3 pore/lesion forms is still lacking. To this end, the effect of the stereochemistry of sterol 3-OH on the membrane permeabilizing activity of AM3 was investigated and direct interaction between sterols and AM3 was demonstrated using solid state ^{2}H NMR. Moreover, the assumption of a toroidal pore being formed by AM3 was evaluated with solid state ^{31}P NMR. It is also worth mentioning that the AM3:lipid molar ratios used in the above experiments were similar (1:27, 1:17, and 1:19 for calcein leakage, lowest concentration in SPR, and both ^{2}H and ^{31}P NMR respectively), thus results may be reasonably compared with one another.

To gain further insight into how AM3 recognizes sterols in membrane, calcein leakage experiments were carried out with POPC liposomes containing epicholesterol (3α-cholesterol). As shown clearly in Figure 4-3, pore formation by AM3 does not just require the presence of a sterol in the membrane, but also of the correct orientation of the 3-OH group: the lack of activity in epicholesterol-containing membranes was almost identical to pure POPC liposomes, in contrast to cholesterol- or ergosterol-containing (3β-hydroxysterol) liposomes. These results reveal the functional role that stereospecific recognition of the 3-OH group plays in formation of pores/lesions by AM3. Pore formation was also closely coupled to the extent of membrane binding as demonstrated by SPR sensorgrams in Figure 4-4. Bound AM3 in cholesterol- or ergosterol-containing membranes were about 7 times as much compared with epicholesterol-containing or pure POPC membranes. This increase in affinity of AM3 towards 3β-hydroxysterol-containing membranes was brought about by direct intermolecular interaction between AM3 and 3β-hydroxysterol as evidenced by characteristic changes in the spectral patterns in solid state ^{2}H NMR spectra (Figure 4-5). Since epicholesterol has its hydroxyl group around the water-membrane interface and thus is still accessible,[59-61] suggests that AM3 stereospecifically and directly recognizes the hydroxyl group of 3β-sterols, probably via hydrogen bonding, in this shallow region resulting in increased AM3 accumulation and subsequent membrane permeabilization. Lack of activity and binding

towards 3α-cholesterol is not surprising as a number of well-known bacterial pore-forming toxins have been demonstrated to be inactive in membranes containing this sterol,[62,63] which accounts for their potent selective toxicity against animal/mammalian cells, which contains 3β-cholesterol. Overall, 3β-sterol exhibits dual effects on the action of AM3: it facilitates both membrane binding and pore/lesion formation.

As described in Chapter 4.1.6, membrane destabilization of AM3 is assumed to follow the toroidal pore model on the basis of its hairpin conformation in membranes and independence of activity on membrane thickness.[49,51,53] This mechanism of pore formation, which has also been described as transient holes prior to membrane collapse in the carpet mechanism (Figure 1-7),[64] shows distinct powder patterns in solid state ^{31}P NMR spectra, e.g. isotropic signals, as was demonstrated for a number of antimicrobial peptides.[55,57,58] Surprisingly, however, no spectral changes were observed in cholesterol- or ergosterol-containing POPC liposomes in the presence of AM3; in fact, the spectra were identical with pure POPC membranes (Figure 4-8). As shown in Figure 4-3, significant membrane destabilization evidenced by calcein leakage was observed at the lowest AM3 concentration tested (1 μM), corresponding to an AM3:lipid molar ratio of 1:27. In the ^{31}P NMR samples, the mole ratio of AM3:lipid was a little higher, at 1:19 (Figure 4-6B and 4-7B), and thus should also result in membrane permeabilization, i.e. changes in spectral patterns should occur, based on its concentration-dependent dye leakage activity (Figure 4-3). Even at a higher AM3:lipid molar ratio of 3:17 (Figure 4-6C) in cholesterol-containing POPC membranes, no noticeable changes in ^{31}P NMR spectrum was observed, undoubtedly indicating that no change in the orientation of a phospholipid headgroup occurs in the presence of AM3.

Previous SPR experiments have suggested that AM3 penetrates the membrane interior of cholesterol- or ergosterol-containing POPC liposomes, based on the sensorgrams' fitting to the two-state reaction model (Figure 2-8 and Equations 6-1 – 6-4).[52] In particular, the formation of the membrane-inserted complex ABx was about 31 times higher in ergosterol-containing POPC membranes than in pure POPC ones as depicted by their respective K_{A2} values.[52] Penetration of AM3 into the hydrophobic core is similar to that observed with amphotericin B, whose pore complex was also stabilized by the presence of cholesterol or ergosterol,[65] but is different from that of TNM-A described in Chapter 2.2. From these previous and current observations, therefore, it is not far-fetched to suggest that membrane insertion and subsequent permeabilization by AM3 does not involve any significant disturbance of the surrounding lipids. In other words, AM3 may not actually form toroidal pores in membranes. A barrel-stave mechanism cannot be ruled out since alamethicin, a

known barrel-stave pore former, also hardly affected the spectra of lipid vesicles in solid state ^{31}P NMR.[58] Although AM3 activity was also independent of membrane thickness, thus the assumption of a toroidal pore,[51] it is worth mentioning that a recent report argues that differentiating the mechanism of action of antimicrobial peptides based on the effect of membrane thickness is an unreliable experimental test.[66] Specfically, mastoparan-X, which disrupts membranes via the toroidal pore/carpet model, exhibited an activity that was much more strongly dependent on bilayer thickness than did the barrel-stave pore-former alamethicin.[66] Another toroidal pore former, colicin E1, was also found to form a larger conductance channel, approximately 2 Å wider, in thicker membranes than in thinner ones.[67] These are in contrast with the prevailing knowledge, which holds that membrane thickness-dependent acitivity is generally supportive of the barrel-stave pore model.[66]

In summary, it was demonstrated that AM3 membrane permeabilizing activity was not only dependent on the presence of sterols in membrane, but more importantly, the 3-OH group must be in the β-configuration. On the basis of SPR measurements, it was likewise shown that membrane binding and affinity of AM3 was lost in epicholesterol-conatining membranes, suggesting a dual role of the 3β-OH group: it serves a critical functional role both in the initial AM3 binding to membrane surface and in the subsequent pore/lesion formation. This enhanced affinity and acitivity towards the 3β-hydroxysterol-containing membranes was explicitly shown to arise from direct intermolecular interaction between AM3 and sterols in membranes as evidenced by characteristic changes in solid state ^{2}H NMR spectral patterns. Finally, solid state ^{31}P NMR data have unambiguously revealed that AM3 perforates the membranes without significant disruption of surrounding lipids, implying a different mechanism of action from the originally proposed toroidal pore model. However, additional experiments will have to be carried out to provide a better picture of the mechanism of AM3 action. To this end, freeze fracture microscopy observations will be useful to probe in more detail the state of AM3 as well as the membrane in the presence of this compound. Similarly, NMR-based experiments may provide significant insights into the nature of AM3-sterol complex in the bilayer environment.

References

1. Garcia Camacho, F.; Gallardo Rodríguez, J.; Sánchez Mirón, A.; Cerón García, M.C.; Belarbi, E.H.; Chrsti, Y.; Molina Grima, E. *Biotech. Adv.* **2007**, 25, 176-194.
2. Guéret, S.M.; Brimble, M.A. *Nat. Prod. Rep.* **2010**, 27, 1350-1366.
3. Hackett, J.D.; Anderson, D.M.; Erdner, D.M.; Bhattacharya, D. *Am. J. Bot.* **2004**, 91, 1523-1534.
4. Kellman, R.; Stüken, A.; Orr, R.J.S.; Svendsen, H.M.; Jakobsen, K.S. *Mar. Drugs.* **2010**, 8, 1011-1048.
5. Moeller, P.D.R.; Beauchesne, K.R.; Huncik, K.M.; Davis, W.C.; Christopher, S.J.; Riggs-Gelasco, P.; Gelasco, A.K. *Environ. Sci. Technol.* **2007**, 41, 1166-1172.
6. Wiese, M.; D'Agostino, P.M.; Mihali, T.K.; Moffitt, M.C.; Neilau, B.A. *Mar. Drugs.* **2010**, 8, 2185-2211.
7. Riobó, P.; Franco, J.M. *Toxicon.* **2011**, 57, 368-375.
8. Nicholson, G.M.; Lewis, R.J. *Mar. Drugs.* **2006**, 4, 82-118.
9. Pérez, S.; Vale, C.; Alonso, E.; Fuwa, H.; Sasaki, M.; Konno, Y.; Goto, T.; Suga, Y.; Vieytes, M.R.; Botana, L.M. *Chem. Res. Toxicol.* **2012**, 25, 1929-1937.
10. Dominguez, H.J.; Paz, B.; Daranas, A.H.; Norte, M.; Franco, J.M.; Fernández, J.A. *Toxicon.* **2010**, 56, 191-217.
11. Otero, A.; Chapela, M.; Atanassova, M.; Vieites, J.M.; Cabado, A.G. *Chem. Res. Toxicol.* **2011**, 24, 1817-1829.
12. Rhodes, L.; Smith, K.; Selwood, A.; McNabb, P.; Munday, R.; Suda, S.; Molenaar, S.; Hallegraeff, G. *Phycologia*. **2011**, 50, 624-628.
13. Leflaive, J.; Ten-Hage, L. *Freshwater Biol.* **2007**, 52, 199-214.
14. Guisande, C.; Frangópulos, M.; Maneiro, I.; Vergara, A.R.; Riveiro, I. *Mar. Ecol. Prog. Ser.* **2002**, 225, 169-176.
15. Wyatt, T.; Jenkinson, I.R. *J. Plankton Res.* **1997**, 19, 551-575.
16. Sheng, J.; Malkiel, E.; Katz, J.; Adolf, J.E.; Place, A.R. *Proc. Natl. Acad. Sci. USA.* **2010**, 107, 2082-2087.
17. Murray, S.; Patterson, D.J. *Eur. J. Phycol.* **2002**, 37, 279-298.
18. Tsuda, M.; Oguchi, K.; Iwamoto, R.; Okamoto, Y.; Kobayashi, J.; Fukushi, E.; Kawabata, J.; Ozawa, T.; Masuda, A.; Kitaya, Y.; Omasa, K. *J. Org. Chem.* **2007**, 72, 4469-4474.
19. Lorente, A.; Lamariano-Merketegi, J.; Albericio, F.; Álvarez, M. Chem. Rev. **In Press**. DOI: 10.1021/cr3004778.

20. Kobayashi, J. *J. Antibiot.* **2008**, 61, 271-284.
21. Tsuda, M.; Oguchi, K.; Iwamoto, R.; Okamoto, Y.; Kobayashi, J.; Fukushi, E.; Kawabata, J.; Ozawa, T.; Masuda, A.; Kitaya, Y.; Omasa, K. *J. Org. Chem.* **2007**, 72, 4469-4474.
22. Oguchi, K.; Tsuda, M.; Iwamoto, R.; Okamoto, Y.; Kobayashi, J.; Fukushi, E.; Kawabata, J.; Ozawa, T.; Masuda, A.; Kitaya, Y.; Omasa, K. *J. Org. Chem.* **2008**, 73, 1567-1570.
23. Kobayashi, J.; Yamaguchi, N.; Ishibashi, M. *Tetrahedron Lett.* **1994**, 35, 7049-7050.
24. Kubota, T.; Endo, T.; Takahashi, Y.; Tsuda, M.; Kobayashi, *J. J. Antibiot.* **2006**, 59, 512-516.
25. Kobayashi, J.; Kubota, T.; Takahashi, M.; Ishibashi, M.; Tsuda, M.; Naoki, H. *J. Org. Chem.* **1994**, 64, 1478-1482.
26. Kubota, T.; Tsuda, M.; Takahashi, M.; Ishibashi, M.; Naoki, H.; Kobayashi, J. *J. Chem. Soc., Perkin Trans. 1*. **1999**, 3483-3487.
27. Kubota, T.; Tsuda, M.; Takahashi, M.; Ishibashi, M.; Oka, S.; Kobayashi, J. *Chem. Pharm. Bull.* **2000**, 48, 1447-1451.
28. Satake, M.; Murata, M.; Yasumoto, T.; Fujita, T.; Naoki, H. *J. Am. Chem. Soc.* **1991**, 113, 9859-9861.
29. Paul, G.K.; Matsumori, N.; Murata, M.; Tachibana, K. *Tetrahedron Lett.* **1995**, 36, 6279-6282.
30. Paul, G. K.; Matsumori, N.; Konoki, K.; Murata, M.; Tachibana, K. *J. Mar. Biotechnol.,* **1997**, *5*, 124-128.
31. Murata, M.; Matsuoka, S.; Matsumori, N.; Paul, G.K.; Tachibana, K. *J. Am. Chem. Soc.* **1999**, 121, 870-871.
32. Morsy, N.; Matsuoka, S.; Houdai, T.; Matsumori, N.; Adachi, S.; Murata, M.; Iwashita, T.; Fujita, T. *Tetrahedron.* **2005**, 61, 8606-8610.
33. Echigoya, R.; Rhodes, L.; Oshima, Y.; Satake, M. *Harmful Algae.* **2005**, 4, 383-389.
34. Morsy, N.; Houdai, T.; Matsuoka, S.; Matsumori, N.; Adachi, S.; Oishi, T.; Murata, M.; Iwashita, T.; Fujita, T. *Bioorg. Med. Chem.* **2006**, 14, 6548-6554.
35. Meng, Y.; Van Wagoner, R.M.; Misner, I.; Tomas, C.; Wright, J.L.C. *J. Nat. Prod.* **2010**, 73, 409-415.
36. Doi, Y.; Ishibashi, M.; Nakamichi, H.; Kosaka, T.; Ishikawa, T.; Kobayashi, J. *J. Org. Chem.* **1997**, 62, 3820-3823.
37. Kubota, T.; Tsuda, M.; Doi, Y.; Takahashi, A.; Nakamichi, H.; Ishibashi, M.; Fukushi, E.; Kawabata, J.; Kobayashi, J. *Tetrahedron.* **1998**, 54, 14455-14464.

38. Kubota, T.; Takahashi, A.; Tsuda, M.; Kobayashi, J. *Mar. Drugs.* **2005**, 3, 113-118.
39. Huang, X.C.; Zhao, D.; Guo, Y.W.; Wu, H.M.; Trivellone, E.; Cimino, G. *Tetrahedron Lett.* **2004**, 45, 5501-5504.
40. Qi, X.M.; Yu, B.; Huang, X.C.; Guo, Y.W.; Zhai, Q.; Jin, R. *Toxicon.* **2007**, 50, 278-282.
41. Hanif, N.; Ohno, O.; Kitamura, M.; Yamada, K.; Uemura, D. *J. Nat. Prod.* **2010**, 73, 1318-1322.
42. Washida, K.; Koyama, T.; Yamada, K.; Kita, M.; Uemura, D. *Tetrahedron Lett.* **2006**, 47, 2521-2525.
43. Huang, S.J.; Kuo, C.M.; Lin, Y.C.; Chen, Y.M.; Lu, C.K. *Tetrahedron Lett.* **2009**, 50, 2512-2515.
44. Van Wagoner, R.M.; Deeds, J.R.; Satake, M.; Ribeiro, A.A.; Place, A.R.; Wright, J.L.C. *Tetrahedron Lett.* **2008**, 49, 6457-6461.
45. Van Wagoner, R.M.; Deeds, J.R.; Tatters, A.O.; Place, A.R.; Tomas, C.R.; Wright, J.L.C. *J. Nat. Prod.* **2010**, 73, 1360-1365.
46. Peng, J.; Place, A.R.; Yoshida, W.; Anklin, C.; Hamann, M.T. *J. Am. Chem. Soc.* **2010**, 132, 3277-3279.
47. Sugahara, K.; Kitamura, Y.; Murata, M.; Satake, M.; Tachibana, K. *J. Org. Chem.* **2011**, 76, 3131-3138.
48. Inuzuka, T.; Yamamoto, Y.; Yamada, K.; Uemura, D. *Tetrahedron Lett.* **2012**, 53, 239-242.
49. Houdai, T.; Matsuoka, S.; Morsy, S.; Matsumori, N.; Satake, M.; Murata, M. *Tetrahedron.* **2005**, 61, 2795-2802.
50. Houdai, T.; Matsuoka, S.; Matsumori, N.; Murata, M. *Biochim. Biophys. Acta.* **2004**, *1667*, 91-100.
51. Morsy, N.; Houdai, T.; Konoki, K.; Matsumori, N.; Oishi, T.; Murata, M. *Bioorg. Med. Chem.* **2008**, 16, 3084-3090.
52. Swasono, R.T.; Mouri, R.; Morsy, N.; Matsumori, N.; Oishi, T.; Murata, M. *Bioorg. Med. Chem. Lett.* **2010**, 20, 2215-2218.
53. Houdai, T.; Matsumori, N.; Murata, M. *Org. Lett.* **2008**, 10, 4191-4194.
54. Matsumori, N.; Tahara, K.; Yamamoto, H.; Morooka, A.; Doi, M.; Oishi, T.; Murata, M. *J. Am. Chem. Soc.* **2009**, 131, 11855-11860.
55. Ramamoorthy, A.; Thennarasu, S.; Lee, D-K.; Tan, A.; Maloy, L. *Biophys. J.* **2006**, 91, 206-216.
56. Hallock, K.J.; Lee, D-K.; Ramamoorthy, A. *Biophys. J.* **2003**, 84, 3052-3060.

57. Bechinger, B. *Biochim. Biophys. Acta.* **2005**, 1712, 101-108.
58. Bertelsen, K.; Dorosz, J.; Hansen, S.K.; Nielsen, N.C.; Vosegaard, T. *PLOS One.* **2012**, 7, e47745.
59. Kessel, A.; Ben-Tal, N.; May, S. *Biophys. J.* **2001**, 81, 643-658.
60. Róg, T.; Pasenkiewicz-Gierula, M. *Biophys. J.* **2003**, 84, 1818-1826.
61. Róg, T.; Pasenkiewicz-Gierula, M.; Vattulainen, I. Karttunen, M. *Biochim. Biophys. Acta.* **2009**, 1788, 97-121.
62. Ikigai, H.; Otsuru, H.; Yamamoto, K.; Shimamura, T. *Microbiol. Immunol.* **2006**, 50, 751-757.
63. Flanagan, J.J.; Tweten, R.K.; Johnson, A.E.; Heuck, A.P. *Biochemistry.* **2009**, 48, 3977-3987.
64. Shai, Y. *Biopolymers.* **2002**, 66, 236-248.
65. Mouri, R.; Konoki, K.; Matsumori, N.; Oishi, T.; Murata, M. *Biochemistry.* **2008**, 47, 7807-7815.
66. Bobone, S.; Roversi, D.; Giordano, L.; De Zotti, M.; Formaggio, F.; Toniolo, C.; Park, Y.; Stella, L. *Biocehmistry.* **2012**, 51, 10124-10126.
67. Sobko, A.A.; Kotova, E.A.; Antonenko, Y.N.; Zakharov, S.D.; Cramer, W.A. *J. Biol. Chem.* **2006**, 281, 14408-14416.

Chapter 5

Conclusions

Theonellamides (TNMs) and amphidinols (AMs) are among the several promising marine natural products that may find potential use as efficient therapeutic agents.

Theonellamides are bicyclic dodecapeptides isolated from the marine sponge *Theonella* sp. that exhibit potent antigfungal and cytotoxic activities, with the former attributed to its stereospecific interaction with 3β-hydroxysterol, in particular ergosterol, in fungal membranes. Amphidinols, on the other hand, are polyketide metabolites from the dinoflagellate *Amphidinium klebsii* whose unique structure is characterized by linear polyhydroxyl and polyene chains, separated by an aliphatic region containing two tetrahydropyran rings. Amphidinols are believed to exert their antifungal and cytotoxic action by interacting with the phospholipid bilayer; in particular, amphidinol 3 requires the presence of membrane-embedded sterols. This unique structure of amphidinols, lacking nitrogenous macrocylces present in other antifungals, makes them novel tools to probe the mechanism of antifungal action.

From this study, comparison between the probable mechanism of action of TNM-A and AM3 is possible and the following conclusions can be made:

1. SPR experiments using a dodecylamine-modified CM5 sensor chip demonstrated the preference of both TNM-A and AM3 towards cholesterol- or ergosterol (3β-hydroxyterol)- containing POPC liposomes over epicholesterol (3α-cholesterol)-containing ones.
2. In the case of TNM-A, two state reaction model clearly showed that the presence of 3β-hydroxyterols significantly enhance binding to the membrane surface (first step), but membrane insertion (second step) proceeds and is not significantly affected by the presence or absence of sterol.
3. For both TNM-A and AM3, the increase in membrane affinity was due to direct intermolecular interaction with 3β-hydroxyterols as evidenced by characteristic changes in splitting patterns from solid state ^{2}H NMR suggesting a critical role played by the 3β-OH moiety.
4. TNM-A most likely disrupts membranes not by distinct pore formation, but rather via membrane deformations or morphological changes which explains its moderate

activity in calcein lekagae assay in both sterol-free and sterol-containing membranes; this is in contrast with AM3 that exhibits very potent dye leakage property, which was further shown to require the presence of not just sterols in membranes, but 3β-hydroxysterols. This implies a dual role for 3β-OH group in AM3 action: membrane binding and pore formation.

5. Membrane disruption and morphological changes induced by TNM-A were clearly observed using differential interference and confocal microscopy supporting the dye leakage results. This was also consistent with the observations of solid state ^{31}P NMR which revealed the presence of isotropic signals both in sterol-free and sterol-containing liposomes indicating disruption of phospholipid packing.
6. Unlike TNM-A, the presence of AM3 in membrane does not involve any significant disruption of surrounding phospholipids in 3β-hydroxysterol-containing membranes, explicitly shown based on the absence of isotropic signals from solid state ^{31}P NMR. These results contradict the earlier hypothesis of a toroidal pore formed by AM3 to account for its membrane permeabilizng action, and thus imply a different mode of action for this compound.

Chapter 6

Experimental Section

6.1 Materials

Salt for artificial seawater, Marin Art Hi® was from Tomita Pharmaceutical. (Osaka, Japan) and silica gel YMC ODS-AQ was from YMC Co. (Kyoto, Japan). Glass plates coated with 60 F_{254} silica gel or RP-18 F_{254} were used for normal phase or reverse phase thin layer chromatography (TLC), respectively. NMR solvents CD_3OD and D_2O were from Merck (Darmstadt, Germany), while DMSO-d_6 was from Euriso-Top (Saint-Aubin Cedex, France). Deuterium-depleted water was from Isotec Inc (St. Louis, MO, USA). 1-palmitoyl-2-oleoyl-*sn*-glycero-3-phosphocholine (POPC) was purchased from NOF Corporation (Tokyo, Japan), Cholesterol, chloroform, methanol (MeOH), 1-propanol (1-PrOH), 2-propanol, 1-butanol, ethyl acetate, acetonitrile, sodium chloride (NaCl), potassium chloride (KCl), disodium hydrogen phosphate, potassium dihydrogen phosphate, sodium nitrate, tris(hydroxymethyl)aminoethane, magnesium sulfate (anhydrous), zinc sulfate heptahydrate, cyanocobalamin (Vitamin B_{12}), biotin (Vitamin H), thiamine hydrochloride (Vitamin B_1), triton X-100, and Celite® 545RVS were purchased from Nacalai Tesque, Inc. (Kyoto, Japan). Ergosterol and disodium ethylenediamine tetraacetic acid were purchased from Tokyo Chemical Industry Co., Ltd. (Tokyo, Japan). Disodium β-glycerophsphtae *n* hydrate, boric acid, cobalt (II) sulfate hexahydrate, and Phospholipid C-Test were from Wako Pure Chemical Industries, Ltd. (Osaka, Japan). 1-Ethyl-3-[3-(dimethylamino)propyl]carbodiimide hydrochloride (EDC), *N*-hydroxysuccinimide (NHS), 10 mM acetate buffer (pH 5.0), 1 M ethanolamine (pH 8.5), 50 mM sodium hydroxide (NaOH), 0.5% (w/v) sodium dodecyl sulfate (SDS), and 10× PBS buffer (pH 7.4) were purchased from GE Healthcare (Uppsala, Sweden). Dodecylamine and dimethyl sulfoxide (DMSO) were purchased from Sigma-Aldrich Co. (St. Louis, MO). Calcein and iron (III)-ethylenediamine tetraacetic acid were from Dojindo Laboratories (Kumamoto, Japan). Epicholesterol was obtained from Steraloids Inc. (Newport, RI, USA). All of these chemicals were of the highest grade and used without further purification. Water was purified with a Millipore Simpli Lab System (Millipore Inc., Bedford, MA). 3-*d*-Cholesterol, 3-*d*-ergosterol, and 3-*d*-epicholesterol (Figure 2-3) and fluorescein-labeled TNM-A (Figure 3-1) were synthesized as previously reported.[1-3]

6.2 Instruments

HPLC System	:	Shimadzu SCL-10Avp, SPD-M10Avp, LC-10ADvp, LC-10ADvp, DGU-12A
UV Spectrophotometer	:	Shimadzu UV-2500 JASCO V-630 BIO
Spectrofluorometer	:	JASCO FP-6500
Mass Spectrometer	:	Thermo Finnigan LCQ Deca XP Thermo Scientific LTQ Orbitrap XL
NMR Spectrometer	:	JEOL ECA400, ECS400 Varian Chemagnetics CMX300 Bruker AVANCE700
Surface Plasmon Resonance	:	GE Healthcare Biacore™ T200
Particle Size Analyzer	:	Horiba LB-550
Microplate Reader	:	Molecular Devices Emax
Clean Bench	:	Sanyo MCV-710ATS
Confocal Microscope	:	Olympus FluoView™ FV1000-D
Autoclave	:	TOMY BS-325, LSX-500
Water Purifying Apparatus	:	Millipore Elix-UV, Simpli Lab
Electronic Balance	:	A&D GR-202,HF-3200
pH Meter	:	TOA HM-40S
Rotary Evaporator	:	Technosigma N-1000, Iwaki Thermo Bath THB-3N; EYELA COOL ACE CA-1111, NVC-2000
Centrifuge	:	WEALTEC KUBOTA5200 Hitachi Himac CF 15R, CR 22GIII
Lyophilizer	:	EYELA FDU-1200, FDU-2200
Vortex Mixer	:	Scientific Industries VORTEX GENIE-2
Sonicator	:	Yamato BRANSON 1510
Micropipette	:	Nichiryo Nichipet EX

6.3 Methods

6.3.1 Isolation of Theonellamide A

TNM-A (20 mg) was a kind gift from Dr. Shinichi Nishimura (Kyoto University) while subsequent sample was isolated as reported previously, summarized in Scheme 6-1.[4]

Briefly, the sponge (provided by Prof. Shigeki Matsunaga, The University of Tokyo) was homogenized using a blender. It was then soaked in a mixture of 1-PrOH:H_2O (2:1 v/v) overnight. Celite was then added and mixed extensively. The sample was filtered using a Buchner funnel and the residue was washed several times with 1-PrOH:H_2O (2:1 v/v). The filtrate and washings were combined and 1-propanol was removed using a rotary evaporator. The aqueous mixture was charged in an ODS column and then subjected to HPLC purification to afford 10 mg TNM-A.

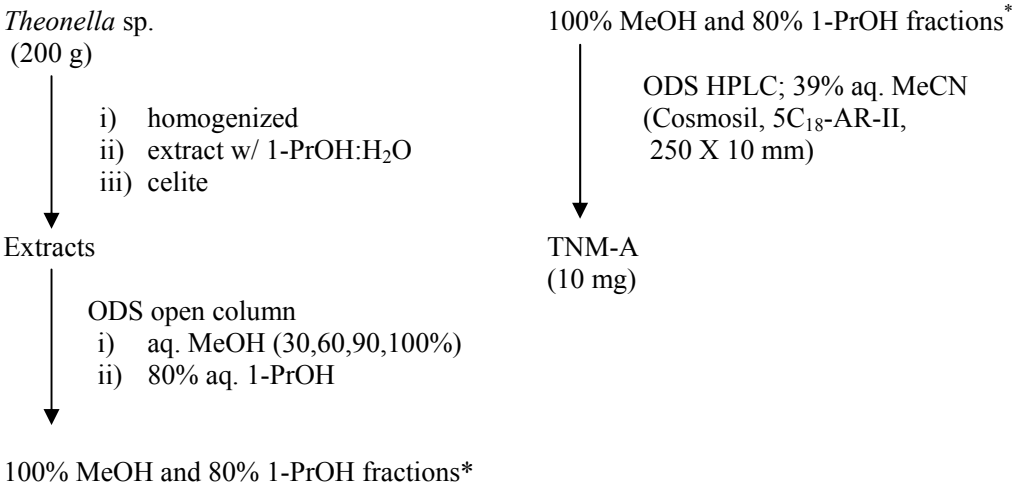

Scheme 6-1. Schematic diagram of TNM-A isolation from sponge.

6.3.2 TNM-A Liquid Chromatography Using an Open Column and HPLC

The aqueous extract (Scheme 6-1), after removing 1-PrOH by a rotary evaporator, was charged to an ODS open column (YMC Gel ODS-AQ; 12 X 2 cm) and initially washed with H_2O. It was then eluted with increasing ratio of MeOH in H_2O (30, 60, 90, and 100%) followed by 80% 1-PrOH in H_2O. TNM-A was found to be mostly in the latter two fractions. After evaporation of the solvent, the residues containing TNM-A were dissolved in MeOH and subjected to further purification by HPLC.

Two pre-packed columns (Cosmosil, 5C_{18}-AR-II, 250 X 10 mm) were connected in series on a Shimadzu HPLC system. 25 µL of the TNM-A containing mixture was injected for each separation. Eluent used was aqueous acetonitrile (39%), which was first degassed using a sonicator. Flow rate was 2 mL/min. TNM-A was collected with a retention time of 12 min (Figure 6-1 and 6-2).

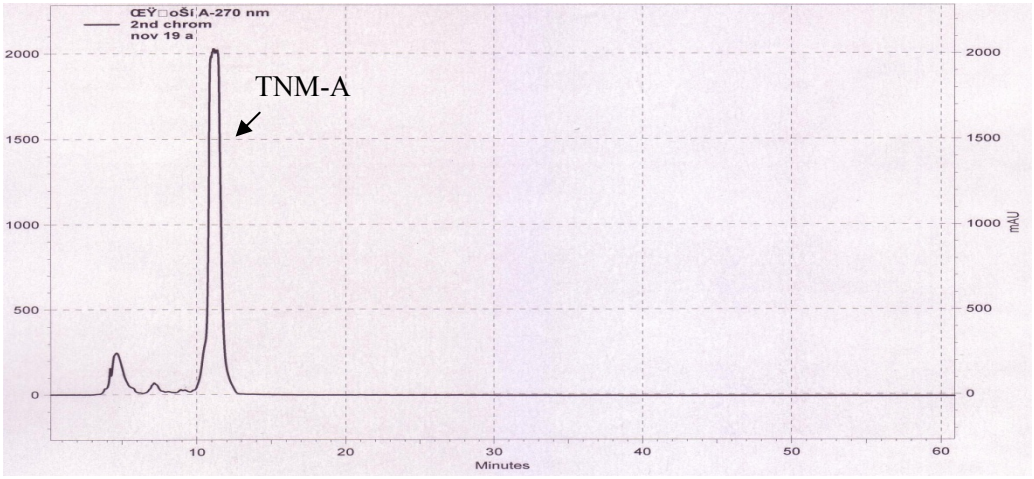

Figure 6-1. Typical chromatogram of TNM-A isolation.

Figure 6-2. UV spectrum of TNM-A obtained from HPLC purification with retention time of 12 min.

6.3.3 Culture of *Amphidinium klebsii*

The dinoflagellate *Amphidinium klebsii* was originally isolated from the surface wash of seaweeds collected from Aburatsubo-Bay, Miura Peninsula, Japan and deposited in the Microbial Culture Collection of the National Institute for Environmental Studies having the identification code NIES 613.[5] Identification of the species was previously carried out by Prof. Y. Fukuyo (Faculty of Agriculture, The University of Tokyo).

Table 6-1. Composition of ES-1 supplement.

Ingredients	Volume or Weight
Artificial sea water	1000 mL
$NaNO_3$	70 mg
Na_2-β-glycerophosphate	10 mg
Tris(hydroxymethyl)aminomethane	100 mg
H_3BO_3	1 mg
$MgSO_4$	200 µg
$ZnSO_4$	25 µg
Na_2-EDTA	5 mg
Fe(III)-EDTA	550 µg
$CoSO_4$	1 µg
Cyanocobalamin (Vitamin B_{12})	2 µg
Biotin (Vitamin H)	1 µg
Thiamine-HCl (Vitamin B_1)	100 µg

Amphidinium klebsii was grown unialgally in 2- or 3-L flasks using artificial seawater (Marin Art Hi, Tomita Pharmaceutical, 3% w/v) enriched with ES-1 supplement (Table 6-1) at 25 ^{o}C for 3-4 weeks under a 16-8 light-dark photocycle (Figure 6-3). The cells were then harvested by filtration and subjected to AM3 isolation.

Figure 6-3. Culture of the dinoflagellate *A. klebsii* in artificial seawater enriched with ES-1 supplement.

Large scale, 1000 liters, culturing of dinoflagellates was also carried out with the assistance of Prof. Masashi Tsuda (Kochi University) using sterile seawater enriched with Pravasoli's ES (PES) supplement (Table 6-2), added to a final concentration of 1% (v/v), at 22 ~ 28 ^{o}C under a 16-8 light-dark photocycle (light intensity at 3000 lux) with constant stirring. *A.klebsii* was first grown in a 10-L medium for two weeks, then transferred to a 200-L medium for another two weeks, and finally to a 1000-L medium for three weeks (Figure 6-4), after which the cells were harvested. Briefly, the culture medium was filtered and concentrated with a MOLSEP® Fiber FS03-FC-FUS1582 (Daicen Membrane-Systems Ltd., Tokyo, Japan) shown in Figure 6-5. The cell concentrate (~80 L) was centrifuged at 5000 rpm, 20 ºC for 2-3 hours using a Hitachi CR 22GIII high speed refrigerated centrifuge (Hitachi Koki Co., Ltd., Tokyo, Japan) to facilitate sedimentation of the cells (Figure 6-6). Water removed from centrifugation was observed under a microscope to ensure that no cells remained in the supernatant.

Table 6-2. Composition of PES supplement.*

Ingredients	Volume or Weight
Distilled water	1000 mL
$NaNO_3$	3.5 g
Na_2-glycerophosphate	500 mg
Tris	5 g
Fe (as EDTA; 1:1 mol)	25 mg
PII solution of metals	250 mL
Cyanocobalamin (Vitamin B_{12})	100 mg
Biotin (Vitamin H)	50 mg
Thiamine-HCl (Vitamin B_1)	5 mg

* pH = 7.8

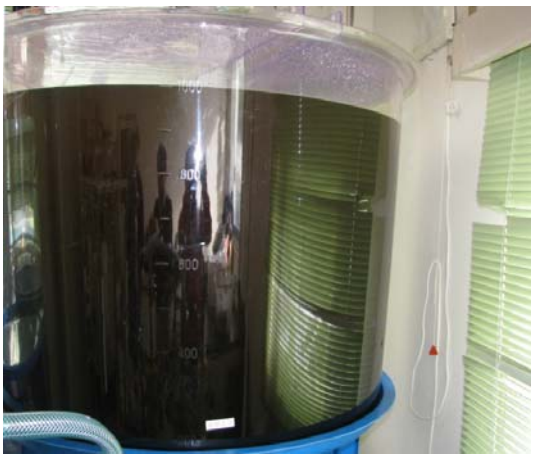

Figure 6-4. Culture of the dinoflagellate *A. klebsii* in 1000-L seawater enriched with PES supplement.

Figure 6-5. Filtration and concentration of *A. klebsii*.

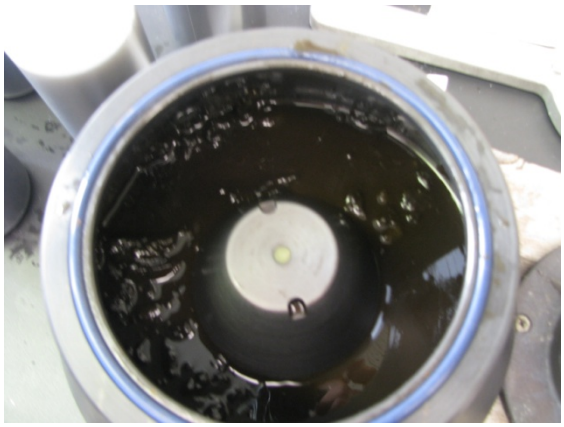

Figure 6-6. *A. klebsii* cells collected after centrifugation.

6.3.4 Isolation of Amphidinol 3

Amphidinol 3 was isolated from harvested cells as reported previously,[6] summarized in Scheme 6-2, corresponding to 198 L and ~200 L of the small and large scale (about 20% of total weight of cells collected) cultures, respectively. Briefly, cells were extracted with MeOH twice, followed by 50% aq. MeOH once, and the solvent was removed with a rotary evaporator at 30 ºC until about 200 mL mixture remained. Then, an excess of lead acetate was added to remove most of the coloring materials/pigments in the mixture, after which excess

lead was removed with an equal volume of Na_2HPO_4. The resulting supernatant was partitioned between H_2O/EtOAc, and the aqueous layer further partitioned between 1-BuOH/H_2O. The organic layer was collected, dried, and charged into an ODS open column. The AM3-containing fractions were then purified by HPLC to afford 27.2 mg and 4.7 mg AM3 from the small and large scale culture media, respectively.

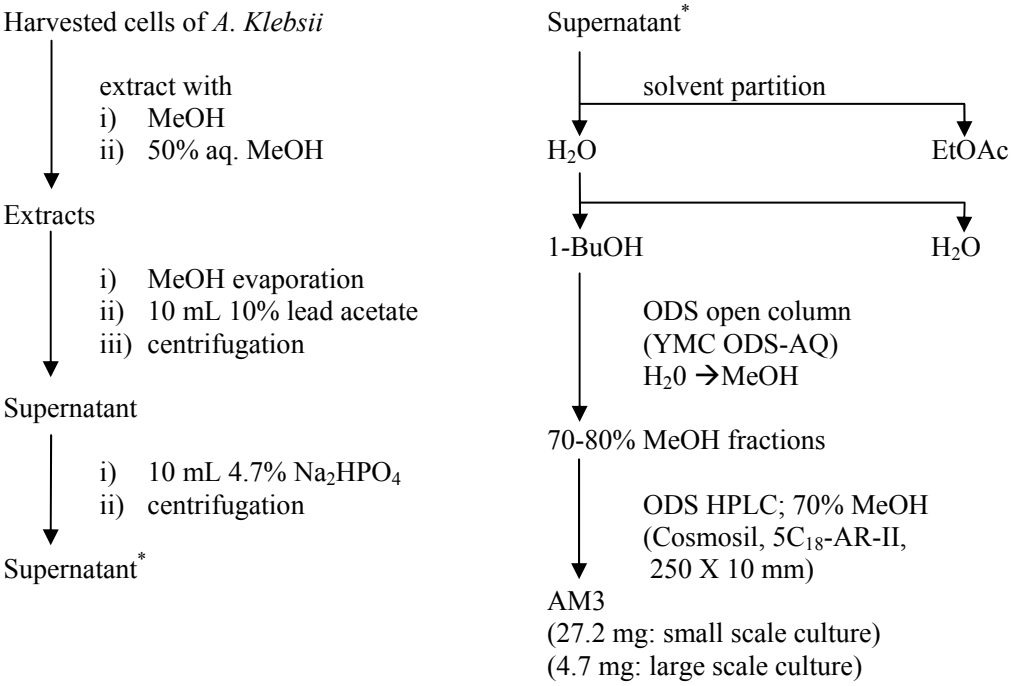

Scheme 6-2. Schematic diagram of AM3 isolation from harvested *A. klebsii* cells.

6.3.5 AM3 Liquid Chromatography Using an Open Column and HPLC

The residue from the 1-BuOH layer (Scheme 6-2) was dissolved in a few mL of H_2O and charged to an ODS open column (YMC Gel ODS-AQ; 12 X 2 cm). The ODS column was initially washed with 3 column volumes of H_2O prior to sample introduction. It was then eluted with increasing ratio of MeOH in H_2O (0 to 100%). AM3 was found to be mostly in the 70 and 80% aq. MeOH fractions. After evaporation of the solvent, the residues containing AM3 were dissolved in MeOH and subjected to further purification by HPLC.

Two pre-packed columns (Cosmosil, $5C_{18}$-AR-II, 250 X 10 mm) were connected in series on a Shimadzu HPLC system. 30 µL of the AM3- containing mixture was injected for each separation. Isocratic elution was carried out using 70% aq. MeOH, which was first

degassed using a sonicator. Flow rate was 1.5 mL/min. AM3 was collected with a retention time of about 60-65 min (Figure 6-7 and 6-8).

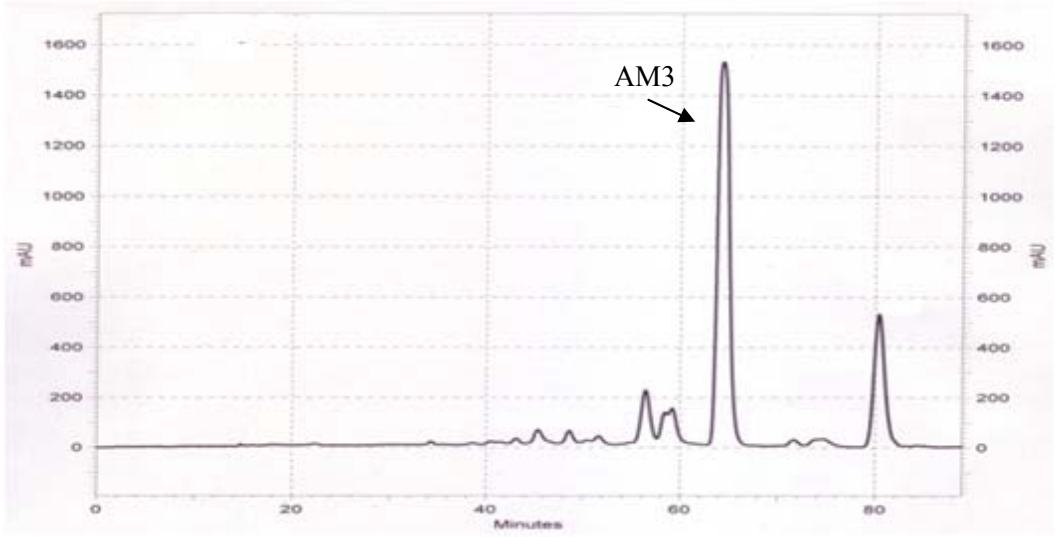

Figure 6-7. Typical chromatogram of AM3 isolation from the 80% aq. MeOH fraction.

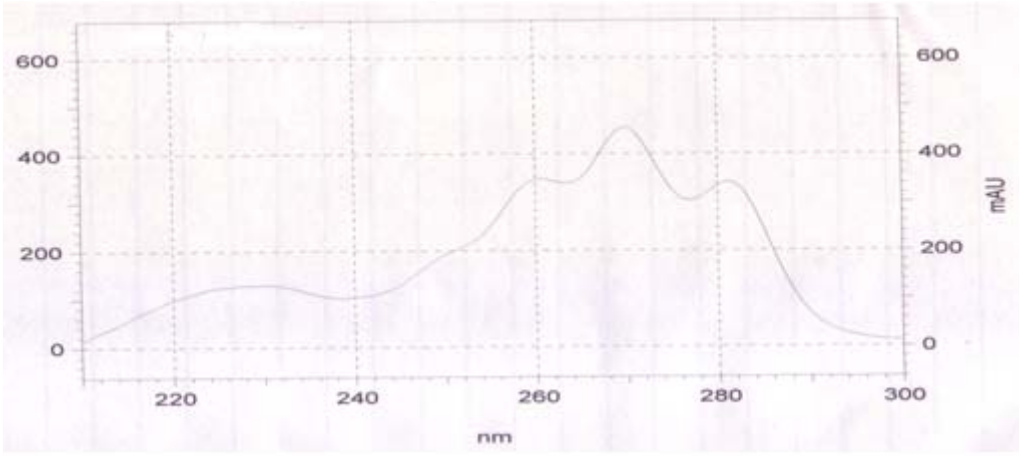

Figure 6-8. UV spectrum of AM3 obtained from HPLC purification with retention time of 64 min.

6.3.6 Surface Plasmon Resonance Experiments

Investigation of the binding interaction between TNM-A or AM3 and POPC liposomes, with or without sterols, was carried out using SPR as reported previously.[6,7]

6.3.6.1 Liposome Preparation

Large unilamellar vesicles (LUVs) were prepared as follows. POPC (10 mg) with or without 10 mol % (~0.5 mg) sterol (cholesterol, ergosterol, or epicholesterol) were dissolved together in chloroform in a round-bottom flask. The solvent was evaporated, and the resulting lipid film was further dried in vacuo overnight. It was then hydrated with 1 mL of PBS buffer [10 mM phosphate buffer (pH 7.4), 2.7 mM potassium chloride, and 137 mM sodium chloride]. The mixture was vortexed, sonicated, and subjected to three cycles of freezing (−80 °C), thawing (60 °C), and vortexing (5 sec) to form multilamellar vesicles (MLVs). The MLV suspension was passed through double 100 nm polycarbonate filters 19 times with LiposoFast-Basic (AVESTIN Inc., Ottawa, Canada) at room temperature to form LUVs. The lipid concentration of the LUVs was determined using a phospholipid C-Test (Wako Pure Chemical Industries Ltd.). The LUVs were then diluted with the same PBS buffer to produce a suspension with a final lipid concentration of 0.5 mM for injection into the SPR instrument.

6.3.6.2 Analyte-Ligand Binding Interaction

TNM-A (1 mg, 0.57 μmol) or AM3 (1 mg, 0.75 μmol) was first dissolved in DMSO (1 mL) or H_2O (1 mL) and stored as a 0.57 mM or 0.75 mM stock solution, respectively. 50 μL of the TNM-A stock solution was diluted to 28 μM with 950 μL of PBS buffer. This solution was further diluted with PBS buffer containing 5% DMSO to give 10, 15, and 20 μM TNM-A solutions. All these solutions, together with the running buffer, were ensured to have the same DMSO concentration. For AM3, an aliquot of the stock solution was diluted to 250 μM with PBS buffer, and subsequently diluted to give 30, 40, and 50 μM AM3 solutions for SPR analysis.

The SPR experiments were performed at 25 °C using a dodecylamine-modified CM5 sensor chip mounted on a Biacore T200 system (GE Healthcare), and the running buffer was PBS containing 5% DMSO (pH 7.4) or PBS buffer (pH 7.4) for TNM-A and AM3, respectively. The unmodified CM5 sensor chip was first washed three times with a 50 mM NaOH/2-propanol solution [3:2 (v/v)] at a flow rate of 20 μL/min for 2 min. Dodecylamine was immobilized in one of the flow cells (fc2) of the CM5 chip with an amino coupling method while the other flow cell (fc1) was left

untouched to serve as the control lane. This chip was activated by injecting a solution of 390 mM EDC and 100 mM *N*-hydroxysuccinimide [1:1 (v/v), 70 μL] and then dodecylamine (1 mg/mL) in 10 mM acetate buffer containing 10% DMSO (pH 5.0) at a flow rate of 10 μL/min and a contact time of 7 min. The remaining *N*-hydroxysuccinimide ester groups on the sensor chip were deactivated by converting them to amide groups with an injection of 1 M ethanolamine hydrochloride (pH 8.5). Thus, the obtained modified sensor chip was then washed with 10% DMSO to remove nonspecifically bound molecules.

For the immobilization of liposomes on the sensor surface, the dodecylamine-modified sensor chip was first conditioned by an injection of running buffer at a flow rate of 10 μL/min for 5 min. The liposome suspension (0.5 mM) was then injected at a flow rate of 2 μL/min for 40 min, followed by the injection of 50 mM NaOH at a flow rate of 20 μL/min for 2 min, three times to generate a stable sensorgram, which indicated the formation of a stable liposome layer on the sensor surface.

TNM-A or AM3 solutions, at concentrations of 10, 15, 20 μM, and 30, 40, 50 μM, respectively, were then injected at a flow rate of 10 μL/min; its association was observed for 300 s. Then running buffer was injected at the same flow rate for 300 s, and the dissociation of TNM-A or AM3 from the surface was monitored. A new liposome surface was prepared for each injection of the TNM-A or AM3 solution. To remove the liposomes from the sensor surface, injections of 0.5% (w/v) SDS, followed by a 50 mM NaOH/2-propanol solution [3:2 (v/v)] both at a flow rate of 20 μL/min for 2 min, were conducted twice to ensure a return to the original baseline.

6.3.6.3 Data Analysis

The sensorgrams obtained from the peptide–lipid bilayer interaction were analyzed by curve fitting[8,9] with Biacore T200 Evaluation version 1.0. Global fitting, which is normally done by simultaneously fitting sensorgrams corresponding to different analyte concentrations, was found to be incompatible with TNM-A as in the case with amphotericin B.[7] This is probably because concentration-dependent aggregate formation of TNM-A in the aqueous phase affects its membrane binding, thus leading to the inconsistency in the kinetic parameters at different TNM-A concentrations. Thus, the kinetic parameters were evaluated not by global fitting but by local fitting to the sensorgrams from 20 μM TNM-A. The sensorgrams were fit to a two-state reaction model,[7] in which interaction between the peptide and the lipid bilayers is assumed to occur in two steps (Scheme 6-3). The first step involves the

binding of TNM-A (A) to membrane lipids (B) in a parallel and stoichiometric manner, identical to the simple bimolecular or Langmuir model if the second step does not proceed. The second step involves a conformational or morphological change of the complex (AB) to a second complex (ABx).

$$A + B \underset{k_{d1}}{\overset{k_{a1}}{\rightleftharpoons}} AB \underset{k_{d2}}{\overset{k_{a2}}{\rightleftharpoons}} ABx$$

Scheme 6-3. Two-state reaction model.

In this model, rate equations are given by

$$d[A]/dt = -k_{a1}[A][B] + k_{d1}[AB] \quad \textbf{(Eq. 6-1)}$$

$$d[AB]/dt = (k_{a1}[A][B] - k_{d1}[AB]) - (k_{a2}[AB] - k_{d2}[ABx]) \quad \textbf{(Eq. 6-2)}$$

$$d[ABx]/dt = k_{a2}[AB] - k_{d2}[ABx] \quad \textbf{(Eq. 6-3)}$$

$$K_{A1} = k_{a1}/k_{d1};\ K_{A2} = k_{a2}/k_{d2};\ K_A = K_{A1}K_{A2} \quad \textbf{(Eq. 6-4)}$$

where k_{a1} and k_{d1} correspond to the association and dissociation rate constants for the liposome surface of free TNM-A, respectively, while k_{a2} and k_{d2} correspond to the distribution rate constants from AB to ABx forms and vice versa, respectively. K_{A1}, K_{A2}, and K_A represent the affinity constants for the first, second, and overall equilibrium steps, respectively. A detailed method for determining the kinetic parameters on the basis of this model is given in the literature.[7,9,10]

6.3.7 Sample Preparation for Solid-State NMR

For the measurement of ^{2}H NMR spectra of the deuterated sterols in POPC membranes, 2.6 μmol of 3-*d*-sterol, 46 μmol of POPC, and TNM-A or AM3 (0 or 2.6 μmol) were dissolved in a $CHCl_3$/MeOH solution [2:1 (v/v)] in a round-bottom flask. The solvent was removed in vacuo and further dried overnight. The lipid film was then rehydrated with 1 mL of milli-Q water. After being sonicated and vortexed for a few minutes, the lipid suspension was subjected to three cycles of freezing (−80 °C) and thawing (40 °C) to make MLVs. The vesicle suspension was lyophilized overnight, rehydrated with deuterium-

depleted water [50% (w/w)], and homogenized by being vortexed, frozen, and thawed. It was then transferred to a 5 mm glass tube (Wilmad) and sealed with epoxy glue.

For the measurement of ^{31}P NMR spectra of POPC membranes, 6.6 μmol of POPC, cholesterol or ergosterol (0 or 0.4 μmol) and TNM-A or AM3 (0 or 0.4 μmol) were dissolved in a solution of $CHCl_3$-MeOH (2:1 v/v) in a round bottom flask. For AM3, an additional sample was made by mixing 5.8 μmol POPC, 0.4 μmol cholesterol, and 1.2 μmol AM3. The same procedure as in ^{2}H NMR sample preparation was performed except for the following: deuterium oxide (50% w/w) was used to rehydrate the sample after lyophilization, instead of deuterium-depleted water, and the homogenized sample was transferred to a 7-mm Teflon tube.

6.3.8 Solid-State NMR Measurements

All the ^{2}H NMR spectra were recorded on a 400 MHz ECA400 (JEOL, Tokyo, Japan) or a 300 MHz CMX300 (Chemagnetics, Agilent, Palo Alto, CA) spectrometer. Spectra were collected at 30 °C using a 5 mm ^{2}H static probe (Doty Scientific Inc., Columbia, SC, or Otsuka Electronics, Osaka, Japan) following a quadrupolar echo sequence.[1] The 90° pulse width was 2 μs; the interpulse delay was 30 μs, and the repetition rate was 0.5 s. The sweep width was 200 kHz, and the number of scans was around 400000.

All ^{31}P NMR spectra were recorded on a 400 MHz ECA400 (JEOL, Tokyo, Japan) using a 7-mm CP-MAS probe ((Doty Scientific Inc., Columbia, SC, USA) without rotation. Spectra were collected at 30 ºC. A singe pulse sequence with proton decoupling was employed with the following spectra parameters: acquisition time was 18 ms, 90º pulse width was 5.6 μs, relaxation delay was 2 s, and total number of scans was around 25 000.

6.3.9 Calcein Leakage Experiments

Extent of calcein leakage from liposomes was carried out as reported previously.[11] Large unilamellar vesicles were prepared as follows. POPC (10 mg, Avanti Polar Lipids, Inc., Alabaster, AL) with or without sterol (10 mol%) was dissolved in chloroform in a round-bottom flask. The solvent was removed under vacuum for about 2 hours at 30 ºC and further dried *in vacuo* overnight. The lipid film thus obtained was rehydrated with 1 mL of 60 mM calcein in Tris-HCl containing 1 mM EDTA and 150 mM NaCl (pH 7.4) and subjected to two cycles of vortexing (1 min) and warming-up (65 ºC) followed by five cycles of freezing (-20 ºC) and thawing (65 ºC) to obtain MLVs. Afterwards, the suspension was passed through a polycarbonate membrane filter (pore size, 200 nm) 19 times using a LiposoFast-Basic (AVESTIN Inc., Ottawa, Canada) to prepare LUVs of homogenous size. Excess calcein was

removed by passing the suspension through a Sepharose 4B column (GE Healthcare BioSciences AB, Uppsala, Sweden) with Tris-HCl containing 1 mM EDTA and 150 mM NaCl (pH 7.4). The lipid concentration in the LUV fraction was quantified using phospholipid C-Test Wako (Wako Pure Chemical Industries, Ltd., Osaka, Japan). Resulting stock solution was stored at 4 ºC under nitrogen gas.

Measurement of calcein leakage was performed on a JASCO FP 6500 spectrofluorometer (JASCO Corp., Tokyo, Japan) with an excitation wavelength of 490 nm (slit 1.5 nm) and an emission wavelength of 517 nm (slit 5 nm). To monitor calcein leakage, 20 μL of the LUV suspension was diluted to 980 μL with the same Tris buffer. A 20 μL aliquot of TNM-A or AM3 in MeOH:DMSO (1:1 v/v) or MeOH, respectively, was then added. Subsequently, 20 μL of 10% (v/v) Triton X-100 (Nacalai Tesque Inc., Kyoto, Japan) was added to obtain the condition of 100% leakage. All measurements were carried out at room temperature with a final lipid concentration of 27 μM.

6.3.10 Hemolysis Assay

Human red blood cells (2 mL) were suspended in PBS buffer containing 8.10 mM Na_2HPO_4, 1.47 mM KH_2PO_4, 137 mM NaCl and 2.68 mM KCl (pH 7.4) and immediately separated from the plasma by centrifugation at 2000 rpm for 5 minutes, repeated twice. The sedimented cells were re-suspended in the same PBS buffer to yield 1% hematocrit. Various concentrations of TNM-A or AM3 in DMSO:MeOH (1:1 v/v, 10 μL) or MeOH (10 μL), respectively, was then added to the red blood cell suspension (1% hematocrit, 190 μL) and incubated for 18 hours at 37 ºC. Afterwards, the mixtures were centrifuged at 2000 rpm for 5 minutes and the supernatant (50 μL) was transferred to a 96-well microplate and subjected to colorimetric measurements at 450 nm to determine the absorbance (A_{S450}) using an Emax® Precision Microplate Reader (Molecular Devices Corp., Sunnyvale, CA). Condition for 100% hemolysis was obtained by incubating the blood suspension in water (A_{T450}). The percentage of released hemoglobin from erythrocytes was computed as (A_{S450}/A_{T450}) x 100. The concentration that caused 50% hemolysis (EC_{50}) was determined from the dose-dependent curve.

6.3.11 Particle Size Distribution Measurement

6.6 μmol of POPC, cholesterol (0 or 0.4 μmol) and TNM-A (0 or 0.4 μmol) were dissolved in a solution of $CHCl_3$-MeOH (2:1 v/v) in a round bottom flask. The solvent was removed *in vacuo* and further dried overnight. The lipid film was then rehydrated with 1 mL of Milli-Q water. After a few minutes of vortexing, the lipid suspension was subjected to

three cycles of freezing (-80 ºC) and thawing (40 ºC) to make MLVs. The suspension was then transferred into a cuvette and the size distribution of the vesicles was measured with a Horiba Dynamic Light Scattering Particle Size Analyzer LB-550 (HORIBA, Ltd., Kyoto, Japan) at 30 ºC.

A second mode of analysis was performed wherein TNM-A was added after vesicle formation. The same protocol as in the preceding paragraph was performed to make POPC:cholesterol (95:5) MLVs except that TNM-A was not mixed with the lipids. The resulting suspension obtained after the freeze-thaw cycle was passed through a polycarbonate membrane filter (pore size, 100 nm) 19 times using a LiposoFast-Basic (AVESTIN Inc., Ottawa, Canada) to prepare LUVs of homogenous size. The lipid concentration in the LUV fraction was quantified using Phospholipid C-Test Wako (Wako Pure Chemical Industries, Ltd., Osaka, Japan). Resulting stock solution was stored at 4 ºC under nitrogen gas. TNM-A was then added to a lipid suspension (0.1 mM) in an eppendorf tube to a final concentration of 0, 5, and 10 μM. The solution was mixed and then incubated at 30 ºC for 1, 3, 6, and 21 hours. At the end of each incubation period, the suspension was transferred into a cuvette and the size distribution of the vesicles was measured with the same conditions as above. Final lipid concentration was 20 μM.

6.3.12 Differential Interference and Confocal Microscopy Observations

Giant unilamellar vesicles (GUVs) were obtained by electroformation explored by Angelova and Dimitrov.[12] Briefly, POPC solutions (with or without 5 mol% cholesterol) were prepared in chloroform or chloroform/methanol (4:1 v/v) to a final phospholipid concentration of 1mg/mL. 15 μL aliquots were then deposited on parallel aligned electrodes (Pt wires, φ=100μm) attached to glass slides and the solvent was evaporated under vacuum overnight. 300 μL of Milli-Q water (Simplicity UV, MerckMillipore, Billerica, MA) was then added to completely immerse the electrodes which were then sealed with another glass slide using a rubber spacer with a small fill port for the drag injection. The slide was thermostated at 30 ºC on a temperature control objective plate (Tokai Hit ThermoPlate, Tokai Hit Co., Ltd., Shizuoka, Japan), and an alternating current (10V, 10Hz) was applied (Arbitrary Waveform Generator 33220A, Agilent Technologies, Tokyo, Japan) for 40-50 minutes to form the GUVs.

After GUV formation, TNM-A or TNM-A:TNM-FL (9:1 mol%), dissolved in Milli-Q water, was gently added to the sample to a final volume of 350 μL through the fill port (final concentration of TNM-A was between 1-20 μM) with micropipette. TNM-A induced morphological changes of the GUV were observed by an Olympus FluoView™ FV1000-D

Scanning Unit with the IX81 Inverted Microscope (Olympus Corp., Tokyo, Japan). A LUCPLFLN 60x universal semi-apochromat objective with NA of 0.70 (Olympus Corp., Tokyo, Japan) was used for differential interference and fluorescent observations. Acquisition speed was 8 μs/pixel and images were visualized with FV10-ASW-3.0 software. The sample temperature was kept at 30 ºC for all observation with the temperature control objective plate.

For confocal fluorescence microscopy observations, excitation and emission wavelength used for TNM-FL was 488 and 515 nm, respectively.

References

1. Matsumori, N.; Tahara, K.; Yamamoto, H.; Morooka, A.; Doi, M.; Oishi, T.; Murata, M. *J. Am. Chem. Soc.* **2009**, 131, 11855-11860.
2. Murari, R.; Murari, M.P.; Baumann, W.J. *Biochemistry.* **1986**, 25, 1062-1067.
3. Nishimura, S.; Arita, Y.; Honda, M.; Iwamoto, K.; Matsuyama, A.; Shirai, A.; Kawasaki, H.; Kakeya, H.; Kobayashi, T.; Matsunaga, S.; Yoshida, M. *Nat. Chem. Biol.* **2010**, 6, 519-526.
4. Matsunaga, S.; Fusetani, N. *J. Org. Chem.* **1995**, 60, 1177–1181.
5. Paul, G. K.; Matsumori, N.; Konoki, K.; Murata, M.; Tachibana, K. *J. Mar. Biotechnol.* **1997**, *5*, 124-128.
6. Swasono, R.T.; Mouri, R.; Morsy, N.; Matsumori, N.; Oishi, T.; Murata, M. *Bioorg. Med. Chem. Lett.* **2010**, 20, 2215-2218.
7. Mouri, R.; Konoki, K.; Matsumori, N.; Oishi, T.; Murata, M. *Biochemistry.* **2008**, 47, 7807-7815.
8. Khalifa, M.B.; Choulier, L.; Lortat-Jacob, H.; Altschuh, D.; Vernet, T. *Anal. Biochem.* **2001**, 293, 194-203.
9. Morton, T.A.; Myszka, D.G.; Chaiken, I.M. *Anal. Biochem.* **1995**, 227, 176-185.
10. Papo, N.; Shai, Y. *Biochemistry.* **2003**, 42, 458-466.
11. Morsy, N.; Houdai, T.; Konoki, K.; Matsumori, N.; Oishi, T.; Murata, M. *Bioorg. Med. Chem.* **2008**, 16, 3084-3090.
12. Angelova, M.I.; Dimitrov, D.S. *Faraday Discuss. Chem. Soc.* **1986**, 81, 303-311.

Acknowledgement

First and foremost, I thank God to whom I offer this glory and honor; the source of Wisdom and Life, whose guidance and blessings all these years have brought me to where I am today.

I am grateful to the Japanese Government for providing a Monbukagakusho scholarship for my Ph.D. studies that went far beyond earning my degree.

I would like to express my sincerest gratitude to my supervisor, Professor Michio Murata for giving me this wonderful opportunity to grow, for providing an excellent research environment, for his trust, and genuine kindness and concern that have made my education a truly memorable one.

I extend my deepest appreciation to Associate Professor Nobuaki Matsumori for patiently sharing with me his expertise, for his guidance and invaluable suggestions and insightful discussions to make my research more meaningful. I would also like to thank Dr. Shigeru Matsuoka of ERATO, Dr. Shinya Hanashima and Dr. Hiroshi Tsuchikawa of our laboratory for their helpful contributions.

I also acknowledge with much appreciation the constructive comments of the reviewers of this work, Professor Yasuhiro Kajihara and Professor Kazuhiko Nakatani.

I am extremely thankful to our collaborators, Professor Minoru Yoshida of RIKEN, Professor Shigeki Matsunga of The University of Tokyo, Professor Hideaki Kakeya and Dr. Shinichi Nishimura of Kyoto University, and Professor Masashi Tsuda of Kochi University for their generous assistance during the course of my study.

I would also like to offer my special thanks to Dr. Naoya Inazumi, Dr. Yuichi Umegawa, and Mr. Mototsugu Doi of Osaka University for their help in NMR measurements and to Dr. Masanao Kinoshita of ERATO for his assistance with differential interference and confocal microscopy observations.

My warmest regards to past and present members of the Laboratory for Biomolecular Chemistry for the friendship and support they have extended to me inside and outside the laboratory. In particular, my senpai Dr. Respati Tri Swasono, my “tutor” Mr. Hajime Shibata, Dr. Sarah Goretta, Dr. Toshiyuki Yamaguchi, Mr. Tetsuro Takano, Mr. Masanori Shimada, Ms. Dian Kurniati, Ms. Yuka Suemichi and Ms. Misaki Yofu. I am thankful as well to my fellow international and Filipino students here in Osaka University who have always been kind enough to share in the troubles and joys of studying abroad.

I am deeply indebted to my former teachers and professors who have had tremendous impact on me, more than they ever know, for nourishing my love for the sciences.

This work is a tribute to my parents, who have instilled in us the value of hardwork and patience; for providing us with the best possible education no matter the difficulty, and to my siblings. I would not have made it without them.

Finally, I will always be grateful to my fiancée, Karen, for her love, understanding, encouragement and selfless sacrifice throughout my PhD studies, for making it bearable, and for having brought out and constantly bringing out the best in me.

NMR Spectra

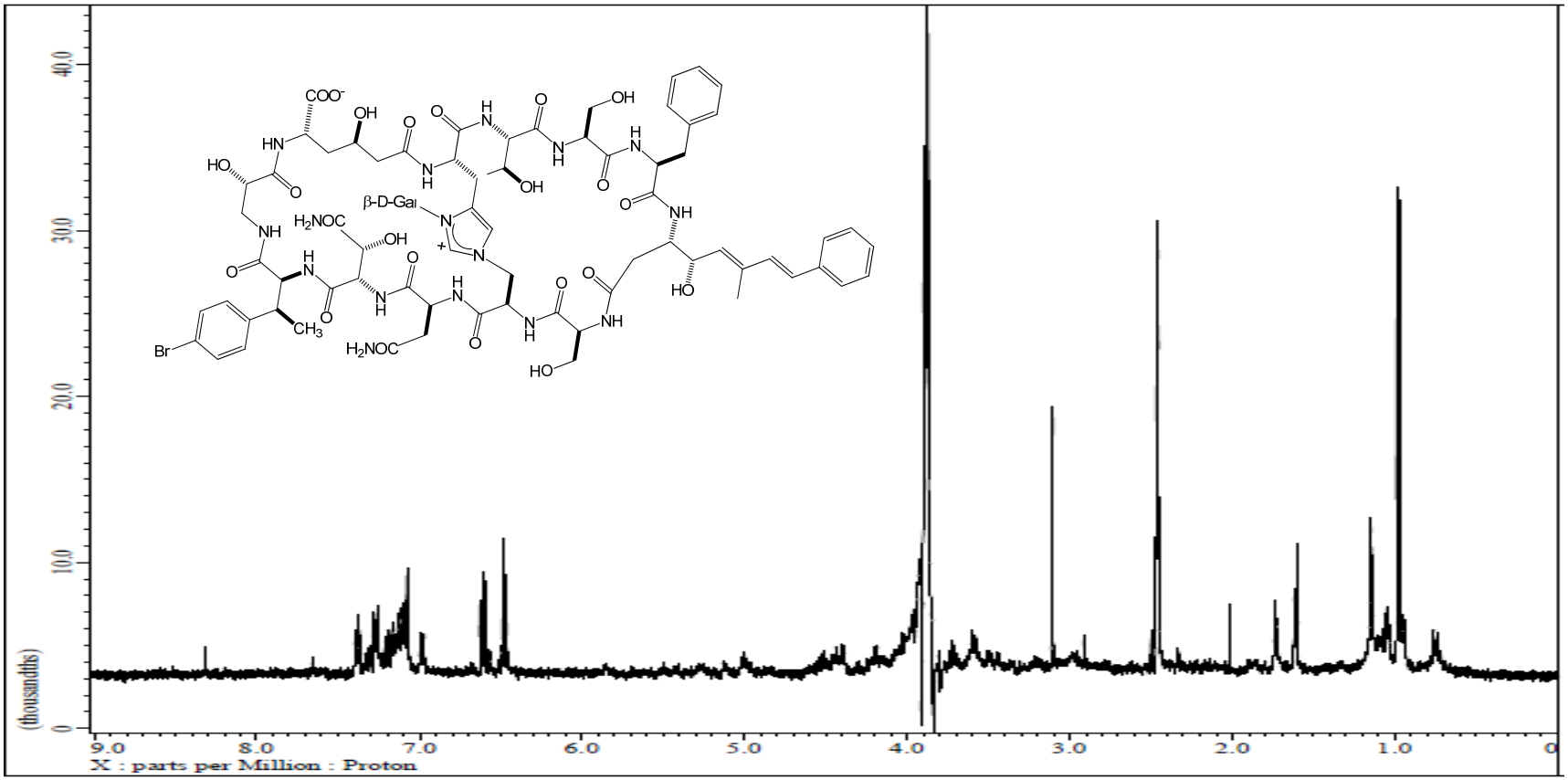

Figure S-1. 400 MHz ^{1}H NMR spectra of TNM-A in DMSO-d_6:D_2O (4:1) obtained at 308K.

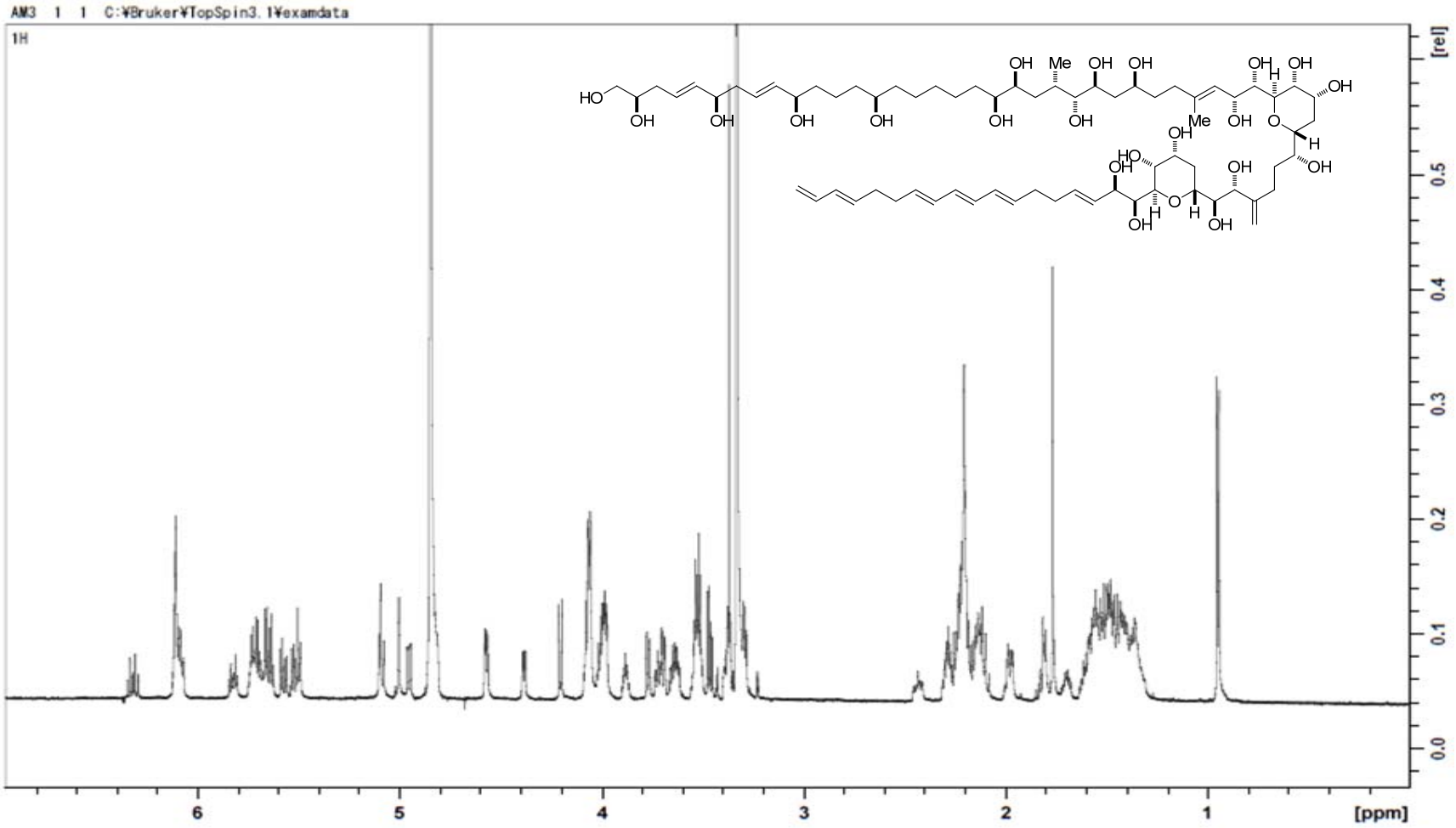

Figure S-2. 700 MHz ^{1}H NMR spectra of AM3 in MeOH-d_4 obtained at 303K.

Appendix

Reprint Permissions

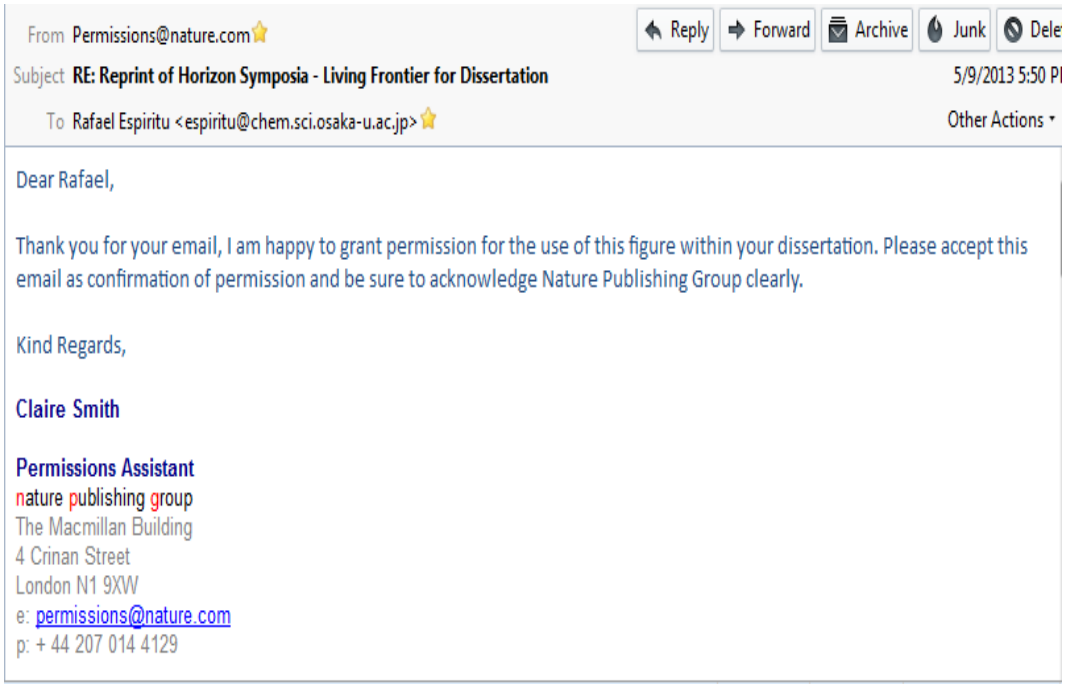

From Permissions@nature.com

Reply | Forward | Archive | Junk | Dele

Subject **RE: Reprint of Horizon Symposia - Living Frontier for Dissertation** 5/9/2013 5:50 PI

To Rafael Espiritu <espiritu@chem.sci.osaka-u.ac.jp> Other Actions

Dear Rafael,

Thank you for your email, I am happy to grant permission for the use of this figure within your dissertation. Please accept this email as confirmation of permission and be sure to acknowledge Nature Publishing Group clearly.

Kind Regards,

Claire Smith

Permissions Assistant
nature publishing group
The Macmillan Building
4 Crinan Street
London N1 9XW
e: permissions@nature.com
p: + 44 207 014 4129

Figure A-1. Reprint permission for *Horizon Symposia: Living Frontier*, **2004**, 1-4. (For Figure 1-1 of thesis).

ELSEVIER LICENSE
TERMS AND CONDITIONS

May 09, 2013

This is a License Agreement between Rafael A Espiritu ("You") and Elsevier ("Elsevier") provided by Copyright Clearance Center ("CCC"). The license consists of your order details, the terms and conditions provided by Elsevier, and the payment terms and conditions.

All payments must be made in full to CCC. For payment instructions, please see information listed at the bottom of this form.

Supplier	Elsevier Limited The Boulevard,Langford Lane Kidlington,Oxford,OX5 1GB,UK
Registered Company Number	1982084
Customer name	Rafael A Espiritu
Customer address	Kuko Golden House 106, Kuko 1-2-13 Ikeda City, Osaka, , 563-0034
License number	3145040492108
License date	May 09, 2013
Licensed content publisher	Elsevier
Licensed content publication	Biochimica et Biophysica Acta (BBA) - Biomembranes
Licensed content title	Membrane assembly of the cholesterol-dependent cytolysin pore complex
Licensed content author	Eileen M. Hotze,Rodney K. Tweten
Licensed content date	April 2012
Licensed content volume number	1818
Licensed content issue number	4
Number of pages	11
Start Page	1028
End Page	1038
Type of Use	reuse in a thesis/dissertation
Portion	figures/tables/illustrations
Number of figures/tables/illustrations	1
Format	both print and electronic
Are you the author of this Elsevier article?	No
Will you be translating?	No
Order reference number	
Title of your thesis/dissertation	Mechanism of Action of Membrane-Active Marine Natural Products Theonellamide A and Amphidinol 3
Expected completion date	Sep 2013
Estimated size (number of pages)	150
Elsevier VAT number	GB 494 6272 12
Permissions price	0 JPY
VAT/Local Sales Tax	0.0 USD / 0.0 GBP
Total	0 JPY
Terms and Conditions	

Figure A-2. Reprint permission for *Biochim, Biophys. Acta*., **2012**, 1818, 1028-1038. (For Figure 1-2 of thesis).

ELSEVIER LICENSE
TERMS AND CONDITIONS

May 09, 2013

This is a License Agreement between Rafael A Espiritu ("You") and Elsevier ("Elsevier") provided by Copyright Clearance Center ("CCC"). The license consists of your order details, the terms and conditions provided by Elsevier, and the payment terms and conditions.

All payments must be made in full to CCC. For payment instructions, please see information listed at the bottom of this form.

Supplier	Elsevier Limited The Boulevard,Langford Lane Kidlington,Oxford,OX5 1GB,UK
Registered Company Number	1982084
Customer name	Rafael A Espiritu
Customer address	Kuko Golden House 106, Kuko 1-2-13 Ikeda City, Osaka, , 563-0034
License number	3145050624475
License date	May 09, 2013
Licensed content publisher	Elsevier
Licensed content publication	Cell
Licensed content title	Structure of a Cholesterol-Binding, Thiol-Activated Cytolysin and a Model of Its Membrane Form
Licensed content author	Jamie Rossjohn,Susanne C Feil,William J McKinstry,Rodney K Tweten,Michael W Parker
Licensed content date	30 May 1997
Licensed content volume number	89
Licensed content issue number	5
Number of pages	8
Start Page	685
End Page	692
Type of Use	reuse in a thesis/dissertation
Intended publisher of new work	other
Portion	figures/tables/illustrations
Number of figures/tables/illustrations	1
Format	both print and electronic
Are you the author of this Elsevier article?	No
Will you be translating?	No
Order reference number	
Title of your thesis/dissertation	Mechanism of Action of Membrane-Active Marine Natural Products Theonellamide A and Amphidinol 3
Expected completion date	Sep 2013
Estimated size (number of pages)	150
Elsevier VAT number	GB 494 6272 12
Permissions price	0 JPY
VAT/Local Sales Tax	0.0 USD / 0.0 GBP
Total	0 JPY
Terms and Conditions	

Figure A-3. Reprint permission for *Cell*, **1997**, 89, 685-692. (For Figure 1-2 of thesis).

NATURE PUBLISHING GROUP LICENSE TERMS AND CONDITIONS

May 09, 2013

This is a License Agreement between Rafael A Espiritu ("You") and Nature Publishing Group ("Nature Publishing Group") provided by Copyright Clearance Center ("CCC"). The license consists of your order details, the terms and conditions provided by Nature Publishing Group, and the payment terms and conditions.

All payments must be made in full to CCC. For payment instructions, please see information listed at the bottom of this form.

License Number	3145060864369
License date	May 09, 2013
Licensed content publisher	Nature Publishing Group
Licensed content publication	Nature Reviews Microbiology
Licensed content title	Antimicrobial peptides: pore formers or metabolic inhibitors in bacteria?
Licensed content author	Kim A. Brogden
Licensed content date	Mar 1, 2005
Volume number	3
Issue number	3
Type of Use	reuse in a thesis/dissertation
Requestor type	academic/educational
Format	print and electronic
Portion	figures/tables/illustrations
Number of figures/tables/illustrations	2
High-res required	no
Figures	Figure 3 Figure 5
Author of this NPG article	no
Your reference number	
Title of your thesis / dissertation	Mechanism of Action of Membrane-Active Marine Natural Products Theonellamide A and Amphidinol 3
Expected completion date	Sep 2013
Estimated size (number of pages)	150
Total	0 JPY
Terms and Conditions	

Figure A-4. Reprint permission for *Nat. Rev. Microbiol.*, **2005**, 3, 238-250. (For Figure 1-4 and 1-5 of thesis).

JOHN WILEY AND SONS LICENSE TERMS AND CONDITIONS

May 09, 2013

This is a License Agreement between Rafael A Espiritu ("You") and John Wiley and Sons ("John Wiley and Sons") provided by Copyright Clearance Center ("CCC"). The license consists of your order details, the terms and conditions provided by John Wiley and Sons, and the payment terms and conditions.

All payments must be made in full to CCC. For payment instructions, please see information listed at the bottom of this form.

License Number	3145070147734
License date	May 09, 2013
Licensed content publisher	John Wiley and Sons
Licensed content publication	Biopolymers
Licensed content title	Mode of action of linear amphipathic α-helical antimicrobial peptides
Licensed copyright line	Copyright © 1998 John Wiley & Sons, Inc.
Licensed content author	Ziv Oren,Yechiel Shai
Licensed content date	May 6, 1999
Start page	451
End page	463
Type of use	Dissertation/Thesis
Requestor type	University/Academic
Format	Print and electronic
Portion	Figure/table
Number of figures/tables	1
Original Wiley figure/table number(s)	Figure 1
Will you be translating?	No
Total	0.00 USD
Terms and Conditions	

Figure A-5. Reprint permission for *Biopolymers*, **1998**, 47, 451-463. (For Figure 1-4 of thesis).

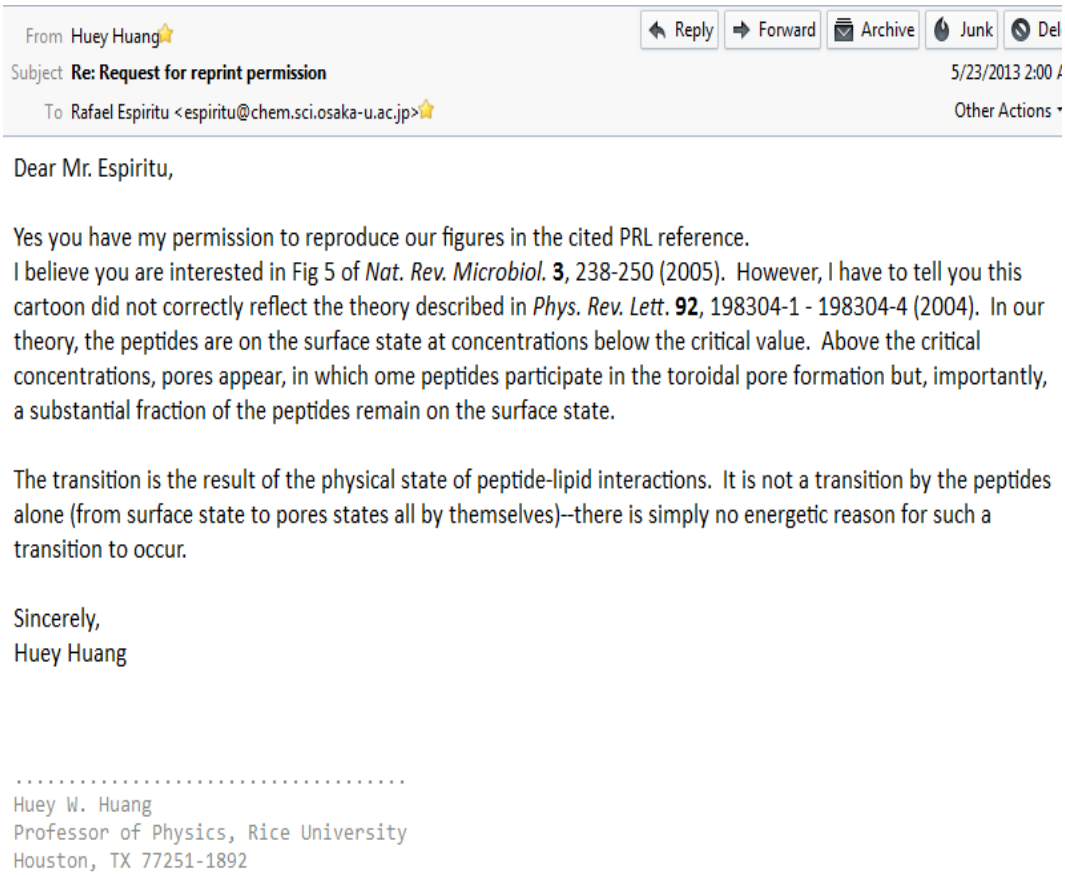

From Huey Huang
Subject Re: Request for reprint permission
To Rafael Espiritu <espiritu@chem.sci.osaka-u.ac.jp>

Reply | Forward | Archive | Junk | Del

5/23/2013 2:00 A

Other Actions

Dear Mr. Espiritu,

Yes you have my permission to reproduce our figures in the cited PRL reference.
I believe you are interested in Fig 5 of *Nat. Rev. Microbiol.* **3**, 238-250 (2005). However, I have to tell you this cartoon did not correctly reflect the theory described in *Phys. Rev. Lett*. **92**, 198304-1 - 198304-4 (2004). In our theory, the peptides are on the surface state at concentrations below the critical value. Above the critical concentrations, pores appear, in which ome peptides participate in the toroidal pore formation but, importantly, a substantial fraction of the peptides remain on the surface state.

The transition is the result of the physical state of peptide-lipid interactions. It is not a transition by the peptides alone (from surface state to pores states all by themselves)--there is simply no energetic reason for such a transition to occur.

Sincerely,
Huey Huang

.....
Huey W. Huang
Professor of Physics, Rice University
Houston, TX 77251-1892

Figure A-6. Reprint permission for *Phys. Rev. Lett.*, **2004**, 92, 198304-1 – 198304-4. (For Figure 1-5 of thesis)

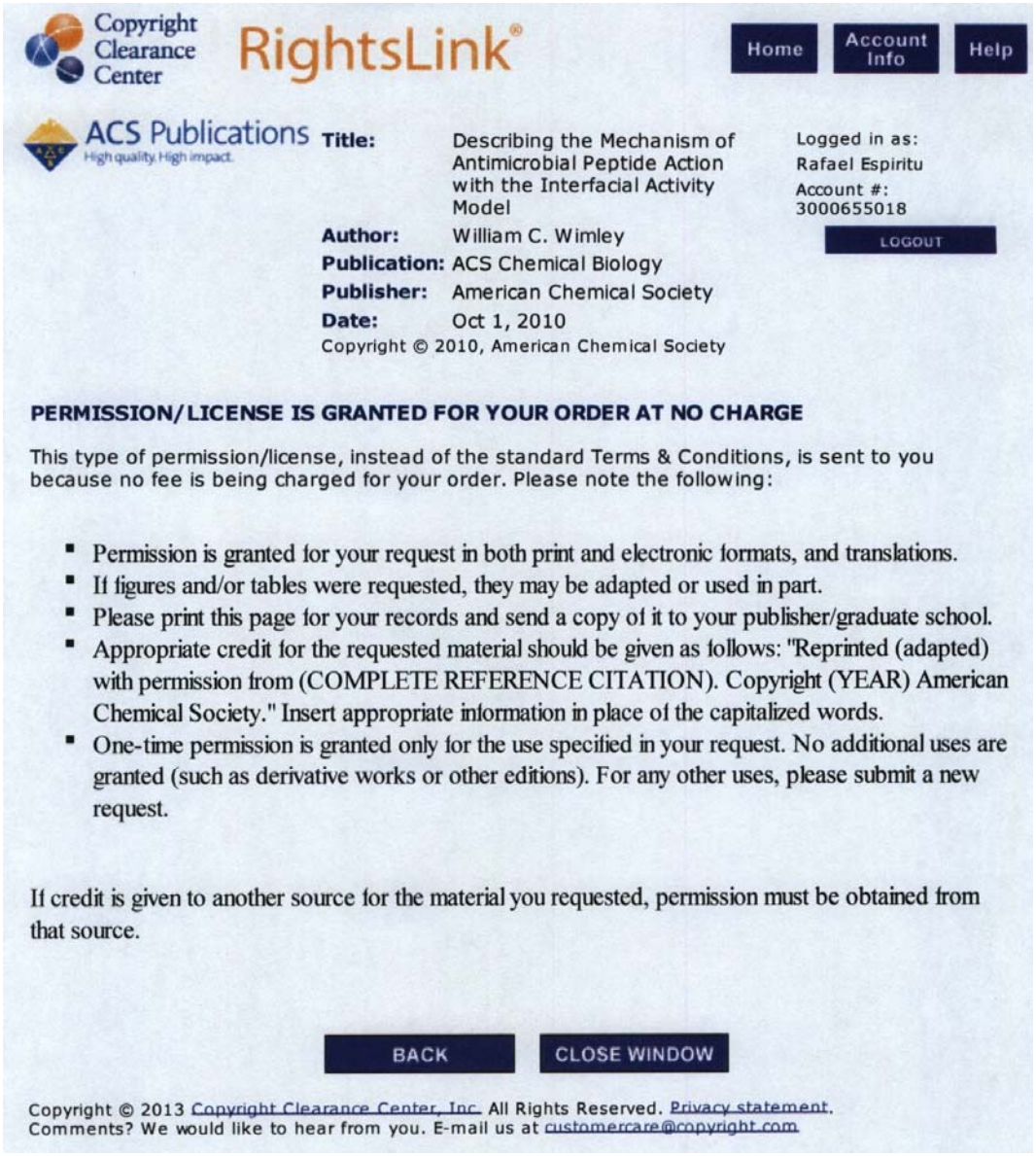

Figure A-7. Reprint permission for *ACS Chem. Biol.,* **2010**, 5, 905-917. (For Figure 1-6, 1-7, and 1-11 of thesis)

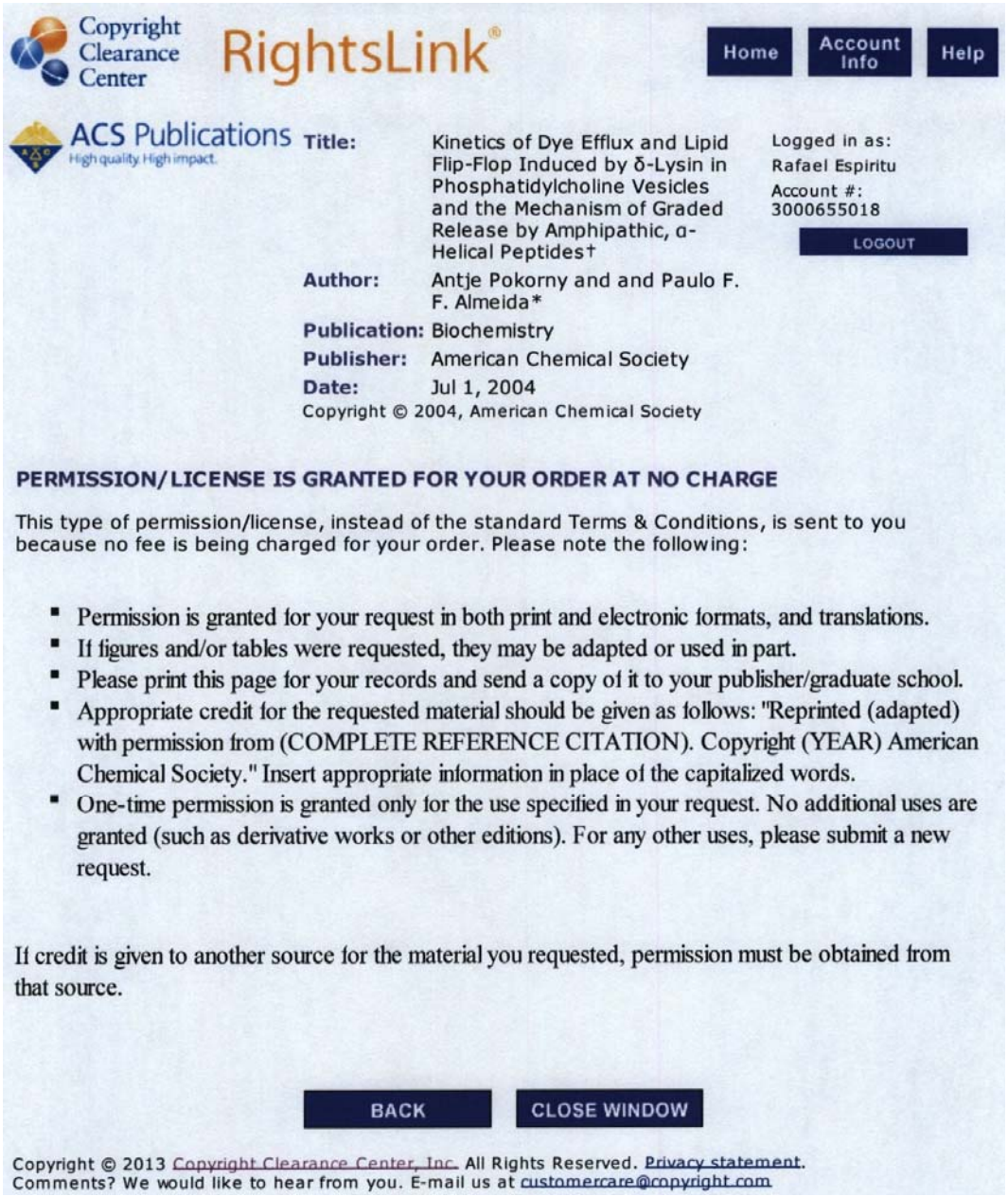

Figure A-8. Reprint permission for *Biochemistry,* **2004**, 43, 8846-8857. (For Figure 1-8 of thesis).

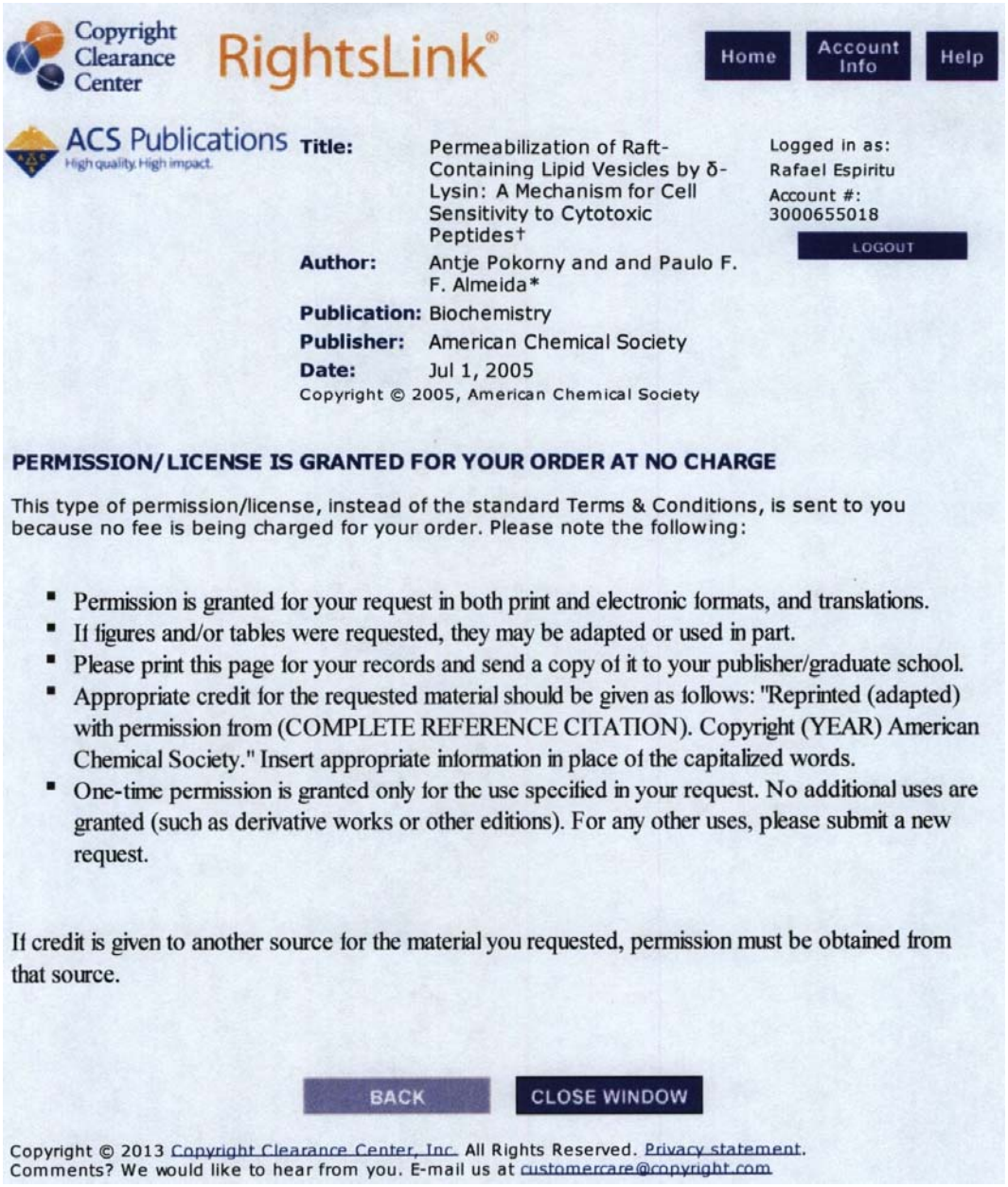

Figure A-9. Reprint permission for *Biochemistry,* **2005**, 44, 9538-9544. (For Figure 1-8 of thesis).

ELSEVIER LICENSE
TERMS AND CONDITIONS

May 09, 2013

This is a License Agreement between Rafael A Espiritu ("You") and Elsevier ("Elsevier") provided by Copyright Clearance Center ("CCC"). The license consists of your order details, the terms and conditions provided by Elsevier, and the payment terms and conditions.

All payments must be made in full to CCC. For payment instructions, please see information listed at the bottom of this form.

Supplier	Elsevier Limited The Boulevard,Langford Lane Kidlington,Oxford,OX5 1GB,UK
Registered Company Number	1982084
Customer name	Rafael A Espiritu
Customer address	Kuko Golden House 106, Kuko 1-2-13 Ikeda City, Osaka, , 563-0034
License number	3145090926968
License date	May 09, 2013
Licensed content publisher	Elsevier
Licensed content publication	Progress in Lipid Research
Licensed content title	Role of lipids in the interaction of antimicrobial peptides with membranes
Licensed content author	Vitor Teixeira,Maria J. Feio,Margarida Bastos
Licensed content date	April 2012
Licensed content volume number	51
Licensed content issue number	2
Number of pages	29
Start Page	149
End Page	177
Type of Use	reuse in a thesis/dissertation
Intended publisher of new work	other
Portion	figures/tables/illustrations
Number of figures/tables/illustrations	1
Format	both print and electronic
Are you the author of this Elsevier article?	No
Will you be translating?	No
Order reference number	
Title of your thesis/dissertation	Mechanism of Action of Membrane-Active Marine Natural Products Theonellamide A and Amphidinol 3
Expected completion date	Sep 2013
Estimated size (number of pages)	150
Elsevier VAT number	GB 494 6272 12
Permissions price	0 JPY
VAT/Local Sales Tax	0.0 USD / 0.0 GBP
Total	0 JPY
Terms and Conditions	

Figure A-10. Reprint permission for *Prog. Lipid Res.,* **2012**, 51, 149-177. (For Figure 1-9 of thesis).

ELSEVIER LICENSE
TERMS AND CONDITIONS

May 09, 2013

This is a License Agreement between Rafael A Espiritu ("You") and Elsevier ("Elsevier") provided by Copyright Clearance Center ("CCC"). The license consists of your order details, the terms and conditions provided by Elsevier, and the payment terms and conditions.

All payments must be made in full to CCC. For payment instructions, please see information listed at the bottom of this form.

Supplier	Elsevier Limited The Boulevard,Langford Lane Kidlington,Oxford,OX5 1GB,UK
Registered Company Number	1982084
Customer name	Rafael A Espiritu
Customer address	Kuko Golden House 106, Kuko 1-2-13
	Ikeda City, Osaka, , 563-0034
License number	3145091332319
License date	May 09, 2013
Licensed content publisher	Elsevier
Licensed content publication	Biochimica et Biophysica Acta (BBA) - Biomembranes
Licensed content title	Interaction of the antimicrobial peptide pheromone Plantaricin A with model membranes: Implications for a novel mechanism of action
Licensed content author	Hongxia Zhao,Rohit Sood,Arimatti Jutila,Shambhunath Bose,Gunnar Fimland,Jon Nissen-Meyer,Paavo K.J. Kinnunen
Licensed content date	September 2006
Licensed content volume number	1758
Licensed content issue number	9
Number of pages	14
Start Page	1461
End Page	1474
Type of Use	reuse in a thesis/dissertation
Intended publisher of new work	other
Portion	figures/tables/illustrations
Number of figures/tables/illustrations	1
Format	both print and electronic
Are you the author of this Elsevier article?	No
Will you be translating?	No
Order reference number	
Title of your thesis/dissertation	Mechanism of Action of Membrane-Active Marine Natural Products Theonellamide A and Amphidinol 3
Expected completion date	Sep 2013
Estimated size (number of pages)	150
Elsevier VAT number	GB 494 6272 12
Permissions price	0 JPY
VAT/Local Sales Tax	0.0 USD / 0.0 GBP
Total	0 JPY
Terms and Conditions	

Figure A-11. Reprint permission for *Biochim. Biophys. Acta.*, **2006**, 1758, 1461-1474. (For Figure 1-10 of thesis).

ELSEVIER LICENSE
TERMS AND CONDITIONS

May 09, 2013

This is a License Agreement between Rafael A Espiritu ("You") and Elsevier ("Elsevier") provided by Copyright Clearance Center ("CCC"). The license consists of your order details, the terms and conditions provided by Elsevier, and the payment terms and conditions.

All payments must be made in full to CCC. For payment instructions, please see information listed at the bottom of this form.

Supplier	Elsevier Limited The Boulevard,Langford Lane Kidlington,Oxford,OX5 1GB,UK
Registered Company Number	1982084
Customer name	Rafael A Espiritu
Customer address	Kuko Golden House 106, Kuko 1-2-13 Ikeda City, Osaka, , 563-0034
License number	3145100336093
License date	May 09, 2013
Licensed content publisher	Elsevier
Licensed content publication	Biochimica et Biophysica Acta (BBA) - Biomembranes
Licensed content title	Toroidal pores formed by antimicrobial peptides show significant disorder
Licensed content author	Durba Sengupta,Hari Leontiadou,Alan E. Mark,Siewert-Jan Marrink
Licensed content date	October 2008
Licensed content volume number	1778
Licensed content issue number	10
Number of pages	10
Start Page	2308
End Page	2317
Type of Use	reuse in a thesis/dissertation
Intended publisher of new work	other
Portion	figures/tables/illustrations
Number of figures/tables/illustrations	1
Format	both print and electronic
Are you the author of this Elsevier article?	No
Will you be translating?	No
Order reference number	
Title of your thesis/dissertation	Mechanism of Action of Membrane-Active Marine Natural Products Theonellamide A and Amphidinol 3
Expected completion date	Sep 2013
Estimated size (number of pages)	150
Elsevier VAT number	GB 494 6272 12
Permissions price	0 JPY
VAT/Local Sales Tax	0.0 USD / 0.0 GBP
Total	0 JPY
Terms and Conditions	

Figure A-12. Reprint permission for *Biophys. Acta*, **2008**, 1778, 2308-2317. (For Figure 1-11 of thesis).

NATURE PUBLISHING GROUP LICENSE TERMS AND CONDITIONS

May 09, 2013

This is a License Agreement between Rafael A Espiritu ("You") and Nature Publishing Group ("Nature Publishing Group") provided by Copyright Clearance Center ("CCC"). The license consists of your order details, the terms and conditions provided by Nature Publishing Group, and the payment terms and conditions.

All payments must be made in full to CCC. For payment instructions, please see information listed at the bottom of this form.

License Number	3145111007833
License date	May 09, 2013
Licensed content publisher	Nature Publishing Group
Licensed content publication	Nature Reviews Microbiology
Licensed content title	Genomic insights into the marine sponge microbiome
Licensed content author	Ute Hentschel, Jörn Piel, Sandie M. Degnan, Michael W. Taylor
Licensed content date	Jul 30, 2012
Volume number	10
Issue number	9
Type of Use	reuse in a thesis/dissertation
Requestor type	academic/educational
Format	print and electronic
Portion	figures/tables/illustrations
Number of figures/tables/illustrations	2
High-res required	no
Figures	Figure 1 Table 2
Author of this NPG article	no
Your reference number	
Title of your thesis / dissertation	Mechanism of Action of Membrane-Active Marine Natural Products Theonellamide A and Amphidinol 3
Expected completion date	Sep 2013
Estimated size (number of pages)	150
Total	0 JPY
Terms and Conditions	

Figure A-13. Reprint permission for *Nat. Rev. Microbiol.*, **2012**, 10, 641-654. (For Figure 2-1 of thesis).

JOHN WILEY AND SONS LICENSE TERMS AND CONDITIONS

May 09, 2013

This is a License Agreement between Rafael A Espiritu ("You") and John Wiley and Sons ("John Wiley and Sons") provided by Copyright Clearance Center ("CCC"). The license consists of your order details, the terms and conditions provided by John Wiley and Sons, and the payment terms and conditions.

All payments must be made in full to CCC. For payment instructions, please see information listed at the bottom of this form.

License Number	3144610443572
License date	May 09, 2013
Licensed content publisher	John Wiley and Sons
Licensed content publication	Environmental Microbiology
Licensed content title	Marine sponges and their microbial symbionts: love and other relationships
Licensed copyright line	© 2011 Society for Applied Microbiology and Blackwell Publishing Ltd
Licensed content author	Nicole S. Webster,Michael W. Taylor
Licensed content date	Mar 28, 2011
Start page	335
End page	346
Type of use	Dissertation/Thesis
Requestor type	University/Academic
Format	Print and electronic
Portion	Figure/table
Number of figures/tables	1
Original Wiley figure/table number(s)	Figure 3
Will you be translating?	No
Total	0.00 USD
Terms and Conditions	

Figure A-14. Reprint permission for *Environ. Microbiol.*, **2012**, 14, 335-346. (For Figure 2-1 of thesis).

NATURE PUBLISHING GROUP LICENSE
TERMS AND CONDITIONS

May 10, 2013

This is a License Agreement between Rafael A Espiritu ("You") and Nature Publishing Group ("Nature Publishing Group") provided by Copyright Clearance Center ("CCC"). The license consists of your order details, the terms and conditions provided by Nature Publishing Group, and the payment terms and conditions.

All payments must be made in full to CCC. For payment instructions, please see information listed at the bottom of this form.

License Number	3145150585079
License date	May 10, 2013
Licensed content publisher	Nature Publishing Group
Licensed content publication	Nature Chemical Biology
Licensed content title	Marine antifungal theonellamides target 3β-hydroxysterol to activate Rho1 signaling
Licensed content author	Shinichi Nishimura, Yuko Arita, Miyuki Honda, Kunihiko Iwamoto, Akihisa Matsuyama, Atsuko Shirai, Hisashi Kawasaki, Hideaki Kakeya, Toshihide Kobayashi, Shigeki Matsunaga, Minoru Yoshida
Licensed content date	Jun 13, 2010
Volume number	6
Issue number	7
Type of Use	reuse in a thesis/dissertation
Requestor type	academic/educational
Format	print and electronic
Portion	figures/tables/illustrations
Number of figures/tables/illustrations	2
High-res required	no
Figures	Figure 3d Figure 5, a, e-g
Author of this NPG article	no
Your reference number	
Title of your thesis / dissertation	Mechanism of Action of Membrane-Active Marine Natural Products Theonellamide A and Amphidinol 3
Expected completion date	Sep 2013
Estimated size (number of pages)	150
Total	0 JPY
Terms and Conditions	

Figure A-15. Reprint permission for *Nat. Chem. Biol.*, **2010**, 6, 519-526. (For Figure 2-2 of thesis).

ELSEVIER LICENSE
TERMS AND CONDITIONS

May 16, 2013

This is a License Agreement between Rafael A Espiritu ("You") and Elsevier ("Elsevier") provided by Copyright Clearance Center ("CCC"). The license consists of your order details, the terms and conditions provided by Elsevier, and the payment terms and conditions.

All payments must be made in full to CCC. For payment instructions, please see information listed at the bottom of this form.

Supplier	Elsevier Limited The Boulevard,Langford Lane Kidlington,Oxford,OX5 1GB,UK
Registered Company Number	1982084
Customer name	Rafael A Espiritu
Customer address	Kuko Golden House 106, Kuko 1-2-13 Ikeda City, Osaka, , 563-0034
License number	3151111336344
License date	May 16, 2013
Licensed content publisher	Elsevier
Licensed content publication	Bioorganic & Medicinal Chemistry
Licensed content title	Effects of lipid constituents on membrane-permeabilizing activity of amphidinols
Licensed content author	Nagy Morsy,Toshihiro Houdai,Keiichi Konoki,Nobuaki Matsumori,Tohru Oishi,Michio Murata
Licensed content date	15 March 2008
Licensed content volume number	16
Licensed content issue number	6
Number of pages	7
Start Page	3084
End Page	3090
Type of Use	reuse in a thesis/dissertation
Intended publisher of new work	other
Portion	figures/tables/illustrations
Number of figures/tables/illustrations	2
Format	both print and electronic
Are you the author of this Elsevier article?	No
Will you be translating?	No
Order reference number	
Title of your thesis/dissertation	Mechanism of Action of Membrane-Active Marine Natural Products Theonellamide A and Amphidinol 3
Expected completion date	Sep 2013
Estimated size (number of pages)	150
Elsevier VAT number	GB 494 6272 12
Permissions price	0 JPY
VAT/Local Sales Tax	0.0 USD / 0.0 GBP
Total	0 JPY
Terms and Conditions	

Figure A-16. Reprint permission for *Bioorg. Med.Chem.*, **2008**, 16, 3084-3090. (For Figure 4-1 and 4-2 of thesis).

Publication

Publication related to this thesis:

Main paper:

1. Interaction between the Marine Sponge Cyclic Peptide Theonellamide A and Sterols in Lipid Bilayers As Viewed by Surface Plasmon Resonance and Solid-State ^{2}H Nuclear Magnetic Resonance.
   Espiritu, R.A.; Matsumori, N.; Murata, M.; Nishimura, S.; Kakeya, H.; Matsunaga, S.; Yoshida, M. *Biochemistry*. **2013**, 52, 2410-2418.

BIOCHEMISTRY
including biophysical chemistry & molecular biology

Article

pubs.acs.org/biochemistry

Interaction between the Marine Sponge Cyclic Peptide Theonellamide A and Sterols in Lipid Bilayers As Viewed by Surface Plasmon Resonance and Solid-State ^{2}H Nuclear Magnetic Resonance

Rafael Atillo Espiritu,[†] Nobuaki Matsumori,*[,†] Michio Murata,[†,‡] Shinichi Nishimura,[§] Hideaki Kakeya,[§] Shigeki Matsunaga,[∥] and Minoru Yoshida[⊥]

[†]Department of Chemistry, Graduate School of Science, Osaka University, Toyonaka, Osaka 560-0043, Japan

[‡]Lipid Active Structure Project, ERATO, Japan Science and Technology Agency, Toyonaka, Osaka 560-0043, Japan

[§]Division of Bioinformatics and Chemical Genomics, Graduate School of Pharmaceutical Sciences, Kyoto University, Sakyo-ku, Kyoto 606-8501, Japan

[∥]Graduate School of Agricultural and Life Sciences, The University of Tokyo, Bunkyo-ku, Tokyo 113-8657, Japan

[⊥]RIKEN Advanced Science Institute, Wako, Saitama 351-0198, Japan

Supporting Information

ABSTRACT: Theonellamides (TNMs) are members of a distinctive family of antifungal and cytotoxic bicyclic dodecapeptides isolated from the marine sponge *Theonella* sp. Recently, it has been shown that TNMs recognize 3β-hydroxysterol-containing membranes, induce glucan overproduction, and damage cellular membranes. However, to date, the detailed mode of sterol binding at a molecular level has not been determined. In this study, to gain insight into the mechanism of sterol recognition of TNM in lipid bilayers, surface plasmon resonance (SPR) experiments and solid-state deuterium nuclear magnetic resonance (^{2}H NMR) measurements were performed on theonellamide A (TNM-A). SPR results revealed that the incorporation of 10 mol % cholesterol or ergosterol into 1-palmitoyl-2-oleoyl-*sn*-glycero-3-phosphocholine (POPC) membranes significantly enhances the affinity of the peptide for the membrane, particularly in the initial binding to the membrane surface. These findings, together with the fact that binding of TNM-A to epicholesterol (3α-cholesterol)-containing liposomes and pure POPC liposomes was comparably weak, confirmed the preference of the peptide for the 3β-hydroxysterol-containing membranes. To further establish the formation of the complex of TNM-A with 3β-hydroxysterols in lipid bilayers, solid-state ^{2}H NMR measurements were conducted using deuterium-labeled cholesterol, ergosterol, or epicholesterol. The ^{2}H NMR spectra showed that TNM-A significantly inhibits the fast rotational motion of cholesterol and ergosterol, but not epicholesterol, therefore verifying the direct complexation between TNM-A and 3β-hydroxysterols in lipid bilayers. This study demonstrates that TNM-A directly recognizes the 3β-OH moiety of sterols, which greatly facilitates its binding to bilayer membranes.

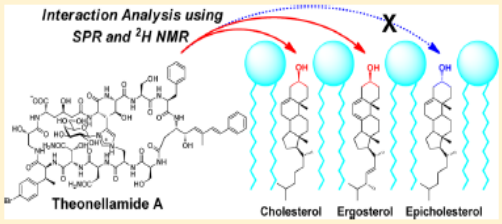

Marine sponges are a rich source of natural products, largely because of their inclination to produce various structurally unique bioactive secondary metabolites.[1] It is believed that, in some cases, these bioactive compounds are actually produced by a diverse and abundant microbial community, which sometimes comprises half of the animals' body weight, rather than the sponge itself.[2−4] Species belonging to the order Lithistida, such as the genus *Theonella*, have been the source of diverse natural products with promising therapeutic potential,[5] e.g., the antifungal theopalauamide,[6] theonegramide, and theonellamides (TNMs),[7−9] HIV entry inhibitor koshikamide F and H,[10] anti-inflammatory solomonamide A,[11] antipsoriatic perthamide C and E,[12] cytotoxic polytheonamides and theopapuamide,[13,14] and rare sterol ligands for human nuclear receptors theonellasterols and conicasterols.[15]

TNMs (Figure 1), isolated from *Theonella* sp., belong to a family of unique bicyclic dodecapeptides first reported in 1989 by Matsunaga et al.[8] Since then, five additional congeners have been isolated.[8,9] These compounds possess a common bis-macrocyclic structure encompassing some unusual amino acids and a bridge of a histidinoalanine moiety. In some of these, a sugar moiety is attached to the bridge yet plays no significant role in the biological activity.[8,9] Structurally related peptides, theopalauamide[6] and theonegramide,[7] have also been isolated from sponges of the same genus. It has previously been reported that TNM-F induces the formation of extraordinarily

Received: January 23, 2013
Revised: March 11, 2013
Published: March 11, 2013

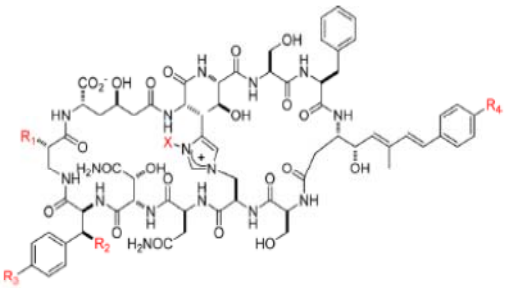

	R_1	R_2	R_3	R_4	X
Theonellamide A	OH	Me	Br	H	β-D-Gal
Theonellamide B	OH	Me	Br	Br	H
Theonellamide C	H	H	H	Br	H
Theonellamide D	H	H	Br	Br	β-L-Ara
Theonellamide E	H	H	Br	Br	β-D-Gal
Theonellamide F	H	H	Br	Br	H

Figure 1. Structures of theonellamides (TNMs).

large vacuoles in 3Y1 rat fibroblasts, and thus, TNM-F is postulated to affect cellular autophagy and inhibit organelle degradation as well as cause the breakdown of their proteins.[16] In addition, by using TNM-A-conjugated gel beads, glutamate dehydrogenase and 17β-hydroxysteroid dehydrogenase IV were identified as its binding proteins from rabbit liver tissues, and in vitro assays revealed that TNM-F activates glutamate dehydrogenase leading to the amination of α-ketoglutarate, although its potency is lower than that of the known activator adenosine diphosphate.[17]

Recently, a series of systematic experiments have provided substantial insights into the mode of action of TNMs and the structurally related theopalauamide.[18,19] Budding yeast genomics, using a collection of molecularly barcoded ORF libraries, revealed that theopalauamide was less effective toward mutated cells in the ergosterol biosynthesis pathway.[19] Indeed, theopalauamide permeabilizes liposomes containing ergosterol.[19] Chemical genomic analysis using a fission yeast ORF collection suggested a mechanistic link between TNMs and 1,3-β-D-glucan synthesis, and an overproduction of 1,3-β-D-glucan was observed following the treatment of yeast cells with TNM-F in a Rho1-dependent manner.[18] Furthermore, in vitro binding assays, using a fluorescently labeled TNM derivative, demonstrated that it specifically binds to 3β-hydroxysterols such as cholesterol and ergosterol (Figure 2).[18] Sterol binding is required for the TNM-induced 1,3-β-D-glucan synthesis and subsequent loss of membrane integrity. Judging from the phenotypic changes in yeasts, the membrane action of TNM-F is apparently distinct from that of polyene antifungals such as amphotericin B, which is also known to bind sterols in membranes; e.g., TNM-F caused fragmentation, instead of enlargement, of vacuoles and exhibited a time-dependent toxicity, as opposed to amphotericin B, which had acute fungicidal activity. Thus, TNMs represent a novel class of sterol-binding compounds whose mode of action is different from that of polyene antibiotics and therefore are expected to be a new tool for exploring the function and localization of sterols in cells. However, as is the case with amphotericin B and other polyene antibiotics, how TNMs recognize the sterols in lipid bilayers is yet to be determined. Therefore, a detailed analysis of the bimolecular interaction between TNMs and sterols is indispensable in understanding the mode of action of TNMs.

In general, interactions between bioactive molecules and cell membranes play a key role in the regulation of several cellular processes such as signal transduction, ion channel formation, and the action of antimicrobial and cytotoxic peptides. Among a wide range of techniques employed to investigate these interactions,[20,21] surface plasmon resonance (SPR) has been proven to be an excellent tool for examining the binding of biomolecules to membranes.[20,22] This technique was successfully employed to characterize the interaction of cationic amphiphilic drugs and antimicrobial peptides with artificial membranes.[23−25] Recently, using SPR, we have also evaluated the binding of amphotericin B[26] and amphidinol 3[27] to palmitoyloleoylphosphatidylcholine [POPC (Figure 2)] liposomes and demonstrated that the affinity of these molecules for the vesicles is significantly enhanced by incorporating cholesterol or ergosterol into the lipid bilayer. Solid-state deuterium NMR (^{2}H NMR) is an invaluable tool in the study of lipid, and sterol dynamics in model membranes, e.g., the membrane perturbing effects, induced by antimicrobial peptides, can be directly observed by the change in quadrupole splitting of deuterated acyl chain segments of phospholipids.[28]

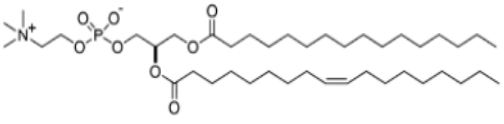

1-Palmitoyl-2-oleoyl-sn-glycero-3-phosphocholine (POPC)

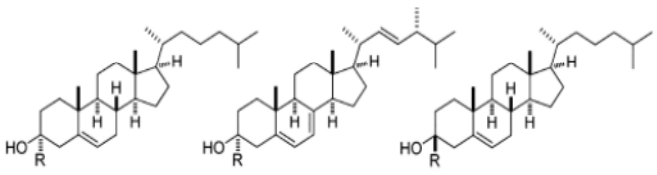

Cholesterol : R = H Ergosterol : R = H Epicholesterol : R = H
3-*d*-Cholesterol : R = D 3-*d*-Ergosterol : R = D 3-*d*-Epicholesterol : R = D

Figure 2. Chemical structures of the lipids used in this study.

dx.doi.org/10.1021/bi4000854 | *Biochemistry* 2013, 52, 2410−2418

More recently, ^{2}H NMR was used to reveal the dynamics of sterols [cholesterol and ergosterol deuterated at C3 (Figure 2)] affected by the presence of amphotericin B.[29] This study has shown that amphotericin B inhibits the fast rotational motion of ergosterol in membranes, thus unequivocally demonstrating the direct amphotericin B–ergosterol interaction in lipid bilayers.

Hence, in this study, we investigate the interaction between TNM-A and POPC liposomes containing cholesterol, ergosterol, or epicholesterol (Figure 2) with SPR to understand its mode of interaction. Then, we observed the direct interaction between TNM-A and sterols incorporated into lipid bilayers using solid-state ^{2}H NMR.

MATERIALS AND METHODS

Materials. Theonellamide A (TNM-A) was isolated as reported previously.[9] 1-Palmitoyl-2-oleoyl-*sn*-glycero-3-phosphocholine (POPC) was purchased from NOF Corp. Cholesterol was from Nacalai Tesque; ergosterol was obtained from Tokyo Kasei, and epicholesterol was obtained from Steraloids, Inc. 3-*d*-Cholesterol, 3-*d*-ergosterol, and 3-*d*-epicholesterol (Figure 2) were synthesized as previously reported.[29,30] 1-Ethyl-3-[3-(dimethylamino)propyl]-carbodiimide hydrochloride (EDC), *N*-hydroxysuccinimide (NHS), 10 mM acetate buffer (pH 5.0), 1 M ethanolamine (pH 8.5), 50 mM sodium hydroxide (NaOH), 0.5% (w/v) sodium dodecyl sulfate (SDS), and 10× PBS buffer (pH 7.4) were purchased from GE Healthcare (Uppsala, Sweden). Dodecylamine and dimethyl sulfoxide (DMSO) were purchased from Sigma-Aldrich Co. (St. Louis, MO). Polycarbonate filters was purchased from AVESTIN Inc. All the other chemicals were standard and analytical quality reagents.

Preparation of Liposomes for SPR Analysis. Large unilamellar vesicles (LUVs) were prepared as follows. POPC (10 mg) with or without 10 mol % (~0.5 mg) sterol (cholesterol, ergosterol, or epicholesterol) were dissolved together in chloroform in a round-bottom flask. The solvent was evaporated, and the resulting lipid film was further dried in vacuo overnight. It was then hydrated with 1 mL of PBS buffer [10 mM phosphate buffer (pH 7.4), 2.7 mM potassium chloride, and 137 mM sodium chloride]. The mixture was vortexed, sonicated, and subjected to three cycles of freezing (−80 °C), thawing (60 °C), and vortexing (5 s) to form multilamellar vesicles (MLVs). The MLV suspension was passed through double 100 nm polycarbonate filters 19 times with LiposoFast-Basic (AVESTIN Inc.) at room temperature to form LUVs. The lipid concentration of the LUVs was determined using a phospholipid C-Test (Wako Pure Chemical Industries Ltd.). The LUVs were then diluted with the same PBS buffer to produce a suspension with a final lipid concentration of 0.5 mM for injection into the SPR instrument.

Surface Plasmon Resonance Experiments. TNM-A (1 mg, 0.57 μmol) was first dissolved in DMSO (1 mL) and stored as a 0.57 mM stock solution; 50 μL of the TNM-A stock solution was diluted to 28 μM with 950 μL of PBS buffer. This solution was further diluted with PBS buffer containing 5% DMSO to give 10, 15, and 20 μM TNM-A solutions. We ensured that all these solutions, together with the running buffer, had the same DMSO concentration.

The SPR experiments were performed at 25 °C using a dodecylamine-modified CM5 sensor chip mounted on a Biacore T200 system (GE Healthcare), and the running buffer was PBS containing 5% DMSO (pH 7.4). The unmodified CM5 sensor chip was first washed three times with a 50 mM NaOH/2-propanol solution [3:2 (v/v)] at a flow rate of 20 μL/min for 2 min. Dodecylamine was immobilized in one of the flow cells (fc2) of the CM5 chip with an amino coupling method while the other flow cell (fc1) was left untouched to serve as the control lane. This chip was activated by injecting a solution of 390 mM EDC and 100 mM *N*-hydroxysuccinimide [1:1 (v/v), 70 μL] and then dodecylamine (1 mg/mL) in 10 mM acetate buffer containing 10% DMSO (pH 5.0) at a flow rate of 10 μL/min and a contact time of 7 min. The remaining *N*-hydroxysuccinimide ester groups on the sensor chip were deactivated by converting them to amide groups with an injection of 1 M ethanolamine hydrochloride (pH 8.5). Thus, the obtained modified sensor chip was then washed with 10% DMSO to remove nonspecifically bound molecules.

For the immobilization of liposomes on the sensor surface, the dodecylamine-modified sensor chip was first conditioned by an injection of running buffer at a rate of 10 μL/min for 5 min. The liposome suspension (0.5 mM) was then injected at a flow rate of 2 μL/min for 40 min, followed by the injection of 50 mM NaOH at a rate of 20 μL/min for 2 min, three times to generate a stable sensorgram, which indicated the formation of a stable liposome layer on the sensor surface.

TNM-A solutions, at concentrations of 10, 15, and 20 μM, were then injected at a flow rate of 10 μL/min; its association was observed for 300 s. Then running buffer was injected at the same flow rate for 300 s, and the dissociation of TNM-A from the surface was monitored. A new liposome surface was prepared for each injection of the TNM-A solution. To remove the liposomes from the sensor surface, injections of 0.5% (w/v) SDS, followed by a 50 mM NaOH/2-propanol solution [3:2 (v/v)] both at a flow rate of 20 μL/min for 2 min, were conducted twice to ensure a return to the original baseline.

Data Analysis. The sensorgrams obtained from the peptide–lipid bilayer interaction were analyzed by curve fitting[31,32] with Biacore T200 Evaluation version 1.0. Global fitting, which is normally done by simultaneously fitting sensorgrams corresponding to different analyte concentrations, was found to be incompatible with TNM-A as in the case with amphotericin B.[26] This is probably because concentration-dependent aggregate formation of TNM-A in the aqueous phase affects its membrane binding, thus leading to the inconsistency in the kinetic parameters at different TNM-A concentrations. Thus, we evaluated the kinetic parameters not by global fitting but by local fitting to the sensorgrams from 20 μM TNM-A. The sensorgrams were fit to a two-state reaction model,[26] in which interaction between the peptide and the lipid bilayers is assumed to occur in two steps (Scheme 1). The first

Scheme 1

$$A + B \underset{k_{d1}}{\overset{k_{a1}}{\rightleftharpoons}} AB \underset{k_{d2}}{\overset{k_{a2}}{\rightleftharpoons}} ABx$$

step involves the binding of TNM-A (A) to membrane lipids (B) in a parallel and stoichiometric manner, identical to the simple bimolecular or Langmuir model if the second step does not proceed. The second step involves a conformational or morphological change of the complex (AB) to a second complex (ABx).

In this model, rate equations are given by

$$d[A]/dt = -k_{a1}[A][B] + k_{d1}[AB] \quad (1)$$

$$d[AB]/dt = (k_{a1}[A][B] - k_{d1}[AB]) - (k_{a2}[AB] - k_{d2}[ABx]) \quad (2)$$

$$d[ABx]/dt = k_{a2}[AB] - k_{d2}[ABx] \quad (3)$$

$$K_{A1} = k_{a1}/k_{d1};\ K_{A2} = k_{a2}/k_{d2};\ K_A = K_{A1}K_{A2} \quad (4)$$

where k_{a1} and k_{d1} correspond to the association and dissociation rate constants for the liposome surface of free TNM-A, respectively, while k_{a2} and k_{d2} correspond to the distribution rate constants from AB to ABx forms and vice versa, respectively. K_{A1}, K_{A2}, and K_A represent the affinity constants for the first, second, and overall equilibrium steps, respectively. A detailed method for determining the kinetic parameters on the basis of this model is given in the literature.[24,26,32]

Sample Preparation for Solid-State ^{2}H NMR. For the measurement of ^{2}H NMR spectra of the deuterated sterols in POPC membranes, 2.6 μmol of 3-*d*-sterol, 46 μmol of POPC, and TNM-A (0 or 2.6 μmol) were dissolved in a $CHCl_3$/MeOH solution [2:1 (v/v)] in a round-bottom flask. The solvent was removed in vacuo and further dried overnight. The lipid film was then rehydrated with 1 mL of milli-Q water. After being sonicated and vortexed for a few minutes, the lipid suspension was subjected to three cycles of freezing (−80 °C) and thawing (40 °C) to make MLVs. The vesicle suspension was lyophilized overnight, rehydrated with deuterium-depleted water [50% (w/w)], and homogenized by being vortexed, frozen, and thawed. It was then transferred to a 5 mm glass tube (Wilmad) and sealed with epoxy glue.

^{2}H NMR Measurements. All the ^{2}H NMR spectra were recorded on a 400 MHz ECA400 (JEOL, Tokyo, Japan) or a 300 MHz CMX300 (Chemagnetics, Agilent, Palo Alto, CA) spectrometer. Spectra were collected at 30 °C using a 5 mm ^{2}H static probe (Doty Scientific Inc., Columbia, SC, or Otsuka Electronics, Osaka, Japan) following a quadrupolar echo sequence.[29] The 90° pulse width was 2 μs; the interpulse delay was 30 μs, and the repetition rate was 0.5 s. The sweep width was 200 kHz, and the number of scans was around 400000.

RESULTS

Binding of TNM-A to POPC Liposomes Measured by SPR. A dodecylamine-modified CM5 sensor chip was utilized to evaluate the interaction of TNM-A with POPC/sterol (10 mol %) and pure POPC liposomes as we previously reported for amphotericin B.[26] The liposomes were captured by the modified lane with an immobilization level of around 12700 ± 800 RU.[26,27] The response from the control lane was subtracted from that in the liposome-immobilized lane. Figure 3 shows typical sensorgrams representing the binding of TNM-A to various POPC liposomes. Interaction of the peptide with the membranes showed clear concentration dependence, regardless of the presence or absence of sterol, indicating that the amount of membrane-bound peptide is directly proportional to the peptide concentration in the bulk solution. Moreover, as evidenced by the RU increase, the presence of cholesterol and ergosterol significantly enhanced the binding of the peptide to POPC liposomes by approximately 3-fold compared with that of pure POPC liposomes, while the binding of the peptide to epicholesterol (3α-cholesterol)-containing liposomes was comparable to that of pure liposomes. These observations clearly demonstrate the preference of the peptide for 3β-hydroxysterols, which is consistent with the previous findings obtained with fluorescently labeled TNM.[18]

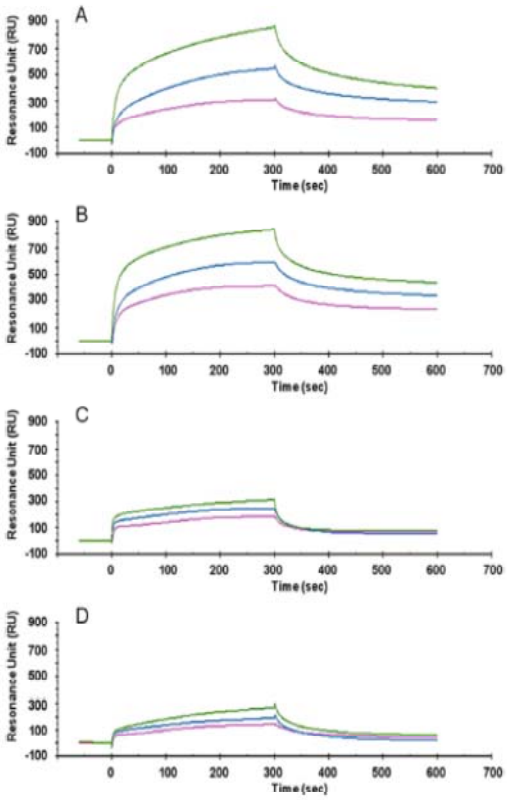

Figure 3. SPR sensorgrams for binding of TNM-A to liposomes captured on a dodecylamine-modified CM5 sensor chip: (A) 10 mol % cholesterol-containing POPC liposomes, (B) 10 mol % ergosterol-containing POPC liposomes, (C) 10 mol % epicholesterol-containing POPC liposome, and (D) pure POPC liposomes. Sensorgrams correspond to 20 (green), 15 (blue), and 10 μM TNM-A (violet).

Next we analyzed the kinetics of binding of TNM-A to lipid membranes by fitting the experimental curves to those calculated from a theoretical model. On the basis of the possible mechanism of action of antimicrobial and membrane-active peptides,[20,24] the sensorgrams could be fit to a two-state reaction model (Scheme 1). This model assumes that the interaction between the peptide and membrane lipids occurs via a two-step process: the first step involving the actual binding of TNM-A to the membrane surface and the second step probably corresponding to a conformational or morphological change to form a more stable membrane complex. The two-state analysis was first applied to well-known membrane peptides melittin and magainin[24,25] and then successfully used for antifungal natural products amphotericin B[26] and amphidinol 3.[27] For these compounds, the two-state model reproduced the experimental SPR sensorgrams better than the conventional Langmuir model, which is consistent with the mechanisms of their membrane activities. Figure 4 shows the curve fitting of the experimental sensorgrams to the two-state reaction model (Scheme 1 and eqs 1−4) together with the components of the theoretical curve, demonstrating that theoretical curves using the two-state model excellently reproduced the experimental sensorgrams. As is evident from

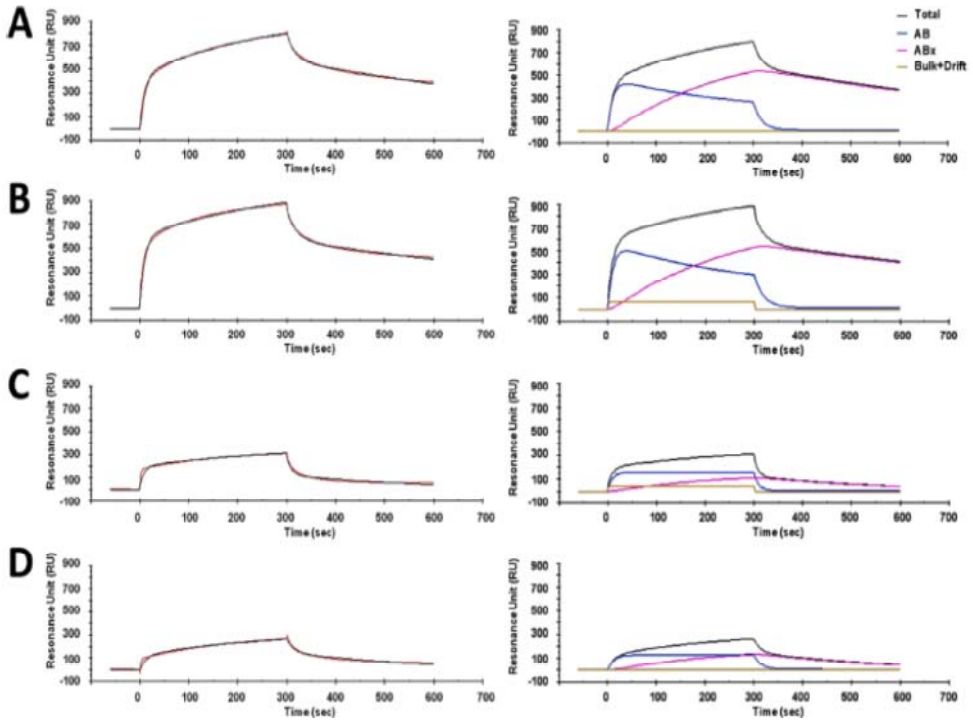

Figure 4. Curve fitting of the SPR sensorgrams to the two-state reaction model (left) and components of the fitting curves (right): (A) 10 mol % cholesterol-containing POPC liposomes, (B) 10 mol % ergosterol-containing POPC liposomes, (C) 10 mol % epicholesterol-containing POPC liposomes, and (D) pure POPC liposomes. Experimental RU values were recorded for 20 μM TNM-A. Red and black traces in the left panels depict experimental and theoretical curves, respectively. Blue, pink, and yellow traces in the right panels represent contributions from the AB complex, the ABx complex, and the bulk effect of the solvent, respectively, to the total component (black line).

Table 1. Kinetic Parameters for the Binding of TNM-A to Liposomes Obtained from the Two-State Reaction Model[a]

	POPC/cholesterol (10 mol %)	POPC/ergosterol (10 mol %)	POPC/epicholesterol (10 mol %)	POPC
k_{a1} ($\times 10^3$ M^{-1} s^{-1})	1.6 ± 0.3	2.5 ± 0.2	0.22 ± 0.09	0.15 ± 0.05
k_{d1} ($\times 10^{-2}$ s^{-1})	5.3 ± 0.5	4.73 ± 0.06	7.5 ± 3.7	7.7 ± 1.1
k_{a2} ($\times 10^{-3}$ s^{-1})	6.6 ± 0.4	5.7 ± 0.2	3.4 ± 0.7	6.1 ± 0.4
k_{d2} ($\times 10^{-3}$ s^{-1})	1.8 ± 0.2	1.2 ± 0.1	2.4 ± 1.3	4.7 ± 0.3
K_{A1} ($\times 10^3$ M^{-1})	30 ± 4	52 ± 4	3.0 ± 0.5	1.8 ± 0.4
K_{A2}	3.6 ± 0.6	4.8 ± 0.4	1.6 ± 0.5	1.3 ± 0.1
K_A ($\times 10^3$ M^{-1})	109 ± 32	250 ± 26	4.9 ± 1.9	2.4 ± 0.5

[a]The concentration of TNM-A was 20 μM.

the right panels of Figure 4, progression of the second step is much slower than that of the first step in all four cases, thus showing that the second step is rate-limiting. We also tried to fit the sensorgrams to the Langmuir or 1:1 bimolecular interaction model but could not reproduce the theoretical curve (Figure S1 of the Supporting Information), thus supporting the notion that the binding of TNM-A to the lipid bilayers occurs via two different processes. Table 1 lists the kinetic and affinity constants obtained from the fitting, showing that the presence of 3β-hydroxysterol, cholesterol, or ergosterol significantly enhanced the affinity (K_A) of TNM-A for the membranes compared with those of epicholesterol (3α-hydroxysterol)-containing and pure POPC liposomes. This enhanced affinity of the peptide for the 3β-hydroxysterol-containing membranes is mainly due to the first binding step, because the rate constants (k_{a1}) are ~10 times larger in cholesterol- and ergosterol-containing liposomes than in epicholesterol-containing and pure POPC liposomes. In contrast, the second rate constants (k_{a2} and K_{A2}) were approximately the same for all systems tested, thus indicating that the second process is less affected by the presence of 3β-hydroxysterol.

In these measurements, the binding of TNM-A to POPC liposomes was very strong, especially with cholesterol- or ergosterol-containing membranes, such that regeneration of the liposome surface via repeated washing with NaOH was not successful (Figure S2 of the Supporting Information). Thus, the liposomes once used for analysis had to be removed, and then fresh liposomes were immobilized on the sensor chip for the next analysis, which resulted in the relatively large standard deviations shown in Table 1. Nevertheless, we can safely compare the kinetic data because the differences in the kinetic

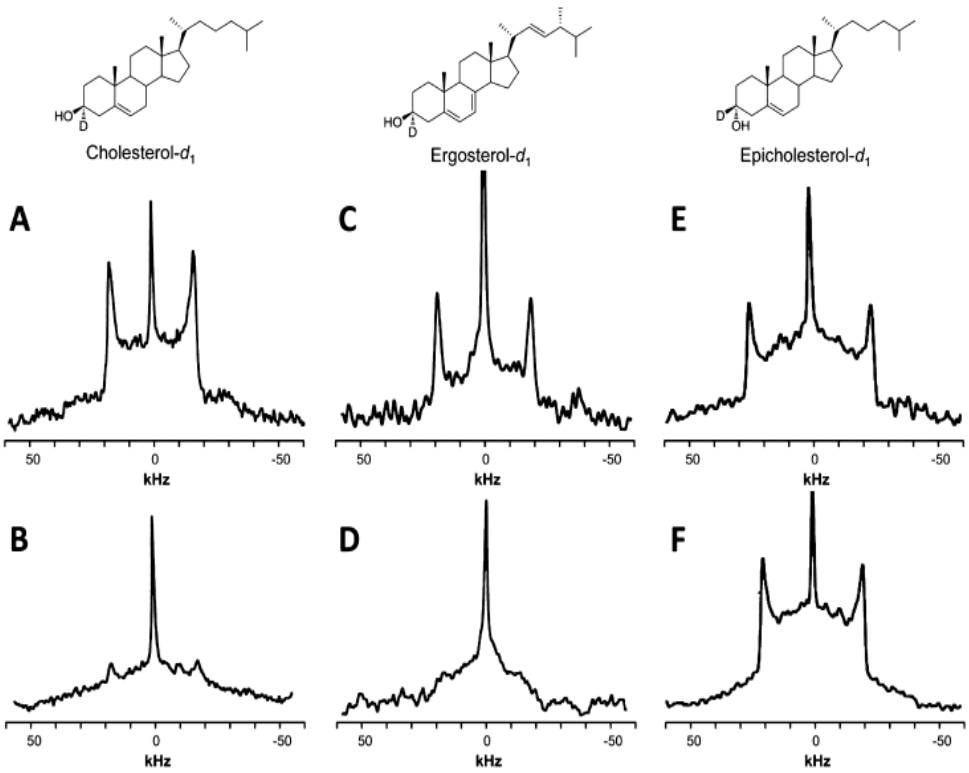

Figure 5. ^{2}H NMR spectra of 3-*d*-sterol incorporated into POPC bilayers in the absence (A, C, and E) and presence (B, D, and F) of TNM-A. 3-*d*-Cholesterol (A and B), 3-*d*-ergosterol (C and D), and 3-*d*-epicholesterol (E and F) were used. 3-*d*-Sterol:TNM-A:POPC molar ratios of 1:0:18 (A, C, and E) and 1:1:18 (B, D, and F) were used. Isotropic signals are mostly from residual deuterium water.

constants between membrane systems significantly exceed the deviations.

Interaction between TNM-A and Sterol As Viewed by Solid-State ^{2}H NMR. Although the SPR experiments described above clearly show the preferential binding of TNM-A to 3β-hydroxysterol-containing membranes, it does not necessarily indicate that TNM-A directly interacts with 3β-hydroxysterol in lipid bilayers; it is also possible to assume that the presence of 3β-hydroxysterols changes the physicochemical properties of the membrane and consequently enhances the membrane affinity of TNM-A. Hence, to gain decisive evidence of the direct binding of TNM-A to membrane sterols, we conducted solid-state ^{2}H NMR measurements using 3-*d*-sterols (Figure 2) incorporated into POPC liposomes. Sterol molecules in lipid bilayers undergo fast lateral diffusion, which can be regarded as an axial rotation in NMR, and quadrupolar splitting observed in the ^{2}H NMR spectra depends both on the tilt angle of the C–^{2}H bond with respect to the rotation axis and the wobbling of the molecule.[29] Figure 5 shows the spectra of the 3-*d*-sterols incorporated into POPC bilayers in the absence and presence of TNM-A. In the absence of TNM-A (Figure 5A), 3-*d*-cholesterol exhibits a characteristic Pake doublet indicative of fast rotational motion of the sterol in the POPC bilayers. However, upon addition of the peptide, a stark attenuation of the splitting signal is observed (Figure 5B), indicating that the molecular rotation falls into an intermediate motional speed with correlation times of 10^{-4} to 10^{-5} s. A similar change in the splitting pattern was observed with 3-*d*-ergosterol (Figure 5C,D). On the other hand, in 3-*d*-epicholesterol-containing POPC liposomes (Figure 5E,F), the characteristic splitting pattern hardly changed, although the splitting value was slightly reduced by the presence of TNM-A, which may be attributable to a morphological change in the liposome induced by TNM-A that will be discussed shortly. Therefore, this demonstrates that the fast rotational motion of both 3-*d*-cholesterol and 3-*d*-ergosterol slows via direct interaction with TNM-A in lipid bilayers, which is indicative of considerable intermolecular interaction. Conversely, no such inhibition with 3-*d*-epicholesterol means that the fast rotational motion occurs even in the presence of TNM-A, indicative of a weaker intermolecular interaction between these two molecules. In addition, these observations strongly support the fact that the presence of either cholesterol or ergosterol, but not epicholesterol, significantly enhances the affinity of TNM-A for POPC liposomes as was shown explicitly in the SPR experiments (Figure 3 and Table 1). These results unequivocally prove the direct interaction between TNM-A and 3β-hydroxysterols in lipid bilayers.

■ DISCUSSION

Although we have reported that fluorescently labeled TNMs bind to 3β-sterols,[18] the detailed mode of interaction is yet to be clarified. In this study, to improve our understanding of the sterol recognition mechanism exhibited by the peptide, we scrutinized the interaction between TNM-A and sterol-containing liposomes using SPR and solid-state ^{2}H NMR and

demonstrated for the first time the direct interaction using TNM-A as an intact TNM. Here it should be mentioned that, although the concentrations of TNM-A are different by 2 orders of magnitude between the two experiments (20 μM and 2.6 mM), the molar ratios between TNM-A and lipid molecules are almost identical (1:25 and 1:19 for SPR and ^{2}H NMR, respectivley), thus rationalizing the concomitant use of both methods.

As described in the introductory section, the presence or absence of a sugar moiety in TNM molecules hardly affects the activity based on comparable results obtained from biological tests.[8,9] Theopalauamide, which is structurally closely related to TNM-A and has a sugar moiety, recognizes sterol molecules as is the case in TNM-F lacking the sugar moiety;[19] therefore, it is reasonable to consider that these results obtained for TNM-A essentially hold true for TNM-F and other TNM congeners.

Using SPR with a dodecylamine-modified CM5 sensor chip that was devised to minimize nonspecific hydrophobic interactions, we successfully demonstrated that the presence of 3β-hydroxysterols, as seen in cholesterol and ergosterol, significantly increases the affinity of the peptide for POPC membranes (Figures 3 and 4 and Table 1). In contrast, TNM-A had a lower affinity for epicholesterol-containing or pure POPC liposomes. The kinetic parameters listed in Table 1 further revealed that the 3β-sterols markedly promote the initial binding of TNM-A to the membrane surfaces (k_{a1}). The membrane affinity is enhanced by direct interaction between the peptide and the sterols that was explicitly shown on the basis of characteristic spectral changes in solid-state ^{2}H NMR. These findings, together with the fact that the alcohol groups of sterols are located close to the membrane interface,[33−35] imply that TNM-A has a direct interaction with the hydroxy moieties of 3β-sterols at the initial binding of TNM-A to the membrane surface, resulting in the greater level of accumulation of the peptide in the shallow area of the membrane. The direct recognition of the sterol hydroxy groups at the membrane surface is consistent with the relatively small difference (a factor of approximately 2) in the affinity between cholesterol and ergosterol (Table 1), indicating that TNM-A does not strictly recognize the difference in the steroid skeleton or side chain structure. It is not so far-fetched to assume that intermolecular hydrogen bonds play a crucial functional role in the interaction between TNM-A and the sterol hydroxy group.

In a previous report,[18] it was demonstrated that calcein, a membrane-impermeable fluorescent dye, was able to enter yeast cells in the presence of TNM-F (11 μM), indicating that membrane integrity is compromised by the peptide. Although the presence of 3β-hydroxysterols had a weaker effect on the second step of the binding process (K_{A2} in Table 1), the greater level of accumulation of TNM-A on the membrane surface, in the presence of cholesterol or ergosterol, results in an increased level of formation of the second complex (ABx) (Figure 4A,B). This presumably corresponds to the relocation of the peptide from the surface-binding form to a more stable membrane-complex form. We have recently observed through microscope and ^{31}P NMR experiments that TNM-A induced a microscopic morphological change in liposome features such as the occurrence of high-curvature regions (to be published in due course), which is consistent with the reduced quadrupole splitting value of epicholesterol by the presence of TNM-A (Figure 5E,F). Therefore, the second step may correspond to deformation of membrane morphology through the binding of the peptide. Namely, the accumulated TNM-A in the 3β-sterol-containing membranes could change the membrane morphology and integrity, ultimately resulting in membrane damage as previously reported for yeast cells.[18] In fact, TNM-induced membrane damage as well as cytotoxicity is reported to be time-dependent,[18] consistent with the slow progression of the second process as shown in Figure 4.

As described in the introductory section, the membrane action of TNM-F is apparently different from that of amphotericin B, a representative polyene antibiotic forming sterol-dependent pores in fungal membranes; e.g., TNM-F exhibited a time-dependent toxicity, while amphotericin B has acute fungicidal activity.[18] In our experiments using artificial membranes, distinct pore formation by TNM-A could not be observed (Figure S3 of the Supporting Information), although it induced hemolysis (Table S1 of the Supporting Information). Here it may be meaningful to compare the SPR kinetic parameters of TNM-A with those of amphotericin B. We previously reported that sterols, particularly ergosterol, prominently promote not only the initial surface binding step of amphotericin B but also the subsequent reorientation process presumably corresponding to pore formation.[26] In particular, the second step of amphotericin B hardly proceeds without sterols being present, thus suggesting that the sterol is involved in the pore complex. In contrast, as clearly shown in Table 1, the second step of TNM-A binding proceeds without sterols and is not significantly accelerated by the presence of sterols. In addition, amphotericin B shows a more than 10-fold difference in the K_A values between cholesterol and ergosterol, which is largely attributed to the second reorientation step, while TNM-A exhibits a smaller difference (a factor of ~2) as shown in Table 1. More recently, we have found that amphotericin B does not interact with epiergosterol (manuscript in preparation). Taken together, this means that amphotericin B recognizes not only the 3-hydroxy group but also steroid rings and side chains, the latter of which would provide ergosterol selectivity and promote the second reorientation process corresponding to pore formation, while TNM-A mostly recognizes the sterol hydroxy group in the initial binding process. This difference is consistent with the observation that TNM-A is unlikely to form distinctive pores as does amphotericin B. Rather, as mentioned previously, it is more plausible that the accumulation of TNM-A in the sterol-containing membrane disturbs and damages the bilayer morphology and integrity, which would correspond to the second process in TNM-A binding. Here it should be mentioned that the weaker sterol dependency in the second process of the binding of TNM to the membrane does not indicate the lack of the interaction between TNM-A and sterol in the second step, because ^{2}H NMR spectra demonstrate the persistent interaction in the membrane, but rather suggests that TNM-A induces the second step irrespective of the presence or absence of the interaction with the sterol molecules.

In conclusion, we have demonstrated using SPR that the presence of cholesterol or ergosterol significantly enhances the affinity of TNM-A for POPC liposomes and the peptide exhibits a preference for sterols with a 3β configuration. This enhanced affinity is caused by direct interaction between the peptide and 3β-hydroxysterols that is explicitly shown by characteristic spectral patterns in solid-state ^{2}H NMR. These results are consistent with the selective binding of fluorescently labeled TNM to 3β-hydroxysterols.[18] Our kinetic data show that 3β-hydroxysterols accelerate the initial binding of TNM-A to the membrane surface, thus suggesting that TNM-A directly

recognizes the 3β-OH moiety upon binding to the membrane surface. Although the presence of 3β-hydroxysterols had a weaker effect on the kinetic constants of the second process corresponding to some deformation of bilayer morphology, the accumulation of TNM-A in the sterol-containing membranes eventually promotes the second process, thus causing the damage to the integrity of the membrane as reported previously.[18] However, the nature of these membrane effects as well as that of the molecular recognition is still a subject of further investigation. To this end, further microscopic and NMR-based experiments will be necessary to observe changes in membrane morphology caused by the peptide and to determine the peptide's structure complexed with sterols in bilayer systems; such studies are currently underway in our group.

■ ASSOCIATED CONTENT

Supporting Information

Fitting of experimental sensorgrams corresponding to 20 μM TNM-A to the Langmuir 1:1 bimolecular interaction model, regeneration of the liposome surface by 50 mM NaOH washing, and experimental details and results of the calcein leakage assay using POPC liposomes as well as the hemolysis assay using human erythrocytes. This material is available free of charge via the Internet at http://pubs.acs.org.

■ AUTHOR INFORMATION

Corresponding Author

*Telephone: +81-6-6850-5790. E-mail: matsmori@chem.sci.osaka-u.ac.jp.

Funding

This work was supported by Grants-in-Aid for Scientific Research (B) (20310132) and (S) (18101010) and in part by JST, ERATO Lipid Active Structure Project. R.A.E. expresses his special thanks to MEXT, Japan, for providing a Ph.D. scholarship.

Notes

The authors declare no competing financial interest.

■ ACKNOWLEDGMENTS

We are grateful to Dr. Y. Umegawa, Dr. N. Inazumi, and Mr. M. Doi (Osaka University) for their help in NMR measurements.

■ ABBREVIATIONS

LUV, large unilamellar vesicle; MLV, multilamellar vesicle; NMR, nuclear magnetic resonance; PBS, phosphate-buffered saline; POPC, 1-palmitoyl-2-oleoyl-*sn*-glycero-3-phosphocholine; RU, resonance unit; SPR, surface plasmon resonance; TNMs, theonellamides; TNM-A, theonellamide A; EDC, 1-ethyl-3-[3-(dimethylamino)propyl]carbodiimide hydrochloride.

■ REFERENCES

(1) Faulkner, D. J. (2002) Marine Natural Products. *Nat. Prod. Rep.* *19*, 1−48.

(2) Tabares, P., Pimentel-Elardo, S. M., Schirmeister, T., Hünig, T., and Hentschel, U. (2011) Anti-protease and immunomodulatory activities of bacteria associated with Caribbean sponges. *Mar. Biotechnol.* *13*, 883−892.

(3) Proksch, P., Putz, A., Ortlepp, S., Kjer, J., and Bayer, M. (2010) Bioactive natural products from marine sponges and fungal endophytes. *Phytochem. Rev.* *9*, 475−489.

(4) Taylor, M. W., Radax, R., Steger, D., and Wagner, M. (2007) Sponge-associated microorganisms: Evolution, ecology, and biotechnological potential. *Microbiol. Mol. Biol.* *71*, 295−347.

(5) Wright, A. E. (2010) The Lithistida: Important sources of compounds useful in biomedical research. *Curr. Opin. Biotechnol.* *21*, 801−807.

(6) Schmidt, E. W., Bewley, C. A., and Faulkner, D. J. (1998) Theopalauamide, a bicyclic glycopeptide from filamentous bacterial symbionts of the lithistid sponge *Theonella swinhoei* from Palau and Mozambique. *J. Org. Chem.* *63*, 1254−1258.

(7) Bewley, C. A., and Faulkner, D. J. (1994) Theonegramide, an antifungal glycopeptide from the Philippine lithistid sponge *Theonella swinhoei*. *J. Org. Chem.* *59*, 4849−4852.

(8) Matsunaga, S., Fusetani, N., Hashimoto, K., and Wälchli, M. (1989) Theonellamide F. A novel antifungal bicyclic peptide from a marine sponge *Theonella* sp. *J. Am. Chem. Soc.* *111*, 2582−2588.

(9) Matsunaga, S., and Fusetani, N. (1995) Theonellamides A-E, cytotoxic bicyclic peptides, from a marine sponge *Theonella* sp. *J. Org. Chem.* *60*, 1177−1181.

(10) Plaza, A., Bifulco, G., Masullo, M., Lloyd, J. R., Keffer, J. L., Colin, P. L., Hooper, J. N. A., Bell, L. J., and Bewley, C. A. (2010) Mutremdamide A and koshikamides C-H, peptide inhibitors of HIV-1 entry from different *Theonella* species. *J. Org. Chem.* *75*, 4344−4355.

(11) Festa, C., De Marino, S., Sepe, V., D'Auria, M. V., Bifulco, G., Debitus, C., Bucci, M., Vellecco, V., and Zampella, A. (2011) Solomonamides A and B, new anti-inflammatory peptides from *Theonella swinhoei*. *Org. Lett.* *13*, 1532−1535.

(12) Festa, C., De Marino, S., Sepe, V., D'Auria, M. V., Bifulco, G., Andrés, R., Terencio, M. C., Payá, M., Debitus, C., and Zampella, A. (2011) Perthamides C-F, potent human antipsoriatic cyclopeptides. *Tetrahedron* *67*, 7780−7786.

(13) Hamada, T., Matsunaga, S., Yano, G., and Fusetani, N. (2005) Polytheonamides A and B, highly cytotoxic, linear polypeptides with unprecedented structural features, from the marine sponge, *Theonella swinhoei*. *J. Am. Chem. Soc.* *127*, 110−118.

(14) Ratnayake, A. S., Bugni, T. S., Feng, X., Harper, M. K., Skalicky, J. J., Mohammed, K. A., Andjelic, C. D., Barrows, L. R., and Ireland, C. M. (2006) Theopapuamide, a cyclic depsipeptide from a Papua New Guinea lithistid sponge *Theonella swinhoei*. *J. Nat. Prod.* *69*, 1582−1586.

(15) De Marino, S., Ummarino, R., D'Auria, M. V., Chini, M. G., Bifulco, G., Renga, B., D'Amore, C., Fiorucci, S., Debitus, C., and Zampella, A. (2011) Theonellasterols and conicasterols from *Theonella swinhoei*. Novel marine natural ligands for human nuclear receptors. *J. Med. Chem.* *54*, 3065−3075.

(16) Wada, S., Matsunaga, S., Fusetani, N., and Watabe, S. (1999) Theonellamide F, a bicyclic peptide marine toxin, induces formation of vacuoles in 3Y1 rat embryonic fibroblast. *Mar. Biotechnol.* *1*, 337−341.

(17) Wada, S., Matsunaga, S., Fusetani, N., and Watabe, S. (2000) Interaction of cytotoxic bicyclic peptides, theonellamides A and F, with glutamate dehydrogenase and 17β-hydroxysteroid dehydrogenase IV. *Mar. Biotechnol.* *2*, 285−292.

(18) Nishimura, S., Arita, Y., Honda, M., Iwamoto, K., Matsuyama, A., Shirai, A., Kawasaki, H., Kakeya, H., Kobayashi, T., Matsunaga, S., and Yoshida, M. (2010) Marine antifungal theonellamides target 3β-hydroxysterol to activate Rho1 signaling. *Nat. Chem. Biol.* *6*, 519−526.

(19) Ho, C. H., Magtanong, L., Barker, S. L., Gresham, D., Nishimura, S., Natarajan, P., Koh, J. L. Y., Porter, J., Gray, C. A., Andersen, R. J., Giaever, G., Nislow, C., Andrews, B., Botstein, D., Graham, T. R., Yoshida, M., and Boone, B. (2009) A molecular barcoded yeast ORF library enables mode-of-action analysis of bioactive compounds. *Nat. Biotechnol.* *27*, 369−377.

(20) Mozsolits, H., and Aguilar, M. (2002) Surface plasmon resonance spectroscopy: An emerging tool for the study of peptide-membrane interactions. *Biopolymers* *66*, 3−18.

(21) Seddon, A. M., Casey, D., Law, R. V., Gee, A., Templer, R. H., and Ces, O. (2009) Drug interactions with lipid membranes. *Chem. Soc. Rev.* *38*, 2509−2519.

(22) Hall, D. (2001) Use of optical biosensors for the study of mechanistically concerted surface adsorption processes. *Anal. Biochem. 288*, 109−125.
(23) Nussio, M. R., Sykes, M. J., Miners, J. O., and Shapter, J. G. (2007) Characterisation of the binding of cationic amphiphilic drugs to phospholipid bilayers using surface plasmon resonance. *ChemMedChem 2*, 366−373.
(24) Papo, N., and Shai, Y. (2003) Exploring peptide membrane interaction using surface plasmon resonance: Differentiation between pore formation versus membrane disruption by lytic peptides. *Biochemistry 42*, 458−466.
(25) Hall, K., Mozsolits, H., and Aguilar, M. (2003) Surface plasmon resonance analysis of antimicrobial peptide-membrane interactions: Affinity & mechanism of action. *Lett. Pept. Sci. 10*, 475−485.
(26) Mouri, R., Konoki, K., Matsumori, N., Oishi, T., and Murata, M. (2008) Complex formation of amphotericin B in sterol-containing membranes as evidenced by surface plasmon resonance. *Biochemistry 47*, 7807−7815.
(27) Swasono, R. T., Mouri, R., Morsy, N., Matsumori, N., Oishi, T., and Murata, M. (2010) Sterol effect on interaction between amphidinol 3 and liposomal membrane as evidenced by surface plasmon resonance. *Bioorg. Med. Chem. Lett. 20*, 2215−2218.
(28) Strandgerg, E., and Ulrich, A. S. (2004) NMR Methods for Studying Membrane-Active Antimicrobial Peptide. *Concepts Magn. Reson., Part A 23*, 89−120.
(29) Matsumori, N., Tahara, K., Yamamoto, H., Morooka, A., Doi, M., Oishi, T., and Murata, M. (2009) Direct interaction between amphotericin B and ergosterol in lipid bilayers as revealed by ^{2}H NMR spectroscopy. *J. Am. Chem. Soc. 131*, 11855−11860.
(30) Murari, R., Murari, M. P., and Baumann, W. J. (1986) Sterol orientations in phosphatidylcholine liposomes as determined by deuterium NMR. *Biochemistry 25*, 1062−1067.
(31) Khalifa, M. B., Choulier, L., Lortat-Jacob, H., Altschuh, D., and Vernet, T. (2001) BIACORE data processing: An evaluation of the global fitting procedure. *Anal. Biochem. 293*, 194−203.
(32) Morton, T. A., Myszka, D. G., and Chaiken, I. M. (1995) Interpreting complex binding kinetics from optical biosensors: A comparison of analysis by linearization, the integrated rate equation, and numerical integration. *Anal. Biochem. 227*, 176−185.
(33) Kessel, A., Ben-Tal, N., and May, S. (2001) Interactions of cholesterol with lipid bilayers: The preferred configurations and fluctuations. *Biophys. J. 81*, 643−658.
(34) Róg, T., and Pasenkiewicz-Gierula, M. (2003) Effects of epicholesterol on the phosphatidylcholine bilayer: A molecular simulation study. *Biophys. J. 84*, 1818−1826.
(35) Róg, T., Pasenkiewicz-Gierula, M., Vattulainen, I., and Karttunen, M. (2009) Ordering effects of cholesterol and its analogues. *Biochim. Biophys. Acta 1788*, 97−121.